frontiers | Research Topics

# Pharmacological and non-pharmacological therapy for obesity and diabetes, volume II

**Edited by**
Guilherme Zweig Rocha, Alexandre Gabarra Oliveira and Bruno Melo Carvalho

**Published in**
Frontiers in Endocrinology

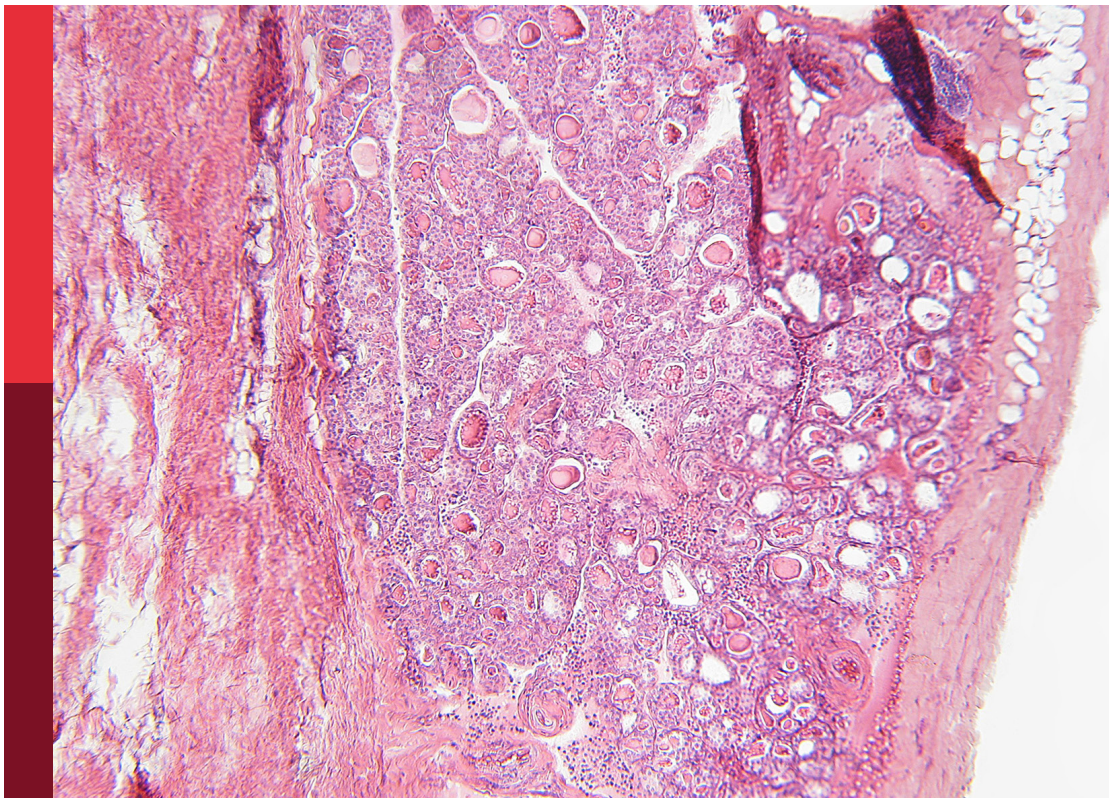

ISSN 1664-8714
ISBN 978-2-8325-3871-5
DOI 10.3389/978-2-8325-3871-5

## About Frontiers

Frontiers is more than just an open access publisher of scholarly articles: it is a pioneering approach to the world of academia, radically improving the way scholarly research is managed. The grand vision of Frontiers is a world where all people have an equal opportunity to seek, share and generate knowledge. Frontiers provides immediate and permanent online open access to all its publications, but this alone is not enough to realize our grand goals.

## Frontiers journal series

The Frontiers journal series is a multi-tier and interdisciplinary set of open-access, online journals, promising a paradigm shift from the current review, selection and dissemination processes in academic publishing. All Frontiers journals are driven by researchers for researchers; therefore, they constitute a service to the scholarly community. At the same time, the *Frontiers journal series* operates on a revolutionary invention, the tiered publishing system, initially addressing specific communities of scholars, and gradually climbing up to broader public understanding, thus serving the interests of the lay society, too.

## Dedication to quality

Each Frontiers article is a landmark of the highest quality, thanks to genuinely collaborative interactions between authors and review editors, who include some of the world's best academicians. Research must be certified by peers before entering a stream of knowledge that may eventually reach the public - and shape society; therefore, Frontiers only applies the most rigorous and unbiased reviews. Frontiers revolutionizes research publishing by freely delivering the most outstanding research, evaluated with no bias from both the academic and social point of view. By applying the most advanced information technologies, Frontiers is catapulting scholarly publishing into a new generation.

## What are Frontiers Research Topics?

Frontiers Research Topics are very popular trademarks of the *Frontiers journals series*: they are collections of at least ten articles, all centered on a particular subject. With their unique mix of varied contributions from Original Research to Review Articles, Frontiers Research Topics unify the most influential researchers, the latest key findings and historical advances in a hot research area.

Find out more on how to host your own Frontiers Research Topic or contribute to one as an author by contacting the Frontiers editorial office: frontiersin.org/about/contact

# Pharmacological and non-pharmacological therapy for obesity and diabetes, volume II

**Topic editors**

Guilherme Zweig Rocha — State University of Campinas, Brazil
Alexandre Gabarra Oliveira — São Paulo State University, Brazil
Bruno Melo Carvalho — Universidade de Pernambuco, Brazil

**Citation**

Rocha, G. Z., Oliveira, A. G., Carvalho, B. M., eds. (2024). *Pharmacological and non-pharmacological therapy for obesity and diabetes, volume II*. Lausanne: Frontiers Media SA. doi: 10.3389/978-2-8325-3871-5

# Table of contents

frontiers | Frontiers in Endocrinology

TYPE Editorial
PUBLISHED 20 October 2023
DOI 10.3389/fendo.2023.1252536



OPEN ACCESS

EDITED AND REVIEWED BY
Katherine Samaras,
St Vincent's Hospital Sydney, Australia

*CORRESPONDENCE
Guilherme Zweig Rocha
gzrocha@gmail.com

RECEIVED 03 July 2023
ACCEPTED 05 October 2023
PUBLISHED 20 October 2023

CITATION
Oliveira AG, Carvalho BM and Zweig Rocha G (2023) Editorial: Pharmacological and non-pharmacological therapy for obesity and diabetes - volume II. *Front. Endocrinol.* 14:1252536. doi: 10.3389/fendo.2023.1252536



# Editorial: Pharmacological and non-pharmacological therapy for obesity and diabetes - volume II

Alexandre Gabarra Oliveira[1], Bruno Melo Carvalho[2] and Guilherme Zweig Rocha[3]*

[1]Department of Physical Education, Bioscience Institute, São Paulo State University (UNESP), Rio Claro, São Paulo, Brazil, [2]Institute of Biological Sciences, University of Pernambuco (UPE), Recife, Pernambuco, Brazil, [3]Department of Internal Medicine, School of Medical Sciences, University of Campinas (UNICAMP), Campinas, São Paulo, Brazil

KEYWORDS

**obesity, diabetes, morbidity, cardiovascular risk, insulin resistance**

Editorial on the Research Topic

Pharmacological and non-pharmacological therapy for obesity and diabetes - volume II

Obesity is one of the most threatening diseases due to its medium to long term consequences and complications, such as type 2 diabetes, cardiovascular diseases, nonalcoholic fatty liver disease, several types of cancer and others (1–4). Interrelationships between insulin resistance and chronic subclinical inflammation adversely affect cellular metabolic functions, homeostasis with generalised metabolic derangement. It is also associated with other phenomena such as beta-cell dysfunction, inflammasome activation, oxidative stress and endoplasmic reticulum stress (ER stress), which also supports the insulin resistance development and maintenance.

Together, these health conditions inflict a considerable burden on individuals, society, and on the economy, through greater public health costs, morbidity and mortality. In this Research Topic, Genua et al. have shown that obesity is also frequent in people with type 1 diabetes, and that these patients also have a higher prevalence of other cardiovascular risk factors. In line with this connection between obesity and cardiovascular risk factors, Liu et al. showed here that in a meta-analysis regarding the use of SGLT2 inhibitors, a widely used drug class for the treatment of cardiovascular diseases and type 2 diabetes, also has some effects in decreasing visceral and subcutaneous adipose tissue, as well as body weight and triglycerides in type 2 diabetes patient. Additionally, another method that also modestly reduces body weight, fat tissue and triglyceride is the long-term acupoint stimulation, a modified acupuncture technique, that showed some interesting results in a randomized controlled trial, as shown here by Dai et al. It is also suggested by Yang et al., in an interesting review, that the use of plant secondary metabolites, such as flavonoids, alkaloids, terpenoids, resveratrol, lipoic acid and others show lipolytic activities and could be beneficial for weight control and the reduction of obesity related risks. Several of these compounds act by the activation of Hormone Sensitive Lipase (HSL), which increases the fatty acids disposal, and AMPK, which induces lipid β-oxidation.

Insulin resistance is often accompanied by a compensatory elevation in insulin production and secretion that is supported by both hypertrophy and hyperplasia of

pancreatic beta cells (5, 6). Although, during the T2DM onset such compensatory mechanism is missing because many beta-cells are dysfunctional as a consequence of increased oxidative stress among others (7, 8). Besides, obesity also induces important alterations in islet microenvironment organization such as rising pancreatic stellate cells (9). It is already known that the use of TUDCA (tauroursodeoxycholic acid) positively impacts on beta-cell function in obese models (10), and novel features of this molecule show interesting activity on adipose tissue, through G protein-coupled bile acid receptor 1 (TGR5) and farnesoid X Receptor (FXR) receptors activation (Freitas et al.).

On the other hand, N-acetyl-L-cysteine (NAC) may attenuate oxidative stress and insulin resistance due to its anti-inflammatory and antioxidant effects (11). Indeed, in the current Research Topic Schuurman et al. have demonstrated that NAC treatment is able to reduce both beta-cell oxidative stress and pancreatic stellate cell (PaSC) activation, along with a normalization of beta-cell mass and size in high-fat diet-induced diabetic mice. They also observed that there is an optimal timing and dosage. Thus, this study extended the current knowledge by highlighting that an antioxidant treatment such as NAC may have protective effects on beta-cell health in obesity.

It is well-known that the chronic inflammation present in obesity has an important relation with the hypoxia observed in adipose tissue expansion. In fact, hypoxia may have a pivotal role in the development of adipose tissue dysfunction through HIF-1α activity (12, 13). In this regard, this Research Topic brings a study of Wu et al. that deeply addressed this point since they demonstrated that nicotinamide mononucleotide effectively reduced fibrosis induced by HIF-1α in adipose tissue of mice placed in a hypobaric chamber for 4 weeks. They also saw that nicotinamide mononucleotide restores NAD/SIRT1 axis. These findings shed light on the nicotinamide mononucleotide as a regulator of adipose tissue hypoxia.

We also highlight that obese patients are also susceptible for nutritional deficiency, which is a low-observed and -investigated component in obesity, as indicated by Shadai et al. (Sadhai et al.), in a group of south-Africans scheduled for bariatric surgery. The most common nutritional deficiency observed in obese people who will undergo metabolic surgery was vitamin D (57%), followed by iron and folate deficiency (44% and 18%, respectively). They also suggest including these items on the preoperative screening of the patients and to include them in a longitudinal surveillance after surgery.

Within the scientific community it is evident that lack of physical activity and high calorie intake plays causal roles in the epidemic of obesity and in the development of metabolic disorders. Moreover, understanding the causes that lead to obesity and also its prevention or reversion are of public health priority. This can be managed by either modification of lifestyle (through physical activity to restore energy balance or reduction of calorie intake, proper diet that is rich in fiber, increasing energy outlay) or using adequate medication or alternative techniques. Therefore, to address this crucial subject, different research fields must combine their expertise.

## Author contributions

All authors listed have made a substantial, direct, and intellectual contribution to the work and approved it for publication.

## Conflict of interest

The authors declare that the research was conducted in the absence of any commercial or financial relationships that could be construed as a potential conflict of interest.

## Publisher's note



## References

1. Bapat SP, Whitty C, Mowery CT, Liang Y, Yoo A, Jiang Z, et al. Obesity alters pathology and treatment response in inflammatory disease. *Nature* (2022) 604:337–42. doi: 10.1038/s41586-022-04536-0

2. Ortega FB, Lavie CJ, Blair SN. Obesity and cardiovascular disease. *Circ Res* (2016) 118(11):1752–70.

3. Koliaki C, Liatis S, Kokkinos A. Obesity and cardiovascular disease: revisiting an old relationship. *Metabolism* (2019) 92:98–107.

4. Jin X, Qiu T, Li L, Yu R, Chen X, Li C, et al. Pathophysiology of obesity and its associated diseases. *Acta Pharm Sin B* (2023) 13(6):2403–24.

5. Prentki M, Nolan CJ. Islet β cell failure in type 2 diabetes. *J Clin Invest* (2006) 116:1802–12. doi: 10.1172/JCI29103

6. Butler AE, Janson J, Bonner-Weir S, Ritzel R, Rizza RA, Butler PC. β-cell deficit and increased β-cell apoptosis in humans with type 2 diabetes. *Diabetes* (2003) 52:102–10. doi: 10.2337/diabetes.52.1.102

7. Swisa A, Glaser B, Dor Y. Metabolic stress and compromised identity of pancreatic beta cells. *Front Genet* (2017) 8:21. doi: 10.3389/fgene.2017.00021

8. Sekhar RV, Mckay SV, Patel SG, Guthikonda AP, Reddy VT, Balasubramanyam A, et al. Glutathione synthesis is diminished in patients with uncontrolled diabetes and restored by dietary supplementation with cysteine and glycine. *Diabetes Care* (2011) 34:162–7. doi: 10.2337/DC10-1006

9. Lee E, Ryu GR, Ko SH, Ahn YB, Song KH. A role of pancreatic stellate cells in islet fibrosis and β-cell dysfunction in type 2 diabetes mellitus. *Biochem Biophys Res Commun* (2017) 485:328–34. doi: 10.1016/j.bbrc.2017.02.082

10. Vettorazzi JF, Ribeiro RA, Borck PC, Branco RC, Soriano S, Merino B, et al. The bile acid TUDCA increases glucose-induced insulin secretion via the cAMP/PKA pathway in pancreatic beta cells. *Metabolism* (2016) 65(3):54–63. doi: 10.1016/j.metabol.2015.10.021

11. Roma LP, Oliveira CAM, Carneiro EM, Albuquerque GG, Boschero AC, Souza KLA. N-acetylcysteine protects pancreatic islet against glucocorticoid toxicity. *Redox Rep* (2011) 16:173–80. doi: 10.1179/1351000211Y.0000000006

12. Sun K, Tordjman J, Clement K, Scherer PE. Fibrosis and adipose tissue dysfunction. *Cell Metab* (2013) 18(4):470–7. doi: 10.1016/j.cmet.2013.06.016

13. Semenza GL. Hypoxia-inducible factors in physiology and medicine. *Cell* (2012) 148(3):399–408. doi: 10.1016/j.cell.2012.01.021

frontiers | Frontiers in Endocrinology

ORIGINAL RESEARCH
published: 19 July 2022
doi: 10.3389/fendo.2022.927067

# The Relative Body Weight Gain From Early to Middle Life Adulthood Associated With Later Life Risk of Diabetes: A Nationwide Cohort Study

*Min Xu[1,2†], Yan Qi[1,2†], Gang Chen[3†], Yingfen Qin[4†], Shengli Wu[5†], Tiange Wang[1,2], Zhiyun Zhao[1,2], Yu Xu[1,2], Mian Li[1,2], Li Chen[6], Lulu Chen[7], Yuhong Chen[1,2], Huacong Deng[8], Zhengnan Gao[9], Yanan Huo[10], Qiang Li[11], Chao Liu[12], Zuojie Luo[4], Yiming Mu[13], Guijun Qin[14], Feixia Shen[15], Lixin Shi[16], Qing Su[17], Qin Wan[18], Guixia Wang[19], Shuangyuan Wang[1,2], Youmin Wang[20], Ruying Hu[21], Yiping Xu[22], Li Yan[23], Tao Yang[24], Xuefeng Yu[25], Yinfei Zhang[26], Tianshu Zeng[7], Xulei Tang[27], Zhen Ye[21], Jiajun Zhao[28], Yufang Bi[1,2], Guang Ning[1,2*†], Jieli Lu[1,2*†] and Weiqing Wang[1,2*†] on behalf of the 4C Study Group*

[1] Department of Endocrine and Metabolic Diseases, Shanghai Institute of Endocrine and Metabolic Diseases, Ruijin Hospital, Shanghai Jiao Tong University School of Medicine, Shanghai, China, [2] Shanghai National Clinical Research Center for metabolic Diseases, Key Laboratory for Endocrine and Metabolic Diseases of the National Health Commission of the People's Republic of China, Shanghai Key Laboratory for Endocrine Tumor, State Key Laboratory of Medical Genomics, Ruijin Hospital, Shanghai Jiao Tong University School of Medicine, Shanghai, China, [3] Department of Endocrinology, Fujian Provincial Hospital, Fujian Medical University, Fuzhou, China, [4] Department of Endocrinology, The First Affiliated Hospital of Guangxi Medical University, Nanning, China, [5] Department of Endocrinology, Karamay Municipal People's Hospital, Xinjiang, China, [6] Department of Endocrinology, Qilu Hospital of Shandong University, Jinan, China, [7] Department of Endocrinology, Union Hospital, Tongji Medical College, Huazhong University of Science and Technology, Wuhan, China, [8] Department of Endocrinology, The First Affiliated Hospital of Chongqing Medical University, Chongqing, China, [9] Department of Endocrinology, Dalian Municipal Central Hospital, Dalian, China, [10] Department of Endocrinology, Jiangxi Provincial People's Hospital Affiliated to Nanchang University, Nanchang, China, [11] Department of Endocrinology, The Second Affiliated Hospital of Harbin Medical University, Harbin, China, [12] Department of Endocrinology, Jiangsu Province Hospital on Integration of Chinese and Western Medicine, Nanjing, China, [13] Department of Endocrinology, Chinese People's Liberation Army General Hospital, Beijing, China, [14] Department of Endocrinology, The First Affiliated Hospital of Zhengzhou University, Zhengzhou, China, [15] Department of Endocrinology, The First Affiliated Hospital of Wenzhou Medical University, Wenzhou, China, [16] Department of Endocrinology, Affiliated Hospital of Guiyang Medical College, Guiyang, China, [17] Department of Endocrinology, Xinhua Hospital Affiliated to Shanghai Jiao Tong University, School of Medicine, Shanghai, China, [18] Department of Endocrinology, The Affiliated Hospital of Southwest Medical University, Luzhou, China, [19] Department of Endocrinology, The First Hospital of Jilin University, Changchun, China, [20] Department of Endocrinology, The First Affiliated Hospital of Anhui Medical University, Hefei, China, [21] Institute of Chronic Diseases, Zhejiang Provincial Center for Disease Control and Prevention, Hangzhou, China, [22] Clinical Trials Center, Ruijin Hospital Affiliated to Shanghai Jiao Tong University School of Medicine, Shanghai, China, [23] Department of Endocrinology, Sun Yat-sen Memorial Hospital, Sun Yat-sen University, Guangzhou, China, [24] Department of Endocrinology, The First Affiliated Hospital of Nanjing Medical University, Nanjing, China, [25] Department of Endocrinology, Tongji Hospital, Tongji Medical College, Huazhong University of Science and Technology, Wuhan, China, [26] Department of Endocrinology, Central Hospital of Shanghai Jiading District, Shanghai, China, [27] Department of Endocrinology, The First Hospital of Lanzhou University, Lanzhou, China, [28] Department of Endocrinology, Shandong Provincial Hospital, Jinan, China

**Aim:** To determine the effect of decade-based body weight gain from 20 to 50 years of age on later life diabetes risk.

**Methods:** 35,611 non-diabetic participants aged ≥ 50 years from a well-defined nationwide cohort were followed up for average of 3.6 years, with cardiovascular diseases and cancers at baseline were excluded. Body weight at 20, 30, 40, and 50 years was reported. The overall 30 years and each 10-year weight gain were calculated

OPEN ACCESS

**Edited by:**
Alexandre Gabarra Oliveira,
São Paulo State University, Brazil

**Reviewed by:**
Heng Wan,
Southern Medical University, China
Jatinderkumar R. Saini,
Symbiosis Institute of Computer Studies and Research (SICSR), India

***Correspondence:**
Weiqing Wang
wqingw61@163.com
Jieli Lu
jielilu@hotmail.com
Guang Ning
gning@sibs.ac.cn

[†]These authors have contributed equally to this work

**Specialty section:**
This article was submitted to Obesity, a section of the journal Frontiers in Endocrinology

**Received:** 23 April 2022
**Accepted:** 15 June 2022
**Published:** 19 July 2022

**Citation:**
Xu M, Qi Y, Chen G, Qin Y, Wu S, Wang T, Zhao Z, Xu Y, Li M, Chen L, Chen L, Chen Y, Deng H, Gao Z, Huo Y, Li Q, Liu C, Luo Z, Mu Y, Qin G, Shen F, Shi L, Su Q, Wan Q, Wang G, Wang S, Wang Y, Hu R, Xu Y, Yan L, Yang T, Yu X, Zhang Y, Zeng T, Tang X, Ye Z, Zhao J, Bi Y, Ning G, Lu J and Wang W (2022) The Relative Body Weight Gain From Early to Middle Life Adulthood Associated With Later Life Risk of Diabetes: A Nationwide Cohort Study. Front. Endocrinol. 13:927067. doi: 10.3389/fendo.2022.927067

from the early and middle life. Cox regression models were used to estimate risks of incident diabetes.

**Results:** After 127,745.26 person-years of follow-up, 2,789 incident diabetes were identified (incidence rate, 2.18%) in 25,289 women (mean weight gain 20-50 years, 7.60 kg) and 10,322 men (7.93 kg). Each 10-kg weight gain over the 30 years was significantly associated with a 39.7% increased risk of incident diabetes (95% confidence interval [CI], 1.33-1.47); weight gain from 20-30 years showed a more prominent effect on the risk of developing diabetes before 60 years than that of after 60 years (Hazard ratio, HR = 1.084, 95% CI [1.049-1.121], $P$ <0.0001 vs. 1.015 [0.975-1.056], $P$ = 0.4643; $P_{Interaction}$=0.0293). It showed a stable effect of the three 10-year intervals weight gain on risk of diabetes after 60 years (HR=1.055, 1.038, 1.043, respectively, all $P$ < 0.0036).

**Conclusions:** The early life weight gain showed a more prominent effect on developing diabetes before 60 years than after 60 years; however, each-decade weight gain from 20 to 50 years showed a similar effect on risk developing diabetes after 60 years.

**Keywords: Body weight gain, early life adulthood, prospective cohort, type 2 diabetes, later life risk, obesity**

## INTRODUCTION

Compelling evidence has demonstrated that overweight and obesity are major established and modifiable risk factors for cardiovascular risk, such as type 2 diabetes (T2D) (1–3). Majority of the studies focused on body weight close to the time of the disease diagnosis, usually the middle-aged and elderly life. Accumulating evidence supported that early adulthood weight could affect subsequent T2D risks regardless of weight close to the time of diagnosis, which suggested a longer history of relative overweight, starting earlier in life, poses an additional risk for developing diabetes (4–7). Besides initial body weight, weight change during early adulthood has also been demonstrated to have an independent effect on subsequent diabetes and other cardio-metabolic risk (7–12).

In China, the largest increase in the prevalence of obesity was seen in men between the ages of 20 and 40 and in women between 30 and 40 (13), which was similar with many other countries. The rising trend of obesity in China, especially in young people, will undoubtedly increase the prevalence of chronic diseases, leading to poor cardiovascular health (13, 14). Given that a large segment of the population is starting to gain weight early in adulthood, after settling into an occupation or family life, which is contributing to the obesity epidemic, it is important to determine whether elevated body weight in earl-life adulthood, or during the transition from early to middle-life adulthood, contributes independently to the disease risk. However, less is known whether body weight gain during different periods in early to middle adult life, usually 20 to 50 years old, are differently related to risk of T2D and how much such weight changes influence the diagnosis age of diabetes.

In this follow-up investigation, we used data from a large sample size well-defined community-based nation-wide cohort in China to determine the effect of decade- based body weight gain from 20 to 50 years old on developing diabetes risk of the later life.

## MATERIALS AND METHODS

### Study Population

The study participants were from the China Cardiometabolic Disease and Cancer Cohort (4C) Study, which was an ongoing multicenter, population-based cohort study investigating associations of glucose homeostasis with clinical outcomes, including diabetes, cardiovascular diseases (CVDs), cancers, and all-cause mortality (15, 16). Briefly, a total of 20 communities from seven general geographic regions in China were selected during 2011-2012 (**Supplementary Table S1**). Eligible men and women aged ≥40 years were identified from local resident registration systems and invited to the study by home visiting by the trained community health workers. At baseline, a standard questionnaire was used to collect the lifestyle factors, disease and medical history, etc. Anthropometry measurements, 2-hour oral glucose tolerance tests (OGTTs), blood and urine sampling were conducted. During 2014-2015, we performed the first round of follow-up examination.

A total of 193,846 individuals were recruited for the baseline and 170,240 participants attended the follow-up examination. In the present analysis, we excluded subjects who died during the follow-up (n=2,993); the baseline diagnosed diabetic patients (n=39,821) or un-determined glucose metabolism status (n=4,602); CVDs or cancers (n=1,836); or those who did not attend the on-site follow-up visit, but have major diseases status information by short questionnaire (n=16,084). For the specific aim of studying the effect of body weight during 20 to 50 years of age on the later life diabetes risk, we further excluded those

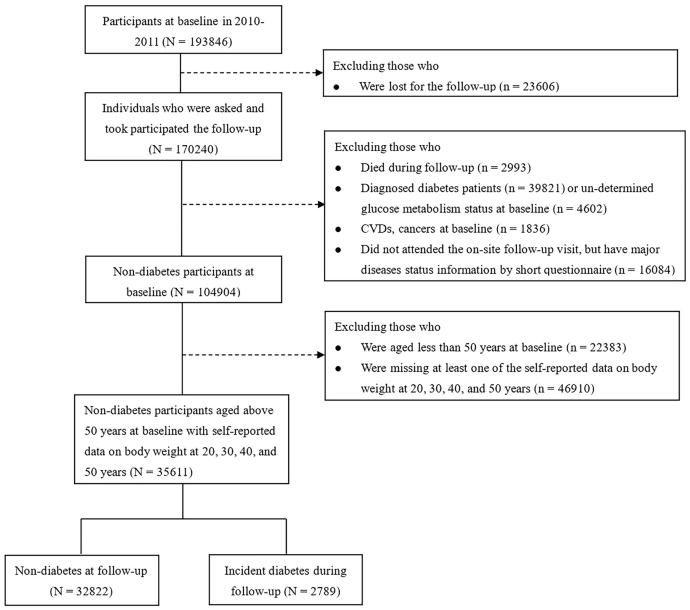


**FIGURE 1** | Flow chart of the present study.

people who were aged less than 50 years at baseline (n=22,383); or missing at least one of the self-reported data on body weight at 20, 30, 40 and 50 years (n=46,910). Thus, a total of 35,611 non-diabetic participants (25,289 women, 10,322 men) aged 50 years and above were finally included in the main analyses. The flow chart of participants selecting was described in **Figure 1**.

The study was approved by the Medical Ethics Committee of Ruijin Hospital, Shanghai Jiao-Tong University. Each participant provided written informed consent.

## Incident Diabetes Ascertainments

Incident T2D cases was defined according to the 2010 American Diabetes Association (ADA) criteria (fasting plasma glucose level ≥7.0 mmol/l or 2h OGTT glucose ≥11.1 mmol/l, or HbA1c ≥6.5%, or receiving glucose-lowering drugs or insulin injection) and/or a self-reported diagnosis by healthcare professionals.

## Exposure Assessment

Participants were asked to recall their body weight (kg) at their twenty, thirty, forty and fifty years old and record on the questionnaire. Weight gain over the 30 years (from 20 to 50 year of age) and decade-based weight gain were calculated by subtracting the self-reported body weight at the former time point from the one at the later time point. We assumed that body height is relatively stable during adulthood, and weight gain can represent one's changes in adiposity during the early to middle life.

## Covariates Assessment

In the baseline questionnaires, we inquired information on risk factors for chronic diseases, such as cigarette smoking (current, former, or never smoker), and alcoholic intake, physical activity and sedentary time, education level (high school and above, or below high school) and family history of diabetes. Smoking status was defined as current, former, and never smokers. Current smokers were defined as smoking cigarettes every day or almost every day, with at least 7 cigarettes per week for at least 6 months. Former smokers were defined as cessation of smoking for more than 6 months. To assess the intensity of the smoking, the current/former smokers were used as two dummy variables, which was defined as the number of cigarettes each day, that were 0 cigarettes/day, 1–9 cigarettes/day, 10-19 cigarettes/day and ≥20 cigarettes/day. Never smokers were defined as participants who reported never smoked or had not smoked cigarettes regularly (<100 cigarettes in a lifetime). Alcohol intake was defined as drinker or non-drinker. Information regarding alcohol intake was collected by inquiring the information on the amount and type of alcoholic beverages consumed in the past 6 months, including beer, wine (e.g. red wine, or yellow wine, a typical wine made from rice and widely consumed in south China), and hard liquor. Beers are sold in 750-mL bottles, and wine and hard liquor in units of 0.5 kg. One unit of beer, wine, and liquor on average contains 30, 90, and 200 g ethanol, respectively. Average alcohol consumption was calculated by multiplying amount of alcohol consumed per drinking day by frequency (g/day). We used the Global Physical Activity Questionnaire to collect intensity, duration, and frequency of physical activity, the Metabolic Equivalent of Task (MET) minutes per week was used to measure physical activity level (17). Baseline body weight and height were measured according to a standard protocol by trained study staff. Baseline body weight and height were measured while they wore minimal clothing and no shoes, with values rounded to the nearest

0.1 kg and 0.1 cm, respectively. Body mass index (BMI) was calculated as body weight in kilograms divided by the square of body height in meters.

## Biochemical Measurements

Fasting and 2h post-loading blood sampling was performed during the OGTT. Participants were required to fast for ≥10 hours prior to filed examination. Plasma glucose concentrations were analyzed locally using a glucose oxidase or hexokinase method within two hours after blood sample collection under a stringent quality control program. Hemoglobin Capillary Collection System (Bio-Rad Laboratories, CA, USA) was used to collect finger capillary whole blood and shipped at 2-8°C to a certificated central laboratory at Ruijin Hospital. HbA1c was determined by high-performance liquid chromatography (VARIANT II System, Bio-Rad Laboratories, CA, USA). Fasting serum insulin was measured at the central laboratory using an auto-analyzer (ARCHITECT ci16200 analyzer, Abbott Laboratories, Illinois, USA). Homeostasis model assessment of insulin resistance (HOMA_IR) was calculated as fasting insulin × fasting plasma glucose/22.5, and beta cell function index (HOMA_β) was 20 × fasting insulin / (fasting plasma glucose − 3.5), where fasting insulin was in mIU/L and fasting plasma glucose in mmol/L.

## Statistical Analysis

Comparison of the baseline characteristics of the non-diabetic participants according to diabetes status at follow up examination by sex were conducted by ANOVA for continuous variables, and $\chi 2$ tests for categorical variables. The skewed distribution data were logarithmically transformed before statistical analysis.

We used Cox proportional hazards models to calculate multivariable-adjusted hazard ratios (HR) and 95% confidence intervals (CI) for the risk of T2D. For incident T2D, person-years were calculated from self-reported date of T2D diagnosis or the respective follow-up examination date for each individual or death or to end of follow-up (June 1, 2015), whichever came first. The following covariates were included in multivariable-adjusted models: age (continuous), sex, BMI at 20 years (continuous), baseline BMI (continuous), physical activity and sedentary time (in quintiles), smoking status (never, past, current), alcohol intake (g/day), high school and above (yes or no) and family history of diabetes (yes or no). The missing data were coded as a missing indicator category for categorical variables. We also tested the potential collinearity of BMI at 20 years age and BMI at baseline, and it showed that there was no collinearity of BMI at 20 years age and at baseline (the variance inflation factor, VIF was 1).

We tested interactions of age and other predictors of T2D by putting body weight gain in each 10 year from 20-50 years or the overall weight gain over the 30 years, each strata variable and the interaction terms (weight gain x the strata variable) in the same multivariate model. We also conducted stratified analysis according to baseline age (< or ≥60 years), sex, BMI at 20 years (< or ≥the median value, 21 kg/m$^2$), baseline BMI (< or ≥25 kg/m$^2$), physical activity (in quintiles), current smoking (yes or no).

All the analyses were carried out with SAS software, version 9.3 (SAS Institute), at a two-tailed alpha level of 0.05.

# RESULTS

We determined 2,789 incident diabetes after a follow up of 127,745.26 person-years from the 35,611 non-diabetic participants aged ≥ 50 years. The incidence rate of T2D was 2.18%, 95% CI (2.10% - 2.17%), with 2.43% in men and 2.08% in women.

From early to middle adulthood, the mean weight gain from 20 to 50 years [SD] was: 7.60 [7.95] kg in women and 7.93 [8.54] kg in men; each 10-year weight gain from 20-30, 30-40, and 40-50 years were: 2.78 [4.88], 2.39 [4.26], and 2.42 [4.40] kg in women; and 2.67 [4.12], 2.76 [4.66], and 2.50 [4.92] kg in men, respectively.

Baseline characteristics of participants were summarized in **Table 1**. Consistently among total participants, men and women, those who developed diabetes had a higher body weight at 20 years, more weight gain from 20 to 50 years, as well as each-decade based weight gain (**Table 1**). Body weight at 20 years and each-decade weight gain from 20 to 50 years were independently and significantly associated with an increased risk of incident diabetes (**Supplementary Table S2**).

Among total cohort, each 10-kg weight gain over the 30 years period (20-50 years) was significantly associated with 39.7% increased risk of incident diabetes (95% CI, 1.33-1.47) (HR 1.37, 95% CI [1.26-1.49] in men; and 1.40 [1.32-1.49] in women) after adjustments for a full list of confounders. The corresponding HRs and 95%CI for each 1-kg/m$^2$ weight gain from 20-50 years were 1.036, 95% CI 1.001-1.071, P = 0.0427 in men and 1.047, 95% CI 1.025-1.069, P <.0001 in women (**Table 2**). However, the associations were not significantly different between men and women (P for interaction = 0.286). The HR and 95% CI of T2D in weight gain (each 1-kg/m$^2$ BMI) from 20-30 years was 1.055 (1.029-1.081), 1.038 (1.012-1.064) for weight gain form 30-40 years and 1.043 (1.017-1.069) for 40-50 years, respectively. In both sexes, the weight gain from 20-30 years showed a nominally higher risk of developing diabetes than the other two-decades interval; however, no significant interaction between sex and the different life stage weight gain was detected (all P for interaction > 0.344 in men, and 0.329 in women) (**Table 2**).

We further performed stratified analysis according to age, BMI at 20 years and lifestyle factors at baseline. In the participants younger than 60 years, weight gain from 20-30 years showed more prominent effect on risk of developing diabetes than that in those older than 60 years (HR 1.084, 95% CI [1.049-1.121] vs. 1.015, 95% CI [0.975-1.056], $P_{interaction}$=0.0293) (**Table 3**, **Figure 2A**). Same trend was found with regard to total weight gain over the 30 years (**Table 3**, **Figure 2B**). It showed a stable effect of the three 10-year intervals weight gain from 20 to 50 years on risk of developing diabetes after 60 years; however, the results did not remain significant after adjusted for the baseline BMI.

**TABLE 1 |** Baseline characteristics of the non-diabetic participants according to sex and diabetes status at follow up examination.

| | Total cohort | | | Men | | | Women | | |
|---|---|---|---|---|---|---|---|---|---|
| | Non-diabetes | Diabetes | *P* | Non-diabetes | Diabetes | *P* | Non-diabetes | Diabetes | *P* |
| *n*. of participants | 32,822 | 2,789 | | 9,422 | 900 | | 23,400 | 1,889 | |
| Age at baseline, years | 58.8 (6.7) | 59.7 (6.7) | <.0001 | 60.0 (7.0) | 60.2 (6.9) | 0.4584 | 58.3 (6.5) | 59.4 (6.6) | <.0001 |
| BMI at baseline, kg/m$^2$ | 24.5 (3.5) | 25.6 (3.4) | <.0001 | 24.6 (3.4) | 25.6 (3.2) | <.0001 | 24.5 (3.5) | 25.6 (3.5) | <.0001 |
| BMI at age of 20 y, kg/m$^2$ | 21.2 (2.9) | 21.3 (2.8) | 0.0327 | 21.4 (2.6) | 21.4 (2.5) | 0.7896 | 21.2 (3.0) | 21.3 (2.9) | 0.0292 |
| BMI at age of 30 y, kg/m$^2$ | 22.3 (2.9) | 22.7 (2.9) | <.0001 | 22.3 (2.6) | 22.6 (2.5) | 0.0003 | 22.3 (3.0) | 22.7 (3.0) | <.0001 |
| BMI at age of 40 y, kg/m$^2$ | 23.2 (3.0) | 23.9 (3.1) | <.0001 | 23.3 (2.9) | 23.9 (2.9) | <.0001 | 23.2 (3.1) | 23.9 (3.2) | <.0001 |
| BMI at age of 50 y, kg/m$^2$ | 24.2 (3.3) | 25.1 (3,3) | <.0001 | 24.1 (3.2) | 25.0 (3.1) | <.0001 | 24.2 (3.3) | 25.1 (3.4) | <.0001 |
| Height at baseline, cm | 159.3 (7.6) | 159.4 (7.7) | 0.4918 | 166.5 (6.5) | 166.3 (6.2) | 0.4196 | 156.4 (5.8) | 156.1 (5.9) | 0.0371 |
| Weight at age of 20 y, kg | 53.8 (7.9) | 54.2 (8.0) | 0.0136 | 59.2 (7.3) | 59.2 (7.6) | 0.9391 | 51.7 (7.1) | 51.8 (7.1) | 0.2566 |
| Each decade weight gain, kg | | | | | | | | | |
| 20-30 y | 2.49 (4.67) | 3.44 (4.63) | <.0001 | 2.59 (4.09) | 3.45 (4.32) | <.0001 | 2.73 (4.89) | 3.43 (4.77) | <.0001 |
| 30-40 y | 2.45 (4.36) | 3.09 (4.69) | <.0001 | 2.70 (4.63) | 3.43 (4.93) | <.0001 | 2.35 (4.24) | 2.93 (4.56) | <.0001 |
| 40-50 y | 2.39 (4.54) | 3.04 (4.79) | <.0001 | 2.44 (4.90) | 3.12 (5.12) | <.0001 | 2.38 (4.38) | 3.00 (4.62) | <.0001 |
| Glucose traits at baseline | | | | | | | | | |
| Fasting glucose, mmol/L | 5.46 (0.51) | 5.77 (0.57) | <.0001 | 5.50 (0.52) | 5.78 (0.59) | <.0001 | 5.44 (0.51) | 5.76 (0.55) | <.0001 |
| OGTT 2h post-loading glucose, mmol/L | 6.84 (1.62) | 7.93 (1.79) | <.0001 | 6.65 (1.73) | 7.78 (1.89) | <.0001 | 6.91 (1.56) | 8.00 (1.73) | <.0001 |
| HbA1c level, % | 5.75 (0.36) | 5.90 (0.36) | <.0001 | 5.70 (0.36) | 5.87 (0.38) | <.0001 | 5.77 (0.35) | 5.91 (0.36) | <.0001 |
| HOMA_β, % | 69.0 (49.5-95.9) | 68.9 (46.5-96.6) | 0.8177 | 58.4 (40.3-84.2) | 59.6 (39.6-86.4) | 0.6236 | 72.9 (53.7-100) | 72.6 (51.0-101.7) | 0.7730 |
| HOMA_IR | 1.60 (1.13-2.24) | 2.02 (1.39-2.80) | <.0001 | 1.39 (0.94-2.02) | 1.79 (1.20-2.50) | <.0001 | 1.68 (1.22-2.32) | 2.11 (1.52-2.89) | <.0001 |
| Physical activity, MET-h/wk | | | | | | | | | |
| Quintile 1 | 0 | 0 | 0.3773 | 0 | 0 | 0.0397 | 0 | 0 | 0.3452 |
| Quintile 2 | 9.46 (2.93) | 9.70 (2.81) | | 9.59 (2.87) | 9.73 (2.63) | | 9.41 (2.95) | 9.68 (2.90) | |
| Quintile 3 | 22.0 (2.65) | 21.9 (2.71) | | 21.9 (2.69) | 22.0 (2.62) | | 22.0 (2.64) | 21.9 (2.74) | |
| Quintile 4 | 40.9 (7.11) | 41.0 (7.06) | | 41.0 (7.14) | 41.1 (7.23) | | 40.8 (7.10) | 41.0 (6.99) | |
| Quintile 5 | 94.1 (51.9) | 96.7 (61.4) | | 99.2 (55.9) | 98.6 (54.8) | | 92.0 (55.0) | 95.5 (65.0) | |
| Sedentary time, hours/day | | | | | | | | | |
| Quintile 1 | 1.45 (0.69) | 1.50 (0.66) | 0.0787 | 1.45 (0.69) | 1.52 (0.63) | 0.2043 | 1.46 (0.69) | 1.49 (0.67) | 0.1344 |
| Quintile 2 | 2.87 (0.25) | 2.91 (0.22) | | 2.86 (0.25) | 2.92 (0.21) | | 2.87 (0.24) | 2.90 (0.22) | |
| Quintile 3 | 3.87 (0.24) | 3.89 (0.23) | | 3.87 (0.24) | 3.89 (0.22) | | 3.88 (0.24) | 3.89 (0.23) | |
| Quintile 4 | 4.97 (0.34) | 4.93 (0.32) | | 5.00 (0.34) | 4.96 (0.35) | | 4.96 (0.34) | 4.92 (0.30) | |
| Quintile 5 | 7.35 (1.59) | 7.37 (1.62) | | 7.45 (1.68) | 7.66 (1.91) | | 7.30 (1.55) | 7.22 (1.42) | |
| Alcohol consumption, grams/day | | | | | | | | | |
| 0 | 29,334 (89.4) | 2,458 (88.1) | 0.0385 | 6,349 (67.4) | 594 (66.0) | 0.2743 | 22,985 (98.2) | 1,864 (98.7) | 0.4749 |
| 0-20 | 809 (2.46) | 70 (2.51) | | 579 (6.15) | 58 (6.44) | | 230 (0.98) | 12 (0.64) | |
| 20-40 | 720 (2.19) | 57 (2.04) | | 639 (6.78) | 51 (5.67) | | 81 (0.35) | 6 (0.32) | |
| ≥ 40 | 1,959 (5.57) | 204 (7.31) | | 1,855 (19.7) | 197 (21.9) | | 104 (0.44) | 7 (0.37) | |
| Smoking status | | | | | | | | | |
| Never smoker | 26,760 (82.7) | 2,222 (80.2) | 0.002 | 4,009 (43.1) | 395 (44.2) | | 22,751 (98.6) | 1,827 (97.6) | 0.0003 |
| Past smoker | | | | | | | | | |
| 0 | 31,341 (95.5) | 2,649 (94.9) | 0.6265 | 8,027 (85.2) | 771 (85.7) | 0.7791 | 23,314 (99.6) | 1,878 (99.4) | 0.0330 |
| 0-10 cigarettes/day | 374 (1.14) | 35 (1.25) | | 315 (3.34) | 27 (3.00) | | 59 (0.25) | 8 (0.42) | |
| 10-20 cigarettes/day | 318 (0.97) | 28 (1.00) | | 309 (3.28) | 25 (2.78) | | 9 (0.04) | 3 (0.16) | |
| ≥ 20 cigarettes/day | 77 (2.76) | 77 (2.76) | | 771 (8.18) | 77 (8.56) | | 18 (0.08) | 0 | |
| Current smoker | | | | | | | | | |
| 0 | 28,691 (87.4) | 2,385 (85.5) | 0.0384 | 5,518 (58.6) | 530 (58.9) | 0.9314 | 23,173 (99.0) | 1,855 (98.2) | 0.0036 |
| 0-10 cigarettes/day | 678 (2.07) | 68 (2.44) | | 584 (6.20) | 51 (5.67) | | 94 (0.40) | 17 (0.90) | |
| 10-20 pack-years | 1,195 (3.64) | 116 (4.16) | | 1,132 (12.0) | 107 (11.9) | | 63 (0.27) | 9 (0.48) | |
| ≥ 20 cigarettes/day | 2,258 (6.88) | 220 (7.89) | | 2,188 (23.2) | 212 (23.6) | | 70 (0.30) | 8 (0.42) | |
| Education level | | | | | | | | | |
| High school and above | 19,833 (60.4) | 1,691 (60.6) | 0.8316 | 5,545 (58.9) | 498 (55.3) | 0.0407 | 14,288 (61.1) | 1,193 (63.2) | 0.0722 |
| Junior high school and below | 12,989 (39.6) | 1,098 (39.4) | | 3,877 (41.2) | 402 (44.7) | | 9,112 (38.9) | 696 (36.8) | |
| Family history of diabetes | 4,032 (12.3) | 434 (15.6) | <.0001 | 883 (9.37) | 131 (14.6) | <.0001 | 3,149 (13.5) | 303 (16.0) | 0.0017 |

*Data are presented as means ± standard deviation (SD), or medians (inter-quartile ranges) for skewed variables, or number (proportions) for categorical variables. P values were from the ANOVA without any adjustments. Abbreviations: IQR, inter quartile range; MET, metabolic equivalent task.*

It also showed that weight gain in each-decade was significantly associated with risk of later life diabetes in participants with higher BMI at their 20 years (≥21 kg/m$^2$); while no significant association was found in those with lower level (< 21 kg/m$^2$) (**Table 3**). No significant interactions were found between body weight at 20 years, baseline BMI or the smoking status at baseline with the weight gains of each 10-year intervals on the risk of incident diabetes (all $P_{\text{interaction}} \geq 0.05$).

**TABLE 2 |** Hazard risk of weight gain in different life stage with risk of incident diabetes in total and sex-specific samples.

| | | Model 1 HR, 95% CI | *P* | Model 2 HR, 95% CI | *P* |
|---|---|---|---|---|---|
| Total cohort | | | | | |
| Cases/Participants | 2,789/35,611 | | | | |
| Person-years | 127,745.26 | | | | |
| Incidence rate, 95% CI | 2.18% (2.10%-2.17%) | | | | |
| Weight gain, each 1-kg/m$^2$ | | | | | |
| from 20-30 years age | | 1.060 (1.035-1.085) | <.0001 | 1.055 (1.029-1.081) | <.0001 |
| from 30-40 years age | | 1.042 (1.018-1.067) | <.0001 | 1.038 (1.012-1.064) | 0.0036 |
| from 40-50 years age | | 1.049 (1.024-1.074) | <.0001 | 1.043 (1.017-1.069) | 0.0009 |
| Weight gain, from 20-50 years age, each 1-kg/m$^2$ | | 1.050 (1.032-1.068) | <.0001 | 1.045 (1.027-1.064) | <.0001 |
| Men | | | | | |
| Cases/Participants | 900/10,322 | | | | |
| Person-years | 37,108.18 | | | | |
| Incidence rate, 95% CI | 2.43% (2.27%-2.59%) | | | | |
| Weight gain, each 1-kg/m$^2$ | | | | | |
| from 20-30 years age | | 1.083 (1.032-1.137) | 0.0011 | 1.071 (1.018-1.127) | 0.0259 |
| from 30-40 years age | | 1.026 (0.984-1.070) | 0.2266 | 1.020 (0.975-1.067) | 0.3911 |
| from 40-50 years age | | 1.035 (0.992-1.080) | 0.1137 | 1.027 (0.982-1.074) | 0.2425 |
| Weight gain, from 20-50 years age, each 1- kg/m$^2$ | | 1.044 (1.011-1.077) | 0.0079 | 1.036 (1.001-1.071) | 0.0427 |
| Women | | | | | |
| Cases/Participants | 1,889/25,289 | | | | |
| Person-years | 90,637.08 | | | | |
| Incidence rate, 95% CI | 2.08% (1.99%-2.18%) | | | | |
| Weight gain, each 1-kg/m$^2$ | | | | | |
| from 20-30 years age | | 1.054 (1.026-1.083) | 0.0001 | 1.051 (1.022-1.081) | 0.0006 |
| from 30-40 years age | | 1.048 (1.018-1.078) | 0.0015 | 1.042 (1.010-1.074) | 0.0085 |
| from 40-50 years age | | 1.053 (1.024-1.083) | 0.0003 | 1.048 (1.017-1.079) | 0.0022 |
| Weight gain, from 20-50 years age, each 1-kg/m$^2$ | | 1.052 (1.031-1.073) | <.0001 | 1.047 (1.025-1.069) | <.0001 |

*Data are hazard ratio, 95% confidence interval (CI). P values were calculated from the Cox regression models. Model 1, adjusted for age, sex, BMI at 20 years age and BMI at baseline. Model 2, further adjusted for quintiles of physical activity, quintiles of sedentary time, smoking status (current, former, and never), alcohol drinking (g/day), and education level (high school and above or low), and diabetes family history (yes or no).*

Characteristics of the participants by their BMI at 20 years and baseline BMI categories was shown in **Supplementary Table S3**.

On considering a high proportion of the participants failed to report their body weight at least one time per year (44.7%, 46,910/104,904), we validated the robustness of the present analysis by conducting the multiple imputation analysis. We imputed missing data not only in BMI at 20, 30, 40 and 50 years of age, and but also the above mentioned covariates (n=82,521), using the Markov Chain Monte Carlo (MCMC) method, to estimate the risk ratio of weight gain on diabetes (SAS software, version 9.2, SAS Institute, Cary, North Carolina) (18). **Figure 3** shows the main and stratified analysis results using the procedure of MIANALYZE, which were consistent with that calculating from the previous procedure in which the missing data for weight at each time point were excluded.

## DISCUSSION

In the present large population-based nation-wide follow up study, we found that weight gain from early to middle life was significantly associated with increased later life diabetes risk. Weight gain in early life of the adulthood, usually 20 to 30 years showed more prominent effect on developing diabetes before 60 years than that for developing diabetes after 60 years; however, each-decade weight gain over the adulthood from 20 to 50 years showed similar effect on the risk of developing diabetes after 60 years. The main findings were summarized graphically in **Figure 4**.

The prevalence of obesity gradually increases from 20 to 60 years of old. A large percentage of T2D develops after 40 to 70 years (13, 19–21). Previous studies have demonstrated that besides initial body weight, weight change during early adulthood poses an independent role on subsequent diabetes risk (7, 12), including recent two large, long-term cohorts, which showed that weight change from early to middle adulthood (age of 18 or 21 to 55 years) was associated with increased risk of morbidity and mortality, independent of weight at early adulthood (11). In addition, we have summarized the scientific literature of similar research works as **Supplementary Table 4**. In the present study, we confirmed that body weight gain over 30 years in the early and middle adulthood were significantly associated with later life diabetes risk, independent of the baseline and the early life (in 20s) BMI.

Previous study showed an inverse linear relation was found between BMI and age at diabetes onset (22). Adults with early diagnosed diabetes were more obese and more likely to be female than those with a later onset of T2D. Weight gain in early rather than middle-to-late adulthood played an important role in developing diabetes (23). The relative risk of T2D for a 5-kg m$^{-2}$ increment in BMI was 3.07 for early weight gain (in 18–24s), and 2.12 for late weight-gain (in their 50s) (23). Our results were consistent with the previous studies that investigated the associations of weight change at different period with the risk

**TABLE 3 |** Stratified analysis of the hazard risk of weight gain in different life with risk of incident diabetes.

| | | Model 1 HR, 95% CI | *P* | Model 2 HR, 95% CI | *P* |
|---|---|---|---|---|---|
| Age < 60 years | | | | | |
| Cases/Participants | 1,613/22,585 | | | | |
| Person-years | 80,388.40 | | | | |
| Incidence rate, 95% CI | 2.01% (1.91%-2.11%) | | | | |
| Weight gain, each 1-kg/m$^2$ | | | | | |
| from 20-30 years | | 1.083 (1.049-1.118) | <.0001 | 1.084 (1.049-1.121) | <.0001 |
| from 30-40 years | | 1.053 (1.021-1.087) | 0.0012 | 1.047 (1.013-1.083) | 0.0067 |
| from 40-50 years | | 1.055 (1.022-1.088) | 0.0009 | 1.051 (1.017-1.087) | 0.0032 |
| Age ≥ 60 years | | | | | |
| Cases/Participants | 1,176/13,026 | | | | |
| Person-years | 47,356.86 | | | | |
| Incidence rate, 95% CI | 2.48% (2.34%-2.63%) | | | | |
| Weight gain, each 1-kg/m$^2$ | | | | | |
| from 20-30 years | | 1.023 (0.985-1.063) | 0.2331 | 1.015 (0.975-1.056) | 0.4643 |
| from 30-40 years | | 1.017 (0.978-1.057) | 0.4104 | 1.014 (0.973-1.057) | 0.5094 |
| from 40-50 years | | 1.041 (1.001-1.082) | 0.0451 | 1.032 (0.991-1.075) | 0.1286 |
| BMI at baseline < 25kg/m$^2$ | | | | | |
| Cases/Participants | 1215/20,346 | | | | |
| Person-years | 72,978.38 | | | | |
| Incidence rate, 95% CI | 1.67% (1.57%-1.76%) | | | | |
| Weight gain, each 1-kg/m$^2$ | | | | | |
| from 20-30 years | | 1.071 (1.034-1.109) | 0.0001 | 1.075 (1.036-1.116) | 0.0001 |
| from 30-40 years | | 1.063 (1.027-1.100) | 0.0005 | 1.058 (1.020-1.097) | 0.0027 |
| from 40-50 years | | 1.065 (1.029-1.103) | 0.0004 | 1.066 (1.028-1.106) | 0.0006 |
| BMI at baseline ≥ 25kg/m$^2$ | | | | | |
| Cases/Participants | 1,556/15,004 | | | | |
| Person-years | 53,807.52 | | | | |
| Incidence rate, 95% CI | 2.89% (2.75%-3.04%) | | | | |
| Weight gain, each 1-kg/m$^2$ | | | | | |
| from 20-30 years | | 1.065 (1.031-1.101) | 0.0002 | 1.055 (1.020-1.092) | 0.0022 |
| from 30-40 years | | 1.040 (1.004-1.076) | 0.0267 | 1.034 (0.998-1.072) | 0.0677 |
| from 40-50 years | | 1.045 (1.010-1.080) | 0.0100 | 1.033 (0.997-1.069) | 0.0700 |
| Low BMI at 20 years | | | | | |
| Cases/Participants | 1,313/17,330 | | | | |
| Person-years | 63,539.47 | | | | |
| Incidence rate, 95% CI | 2.07% (196%-2.18%) | | | | |
| Weight gain, each 1-kg/m$^2$ | | | | | |
| from 20-30 years | | 1.031 (0.988-1.077) | 0.1638 | 1.025 (0.979-1.073) | 0.2846 |
| from 30-40 years | | 1.005 (0.959-1.052) | 0.8417 | 0.999 (0.950-1.050) | 0.9642 |
| from 40-50 years | | 1.004 (0.959-1.052) | 0.8645 | 1.009 (0.961-1.060) | 0.7144 |
| High BMI at 20 years | | | | | |
| Cases/Participants | 1,403/17,175 | | | | |
| Person-years | 61,131.70 | | | | |
| Incidence rate, 95% CI | 2.30% (2.18%-2.42%) | | | | |
| Weight gain, each 1-kg/m$^2$ | | | | | |
| from 20-30 years | | 1.044 (1.011-1.078) | 0.0077 | 1.042 (1.008-1.078) | 0.0148 |
| from 30-40 years | | 1.040 (1.008-1.074) | 0.0142 | 1.035 (1.001-1.070) | 0.0433 |

*(Continued)*

**TABLE 3** | Continued

| | Model 1 HR, 95% CI | *P* | Model 2 HR, 95% CI | *P* |
|---|---|---|---|---|
| from 40-50 years | 1.042 (1.010-1.075) | 0.0092 | 1.032 (0.998-1.066) | 0.0631 |
| Never smoker | | | | |
| Cases/Participants | 2,222/28,982 | | | |
| Person-years | 103,916.14 | | | |
| Incidence rate, 95% CI | 2.14% (2.05%-2.23%) | | | |
| Weight gain, each 1-kg/m$^2$ | | | | |
| from 20-30 years | 1.059 (1.032-1.086) | <.0001 | 1.056 (1.028-1.085) | <.0001 |
| from 30-40 years | 1.048 (1.021-1.075) | 0.0003 | 1.042 (1.014-1.070) | 0.0034 |
| from 40-50 years | 1.041 (1.014-1.069) | 0.0026 | 1.035 (1.007-1.064) | 0.0152 |
| Ever-smoker | | | | |
| Cases/Participants | 544/6156 | | | |
| Person-years | 22,155.32 | | | |
| Incidence rate, 95% CI | 2.46% (2.25%-2.67%) | | | |
| Weight gain, each 1-kg/m$^2$ | | | | |
| from 20-30 years | 1.048 (0.981-1.119) | 0.1619 | 1.030 (0.962-1.103) | 0.3983 |
| from 30-40 years | 1.006 (0.944-1.072) | 0.8522 | 0.998 (0.934-1.067) | 0.9580 |
| from 40-50 years | 1.058 (0.998-1.121) | 0.0576 | 1.049 (0.988-1.115) | 0.1194 |

*Data are hazard ratio, 95% confidence interval (CI). P values were calculated from the Cox regression models. Model 1, adjusted for age, sex, BMI at 20 years age and BMI at baseline. Model 2, further adjusted for quintiles of physical activity, quintiles of sedentary time, smoking status (current, former, and never), alcohol drinking (g/day), and education level (percentage of high school and above), and diabetes family history (yes or no).*

of T2D (24). In the EPIC-Potsdam study, it was suggested that severe weight gain between ages 25 and 40 y was more strongly associated with risk of diabetes in men (1.5 times) and in women (4.3 times) than weight gain in later life. In addition, greater weight gain, particularly in early adulthood, may be more likely to lead to a lower age at onset of diabetes in men (5 y) and in women (3 y) (24). Though the definition of early adulthood phase was different in our study and other similar studies, it provides us very impressive evidence that the early life, from the 20 to 30 s years, weight gain exerted more prominent effect on risk of earlier developing diabetes.

One possible explanation is that early adulthood marks the end of a critical period for the development of metabolism (25), such as androgen-induced intra-abdominal fat deposition during adolescence may contribute to subsequent hepatic insulin resistance that, in turn, lead to glucose intolerance (26). Individuals who showed weight gain in early life may differ from those who gained weight in later life in behavior and genetic predisposition that may affect metabolism and disease risk (27). Moreover, weight gain in early life tends to be metabolic disturbances reflected by HbA1c, high density lipoprotein cholesterol, high sensitive C-reactive protein, and adiponectin (28).

Several limitations should be acknowledged. Firstly, the early and middle life body weight data was self-reported, which might yield recall bias. The recall bias should be cautiously concerned in this study. However, several previous studies have characterized the validity of retrospective-recalled self-reported weight and measured weight in longitudinal cohorts (29–32), and provided evidence that self-reported weight is reasonably valid surrogate in epidemiology studies (32). In a subgroup of younger women aged 25 - 42 years in the Nurses' Health Study II, the self-reported and measured weights were highly correlated: the correlation between measured and recalled weight at 18 years was 0.87 (30), and as well in middle aged and elderly study participants: 0.97 for men aged 40-75 years and for women aged 41-65 years (29). In the longitudinal Charleston Heart Study, in elderly study participants aged 60 to 100 years, correlations between reported and measured weights were 0.979 for current, 0.935 for 4-year, and 0.822 for 28-year recall (31). In the present analysis, the average age at baseline were 58.8 years (interquartile range 53.9-62.6). We compared the self-reported body weight at 60 years and the weight measured at baseline examination, the correlation was 0.84 for BMI (kg/m$^2$) and 0.85 for body weight (kg). We could not provide the exact valid data on the early life stage. In one of our ongoing community- based cohort studies at Shanghai local area, we assessed the correlation of two repeated recalled body weight during early life to middle-aged and elderly life with a 5-year interval. We found that the two recalled body weight at 50 years were highly correlated (r = 0.72, n = 2,746), and moderately correlated for body weight at 20 years (r = 0.57, n = 2,783).

Secondly, we carefully excluded the missing values on the early to middle life stage in at least one time points. This procedure could yield solid results, along with some missing value bias. However, the relative homogeneity of the cohort in educational attainment and so on actually may serve to enhance the internal validity of this study. Moreover, we conducted the sensitivity analysis by using

multiple imputation methods. Because of a large proportion of missing data in recalled weights, we increased the number of imputations (n of impute = 50) to achieve reasonable statistical efficiency. Additionally, when we selected the predictors of diabetes, we imputed not only the main exposure but also all the covariates that were input in the analysis models. The results yielded from the multiple imputation method consistently supported the main analysis.

In addition, the values of age, body weight and height in the present study were shown as means and standard deviation with one decimal place. As the values of weight and height were usually rounded during the empirical work, it should be cautious in the data interpretation.

## CONCLUSIONS

Weight gain from early to middle life was linearly and significantly associated with increased risk of incident diabetes. The earlier life weight gain the more strong effect was found on earlier developing

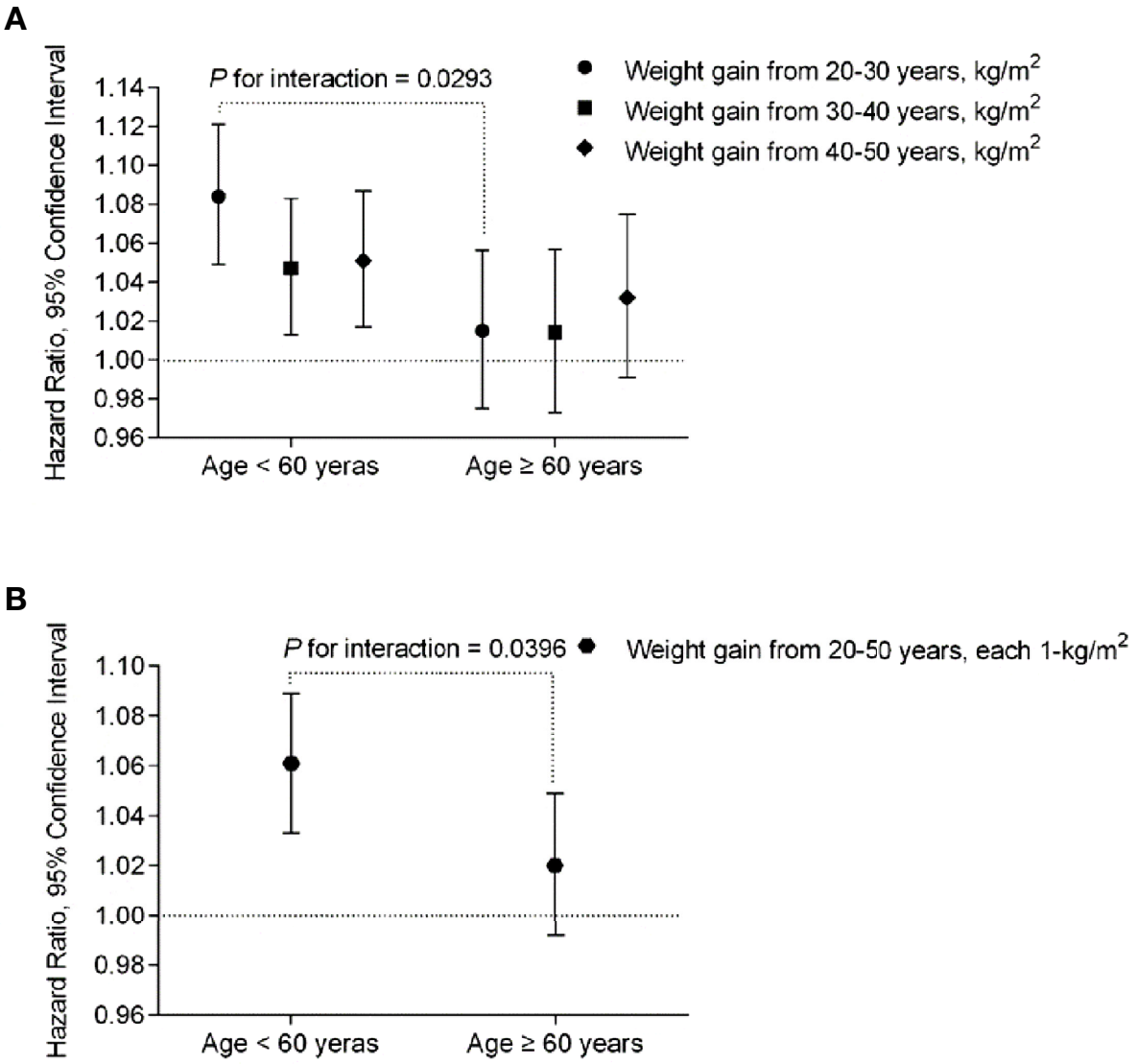


**FIGURE 2** | The risk of each 1-kg/m$^2$ body weight gain during the 3-decade intervals from early to middle life with diabetes risk stratified by age < 60 or ≥ 60 years at baseline, respectively. The multivariable-adjusted hazard ratios (HR) and 95% confidence intervals (CI) for the risk of T2D were calculated by Cox proportional hazards models, after adjustments for age (continuous), sex, body height, BMI at 20 years (continuous), baseline BMI (continuous), physical activity and sedentary time (in quintiles), smoking status (never, past, current), alcohol intake (g/day), high school and above (yes or no) and family history of diabetes (yes or no). $P_{\text{interactions}}$ were from the Cox proportional hazards models, by putting age and body weight gain in each 10 years from 20-50 years or the overall weight gain over the 30 years, and the interaction terms (weight gain x age) in the same multivariable-adjusted model, simultaneously. **(A)** Association of each-decade increase of body weight with risk of incident diabetes stratified by age < 60 or ≥ 60 years at baseline. **(B)** Association of total body weight gain from age 20-50 (each 1 kg/m2) with risk of incident diabetes stratified by age < 60 or ≥ 60 years at baseline.

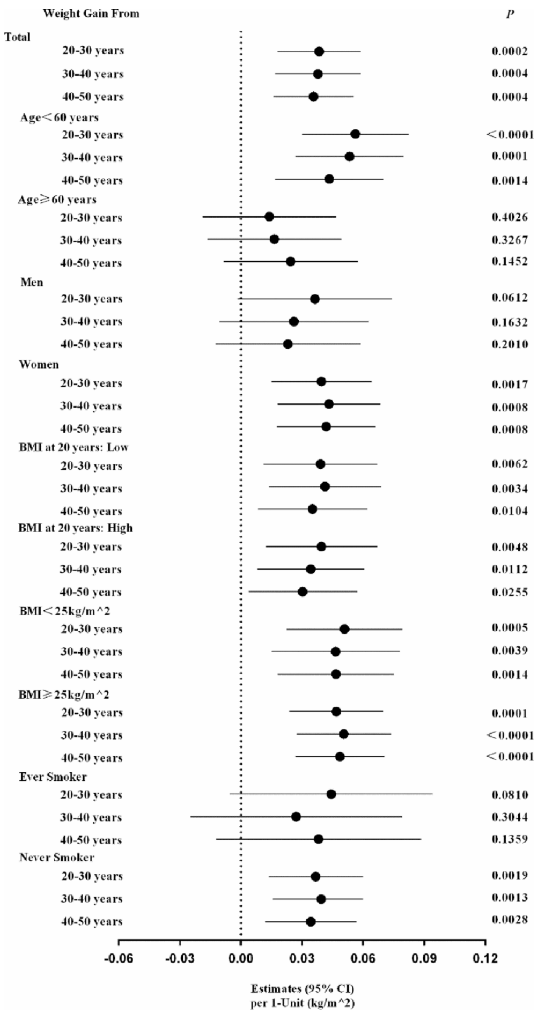


**FIGURE 3** | The estimated risk of each 1-kg/m$^2$ of each-decade body weight gain from early to middle life with diabetes risk: data from the multiple imputation methods. The multiple imputation methods were conducted in dealing with the missing data in BMI at 20, 30, 40 and 50 years of age, and the above-mentioned covariates, using the Markov chain Monte Carlo (MCMC) method, to estimate the risk of weight gains on diabetes in total participants and each risk factors strata.

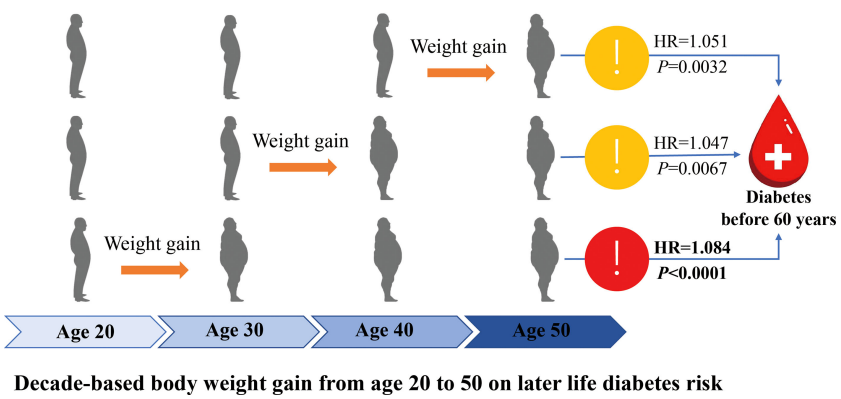


**FIGURE 4** | A graphic presentation of main findings of present study.

diabetes; however, for the risk of developing diabetes after 60 years, each-decade weight gain over the adulthood showed similar effect. It provided evidence that people should pay equal attention to the body weight during the life span, not only after the middle life but also the early stage. More well designed and longitudinal cohort studies with validated early life body weight records or measurements and well documented diseases outcomes are warranted to replicate the present study.

## DATA AVAILABILITY STATEMENT

The original contributions presented in the study are included in the article/**Supplementary Material**. Further inquiries can be directed to the corresponding authors.

## ETHICS STATEMENT

The studies involving human participants were reviewed and approved by Medical Ethics Committee of Ruijin Hospital, Shanghai Jiao-Tong University School of Medicine. The patients/participants provided their written informed consent to participate in this study.

## AUTHOR CONTRIBUTIONS

WW, JL, GN, and MX conceived and designed the study. MX, YQ, ML, YX, JL, TW, and ZZ analyzed data. QW, FS, ZG, GC, JZ, LC, LS, RH, ZY, XT, QS, GQ, GW, ZL, YQ, YH, QL, YZ, YC, CL, YM, YW, SWu, TY, LC, XY, LY, and HD collected data. All authors were involving in writing and revising the manuscript and had final approval of the submitted and published versions. WW, JL and GN are the guarantors of this work and, as such, had full access to all the data in the study and take responsibility for the integrity of the data and the accuracy of the data analysis. All authors contributed to the article and approved the submitted version.

## FUNDING

This work was funded by the National Natural Science Foundation of China (81941017, 81930021, 81970706, 81970728, 91857205, and 82088102), and the Clinical Research Plan of SHDC (SHDC2020CR1001A and SHDC2020CR3064B), and the Shanghai Municipal Education Commission–Gaofeng Clinical Medicine Grant Support (20152508 Round 2). MX, JL, ML, TW, YX, ZZ, YB, WW, and GN are members of innovative research team of high-level local universities in Shanghai.

## ACKNOWLEDGMENTS

The authors thank all study participants.

## SUPPLEMENTARY MATERIAL

The Supplementary Material for this article can be found online at: https://www.frontiersin.org/articles/10.3389/fendo.2022.927067/full#supplementary-material

## REFERENCES

1. Naser KA, Gruber A, Thomson GA. The Emerging Pandemic of Obesity and Diabetes: Are We Doing Enough to Prevent a Disaster? *Int J Clin Pract* (2006) 60(9):1093–7. doi: 10.1111/j.1742-1241.2006.01003.x
2. Schulze MB, Hu FB. Primary Prevention of Diabetes: What can be Done and How Much can be Prevented? *Annu Rev Public Health* (2005) 26:445–67. doi: 10.1146/annurev.publhealth.26.021304.144532
3. Weinstein AR, Sesso HD, Lee IM, Cook NR, Manson JE, Buring JE, et al. Relationship of Physical Activity vs Body Mass Index With T2D in Women. *JAMA* (2004) 292(10):1188–94. doi: 10.1001/jama.292.10.1188
4. Tirosh A, Shai I, Afek A, Dubnov-Raz G, Ayalon N, Gordon B, et al. Adolescent BMI Trajectory and Risk of Diabetes Versus Coronary Disease. *N Engl J Med* (2011) 364(14):1315–25. doi: 10.1056/NEJMoa1006992
5. de Lauzon-Guillain B, Balkau B, Charles MA, Romieu I, Boutron-Ruault MC, Clavel-Chapelon F. Birth Weight, Body Silhouette Over the Life Course, and Incident Diabetes in 91,453 Middle-Aged Women From the French Etude Epidemiologique De Femmes De La Mutuelle Generale De L'education Nationale (E3N) Cohort. *Diabetes Care* (2010) 33(2):298–303. doi: 10.2337/dc09-1304
6. He S, Shu Y, He J, Chen X, Cui K, Feng J, et al. The Effects of Initial and Subsequent Adiposity Status on Diabetes Mellitus. *Int J Cardiol* (2013) 168 (1):511–4. doi: 10.1016/j.ijcard.2012.09.196
7. de Mutsert R, Sun Q, Willett WC, Hu FB, van Dam RM. Overweight in Early Adulthood, Adult Weight Change, and Risk of T2D, Cardiovascular Diseases, and Certain Cancers in Men: A Cohort Study. *Am J Epidemiol* (2014) 179 (11):1353–65. doi: 10.1093/aje/kwu052
8. Black E, Holst C, Astrup A, Toubro S, Echwald S, Pedersen O, et al. Long-Term Influences of Body-Weight Changes, Independent of the Attained Weight, on Risk of Impaired Glucose Tolerance and T2D. *Diabetes Med* (2005) 22(9):1199–205. doi: 10.1111/j.1464-5491.2005.01615.x
9. Zhou L, Li Y, Guo M, Wu Y, Zhao L. Relations of Body Weight Status in Early Adulthood and Weight Changes Until Middle Age With Hypertension in the Chinese Population. *Hypertension Res* (2016) 39(12):913–18. doi: 10.1038/hr.2016.80
10. Chen C, Ye Y, Zhang Y, Pan XF, Pan A. Weight Change Across Adulthood in Relation to All Cause and Cause Specific Mortality: Prospective Cohort Study. *BMJ* (2019) 367:l5584. doi: 10.1136/bmj.l5584
11. Zheng Y, Manson JE, Yuan C, Liang MH, Grodstein F, Stampfer MJ, et al. Associations of Weight Gain From Early to Middle Adulthood With Major Health Outcomes Later in Life. *JAMA* (2017) 318(3):255–69. doi: 10.1001/jama.2017.7092
12. Sun W, Shi L, Ye Z, Mu Y, Liu C, Zhao J, et al. Association Between the Change in Body Mass Index From Early Adulthood to Midlife and Subsequent T2D Mellitus. *Obesity* (2016) 24(3):703–9. doi: 10.1002/oby.21336
13. Tian Y, Jiang C, Wang M, Cai R, Zhang Y, He Z, et al. BMI, Leisure-Time Physical Activity, and Physical Fitness in Adults in China: Results From a Series of National Surveys, 2000-14. *Lancet Diabetes Endocrinol* (2016) 4 (6):487–97. doi: 10.1016/S2213-8587(16)00081-4
14. Bi Y, Jiang Y, He J, Xu Y, Wang L, Xu M, et al. Status of Cardiovascular Health in Chinese Adults. *J Am Coll Cardiol* (2015) 65(10):1013–25. doi: 10.1016/j.jacc.2014.12.044
15. Lu J, He J, Li M, Tang X, Hu R, Shi L, et al. Predictive Value of Fasting Glucose, Postload Glucose, and Hemoglobin A 1c on Risk of Diabetes and

Complications in Chinese Adults. *Diabetes Care* (2019) 42(8):1539–48. doi: 10.2337/dc18-1390
16. Wang T, Lu J, Shi L, Chen G, Xu M, Xu Y, et al. Association of Insulin Resistance and β-Cell Dysfunction With Incident Diabetes Among Adults in China: A Nationwide, Population-Based, Prospective Cohort Study. *Lancet Diabetes Endocrinol* (2020) 8(2):115–24. doi: 10.1016/S2213-8587(19)30425-5
17. World Health Organization. *Global Physical Activity Questionnaire and Analysis Guide* (2019). Available at: https://www.who.int/ncds/surveillance/steps/GPAQ/en/ (Accessed 15 Feb 2019).
18. Yuan YC. *Multiple Imputation for Missing Data: Concepts and New Development (Version 9.0)*. Rockville, MD: SAS Institute (2000).
19. *Centers for Disease Control and Prevention. 2011 National Diabetes Statistic Report* (2017). Available at: https://www.cdc.gov/features/diabetes-statistic-report/index.html (Accessed 15 Feb 2019).
20. Wang L, Gao P, Zhang M, Huang Z, Zhang D, Deng Q, et al. Prevalence and Ethnic Pattern of Diabetes and Prediabetes in China in 2013. *JAMA* (2017) 317(24):2515–23. doi: 10.1001/jama.2017.7596
21. Xu Y, Wang L, He J, Bi Y, Li M, Wang T, et al. 2010 China Noncommunicable Disease Surveillance Group. Prevalence and Control of Diabetes in Chinese Adults. *JAMA* (2013) 310(9):948–59. doi: 10.1001/jama.2013.168118
22. Hillier TA, Pedula KL. Characteristics of an Adult Population With Newly Diagnosed T2D: The Relation of Obesity and Age of Onset. *Diabetes Care* (2001) 24(9):1522–7. doi: 10.2337/diacare.24.9.1522
23. Kodama S, Horikawa C, Fujihara K, Yoshizawa S, Yachi Y, Tanaka S, et al. Quantitative Relationship Between Body Weight Gain in Adulthood and Incident T2D: A Meta-Analysis. *Obes Rev* (2014) 15(3):202–14. doi: 10.1111/obr.12129
24. Schienkiewitz A, Schulze MB, Hoffmann K, Kroke A, Boeing H. Body Mass Index History and Risk of T2D: Results From the European Prospective Investigation Into Cancer and Nutrition (EPIC)-Potsdam Study. *Am J Clin Nutr* (2006) 84(2):427–33. doi: 10.1093/ajcn/84.1.427
25. Brancati FL, Wang NY, Mead LA, Liang KY, Klag MJ. Body Weight Patters From 20 to 49 Years of Age and Subsequent Risk for Diabetes Mellitus. *Arch Inter Med* (1999) 159(9):957–63. doi: 10.1001/archinte.159.9.957
26. Dietz WH. Critical Periods in Childhood for the Development of Obesity. *Am J Clin Nutr* (1994) 59(5):955–9. doi: 10.1093/ajcn/59.5.955
27. Stunkard AJ, Sørensen TI, Hanis C, Teasdale TW, Chakraborty R, Schull WJ, et al. An Adoption Study of Human Obesity. *N Engl J Med* (1986) 314(4):193–8. doi: 10.1056/NEJM198601233140401
28. Montonen J, Boeing H, Schleicher E, Fritsche A, Pischon T. Association of Changes in Body Mass Index During Earlier Adulthood and Later Adulthood With Circulating Obesity Biomarker Concentrations in Middle-Aged Men and Women. *Diabetologia* (2011) 54(7):1676–83. doi: 10.1007/s00125-011-2124-6
29. Rimm EB, Stampfer MJ, Colditz GA, Chute CG, Litin LB, Willett WC. Validity of Self-Reported Waist and Hip Circumferences in Men and Women. *Epidemiology* (1990) 1(6):466–73. doi: 10.1097/00001648-199011000-00009
30. Troy LM, Hunter DJ, Manson JE, Colditz GA, Stampfer MJ, Willett WC. The Validity of Recalled Weight Among Younger Women. *Int J Obes Relat Metab Disord* (1995) 19(8):570–2.
31. Stevens J, Keil JE, Waid LR, Gazes PC. Accuracy of Current, 4-Year, and 28-Year Self-Reported Body Weight in an Elderly Population. *Am J Epidemiol* (1990) 132(6):1156–63. doi: 10.1093/oxfordjournals.aje.a115758
32. Spencer EA, Appleby PN, Davey GK, Key TJ. Validity of Self-Reported Height and Weight in 4808 EPIC-Oxford Participants. *Public Health Nutr* (2002) 5 (4):561–5. doi: 10.1079/PHN2001322

**Conflict of Interest:** The authors declare that the research was conducted in the absence of any commercial or financial relationships that could be construed as a potential conflict of interest.

**Publisher's Note:** All claims expressed in this article are solely those of the authors and do not necessarily represent those of their affiliated organizations, or those of the publisher, the editors and the reviewers. Any product that may be evaluated in this article, or claim that may be made by its manufacturer, is not guaranteed or endorsed by the publisher.

frontiers | Frontiers in Endocrinology

TYPE Original Research
PUBLISHED 28 July 2022
DOI 10.3389/fendo.2022.952373



OPEN ACCESS

EDITED BY
Guilherme Zweig Rocha,
State University of Campinas, Brazil

REVIEWED BY
Huirong Liu,
Shanghai Research Center for Acupuncture and Meridians, China
Hyangsook Lee,
Kyung Hee University, South Korea
Im Quah-Smith,
Royal Hospital for Women, Australia

*CORRESPONDENCE
Guang Ji
jg@shutcm.edu.cn

†These authors have contributed equally to this work and share first authorship

SPECIALTY SECTION
This article was submitted to Obesity, a section of the journal Frontiers in Endocrinology

RECEIVED 25 May 2022
ACCEPTED 05 July 2022
PUBLISHED 28 July 2022

CITATION
Dai L, Wang M, Zhang K-P, Wang L, Zheng H-M, Li C-B, Zhou W-J, Zhou S-G and Ji G (2022) Modified acupuncture therapy, long-term acupoint stimulation versus sham control for weight control: a multicenter, randomized controlled trial. *Front. Endocrinol.* 13:952373. doi: 10.3389/fendo.2022.952373



# Modified acupuncture therapy, long-term acupoint stimulation versus sham control for weight control: a multicenter, randomized controlled trial

Liang Dai[1,2†], Miao Wang[3†], Ke-Pei Zhang[3], Lin Wang[4], Hui-Min Zheng[5], Chun-Bo Li[6], Wen-Jun Zhou[1], Shi-Gao Zhou[3] and Guang Ji[1*]

[1]Institute of Digestive Diseases, Longhua Hospital, Shanghai University of Traditional Chinese Medicine, Shanghai, China, [2]Clinical Research Academy, Peking University Shenzhen Hospital, Peking University, Shenzhen, China, [3]Department of Internal Medicine of Traditional Chinese Medicine, Longhua Hospital, Shanghai University of Traditional Chinese Medicine, Shanghai, China, [4]Department of Internal Medicine of Traditional Chinese Medicine, Shanghai Pudong New Area Peoples' Hospital, Shanghai, China, [5]Department of Acupuncture and Moxibustion, Shanghai Municipal Hospital of Traditional Chinese Medicine, Shanghai University of Traditional Chinese Medicine, Shanghai, China, [6]Shanghai Key Laboratory of Psychotic Disorders, Shanghai Mental Health Center, Shanghai Jiao Tong University School of Medicine, Shanghai, China

**Objective:** Long-term acupoint stimulation (LAS), also called embedding acupuncture, is a modified acupuncture technique. The preliminary results have demonstrated its efficacy in body-weight control. However, the low quality of available trials limited its application. This study aimed to evaluate the efficacy and safety of LAS in body-weight control by using a randomized, parallel, sham-controlled clinical trial design.

**Methods:** This was a randomized, single-blind, sham-controlled clinical trial including 84 adult participants (18–60 years) with a body mass index (BMI) of ≥ 24 kg/m$^2$ conducted in three general hospitals in Shanghai, China. Participants were equally assigned to receive LAS or sham LAS (SLAS) once per 10 days, eight times in total. After completion, an additional intervention with a 3-month follow-up period was set to examine the continued effect of LAS. The primary outcome was the change in body weight from baseline to treatment endpoint within the intention-to-treat (ITT) analysis. Secondary outcomes contained changes in waist-to-hip ratio (WHR), lipid metabolism, and visceral and subcutaneous adipose tissues.

**Results:** From 14 May 2018 to 03 November 2019, 84 participants out of 201 screened individuals met the eligibility criteria, were randomized, and were analyzed (42 participants in each group). From baseline to treatment endpoint, the body-weight reduction in the LAS group was significantly larger than in the sham control (net difference: 1.57 kg, 95% CI: 0.29–2.86, $p$ = 0.012). The superior weight reduction effect persisted in the follow-up period (net difference: 3.20 kg, 95% CI: 1.17–5.21, $p$ = 0.001). LAS therapy also showed

improvement in triglyceride and subcutaneous adipose tissue (SAT) compared with sham control. One participant in the LAS group reported a slightly uncomfortable and tingling sensation after the additional intervention. No other adverse events (AEs) were documented.

**Conclusion:** LAS, a modified acupuncture technique, is safe and effective in body-weight control. It could be used as an alternative choice to classical acupuncture for obesity management.

**Clinical Trial Registration:** [www.chictr.org.cn], identifier [ChiCTR1800015498].

KEYWORDS

acupuncture, long-term acupoint stimulation, weight control, visceral adipose tissue, subcutaneous adipose tissue, randomized controlled trial

# Introduction

Due to an unhealthy lifestyle, overweight and obesity have affected more than one-third of the Chinese population (1). Along with high prevalence, the level of body mass index (BMI) has also presented a consistently increasing trend in recent decades (2). Abundant studies have demonstrated that obesity is an independent risk factor for nonalcoholic fatty liver disease, cardiovascular diseases, and even certain types of cancers (3–5). Hence, active management of overweight and obesity is crucial in daily practice.

Conventional strategies for body-weight control include lifestyle modification, use of chemical agents, and surgical interventions (6–8). Certain pharmacotherapies, in addition to lifestyle modification, indeed present a significant effect on weight loss (9, 10). However, majority of people would experience various adverse events (AEs) as well as benefits in health outcomes except for the quality of life, which was still lacking (11). Surgical treatment is not a conventional option and could only be considered for patients with a BMI of ≥35 kg/m$^2$ (12). Hence, patients and clinicians would introduce alternative therapies to body-weight management, and acupuncture is one of the representative options.

Various studies have illustrated that acupuncture can significantly reduce body weight and BMI compared with sham control (13, 14). However, based on the synthesized data, the effect size of classical acupuncture was not enough to achieve the goal of weight loss (7). Thus, different techniques have been utilized to modify conventional acupuncture. Long-term acupoint stimulation (LAS), also called embedding acupuncture, is a kind of modified technique developed based on extended needle retention. By implanting compatible and self-degradable materials into acupoints, the acupuncture sensation would be amplified and prolonged, and therefore, the efficacy would be enhanced theoretically (15). Previous systematic reviews have summarized the current evidence of LAS in controlling body weight (16, 17). However, the conclusion should be interpreted with caution due to the low quality of included trials and high heterogeneity.

In order to verify the effectiveness and safety of LAS for weight control, we conducted this rigorous multicenter, randomized clinical trial using sham control as the comparator. The results of this trial would also serve as foundational data for further potential head-to-head trials versus conventional acupuncture.

# Materials and methods

## Study design

This was a 6-month, multicenter, single-blind, sham-controlled, parallel clinical trial conducted in Longhua Hospital Affiliated to Shanghai University of Traditional Chinese Medicine, People's Hospital of Pudong District of Shanghai and Shanghai Municipal Hospital of Traditional Chinese Medicine. Qualified participants were randomly assigned to LAS or sham LAS (SLAS) arms according to a ratio of 1:1. LAS or SLAS was given once per 10 days, eight times in total. After completion of treatment, an additional intervention with a 3-month follow-up period was set to assess the continued effect of LAS.

The study protocol was approved by the Clinical Trial Institutional Review Board (IRB) of Longhua Hospital Affiliated to Shanghai University of Traditional Chinese Medicine (No. 2016LCSY321) and registered at the Chinese Clinical Trial Registry (www.chictr.org.cn, No. ChiCTR1800015498) on 10 April 2018. The execution of the

trial strictly followed the Helsinki Declaration and Good Clinical Practice Guideline. The reporting of this clinical trial followed the requirements of the Consolidated Standards of Reporting Trials (CONSORT) and Standards for Reporting Interventions in Controlled Trials of Acupuncture (STRICTA) statements (18, 19), and the corresponding checklists can be found in Supplementary Tables S1, S2.

## Participants

All participants were recruited publicly through advertisements on social media. Potential subjects could choose one of the three study centers to participate in the trial. The definition of overweight and obesity was based on the Guidelines for Prevention and Control of Overweight and Obesity in Chinese Adults, specifically a BMI of ≥24 kg/m$^2$ (20). Other inclusion criteria were age, from 18 to 60 years old, and voluntary informed consent. The exclusion criteria included pregnancy and lactation; allergy to embedding material, namely, poly-*p*-dioxanone (PPDO); severe comorbidities such as cardiovascular, hepatic, renal, or other primary diseases; and mental illness. After eligibility, informed consent was obtained from the participants and then confirmed.

## Interventions

According to previous systematic reviews and consultations with specialists (13, 16), the following acupoints were chosen: Zhongwan (CV12), Tianshu (ST25), Fenglong (ST40), and Pishu (BL20). Previous reports have demonstrated their functions in regulating appetite and energy metabolism (21–23). According to traditional Chinese medicine (TCM) theory, these acupoints have the functions of regulating the qi activity and invigorating the spleen to eliminate dampness (24). The specific anatomical locations are described in Table 1 and shown in Supplementary Figure S1.

The bioabsorbable PPDO suture was chosen as the embedding material. PPDO has been widely used in various surgical procedures (25). It could be completely degraded into water and carbon dioxide in approximately half a year in the body (26, 27). Previous studies have illustrated its satisfactory biocompatibility (28, 29); hence, a low level of inflammatory response was anticipated during the LAS treatment.

The LAS procedure was completed by professional acupuncturists with at least 10 years of clinical practice experience. The embedding needle (size no. 7) was composed of needle tubing and stylet. Before inserting the stylet, a microbic PPDO suture (size: 3–0) was first placed in the tip of a disposable embedding needle. The reason for choosing this size was based on researchers' clinical experience, specifically that previous patients who received this size of suture reported better treatment response and less discomfort sensation. Next, the needle was inserted at a depth of 1.5–2.0 cm into the acupoints. The depth was consistent with routine acupuncture insertion depth in previous trials (30). Choosing this depth matched the aim of LAS therapy, namely, prolonging the needle sensation and avoiding the introduction of other biases. The position of the needle tip should be between the skin and muscle. After obtaining needle sensation (feelings of soreness, numbness, fullness, and heaviness in the acupoints, also defined as "de-qi"), the acupuncturist would gradually pull out the tubing and push in the stylet at the same time. This simultaneous operation would ensure the PPDO suture underneath the acupoint. Afterward, the embedding needle was withdrawn, the pinhole was pressed gently with sterile cotton and then taped. The size of the implanted PPDO suture and the key procedures of LAS therapy could be found in Supplementary Figures S2, S3. For the SLAS arm, the treatment procedure was the same, except that no PPDO suture was in the embedding needle. In order to guarantee the blinding of participants, they were required to keep the supine position first to finish the procedure in CV12, ST25, and ST40. They were asked to keep looking ahead during the procedure and to look down at their body was strictly forbidden. They were then asked to turn over to the prone position to finish the procedure in BL20, which was exactly the vision-blind area of the participants. All participants were informed to gently massage the acupoints before and after meals for 2 min.

The procedure was carried out once every 10 days, eight times in total. The treatment interval could be adjusted by the acupuncturist properly when encountering exceptional circumstances such as a menstrual period. The treatment scheme was established based on a previous systematic review and specialist consultations (31). To be specific, we asked about

TABLE 1 Locations of selected acupoints.

| Acupoints | Anatomical location |
|---|---|
| Zhongwan (CV12) | On the anterior median line of the upper abdomen, 4.0 cun above the umbilicus |
| Tianshu (ST25) | On the middle of the abdomen, 2 cun lateral to the umbilicus |
| Fenglong (ST40) | On the anterior aspect of the lower leg, 8 cun superior to the external malleolus, lateral to ST38, two finger-breadth (middle finger) from the anterior crest of the tibia |
| Pishu (BL20) | On the back, 1.5 cun lateral to the lower border of the spinous process of the 11th thoracic vertebra |

the patients' feelings of sensation during LAS therapy in our daily practice. Most of them reported that the sensation disappeared in approximately 1–2 weeks. Based on the preliminary data, we determined the treatment interval as 10 days after consultation with specialists. For the treatment duration, we noticed that a 12-week period was chosen in the majority of clinical trials regarding body-weight control. According to the previous treatment interval, we ultimately set the treatment strategy as once every 10 days, eight times in total. After completion of treatment, an additional intervention with a 3-month follow-up period was set to examine the continued effect.

Lifestyle modification plays an important role in body-weight management. In order to evaluate the effect of LAS in a real-world setting, participants were informed to follow the lifestyle modification requirements. Dramatic changes in calorie intake and/or physical activities were not allowed. Healthy lifestyle suggestions were provided in every follow-up visit according to overweight and obesity management guidelines, including limiting calorie intake and increasing physical exercise (20). To be specific, the total calorie of a daily diet should be around 1,660 kcal. Moderate physical exercise should be performed four times per week at least, and the whole time should be above 150 min. The suggestions were communicated through brochures and oral education. During every visit, the clinical investigator would ask participants about the execution of lifestyle modification. Refusal to follow lifestyle suggestions was considered a protocol violation.

## Outcomes

Participants were required to complete body measurements and scheduled laboratory tests during every visit before treatment or consultation. The primary outcome was the change in body weight after treatment. Secondary outcomes included the change in waist-to-hip ratio (WHR), total cholesterol (TC), triglyceride (TG), high-density lipoprotein cholesterol (HDL-C), and low-density lipoprotein cholesterol (LDL-C). In addition, on the principle of voluntariness, we recruited some participants to assess the change in body adipose tissue by using magnetic resonance imaging. The specific assessment method is documented in Supplementary File 1. The exploratory outcomes were the changes in visceral adipose tissue (VAT) and subcutaneous adipose tissue (SAT).

Safety assessments involved blood routine tests, urine routine tests, stool routine tests, hepatic and renal function tests, and 12-lead electrocardiograms. AEs were documented during the whole study. Necessary medical interventions were also given to patients experiencing AEs.

## Randomization and blinding

Block randomization was conducted in the ratio of 1:1 according to the random number table generated from NCSS software 11 (NCSS, LLC, Kaysville, UT, USA). An independent research assistant was responsible for the randomization and preparation of treatment assignment envelopes. The opaque sealed envelopes only had coherent randomization numbers on the surface and could not be opened until the eligibility of participants was confirmed. Clinical practitioners were responsible for informed consent and participant screening. All potential participants were informed about the rationale of LAS therapy, the detailed therapy process, and that they would be randomly allocated to a real LAS group or sham control. The allocation was not revealed until the study's completion. For participants who received sham LAS therapy, they can obtain a compensatory nine-time LAS therapy according to their willingness. Eligible participants were to confirm the above information before enrolment. After eligibility confirmation of the participants, the clinical practitioner were to open the envelope based on the inclusion order and perform the procedure accordingly. Participants were blinded during the whole study. Apart from position requirements during treatment, the implanting material made the blinding more reliable. To be specific, before the execution of this trial, we did a survey of patients who had been treated with LAS therapy. The survey indicated that the size of the PPDO suture (size 3–0) we selected was well-tolerated, and most of the patients reported no obvious sense of the implanting material. Due to the specificity of acupuncture trials, the practitioners could not be blinded. Other investigators, including coordinators, assessors, statisticians, and participants were blinded to the specific assignments.

## Statistical analysis

The sample size calculation was based on the primary outcome. According to our pilot study, the mean reduction of body weight by SAT was 6.61 kg with a standard deviation (SD) of 10.53 (unpublished data). NCSS software (NCSS, LLC, Kaysville, UT, USA) was used to estimate the sample size. In order to yield an 80%-statistical power with a two-sided significance level of 0.05, 38 participants per group were needed. Furthermore, assuming a dropout rate of 10%, a total of 84 participants were determined.

All outcome measures were evaluated based on the intention-to-treat (ITT) principle. The analysis set was composed of all randomized participants. The missing data were filled out using the last-observation-carried-forward

method. Furthermore, for the follow-up data, the analysis set was defined as the participants who underwent evaluation at both the baseline and corresponding follow-up timepoints. The R software (Version 3.6) was utilized to conduct statistical analysis. Data were presented in mean values with an SD or as a number with a percentage. The primary outcome, change in body weight, was evaluated by repeated-measures analysis of variance. Baseline differences between groups and other outcome variables were assessed by Student's *t*-test, Chi-square test, or Mann–Whitney *U* test according to the data characteristics. Significance was defined as a two-tailed value of 0.05.

# Results

## Baseline characteristics

From 14 May 2018 to 03 November 2019, 201 individuals were screened. Among them, 84 participants met the eligibility requirements and were randomized. Finally, 79 participants completed the study. The reasons for withdrawal included undesired efficacy ($n$ = 1), time conflict ($n$ = 2), and travel ($n$ = 2). Treatment adherence for the whole intervention was 94%. The participant flowchart is shown in Figure 1. The baseline characteristics of the included participants are presented in Table 2. No statistically significant difference was found between the two groups.

## Changes in body weight and BMI

The mean reduction of body weight was 2.97 kg (SD: 2.98) after eight times of treatment in the LAS group, while it was 1.40 kg (SD: 2.95) in the sham control; a higher amplitude was noticed in the LAS group (net difference: 1.57 kg, 95% confidence interval (CI): 0.29–2.86, $p$ = 0.012) (Table 3). The weight reduction effect persisted in the follow-up period. The mean reduction of body weight was 3.84 kg (SD: 4.17) from baseline to follow-up endpoint in the LAS group, while it was 0.65 kg (SD: 4.49) in the sham control; a larger decrease was still found in the LAS group (net difference: 3.20 kg, 95% CI: 1.17–5.21, $p$ = 0.001) (Table 2). The change in body weight along with time in the two groups is shown in Figure 2. At the end of treatment, 12 (28.6%) and 6 (14.3%) participants achieved at least a 5% reduction in body weight in the LAS group and sham control, respectively.

Similarly, the mean change in BMI was −1.07 kg/m$^2$ (SD: 1.10) in the LAS group after treatment. The reduction was significantly higher than the SLAS group (−0.49 kg/m$^2$ (SD: 1.04)) (net difference: 0.58 kg/m$^2$, 95% CI: 0.12–1.05, $p$ = 0.010) (Table 2). From beginning to follow-up endpoint, the reduction

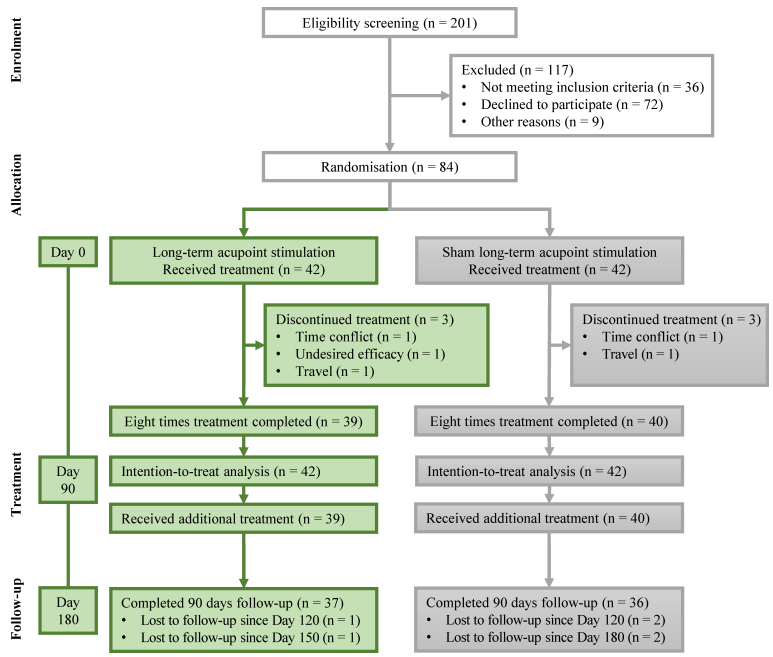


FIGURE 1
Participants' flowchart.

TABLE 2 Baseline characteristics of the intention-to-treat (ITT) population.

| | LAS ($n$ = 42) | SLAS ($n$ = 42) | $p$-value |
|---|---|---|---|
| Gender | | | |
| Male | 14 (33.33%) | 19 (45.24%) | 0.26 |
| Female | 28 (66.67%) | 23 (54.76%) | |
| Age (years) | 33.05 (6.60) | 36.17 (9.71) | 0.25 |
| Body weight (kg) | 83.99 (20.33) | 85.20 (13.46) | 0.69 |
| BMI (kg/m$^2$) | 29.98 (4.78) | 30.18 (3.70) | 0.38 |
| Waist circumference (cm) | 99.79 (13.62) | 101.21 (10.19) | 0.58 |
| Hip circumference (cm) | 107.69 (10.07) | 108.31 (7.42) | 0.75 |
| WHR | 0.92 (0.07) | 0.93 (0.07) | 0.50 |
| TC (mmol/L) | 4.64 (0.91) | 4.76 (0.99) | 0.99 |
| TG (mmol/L) | 1.80 (1.52) | 1.38 (0.55) | 0.06 |
| LDL-C (mmol/L) | 3.11 (0.68) | 3.24 (0.77) | 0.51 |
| HDL-C (mmol/L) | 1.21 (0.24) | 1.29 (0.27) | 0.31 |
| Comorbidities | | | |
| Hypertension | 6 (14.29%) | 4 (9.52%) | 0.50 |
| CHD | 0 (0%) | 0 (0%) | 1.00 |
| Dyslipidemia | 2 (4.76%) | 2 (4.76%) | 1.00 |
| NAFLD | 9 (21.43%) | 8 (19.05%) | 0.79 |
| CKD | 0 (0%) | 0 (0%) | 1.00 |

Data are in n (%) or mean (SD) values.
BMI, body mass index; CHD, coronary heart disease; CKD, chronic kidney disease; HDL-C, low-density lipoprotein cholesterol; LAS, long-term acupoint stimulation; LDL-C, low-density lipoprotein cholesterol; NAFLD, nonalcoholic fatty liver disease; SLAS, sham long-term acupoint stimulation; TC, total cholesterol; TG, triglyceride; WHR, waist-to-hip ratio.

of BMI was still 1.39 kg/m$^2$ (SD: 1.56) in the LAS group, while it was 0.22 kg/m$^2$ (SD: 1.59) in the SLAS group. Statistical significance was found between groups (net difference: 1.16 kg/m$^2$, 95% CI: 0.42–1.89, $p$ = 0.001) (Table 2).

## Secondary outcomes

From baseline to treatment endpoint, a certain reduction was found in both waist circumference and hip circumference in either group. To be specific, the mean change in waist circumference in the LAS group was more significant than SLAS (−5.43 (SD: 5.08) versus −2.96 (SD: 5.34), $p$ = 0.033), while the mean change in hip circumference showed no obvious difference between LAS and SLAS (−3.45 (SD: 4.12) versus −1.86 (SD: 3.94), $p$ = 0.074). Furthermore, no significant difference was found in the change in WHR between the two groups. The detailed information regarding body measurements is presented in Table 4.

At the end of treatment, no significant difference was observed in the change of lipid profiles (TC, HDL-C, or LDL-C) between the two groups, except for TG (Table 4). The mean reduction of TG in the LAS group was 0.32 (SD: 1.43) after the eighth treatment, while a slight elevation of TG was observed in the SLAS group (0.21 (SD: 0.53)); the difference was statistically significant ($p$ = 0.027).

TABLE 3 Change of body weight and body mass index during the whole trial.

| | Baseline to treatment endpoint | | | |
|---|---|---|---|---|
| | LAS ($n$ = 42) | SLAS ($n$ = 42) | Net difference and 95% CI | $p$-value |
| Body weight (kg) | 2.97 (2.98) | 1.40 (2.95) | 1.57 (0.29, 2.86) | 0.012 |
| BMI (kg/m$^2$) | 1.07 (1.10) | 0.49 (1.04) | 0.58 (0.12, 1.05) | 0.010 |
| | Baseline to follow-up endpoint | | | |
| | LAS ($n$ = 37) | SLAS ($n$ = 36) | Net difference and 95% CI | $p$-value |
| Body weight (kg) | 3.84 (4.17) | 0.65 (4.49) | 3.20 (1.17, 5.21) | 0.001 |
| BMI (kg/m$^2$) | 1.39 (1.56) | 0.22 (1.59) | 1.16 (0.42, 1.89) | 0.001 |

Data are in mean (SD) values.
BMI, body mass index; LAS, long-term acupoint stimulation; SLAS, sham long-term acupoint stimulation.

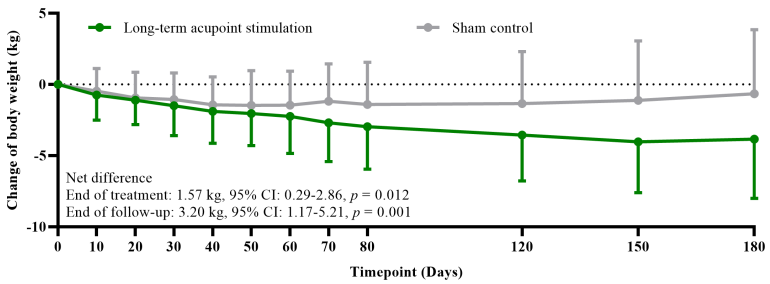


FIGURE 2
Change of body weight from baseline to 180 days follow-up.

## Change of body adipose tissue

Based on voluntariness, the MRI evaluation for body adipose tissue was conducted on 53 participants (29 in the LAS group and 24 in the SLAS group, Table 5). VAT was assessed in the liver, pancreas, and kidney. After treatment, no significant difference was found between the two groups. SAT was investigated in four axial slices, namely, L2-L3, L3-L4, L4-L5, and L5-S1. At the endpoint of the eighth treatment, the SAT in L3-L4 was significantly reduced in the LAS group compared with the SLAS group (−49.74 (SD: 128.67) versus 13.30 (SD: 97.01), $p$ = 0.043). Beyond that, no obvious difference was noticed in other segments between the two groups.

## Safety assessment

No abnormalities were reported in vital signs, laboratory tests, and 12-lead electrocardiograms throughout the whole trial. One participant in the LAS group complained of an uncomfortable and tingling sensation after the additional intervention. Relief was achieved after local hot compress. No other AEs were documented.

# Discussion

This clinical trial demonstrated that LAS could significantly improve body-weight control compared with sham control. In addition, the beneficial effect persisted for at least 3 months after the completion of the interventions. To the best of our knowledge, this is the first LAS clinical trial to use a PPDO suture as an embedding material. Both efficacy and safety profiles indicated that LAS with PPDO sutures could be used as a choice for body-weight management.

Compared with classical acupuncture, LAS is supposed to achieve a more significant effect by using fewer intervention times. The results of our trial confirm this statement. According to a previous systematic review, classical acupuncture could reduce additional body weight of 0.60 kg versus sham control (14). In our trial, by carrying out the procedure every 10 days, we achieved approximately three times the effect compared to the above data. In consideration of satisfactory safety, LAS may have

TABLE 4 Change of secondary outcomes after treatment.

| | LAS ($n$ = 42) | SLAS ($n$ = 42) | Net difference and 95% CI | $p$-value |
|---|---|---|---|---|
| Body measurements | | | | |
| Waist circumference (cm) | −5.43 (5.08) | −2.96 (5.34) | 2.46 (0.20, 4.73) | 0.033 |
| Hip circumference (cm) | −3.45 (4.12) | −1.86 (3.94) | 1.60 (0.16, 3.35) | 0.074 |
| WHR | −0.02 (0.03) | −0.01 (0.04) | 0.01 (-0.03, 0.01) | 0.23 |
| Glucose and lipid metabolism | | | | |
| TC (mmol/L) | 0.06 (0.58) | 0.20 (0.62) | 0.15 (−0.41, 0.11) | 0.27 |
| TG (mmol/L) | −0.32 (1.43) | 0.21 (0.53) | 0.53 (0.06, 1.00) | 0.027 |
| LDL-C (mmol/L) | 0.10 (0.72) | −0.02 (0.60) | 0.01 (−0.21, 0.23) | 0.95 |
| HDL-C (mmol/L) | 0.002 (0.19) | 0.03 (0.22) | 0.03 (−0.12, 0.06) | 0.47 |

Data are in mean (SD) values.
HDL-C, low-density lipoprotein cholesterol; LAS, long-term acupoint stimulation; LDL-C, low-density lipoprotein cholesterol; SLAS, sham long-term acupoint stimulation; TC, total cholesterol; TG, triglyceride; WHR, waist-to-hip ratio.

TABLE 5 Change in visceral adipose tissue and subcutaneous adipose tissue after the treatment.

| | LAS ($n$ = 29) | SLAS ($n$ = 24) | $p$-value |
|---|---|---|---|
| Hepatic fat ($mm^2$) | −0.01 (0.04) | −0.001 (0.02) | 0.074 |
| Pancreatic fat ($mm^2$) | 0.004 (0.04) | −0.003 (0.03) | 0.50 |
| Renal sinus fat ($mm^2$) | −97.26 (164.03) | −161.11 (378.72) | 0.29 |
| SAT L2-L3 ($cm^2$) | −38.50 (95.27) | 3.25 (106.32) | 0.14 |
| SAT L3-L4 ($cm^2$) | −49.74 (128.67) | 13.30 (97.01) | 0.043 |
| SAT L4-L5 ($cm^2$) | −52.23 (218.81) | −42.80 (211.52) | 0.73 |
| SAT L5-S1 ($cm^2$) | −41.38 (121.64) | −14.08 (118.70) | 0.34 |

Data are in mean (SD) values.
BMI, body mass index; LAS, long-term acupoint stimulation; SAT, subcutaneous adipose tissue; SLAS, sham long-term acupoint stimulation.

the potential to replace classical acupuncture in body-weight management with support from further head-to-head trials.

The current guidelines recommend at least 5% weight loss as the treatment goal (7). At the end of treatment, one quarter of the participants have achieved the target. Based on the guidelines, this number is not satisfactory. However, in consideration of the relatively short intervention period (80 days), this result is still gratifying. Furthermore, our result in terms of body-weight change is substantially superior to a recently published randomized controlled trial in which the synthesized data involving 40 participants reported that body-weight reduction was 1.65 kg in the LAS group (32). Although our intervention period was 2 weeks longer, this may not be enough to explain the gap. The potential reason may be the distinct acupoint selection. Further studies could be considered to explore the specific mechanisms of chosen acupoints.

The mean body weight in the SLAS group was also slightly reduced compared with the baseline. This may result from the SLAS intervention. The comparator utilized in our trial was not a real placebo. The procedure still needed to insert the needle into the acupoints and acquire the needle sensation. Only the stimulation time was shortened. Thus, in order to obtain a comprehensive understanding of the effectiveness of LAS, a wait-list control group could be introduced in future trials.

The biocompatible materials of LAS are diverse. Catgut suture is one of the conventional choices. As one of the commonest materials, catgut embedding has been used in treating a variety of diseases other than obesity, such as insomnia, chronic urticaria, and postmenopausal osteoporosis (33–35). However, there were also certain AEs reported (36, 37). Therefore, we selected an innovative material, namely, PPDO suture, as our embedding material. Previous studies reported that PPDO sutures possessed satisfactory stability, biocompatibility, and biodegradability (26, 29). These features would guarantee sustaining the stimulation of acupoints while reducing the potential risk of AEs such as inflammation and discomfort. Our study did demonstrate this hypothesis. Included participants presented good tolerance to the PPDO suture, and no one rejected treatment due to AEs. This embedding material could be prioritized in future practice and extended to other indications of LAS.

Apart from traditional body-weight evaluation, we introduced MRI for objective evaluation of the change of adipose tissue. For visceral fat, the liver is the most affected organ by fat accumulation compared with the pancreas and kidney based on their responsibilities in lipid metabolism (38). This fact can also be supported by the TCM theory (39). The liver governs dispersion and regulates the metabolism of body fluids. Impairment of function would cause accumulation of excess water and grain in the liver, which corresponds to fat accumulation in modern medicine. Based on our results, LAS showed no obvious effect on visceral fat but could significantly reduce subcutaneous fat around the waist (L3-L4) after eight times of treatment. This finding revealed that the relatively short-term improvement in body weight by LAS may come from the decrease in SAT. Furthermore, according to our results of lipid profiles, LAS significantly reduced the level of TG but showed no obvious effect on LDL-C and TC. Considering that TG is one of the main components stored in adipose tissue, we speculated that the short-term beneficial effect of LAS on body weight may result from its regulation of TG metabolism rather than TC or LDL-C. Previous acupuncture studies utilized different acupoint regimes and showed positive effects on TC and LDL-C (40). Hence, we may consider modification of our acupoint regime in future studies, hoping to find a new acupoint combination that benefits cholesterol metabolism. Based on our findings, abdominal fat accumulation is a characteristic of central obesity and serves as an independent risk factor for cardiovascular outcomes (41, 42). In further trials, it will be worth assessing the effectiveness of LAS in this population.

The mechanisms underlying LAS for body-weight control still lack relevant studies. Considering that prolonged needle sensation is the main characteristic of LAS, we speculated that the potential mechanisms are similar. In general, acupuncture treatment involves four main routes, namely, lipid and energy metabolism, inflammatory response, appetite regulation, and adipose-tissue transformation (43). For instance, electroacupuncture on CV12

and Guanyuan (CV4) can regulate the ratio of adiponectin and leptin in obese Zucker diabetic fatty rats and then further restore the balance of glucose and lipid metabolism (44). Huang et al. found that electroacupuncture on CV12, ST40, Zusanli (ST36), and CV4 could activate the silent information regulation factor 1/nuclear factor-kappa B signaling pathway in obese rats and reduce the expression of downstream inflammatory factors (45). Ghrelin and leptin are counter hormones in regulating appetite (46). A previous animal study found that acupuncture could regulate a diet's rhythm by reducing ghrelin levels (47). A randomized controlled trial also reported that acupuncture's effect on weight control may result from its regulation of the balance between leptin and ghrelin (48). Other studies also reported that acupuncture could promote white adipose tissue browning *via* enhancing the expression of uncoupling protein-1 (47, 49). To verify these mechanisms and explore the potential amplifying effect brought by LAS, basic studies utilizing real LAS therapy should be supplemented.

Our study provided a general acupoint regime of LAS therapy for weight control. However, factors such as demographic characteristics, acupuncture techniques, and causes of overweight/obesity may interfere with efficacy (50, 51). In clinical practice, doctors are encouraged to adjust the acupoint regime flexibly based on the patients' status. Further studies can also be considered in exploring individualized acupoint selection in treating overweight/obesity.

Our study has certain limitations. Firstly, participant recruitment was not only limited to simple obesity. Nearly half of the participants possessed BMI levels between 24 and 28 $kg/m^2$. This population may weaken the overall efficacy of LAS treatment. Secondly, only body measurements and lipid metabolism were evaluated in this study. Obesity-related hormones, such as leptin and ghrelin, were not involved. Hence, we could not explain the potential mechanisms of LAS. The sample size of this study was limited. The observed effect size was lower than expected. According to the study results, a larger-scale clinical trial is needed with at least 92 participants in each group. Furthermore, our clinical trial was a simple sham-controlled study. No active intervention or blank control was introduced. Thus, we could not estimate the specific position of LAS in the management algorithm of body weight. Further head-to-head studies are suggested. Lastly, the evaluation for lifestyle modification only served as a compliance indicator in this trial. The lack of lifestyle data partially limited the explanation of study results. Real-time monitoring and documenting of participants' daily lifestyle data *via* smart wearable devices would be a considerable solution.

In summary, the modified acupuncture technique, specifically, LAS with PPDO suture, was superior to sham control in controlling body weight after 80 days of treatment. Also, the therapeutic effect persisted throughout the 3-month follow-up period. The benefit may result from the reduction of SAT. Further studies could focus on mechanism exploration and head-to-head comparison with standard medications.

## Data availability statement

The original contributions presented in the study are included in the article/Supplementary Material. Further inquiries can be directed to the corresponding author.

## Ethics statement

The studies involving human participants were reviewed and approved by Clinical Trial Institutional Review Board of Longhua Hospital Affiliated to Shanghai University of Traditional Chinese Medicine. The patients/participants provided their written informed consent to participate in this study.

## Author contributions

All listed authors met the requirements for authorship. LD and MW designed the trial, interpreted the data, and drafted the manuscript, and were considered as co-first authors. K-PZ, LW, and H-MZ recruited the participants and performed treatments. C-BL conducted an MRI assessment and analysis. W-JZ and S-GZ coordinated the conduct of the study. GJ initiated the trial and supervised the execution. All authors read and approved the final manuscript.

## Funding

This work was supported by the Shanghai Three-year Action Plan for Accelerating the Development of Traditional Chinese Medicine (No. ZY (2018-2020)-CCCX-2002-01) and the Clinical Research Plan of SHDC (No. SHDC12017X16). The funders had no role in the study design, data collection and analysis, the decision to publish, or the preparation of the manuscript.

## Acknowledgments

We thank the research assistants and nurses from the three medical centers for guaranteeing the smooth proceeding of this clinical trial. We also thank Dr. Ying Shan from the Clinical Research Academy, Peking University Shenzhen Hospital, for statistical analysis support.

## Conflict of interest

The authors declare that the research was conducted in the absence of any commercial or financial relationships that could be construed as a potential conflict of interest.

## Publisher's note

All claims expressed in this article are solely those of the authors and do not necessarily represent those of their affiliated organizations, or those of the publisher, the editors and the reviewers. Any product that may be evaluated in this article, or claim that may be made by its manufacturer, is not guaranteed or endorsed by the publisher.

## Supplementary material

The Supplementary Material for this article can be found online at: https://www.frontiersin.org/articles/10.3389/fendo.2022.952373/full#supplementary-material

## References

1. Tian Y, Jiang C, Wang M, Cai R, Zhang Y, He Z, et al. Bmi, leisure-time physical activity, and physical fitness in adults in China: Results from a series of national surveys, 2000-14. *Lancet Diabetes Endocrinol* (2016) 4(6):487–97. doi: 10.1016/s2213-8587(16)00081-4

2. NCD Risk Factor Collaboration. Trends in adult body-mass index in 200 countries from 1975 to 2014: A pooled analysis of 1698 population-based measurement studies with 19·2 million participants. *Lancet* (2016) 387 (10026):1377–96. doi: 10.1016/s0140-6736(16)30054-x

3. Li L, Liu DW, Yan HY, Wang ZY, Zhao SH, Wang B. Obesity is an independent risk factor for non-alcoholic fatty liver disease: Evidence from a meta-analysis of 21 cohort studies. *Obes Rev* (2016) 17(6):510–9. doi: 10.1111/obr.12407

4. Mandviwala T, Khalid U, Deswal A. Obesity and cardiovascular disease: A risk factor or a risk marker? *Curr Atheroscler Rep* (2016) 18(5):21. doi: 10.1007/s11883-016-0575-4

5. Nunez C, Bauman A, Egger S, Sitas F, Nair-Shalliker V. Obesity, physical activity and cancer risks: Results from the cancer, lifestyle and evaluation of risk study (Clear). *Cancer Epidemiol* (2017) 47:56–63. doi: 10.1016/j.canep.2017.01.002

6. Durrer Schutz D, Busetto L, Dicker D, Farpour-Lambert N, Pryke R, Toplak H, et al. European Practical and patient-centred guidelines for adult obesity management in primary care. *Obes Facts* (2019) 12(1):40–66. doi: 10.1159/000496183

7. Garvey WT, Mechanick JI, Brett EM, Garber AJ, Hurley DL, Jastreboff AM, et al. American Association of clinical endocrinologists and American college of endocrinology comprehensive clinical practice guidelines for medical care of patients with obesity. *Endocr Pract* (2016) 22 Suppl 3:1–203. doi: 10.4158/ep161365.Gl

8. Bray GA, Heisel WE, Afshin A, Jensen MD, Dietz WH, Long M, et al. The science of obesity management: An endocrine society scientific statement. *Endocr Rev* (2018) 39(2):79–132. doi: 10.1210/er.2017-00253

9. Khera R, Murad MH, Chandar AK, Dulai PS, Wang Z, Prokop LJ, et al. Association of pharmacological treatments for obesity with weight loss and adverse events: A systematic review and meta-analysis. *JAMA* (2016) 315(22):2424–34. doi: 10.1001/jama.2016.7602

10. Yanovski SZ, Yanovski JA. Long-term drug treatment for obesity: A systematic and clinical review. *JAMA* (2014) 311(1):74–86. doi: 10.1001/jama.2013.281361

11. LeBlanc EL, Patnode CD, Webber EM, Redmond N, Rushkin M, O'Connor EA, et al. *Behavioral and pharmacotherapy weight loss interventions to prevent obesity-related morbidity and mortality in adults: An updated systematic review for the us preventive services task force*. Rockville (MD: Agency for Healthcare Research and Quality (US (2018).

12. Nguyen NT, Varela JE. Bariatric surgery for obesity and metabolic disorders: State of the art. *Nat Rev Gastroenterol Hepatol* (2017) 14(3):160–9. doi: 10.1038/nrgastro.2016.170

13. Fang S, Wang M, Zheng Y, Zhou S, Ji G. Acupuncture and lifestyle modification treatment for obesity: A meta-analysis. *Am J Chin Med* (2017) 45 (2):239–54. doi: 10.1142/s0192415x1750015x

14. Zhang RQ, Tan J, Li FY, Ma YH, Han LX, Yang XL. Acupuncture for the treatment of obesity in adults: A systematic review and meta-analysis. *Postgrad Med J* (2017) 93(1106):743–51. doi: 10.1136/postgradmedj-2017-134969

15. Huo J, Zhao J, Yuan Y, Wang J. [Research status of the effect mechanism on catgut-point embedding therapy]. *Zhongguo Zhen Jiu* (2017) 37(11):1251–4. doi: 10.13703/j.0255-2930.2017.11.031

16. Huang CY, Choong MY, Li TS. Treatment of obesity by catgut embedding: An evidence-based systematic analysis. *Acupunct Med* (2012) 30(3):233–4. doi: 10.1136/acupmed-2012-010176

17. Sheng J, Jin X, Zhu J, Chen Y, Liu X. The effectiveness of acupoint catgut embedding therapy for abdominal obesity: A systematic review and meta-analysis. *Evid Based Complement Alternat Med* (2019) 2019:9714313. doi: 10.1155/2019/9714313

18. MacPherson H, Altman DG, Hammerschlag R, Youping L, Taixiang W, White A, et al. Revised standards for reporting interventions in clinical trials of acupuncture (Stricta): Extending the consort statement. *PLoS Med* (2010) 7(6): e1000261. doi: 10.1371/journal.pmed.1000261

19. Schulz KF, Altman DG, Moher D. Consort 2010 statement: Updated guidelines for reporting parallel group randomised trials. *BMJ* (2010) 340:c332. doi: 10.1136/bmj.c332

20. Chen C, Lu FC. The guidelines for prevention and control of overweight and obesity in Chinese adults. *BioMed Environ Sci* (2004) 17 Suppl:1–36.

21. Figueiredo LM, Silva AH, Prado Neto AX, Hissa MN, Vasconcelos PR, Guimarães SB. Electroacupuncture stimulation using different frequencies (10 and 100 Hz) changes the energy metabolism in induced hyperglycemic rats. *Acta Cir Bras* (2011) 26 Suppl 1:47–52. doi: 10.1590/s0102-86502011000700010

22. Kong XJ, Gao L, Peng H, Shi X. [Effects of electro-acupuncture on expression of obestatin in hypothalamus of rats with simple obesity]. *Zhong Xi Yi Jie He Xue Bao* (2010) 8(5):480–5. doi: 10.3736/jcim20100513

23. Li M, Zhang Y. Modulation of gene expression in cholesterol-lowering effect of electroacupuncture at fenglong acupoint (ST40): A cDNA microarray study. *Int J Mol Med* (2007) 19(4):617–29. doi: 10.3892/ijmm.19.4.617

24. Mo Q, Wu XM, Yang S. [Characteristics and rules of acupoints selection in treatment of simple obesity with acupoint catgut embedding]. *Yunnan Zhong Yi Xue Yuan Xue Bao* (2018) 41(2):67–72. doi: 10.19288/j.cnki.issn.1000-2723.2018.02.019

25. Lerwick E. Studies on the efficacy and safety of polydioxanone monofilament absorbable suture. *Surg Gynecol Obstet* (1983) 156(1):51–5.

26. Boenisch M, Mink A. Clinical and histological results of septoplasty with a resorbable implant. *Arch Otolaryngol Head Neck Surg* (2000) 126(11):1373–7. doi: 10.1001/archotol.126.11.1373

27. Rimmer J, Ferguson LM, Saleh HA. Versatile applications of the polydioxanone plate in rhinoplasty and septal surgery. *Arch Facial Plast Surg* (2012) 14(5):323–30. doi: 10.1001/archfacial.2012.147

28. Boenisch M, Tamás H, Nolst Trenité GJ. Influence of polydioxanone foil on growing septal cartilage after surgery in an animal model: New aspects of cartilage healing and regeneration (Preliminary results). *Arch Facial Plast Surg* (2003) 5 (4):316–9. doi: 10.1001/archfaci.5.4.316

29. Otto J, Binnebösel M, Pietsch S, Anurov M, Titkova S, Ottinger AP, et al. Large-Pore pds mesh compared to small-pore pg mesh. *J Invest Surg* (2010) 23 (4):190–6. doi: 10.3109/08941931003739741

30. Belivani M, Dimitroula C, Katsiki N, Apostolopoulou M, Cummings M, Hatzitolios AI. Acupuncture in the treatment of obesity: A narrative review of the literature. *Acupunct Med* (2013) 31(1):88–97. doi: 10.1136/acupmed-2012-010247

31. Cho WC, Li C, Chen HY. Clinical efficacy of acupoint embedment in weight control: A systematic review and meta-analysis. *Med (Baltimore)* (2018) 97(36): e12267. doi: 10.1097/md.0000000000012267

32. Chen IJ, Yeh YH, Hsu CH. Therapeutic effect of acupoint catgut embedding in abdominally obese women: A randomized, double-blind, placebo-controlled study. *J Womens Health (Larchmt)* (2018) 27(6):782–90. doi: 10.1089/jwh.2017.6542

33. Huang F, Xie Y, Zhao S, Feng Z, Chen G, Xu Y. The effectiveness and safety of acupoint catgut embedding for the treatment of postmenopausal osteoporosis: A systematic review and meta-analysis. *Evid Based Complement Alternat Med* (2019) 2019:2673763. doi: 10.1155/2019/2673763

34. Shi Y, Hou T, Zheng Q, Liu Y, Yang T, Li Y. Acupoint catgut embedding for patients with chronic urticaria: A systematic review protocol. *Med (Baltimore)* (2019) 98(24):e16036. doi: 10.1097/md.0000000000016036

35. Xu F, Xuan LH, Zhou HJ, Chen FY, Zheng ZJ, Bi Y, et al. Acupoint catgut embedding alleviates insomnia in different Chinese medicine syndrome types: A randomized controlled trial. *Chin J Integr Med* (2019) 25(7):543–9. doi: 10.1007/s11655-018-2770-3

36. Wang XL, Lin GH, Xu N, Zeng JC, Xu DH, Wang SX. [Analysis of adverse reactions of acupoint catgut embedding therapy]. *Zhongguo Zhen Jiu* (2020) 40 (2):193–6. doi: 10.13703/j.0255-2930.20190316-k00034

37. Chuang YT, Li TS, Lin TY, Hsu CJ. An unusual complication related to acupuncture point catgut embedding treatment of obesity. *Acupunct Med* (2011) 29 (4):307–8. doi: 10.1136/acupmed.2011.010084

38. Tchernof A, Després JP. Pathophysiology of human visceral obesity: An update. *Physiol Rev* (2013) 93(1):359–404. doi: 10.1152/physrev.00033.2011

39. Huo L, Zhang HR, Zhan XH, Liang Y. [the concept alternation of "Liver govens dispersion"]. *Zhongguo Zhong Yi Ji Chu Yi Xue Za Zhi* (2021) 27(10):1533–5. doi: 10.19945/j.cnki.issn.1006-3250.2021.10.001

40. Zhang K, Zhou S, Wang C, Xu H, Zhang L. Acupuncture on obesity: Clinical evidence and possible neuroendocrine mechanisms. *Evid Based Complement Alternat Med* (2018) 2018:6409389. doi: 10.1155/2018/6409389

41. Zhu S, Wang Z, Heshka S, Heo M, Faith MS, Heymsfield SB. Waist circumference and obesity-associated risk factors among whites in the third national health and nutrition examination survey: Clinical action thresholds. *Am J Clin Nutr* (2002) 76(4):743–9. doi: 10.1093/ajcn/76.4.743

42. Flicker L, McCaul KA, Hankey GJ, Jamrozik K, Brown WJ, Byles JE, et al. Body mass index and survival in men and women aged 70 to 75. *J Am Geriatr Soc* (2010) 58(2):234–41. doi: 10.1111/j.1532-5415.2009.02677.x

43. Wang LH, Huang W, Wei D, Ding DG, Liu YR, Wang JJ, et al. Mechanisms of acupuncture therapy for simple obesity: An evidence-based review of clinical and animal studies on simple obesity. *Evid Based Complement Alternat Med* (2019) 2019:5796381. doi: 10.1155/2019/5796381

44. Peplow PV. Repeated electroacupuncture in obese zucker diabetic fatty rats: Adiponectin and leptin in serum and adipose tissue. *J Acupunct Meridian Stud* (2015) 8(2):66–70. doi: 10.1016/j.jams.2014.06.013

45. Huang Q, Chen R, Peng M, Li L, Li T, Liang FX, et al. [Effect of electroacupuncture on Sirt1/Nf-κb signaling pathway in adipose tissue of obese rats]. *Zhongguo Zhen Jiu* (2020) 40(2):185–91. doi: 10.13703/j.0255-2930.20190324-00054

46. Kojima M, Kangawa K. Ghrelin: Structure and function. *Physiol Rev* (2005) 85(2):495–522. doi: 10.1152/physrev.00012.2004

47. Shen W, Wang Y, Lu SF, Hong H, Fu S, He S, et al. Acupuncture promotes white adipose tissue browning by inducing Ucp1 expression on dio mice. *BMC Complement Altern Med* (2014) 14:501. doi: 10.1186/1472-6882-14-501

48. Güçel F, Bahar B, Demirtas C, Mit S, Cevik C. Influence of acupuncture on leptin, ghrelin, insulin and cholecystokinin in obese women: A randomised, sham-controlled preliminary trial. *Acupunct Med* (2012) 30(3):203–7. doi: 10.1136/acupmed-2012-010127

49. Wang F, Tian DR, Han JS. Electroacupuncture in the treatment of obesity. *Neurochem Res* (2008) 33(10):2023–7. doi: 10.1007/s11064-008-9822-6

50. Chen J, Chen D, Ren Q, Zhu W, Xu S, Lu L, et al. Acupuncture and related techniques for obesity and cardiovascular risk factors: A systematic review and meta-regression analysis. *Acupunct Med* (2020) 38(4):227–34. doi: 10.1136/acupmed-2018-011646

51. Xu L, Ding C, Chen J, Tan R, Chen D, Xu S, et al. [Efficacy difference between warming acupuncture and other acupuncture methods for primary obesity: A meta-analysis]. *Zhongguo Zhen Jiu* (2018) 38(9):1019–26. doi: 10.13703/j.0255-2930.2018.09.031

frontiers | Frontiers in Endocrinology

TYPE Original Research
PUBLISHED 25 August 2022
DOI 10.3389/fendo.2022.938680



OPEN ACCESS

EDITED BY
Alexandre Gabarra Oliveira,
São Paulo State University, Brazil

REVIEWED BY
Ling Li,
Southeast University, China
Ana Ghezzi,
State University of Campinas, Brazil

*CORRESPONDENCE
Rennian Wang
rwang@uwo.ca

SPECIALTY SECTION
This article was submitted to Obesity, a section of the journal Frontiers in Endocrinology

RECEIVED 07 May 2022
ACCEPTED 08 August 2022
PUBLISHED 25 August 2022

CITATION
Schuurman M, Wallace M, Sahi G, Barillaro M, Zhang S, Rahman M, Sawyez C, Borradaile N and Wang R (2022) N-acetyl-L-cysteine treatment reduces beta-cell oxidative stress and pancreatic stellate cell activity in a high fat diet-induced diabetic mouse model. *Front. Endocrinol.* 13:938680. doi: 10.3389/fendo.2022.938680



# N-acetyl-L-cysteine treatment reduces beta-cell oxidative stress and pancreatic stellate cell activity in a high fat diet-induced diabetic mouse model

Meg Schuurman[1,2], Madison Wallace[1,3], Gurleen Sahi[1,2], Malina Barillaro[1,2], Siyi Zhang[1], Mushfiqur Rahman[1,2], Cynthia Sawyez[2], Nica Borradaile[2] and Rennian Wang[1,2]*

[1]Children's Health Research Institute, London, ON, Canada, [2]Department of Physiology & Pharmacology, University of Western Ontario, London, ON, Canada, [3]Department of Pathology and Laboratory Medicine, University of Western Ontario, London, ON, Canada

Obesity plays a major role in type II diabetes (T2DM) progression because it applies metabolic and oxidative stress resulting in dysfunctional beta-cells and activation of intra-islet pancreatic stellate cells (PaSCs) which cause islet fibrosis. Administration of antioxidant N-acetyl-L-cysteine (NAC) *in vivo* improves metabolic outcomes in diet-induced obese diabetic mice, and *in vitro* inhibits PaSCs activation. However, the effects of NAC on diabetic islets *in vivo* are unknown. This study examined if dosage and length of NAC treatment in HFD-induced diabetic mice effect metabolic outcomes associated with maintaining healthy beta-cells and quiescent PaSCs, *in vivo*. Male C57BL/6N mice were fed normal chow (ND) or high-fat (HFD) diet up to 30 weeks. NAC was administered in drinking water to HFD mice in preventative treatment ($HFD^{pNAC}$) for 23 weeks or intervention treatment for 10 ($HFD^{iNAC}$) or 18 ($HFD^{iNAC+)}$ weeks, respectively. $HFD^{pNAC}$ and $HFD^{iNAC+}$, but not $HFD^{iNAC}$, mice showed significantly improved glucose tolerance and insulin sensitivity. Hyperinsulinemia led by beta-cell overcompensation in HFD mice was significantly rescued in NAC treated mice. A reduction of beta-cell nuclear Pdx-1 localization in HFD mice was significantly improved in NAC treated islets along with significantly reduced beta-cell oxidative stress. HFD-induced intra-islet PaSCs activation, labeled by αSMA, was significantly diminished in NAC treated mice along with lesser intra-islet collagen deposition. This study determined that efficiency of NAC treatment is beneficial at maintaining healthy beta-cells and quiescent intra-islet PaSCs in HFD-induced obese T2DM mouse model. These findings highlight an adjuvant therapeutic potential in NAC for controlling T2DM progression in humans.

KEYWORDS

**N-acetyl-L-cysteine (NAC), HFD-induced diabetes, beta-cell oxidative stress, pancreatic stellate cells (PaSCs), collagen fiber**

# Introduction

Type 2 diabetes mellitus (T2DM) is a progressive metabolic disease consisting of whole body and pancreatic islet alterations which culminate in dysregulated glycemia (1). T2DM progression, often facilitated by obesity, typically begins with insulin resistance, where peripheral tissue insulin receptors become insensitive and require increased insulin to initiate a response (2, 3). Subclinical inflammation—elevated pro-inflammatory cytokines— is present during obesity which has been associated with metabolic syndrome and peripheral insulin resistance (4). Initially, pancreatic beta-cells accommodate this increase in demand by increasing insulin production as well as their size and number (1, 5). However, this compensatory mechanism is limited and leads to eventual beta-cell failure. The major cause of the clinical progression of T2DM is a decline in beta-cell mass and function within the pancreatic islets (1, 6). Since islet cellular organization is supported by non-islet cells (i.e., pancreatic stellate cells – PaSCs) and the extracellular matrix; this unique microenvironment is crucial for islet function and survival (7–10).

One of the mechanisms facilitating beta-cell failure is believed to be an imbalance between reactive oxygen species (ROS) and antioxidants leading to increased oxidative stress (11). ROS are by-products of metabolism from mitochondria in response to increased glucose, thus in overnutrition settings (i.e. obesity) increased oxidative stress is observed (12). T2DM patients have increased oxidative stress levels compared to non-diabetic controls (11). In addition, diabetic pancreatic islets display lower antioxidant enzyme (i.e. glutathione [GSH], superoxide dismutase [SOD]) expression compared to controls, this further augments beta-cell susceptibility to oxidative stress-induced damage (13, 14). High levels of oxidative stress progresses beta-cell compensation towards dysfunction indicated by reduced nuclear pancreatic and duodenal homeobox 1 (Pdx-1) localization (15). In addition to the beta-cell-specific changes, prolonged high fat diet (HFD)-induced compensation affects the islet microenvironment by increasing intra-islet PaSCs activation and collagen deposition (16). Under conditions of ROS accumulation, mechanical stress and cytokine stimulation, PaSCs are activated and develop a myofibroblast phenotype, gain expression of alpha-smooth muscle actin (aSMA) and are associated with excessive extracellular matrix (ECM) and cytokines production leading to pancreatic inflammation and fibrosis (17, 18). Activated PaSCs are also associated with impaired beta-cell function, *in vitro* (19). However, whether a definitive relationship exists between activated PaSCs and beta-cell dysfunction has not yet been established. Furthermore, it remains to be questioned whether inhibition of PaSC activation and beta-cell oxidative stress *via* antioxidants is a viable therapeutic target for T2DM progression.

N-acetyl-L-cysteine (NAC), a biosynthetic precursor to GSH, is a well-known antioxidant that has been studied for its effect on numerous physiological processes and diseases including T2DM (20–22). In addition to acting as a precursor to glutathione, NAC contains a thiol group which enables it to act directly as an antioxidant; it also acts as an anti-inflammatory (23, 24). NAC has been shown to reduce levels of oxidative stress and improve insulin release in isolated Wistar rat islets (25). When administered in drinking water to HFD murine models of T2DM, NAC improved glucose and insulin tolerance tests (22) and provided functional protection in beta-cells of female mice (26). However, NAC has been shown to be ineffective in limited T2DM clinical work (27). NAC efficacy is impacted by timing (22) and dosage (21) of administration. It was observed to be most beneficial for improving metabolic outcomes when administered as a long-term interventional lasting 5 months (21). Although clinical research is limited, animal models show promise for NAC as a potential treatment in T2DM (21, 22, 26, 28). However, the reported literature lacks understanding with the changes in pancreatic islets particularly in beta-cells and PaSCs following NAC treatment *in vivo*.

In the present study, we aimed to determine the effects of both dosage and timing of NAC administration on pancreatic beta-cells and islet PaSCs in a HFD-induced diabetic mouse model. We hypothesized that the efficiency of NAC treatment will improve metabolic outcomes and beta-cell function by rescuing beta-cell overcompensation while reducing beta-cell stress and PaSC activation induced by HFD. Here, we show that NAC treatment is beneficial for improving metabolic outcomes and beta-cell function, particularly by preserving beta-cell identity, and reducing beta-cell oxidative stress and PaSC activation. However, efficiency of NAC treatment is dependent on both timing and dosage.

# Materials and methods

## Mouse model of high-fat diet induced obesity T2DM with NAC prevention and intervention treatment

Male C57BL/6N (B6N) mice purchased from Charles River (Charles River Laboratories Quebec, Canada) were housed in our facility under a 12:12 h light/dark cycle with a maximum of 5 mice per cage. At 6-weeks of age, mice maintained a normal chow diet (ND) composed of 22% kcal from fat, 23% kcal protein, and 55% kcal from carbohydrates (Harlan Tekard, Indianapolis, IN, USA) or received a high-fat diet (HFD) composed of 60% kcal from fat, 20% from protein, and 20% from carbohydrates (Research Diets INC, New Brunswick, NJ, USA) ad libitum. Mice received a ND or HFD for 22- or 30-week feeding periods (Supplementary Figure S1).

Antioxidant treatment with N-acetyl-L-cysteine (NAC) (Santa Cruz Biotechnology, Inc., Santa Cruz, CA, USA) was administered in drinking water to HFD fed mice either in 10mM or 50mM dosage (21, 22). Since the effectiveness of 10mM dose did not show improvement of glucose metabolism (Supplementary Figure S2) compared to 50mM dosage, this report was focused on using 50mM NAC for antioxidant groups in a prevention (pNAC) or intervention (iNAC) treatment (Supplementary Figure S1). For pNAC treatment, mice received NAC one week prior to HFD and treated through 22-week HFD feeding ($HFD^{pNAC}$). For iNAC treatment, mice received NAC at week 12 after HFD and continued NAC intake for the duration of the 22-week HFD ($HFD^{iNAC}$) and 30-week HFD ($HFD^{iNAC+}$). NAC intake was assessed in each antioxidant treated group (over a three-day period) by measuring water consumption, expressed as NAC intake (mg) per mouse per day. Control mice were age-matched and consumed either ND or HFD with no NAC treatment.

Body weight was monitored weekly, and food intake was measured at the end of the assigned diet period (29). Food intake is expressed kilocalories per mouse per day. All animal work was conducted based on approved protocols from the University of Western Ontario Animal User Subcommittee (Animal Use Protocol #2021-139) in accordance with the Canadian Council of Animal Care guidelines.

## Metabolic studies in experimental mouse models

At the last week of the assigned diet period, fasting blood glucose was examined followed by an intraperitoneal (i.p.) glucose (IPGTT) or insulin (IPITT) tolerance tests. Tests were conducted in the final 2 weeks of diet intervention and at least 5 days apart from one another. For IPGTT, glucose (Dextrose, Sigma, Saint Louis, MO, USA) was administrated at a dose of 2mg/g body weight after an overnight fast for 22 week feeding mice and a 4 hour fast for 30 week feeding mice. For IPITT, insulin (Humulin, Eli Lilly, Toronto, ON, Canada) was administrated at a dose of 1 U/kg body weight after a 4 hour fast. Blood glucose levels were measured before i.p. injection (0 min) and post-injection (15, 30, 60, and 120 mins) and area under the curve (AUC) was used to measure responsiveness. Results of IPITT were normalized to baseline glucose levels (100%) and AUC values were generated to determine changes in insulin sensitivity (30). To determine *in vivo* glucose-stimulated insulin secretion (GSIS), blood samples were collected following 16 h fasting (0 min) and at 5 and 35 min after i.p. injection of glucose (2mg/g). Plasma insulin levels from GSIS and fed cardiac blood was measured using an ultrasensitive insulin mouse ELISA kit (ALPCO, Salem, NH, USA). Plasma triglycerides and cholesterol were measured using enzymatic, colorimetric assays (Wako Diagnostics, Mountain View, California, USA).

## Immunohistological staining and morphometric analyses

At the end of experimental time points, pancreases from mice were collected, weighed, and fixed in 4% paraformaldehyde. Whole pancreatic tissues were embedded in paraffin and sectioned consecutively at 4-µm throughout the length of the pancreas, from head to tail, to avoid any bias due to regional changes in islet distribution and islet cell composition of the pancreas (31). Sections were incubated with the appropriate dilutions of primary antibodies as listed in Supplementary Table S1. As required, 0.2% Triton treatment and/or microwave antigen retrieval with citric acid solution (pH 6.0) were applied to improve detection. Secondary antibodies consisted of fluorescein isothiocyanate (FITC) and tetramethyl rhodamine isothiocyanate (TRITC) (1:50; Jackson Immunoresearch, West Grove, PA, USA). 4'-6'-diamidino-2-phenylindole (DAPI) was used for nuclear counterstaining (Sigma-Aldrich). Images were captured using Nikon Eclipse Ti2 Confocal Microscope (Nikon, Melville, NY, USA) followed by morphometric analysis of islet density, alpha and beta-cell mass and beta-cell size, as previously described (30, 32). Beta-cell proliferation, expression of Pdx-1 transcription factor and oxidative stress were identified by double immunofluorescence staining and quantification from at least 10 random islets per pancreas section. Double positive cells (nuclear marker-positive with insulin-positive) were divided by the total insulin-positive cell population in islets and expressed as a percentage (33). To quantify the percentage of intra-islet PaSCs population, labeled by αSMA and desmin, the positive intra-islet $\alpha SMA^+$ or $desmin^+$ cell area ($\mu m^2$) was manually traced using Nikon NIS-Element software and divided by the total insulin-positive area ($\mu m^2$).

Trichrome staining kit (Abcam, Cambridge, MA, USA) was used to measure intra-islet collagen deposition (34). Stained images were acquired at 40x magnification using an Aperio AT2 whole slide scanner (Leica Biosystems Inc, Concord, Ontario, Canada). The percentage of islet collagen deposition was determined using an ImageJ macro, which segments blue areas (collagen) from red areas in the image using colour deconvolution and measures total blue area per image as previously described (35).

## Statistical analysis

All data are expressed as means ± SEM. Statistical significance was analyzed using GraphPad Prism (version 6 GraphPad Software, San Diego, CA, USA) with 95% of confidence interval. The difference was analyzed using one-

way ANOVA followed by Tukey's *Post-Hoc* test. Differences were considered to be statistically significant when $p < 0.05$.

# Results

## NAC treatment improves glucose metabolism as dose- and time-dependent in HFD-induced diabetic mice

To determine the efficiency of NAC treatment in HFD-induced diabetic mice, both dose- and time-dependent study was established. Dosages of 10mM and 50mM NAC treatment were administered for prevention and intervention groups. HFD mice with 10mM NAC preventive or interventive treatment did not show changes in body weight or fasting blood glucose and had no improvement of glucose metabolism as determined by glucose and insulin tolerance tests (Supplementary Figure S2). Therefore, this report only focused on 50mM dosage of NAC treatment.

Bi-weekly body weights were recorded for the duration of treatment (Figure 1A). HFD mice showed significantly increased body weight compared to ND. There were no body weight significant differences between HFD, $HFD^{pNAC}$ and $HFD^{iNAC}$ groups (Figure 1B). Significant differences in average NAC intake were noted with highest NAC intake observed in the $HFD^{pNAC}$ group (21mg/mouse/day) compared to $HFD^{iNAC}$ (14mg/mouse/day) group and $HFD^{iNAC+}$ (16mg/mouse/day) group (Supplementary Figure S3A). Only $HFD^{iNAC}$ group showed significantly increased food intake when compared to ND group (Supplementary Figure S3B). A significantly increased fasting blood glucose was determined in the HFD mice when compared to ND (Figure 1C), however, an improved fasting blood glucose level was only observed in $HFD^{pNAC}$, not $HFD^{iNAC}$ mice (Figure 1C). Fed plasma insulin level was found to be significantly elevated in HFD mice compared to all other groups, and both $HFD^{pNAC}$ and $HFD^{iNAC}$ mice displayed a similar plasma insulin level as ND mice (Figure 1D). Fed circulating triglycerides and cholesterol were assessed and showed no significant differences between ND, HFD, and NAC treated HFD groups (Supplementary Figure S4).

Mice under HFD for 22 weeks demonstrated a progressive T2DM-like phenotype with impaired glucose and insulin tolerance when compared to ND mice (Figures 1E, F). Significantly improved glucose tolerance and insulin sensitivity in $HFD^{pNAC}$ mice was determined, which showed similar response as ND mice, however, this improvement was not found in $HFD^{iNAC}$ mice (Figures 1E, F). Furthermore, *in vivo* GSIS showed an observable improvement of glucose stimulated insulin secretion in $HFD^{pNAC}$ mice compared to HFD and $HFD^{iNAC}$ groups (Figure 1G). These data indicate that timing efficiency of NAC treatment is critical to normalize glucose metabolism in HFD-induced diabetic mice.

## NAC treatment preserves beta-cell mass and identity with reduction of beta-cell oxidative stress in HFD-induced diabetic mice

Double immunofluorescence staining for insulin and glucagon were used for determining islet density, beta- and alpha-cell mass, and beta-cell size (Figure 2A). Morphological analysis of beta-cell mass showed an increase in HFD pancreas, with no discernable changes in alpha cell mass or islet density (Figures 2B, C, F). The increased beta-cell mass in HFD mice was due to an enlargement in beta-cell size with low beta-cell number in the insulin positive area (Figures 2D, E) but was not caused by changes in beta-cell proliferation as determined using Ki67 co-staining (Figure 2G). Interestingly, HFD-induced enlargement of beta-cell mass was not observed in $HFD^{pNAC}$ and $HFD^{iNAC}$ groups (Figure 2B). Beta-cell mass, size, and number in $HFD^{pNAC}$ and $HFD^{iNAC}$ mouse islets displayed similar results as ND mice (Figures 2D, E).

When analyzing transcription factors (Pdx-1, MafA, and FoxO1) involved in beta-cell function and insulin secretion, it was found that nuclear Pdx-1 localization was significantly reduced in HFD mouse beta-cells compared to ND, $HFD^{pNAC}$ and $HFD^{iNAC}$ groups (Figures 3A, B). Both $HFD^{pNAC}$ and $HFD^{iNAC}$ groups showed significantly improved Pdx-1 nuclear localization, similar to ND group (Figures 3A, B). No obvious changes were found between experimental mice for MafA and FoxO1 nuclear localization in beta-cells (data not shown).

To examine NAC's impact on beta-cell oxidative stress, presence of 8OHdG in beta-cells was quantified using double staining for 8OHdG and insulin. The percentage of nuclear 8OHdG labelling in insulin-positive cells was significantly higher in the HFD mice than that of $HFD^{pNAC}$ and $HFD^{iNAC}$ groups (Figures 3C, D). A significant reduction of beta-cell 8OHdG labelling occurred in both NAC treated HFD mice, but no change observed in the ND mice when compared to HFD mice (Figures 3C, D).

## NAC treatment reduces active PaSCs in islets leading to lower intra-islet collagen deposition in HFD-induced diabetic mice

To determine whether NAC influenced intra-islet PaSCs activation during HFD induced oxidative stress, quantification of active PaSCs population was performed. Since marker αSMA labels active PaSCs and desmin marks both quiescent and active PaSCs, double immunofluorescence staining for αSMA and desmin was performed to verify their colocalization (Supplementary Figure S5). Quantification of intra-islet activated PaSCs labeled by αSMA staining revealed a significant increase in αSMA area in HFD mouse islets compared to ND and $HFD^{pNAC}$ mice (Figures 4A, B).

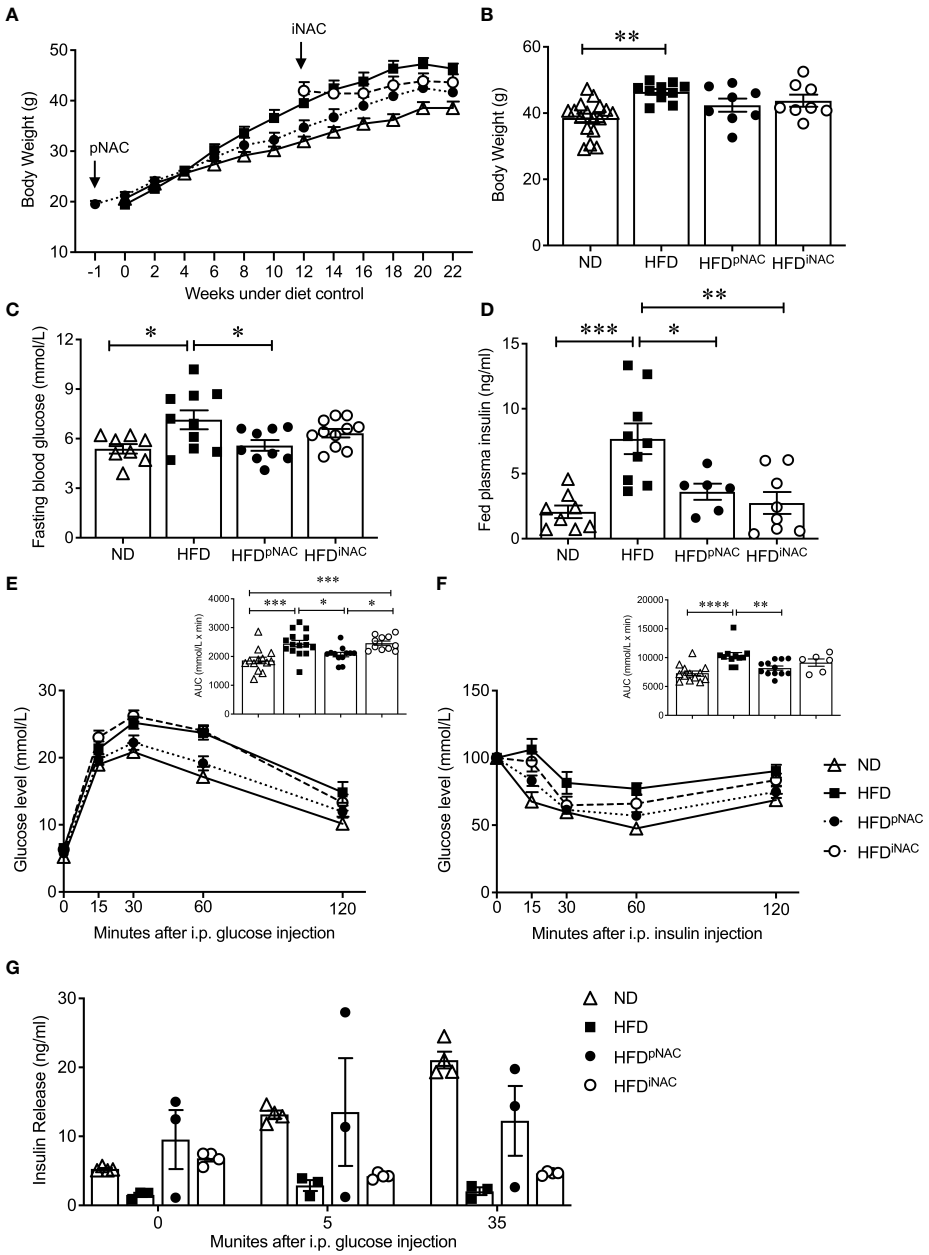


FIGURE 1
Preventive NAC treatment improves glucose metabolism in HFD-induced diabetic mice. **(A)** Recording of bi-weekly body weight for the duration of 22 weeks (n=8-17 mice/group). Measurement of **(B)** body weights, **(C)** overnight (~16 hours) fasting blood glucose and **(D)** fed plasma insulin levels (n=6-17 mice/group). **(E)** IPGTT and area under curve (AUC, n=10-14 mice/group), **(F)** IPITT and AUC (n=6-12 mice/group) and **(G)** *in vivo* GSIS (n=3-5 mice/group) of ND, HFD, $HFD^{pNAC}$ and $HFD^{iNAC}$ mice at 22 weeks. Control diets (ND): open triangle; HFD: closed square; $HFD^{pNAC}$: closed circle; $HFD^{iNAC}$: open circle. Data are expressed as means ± SEM. *$p$<0.05, **$p$<0.01, ***$p$<0.001, ****$p$<0.0001; analyzed using one-way ANOVA followed by Tukey's *Post-Hoc* test.

Although, $\alpha SMA^+$ staining in $HFD^{iNAC}$ islets showed a slight reduction, there was no statistically significant differences between HFD and $HFD^{iNAC}$ mice (Figures 4A, B). Measuring desmin population in the experimental groups showed a significantly higher percentage of $desmin^+$ staining present in HFD mouse islets compared to $HFD^{pNAC}$ and $HFD^{iNAC}$ mouse islets, but no significance observed in ND group (Figures 4C, D). Both data indicate that HFD induced PaSC activation could be diminished by NAC administration.

To further identify whether NAC treatment could abolish HFD-induced PaSC activation and subsequent intra-islet collagen deposition of islet fibrosis, quantification of intra-islet

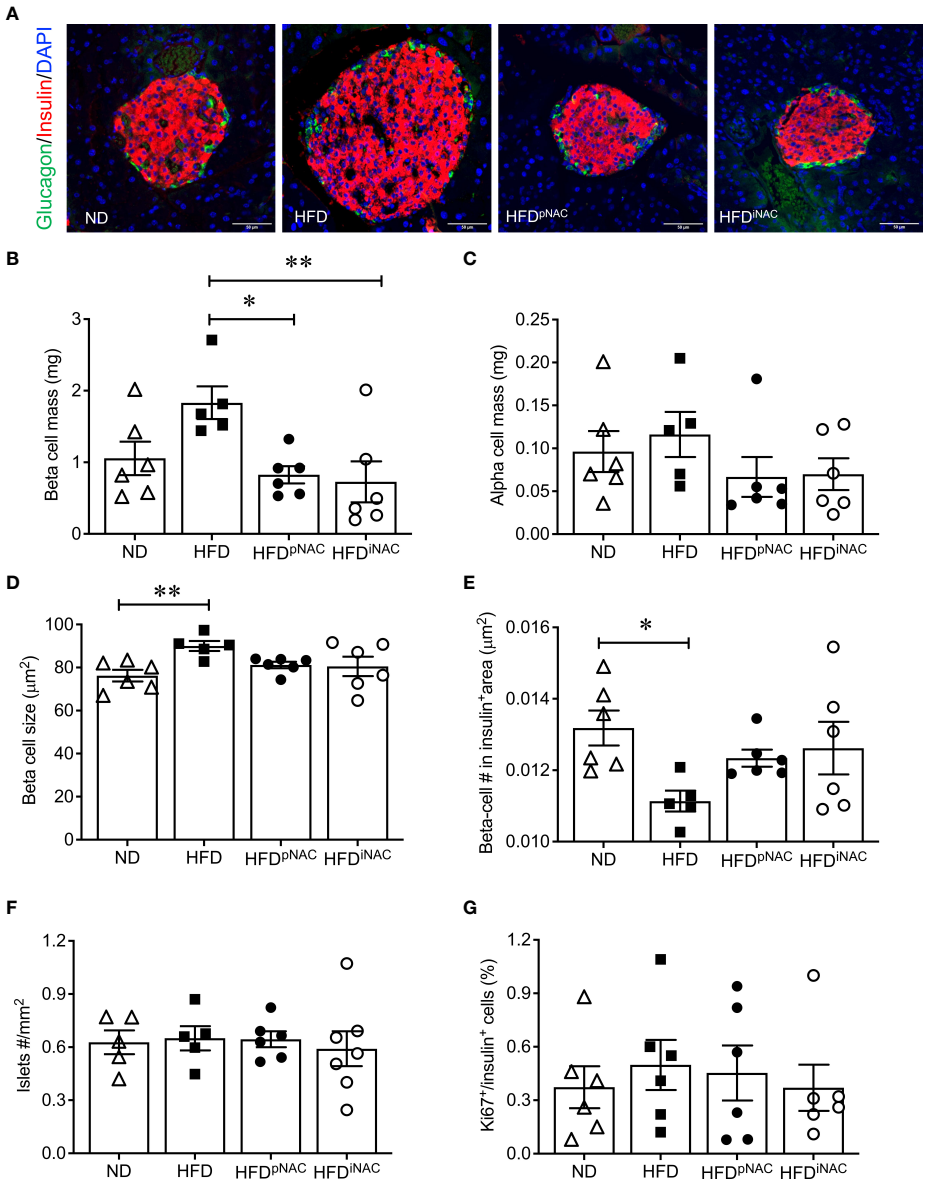


FIGURE 2
Histological analysis of NAC treated HFD pancreata demonstrated preserved beta-cell mass with no change in cell proliferation. **(A)** Representative double immunofluorescence images for islet morphology, detected by insulin (red) and glucagon (green) staining, and DAPI labeled nuclei (blue). Scale bars: 50µm. **(B)** Beta cell mass **(C)** alpha cell mass **(D)** beta cell size and **(E)** number **(F)** islet density in ND, HFD, HFD$^{pNAC}$ and HFD$^{iNAC}$ mouse pancrea at 22 weeks (n=5-6 pancreata/group). **(G)** Proliferation of beta cells quantified using Ki67 co-localization with insulin$^{+}$ cells (n=6 pancreata/group). ND: open triangle; HFD: closed square. HFD$^{pNAC}$: closed circle; HFD$^{iNAC}$: open circle. Data are expressed as means ± SEM. *$p$<0.05, **$p$<0.01, analyzed using one-way ANOVA followed by Tukey's *Post-Hoc* test.

collagen deposition was performed using trichrome stain (Figure 4E). Intra-islet collagen deposition was significantly increased in HFD mouse islets compared to ND mouse islets (Figure 4F), indicating HFD results in progression of islet fibrosis. A significant reduction of intra-islet collagen deposition in HFD$^{pNAC}$ mouse islets was found (Figures 4E, F), but this observation was not present in HFD$^{iNAC}$ mouse islets (Figures 4E, F).

## Prolonged intervention NAC treatment improves glucose metabolism in HFD-induced diabetic mice

Compared to HFD$^{pNAC}$ mice, HFD$^{iNAC}$ mice received NAC treatment 12 weeks after HFD initiation with total duration of 10 weeks NAC treatment. HFD$^{iNAC}$ mice showed no improvement in glucose metabolism, PaSCs activation or collagen deposition,

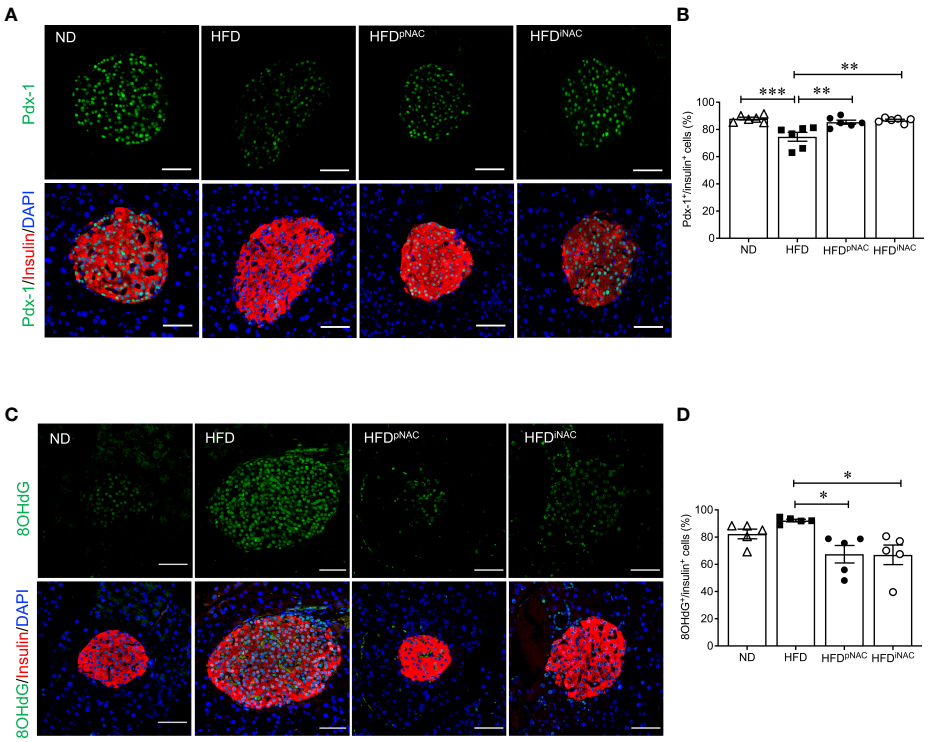


FIGURE 3
NAC treatment preserves beta-cell identity with reduction of beta-cell oxidative stress in HFD-induced diabetic mice. Representative double immunofluorescence images of **(A)** Pdx-1 (green) **(C)** 8OHdG (green) co-stained with insulin (red), nuclei are stained with DAPI (blue). Scale bars: 50µm. Quantification of nuclear **(B)** Pdx-1 **(D)** 8OHdG in insulin$^+$ cells of ND, HFD, HFD$^{pNAC}$ and HFD$^{iNAC}$ mouse pancreas at 22 weeks (n=5-6 pancreata/group). ND: open triangle; HFD: closed square; HFD$^{pNAC}$: closed circle; HFD$^{iNAC}$: open circle. Data are shown as means ± SEM. *$p$<0.05, **$p$<0.01, ***$p$<0.001, analyzed using one-way ANOVA followed by Tukey's *Post-Hoc* test.

indicating the duration of NAC treatment is critical. Therefore, a prolonged NAC treatment of up to 18 weeks (HFD$^{iNAC+}$) was established and investigated. Bi-weekly body weights were recorded up to 30 weeks (Figure 5A). HFD-fed mice had significantly increased body weight compared to ND-fed mice and HFD$^{iNAC+}$ mice (Figure 5B). Reduced body weight was observed in HFD$^{iNAC+}$ mice compared to HFD mice but remained significantly higher than that of ND mice (Figure 5B). Overnight fasting blood glucose was significantly elevated in both HFD and HFD$^{iNAC+}$ mice compared to ND mice (Figure 5C). However, hyperinsulinemia observed in HFD mice were significantly improved in HFD$^{iNAC+}$ mice, but remained significantly higher levels compared to ND mice (Figure 5D). Fed plasma triglyceride levels were significantly lower in HFD mice, but HFD$^{iNAC+}$ mice showed relatively elevated plasma triglycerides similar to ND mice (Figure 5E). Fed plasma cholesterol showed significant increase in both HFD and HFD$^{iNAC+}$ mice when compared to ND mice (Figure 5F). A significant impairment of glucose tolerance was present in HFD mice that was not observed in HFD$^{iNAC+}$ mice. HFD$^{iNAC+}$ mice which displayed similar glucose tolerance as ND mice (Figures 5G, H). A significant impairment of insulin tolerance was observed in HFD mice when compared to ND mice, however, insulin sensitivity showed a trend toward improvement in HFD$^{iNAC+}$ mice compared to HFD mice, but statistical significance was not reached (Figures 5I, J).

## Prolonged intervention NAC treatment preserves beta-cell mass and reduces intra-islet PaSCs activation in HFD-induced diabetic mice

Double immunofluorescence staining images for insulin and glucagon showed large islets present in HFD and HFD$^{iNAC+}$ mouse pancreas compared to ND group (Figure 6A). Morphometric analysis of islet number showed HFD mice have significantly elevated islet numbers compared to ND, however, islet number in HFD$^{iNAC+}$ is comparable to ND (Figure 6B). Beta-cell mass was significantly increased in HFD and was significantly improved in HFD$^{iNAC+}$ mice; HFD$^{iNAC+}$ mice and ND mice showed similar beta-cell masses (Figure 6C). There were no differences observed in alpha-cell mass found between groups (Figure 6D). HFD induced beta-cell dysfunction

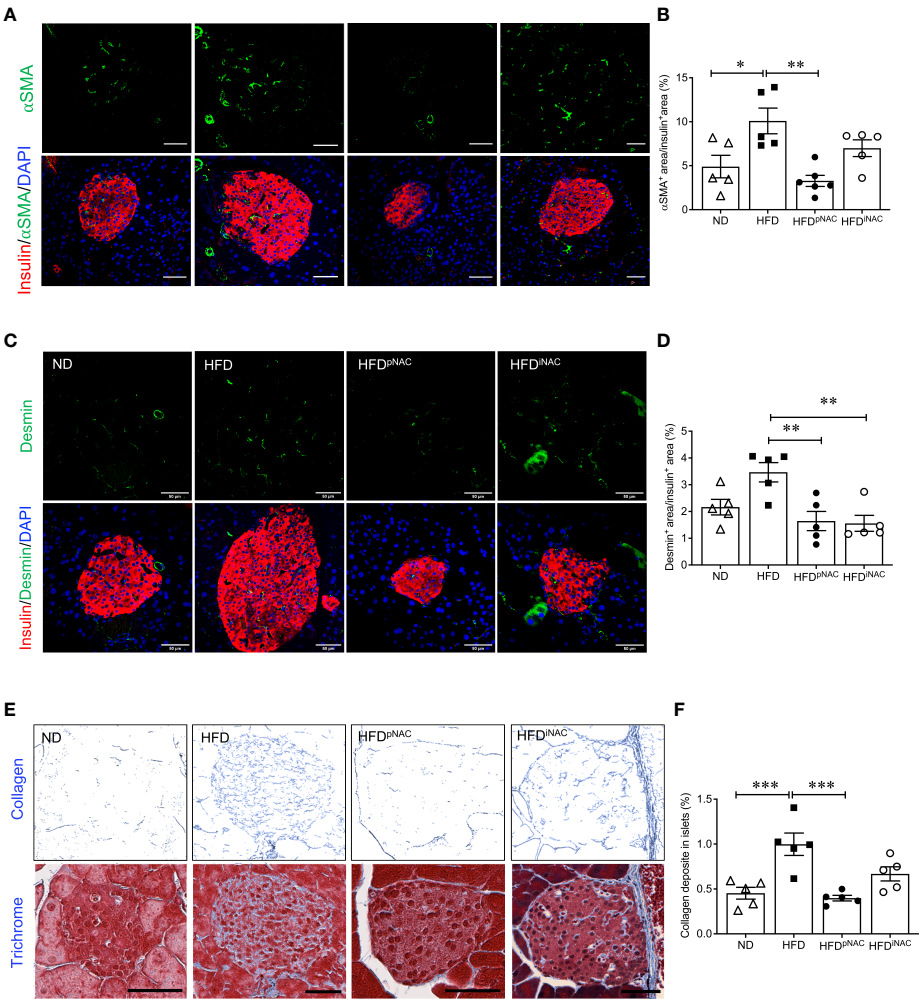


FIGURE 4
Preventive NAC treatment reduces intra-islet PaSCs activation and collagen deposition in HFD-induced diabetic mice. Representative double immunofluorescence images of **(A)** α-SMA (green) or **(C)** desmin (green) co-stained with insulin (red), nuclei are stained with DAPI (blue). Scale bars: 50μm. Quantification of intra-islet α-SMA **(B)** or desmin **(D)** area in ND, HFD, HFD$^{pNAC}$ and HFD$^{iNAC}$ mouse islets at 22 weeks (n=5-6 pancreata/group). **(E)** Representative trichrome staining images, scale bar: 50μm; and **(F)** quantification of intra-islet collagen deposition (n=5 pancreata/group). ND: open triangle; HFD: closed square; HFD$^{pNAC}$: closed circle; HFD$^{iNAC}$: open circle. Data are shown as means ± SEM. *$p$<0.05, **$p$<0.01, ***$p$<0.001, analyzed using one-way ANOVA followed by Tukey's *Post-Hoc* test.

with loss of nuclear Pdx-1 signals was significantly rescued in HFD$^{iNAC+}$ islets, which showed similar nuclear Pdx-1 localization as ND islets (Figure 6F). In parallel, HFD induced beta-cell oxidative stress labeled by 8OHdG$^{+}$ was also significantly improved in HFD$^{iNAC+}$ islets (Figures 6G, H). Furthermore, HFD$^{iNAC+}$ mice showed significantly lower intra-islet αSMA labeling (Figures 7A, B) with improved intra-islet collagen deposition (Figure 7C), which was not observed in HFD$^{iNAC}$ islets receiving a shorter duration of NAC treatment. HFD mice maintained higher level of αSMA labeling and collagen deposition in the intra-islets when compared to ND and HFD$^{iNAC+}$ mice (Figure 7). This data further verified that NAC treatment improves beta-cell identity, oxidative stress and PaSC induced fibrotic in HFD-induced diabetic islets is in a time-dependent manner.

## Discussion

This is a first *in vivo* study investigating the effects of antioxidant NAC on diabetic islets in HFD-induced diabetic mice. It is well documented that mice fed with HFD display dysregulation of glucose metabolism and beta-cell compensation with increased beta-cell oxidative stress and intra-islet PaSC activation, which produces excessive ECM and cytokines resulting in islet fibrosis (Figure 8). When HFD-induced

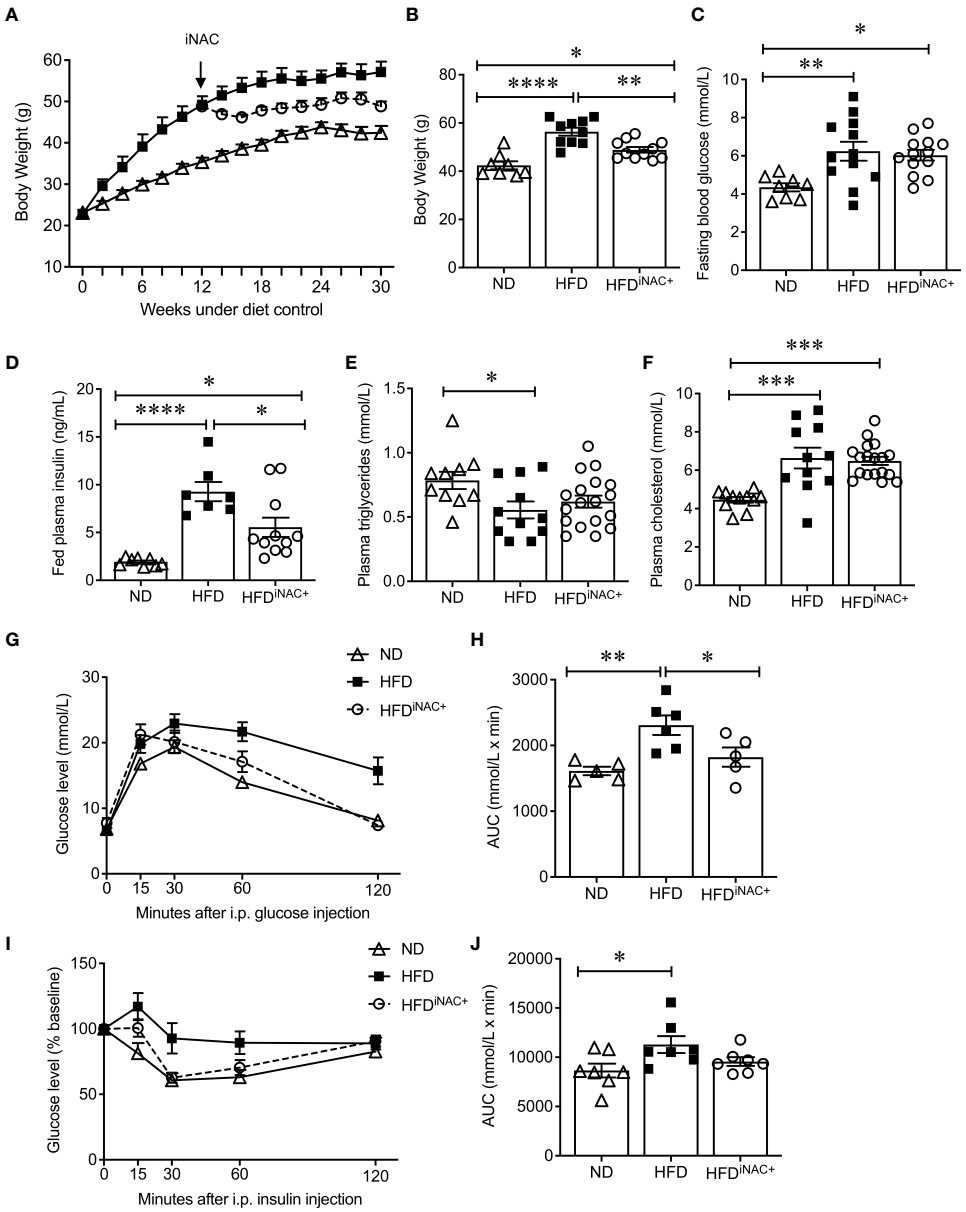


FIGURE 5
Prolonged intervention NAC treatment improves glucose metabolism in HFD-induced diabetic mice. **(A)** Recording of biweekly body weight for the duration of 30 weeks (n=8-12 mice/group). Measurement of **(B)** body weights, **(C)** overnight (~16 hours) fasting blood glucose, **(D)** fed plasma insulin, **(E)** triglycerides and **(F)** cholesterol levels (n=7-18 mice/group). **(G)** IPGTT and **(H)** AUC (n=5-6 mice/group), **(I)** IPITT and **(J)** AUC (n=7 mice/group) of ND, HFD and HFD$^{iNAC+}$ mice at 30 weeks. ND: open triangle; HFD: closed square; HFD$^{iNAC+}$: open circle. Data are expressed as means ± SEM. *$p$<0.05, **$p$<0.01, ***$p$<0.001, ****$p$<0.0001, analyzed using one-way ANOVA followed by Tukey's *Post-Hoc* test.

diabetic mice were administered NAC at an effective dose and time, significantly improved glucose tolerance and insulin sensitivity, and rescue from beta-cell overcompensation was determined. NAC treated HFD mice displayed a normalized beta-cell mass and size with significantly improved beta-cell identity, as Pdx-1 nuclear localization, and reduced beta-cell oxidative stress, labeled by 8-OHdG (Figure 8). Importantly, NAC diminished intra-islet PaSCs activation and PaSC-induced collagen deposition preventing fibrosis caused by HFD (Figure 8). This study suggests that antioxidant therapy using NAC is beneficial for maintaining healthy beta-cells and intra-islet quiescent PaSC population in HFD-induced diabetic mice and provides a better understanding of effective dose and time for antioxidant therapy in obesity related diabetes in humans.

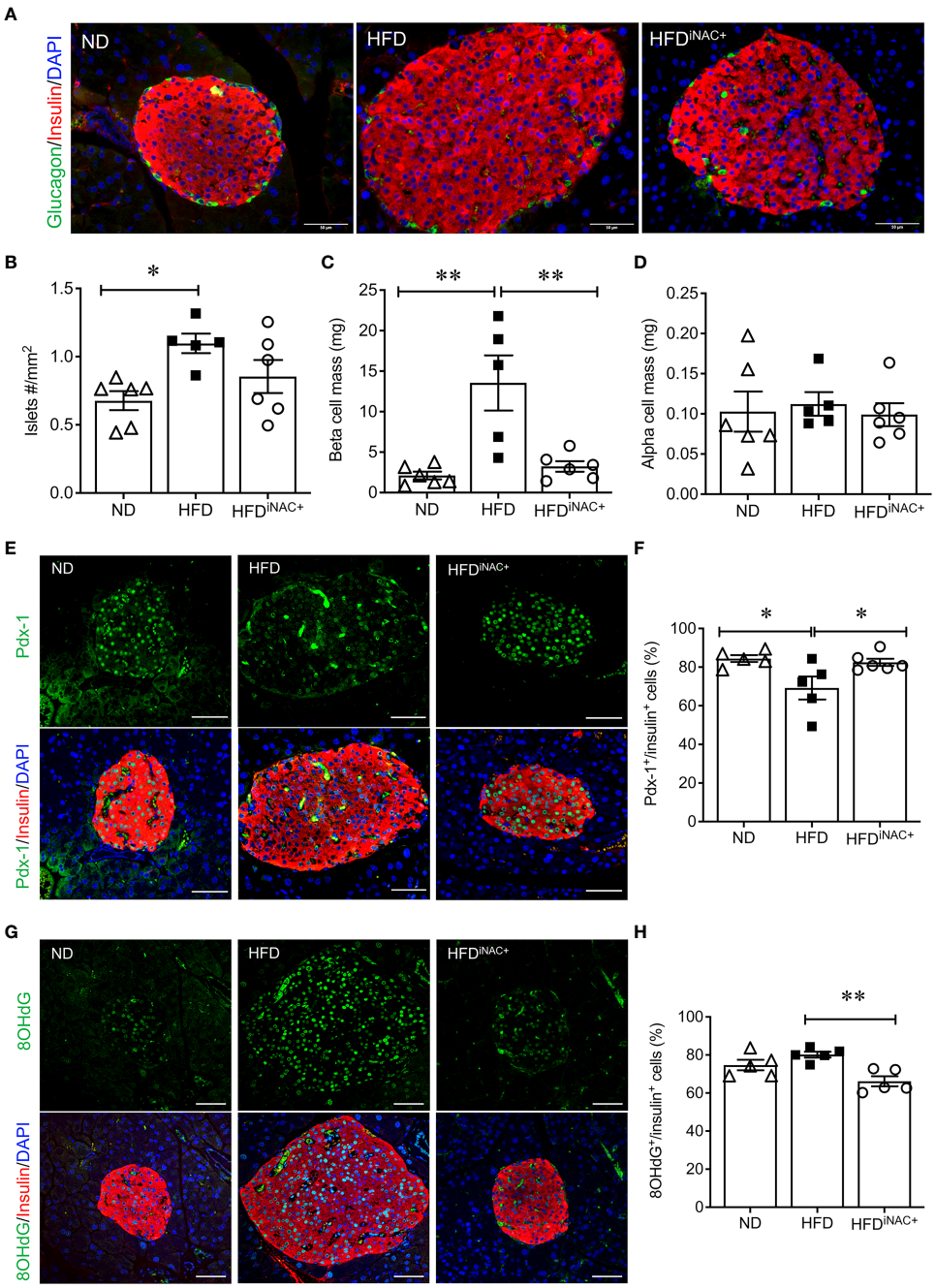


FIGURE 6
Prolonged intervention NAC treatment preserves beta-cell mass and nuclear Pdx-1 with lower 8OHdG in HFD-induced diabetic mice. **(A)** Representative double immunofluorescence images for islet morphology, detected by insulin (red) and glucagon (green) staining and DAPI labeled nuclei (blue). Scale bars: 50μm. Morphometric quantification of islet density **(B)** beta cell mass **(C)** and alpha cell mass **(D)** (n=5-6 pancreata/group). Representative double immunofluorescence images for **(E)** Pdx-1 (green) or **(G)** 8OHdG (green) and insulin (red), nuclei are stained with DAPI (blue). Scale bars: 50μm. Quantification of nuclear Pdx-1 **(F)** or 8OHdG **(H)** in insulin$^+$ cells of ND, HFD and HFD$^{iNAC+}$ mouse pancreas at 30 weeks (n=5-6 pancreata/group). ND: open triangle; HFD: closed square). HFD$^{iNAC+}$: open circle. Data are shown as means ± SEM. *$p$<0.05, **$p$<0.01, analyzed using one-way ANOVA followed by Tukey's *Post-Hoc* test.

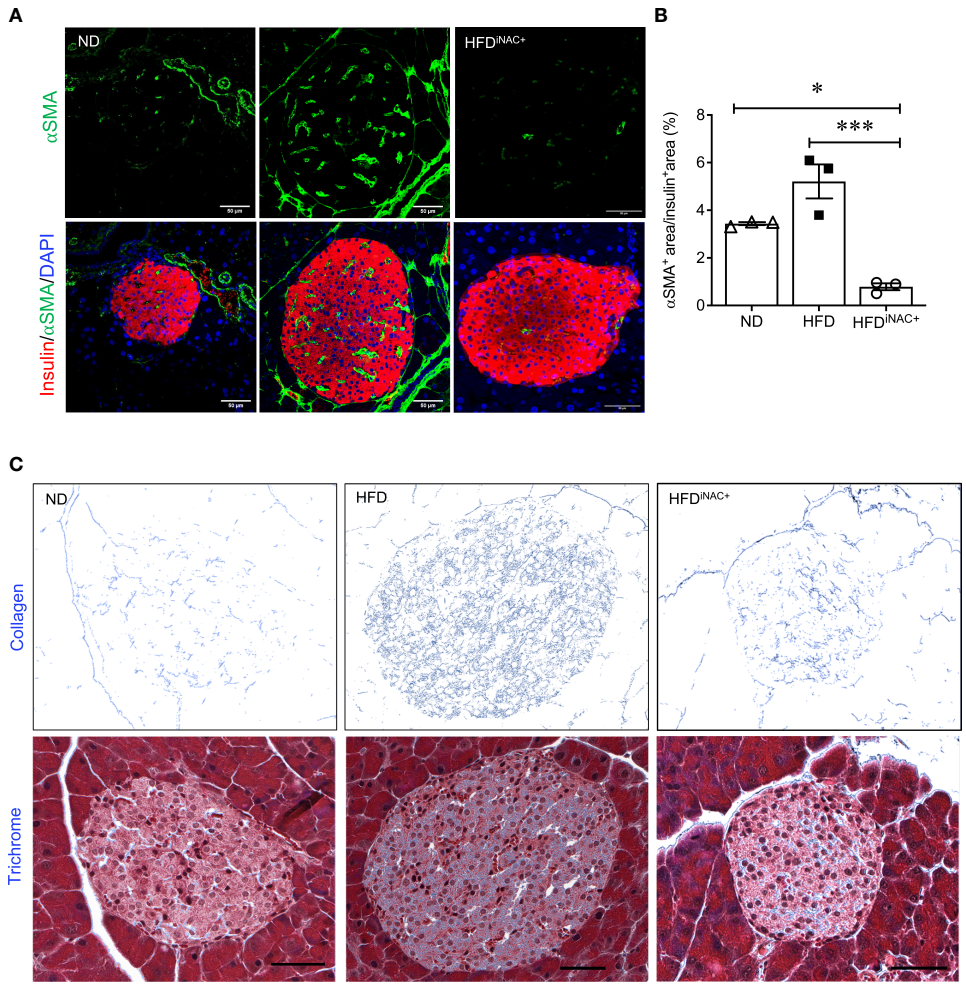


FIGURE 7
Prolonged intervention NAC treatment reduces intra-islet PaSCs activation and collagen deposition in HFD-induced diabetic mice. **(A)** Representative double immunofluorescence images of α-SMA (green) co-stained with insulin (red), nuclei are stained with DAPI (blue). Scale bars, 50μm; **(B)** quantification of intra-islet α-SMA area in ND, HFD and HFD$^{iNAC+}$ mouse islets at 30 weeks (n=3 pancreata/group). **(C)** Representative trichrome staining images of intra-islet collagen deposition. Scale bar: 50μm. ND: open triangle; HFD: closed square; HFD$^{iNAC+}$: open circle) Data are shown as means ± SEM. *$p$<0.05, ***$p$<0.001, analyzed using one-way ANOVA followed by Tukey's *Post-Hoc* test.

Identifying the optimal dosage during NAC therapy is critical for designing clinical trials. Use of sub-optimal or excessive antioxidant dosages of NAC could hinder NAC's positive anti-diabetic effects in T2DM patients (24). Based on previous reports (20, 21), two dosages of NAC (10mM and 50mM) were employed in this study and showed HFD mice that received 10mM NAC in drinking water for up to 22 weeks resulted in no improvements in glucose tolerance and insulin sensitivity. Whereas, administration at 50mM in drinking water showed significant improvements in glucose metabolism, which was consistent with the findings by Falach-Malik et al. (21). It was noted that NAC at 50mM dosage did not cause a significant reduction in body weights, despite increased caloric intake in both HFD$^{pNAC}$ and HFD$^{iNAC}$ mice under 22 weeks HFD feeding. Previous reports suggest that this dosage potentially caused an increase in motor activity and/or metabolic activity which may have been compensated for by increasing food intake resulting in no net loss of weight (22, 36). However, prolonged intervention NAC in HFD$^{iNAC+}$ mice displayed significantly reduced body weights compared to HFD mice under 30 weeks HFD feeding, suggesting NAC treatment is associated with weight loss and may account for required time to take effect.

Previous studies suggest using NAC at an earlier time point increased effectiveness for improving glucose tolerance and insulin sensitivity related to weight loss in HFD mice (21, 22). HFD mice that received preventive NAC treatment for 23 weeks showed significantly improved glucose and insulin tolerance, but this was not observed at 10 weeks. Prolonged intervention NAC

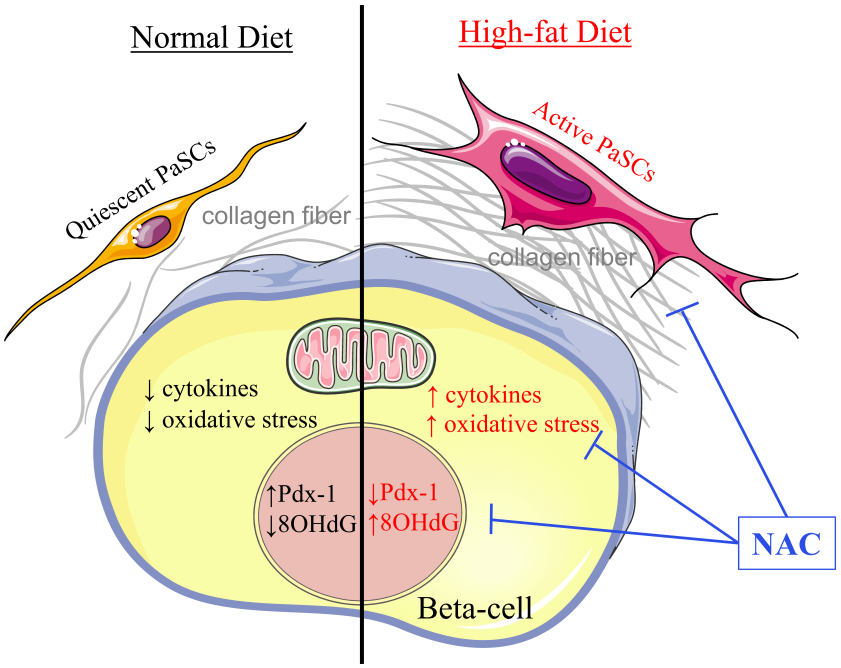


FIGURE 8
Proposed model of NAC maintains healthy beta-cells and quiescent PaSCs in HFD-induced diabetic mouse islet. In a healthy condition under normal chow diet, intra-islet PaSCs are quiescent; they produce suitable cytokines and ECM for maintaining islet structure and facilitating healthy beta-cell function. Under high-fat diet, increased oxidative stress promoted intra-islet PaSC activation resulting in increased cytokine production and ECM deposition which diminished beta-cell identity and function. Given NAC treatment, HFD islets showed significantly reduced oxidative stress and intra-islet PaSC activation with enhanced beta-cell identity and function.

(18 weeks) administration to HFD mice displayed improvement similar to NAC prevention treated mice, indicating that positive anti-diabetic effects of NAC in HFD-induced diabetic mice require up to 18 weeks of prevention or intervention NAC treatment. Although, there was no change in fed plasma lipid level in mice with 22 weeks HFD feeding, HFD-induced hepatic insufficient export of triglycerides was observed in HFD mice with 30 weeks feeding, this impaired liver export of triglycerides was rescued in $HFD^{iNAC+}$ mice that showed normalised triglycerides level comparable to ND mice. This data indicates that NAC improved glucose metabolism and may be associated with improved liver function to reduce hepatic triglyceride accumulation in order to reduce gluconeogenesis and enhance insulin signalling (37, 38). Taken together, this study suggests that adequate duration of administration is crucial for NAC to be effective as an antioxidative therapy in treating diet-induced obesity diabetes.

Mice fed with HFD for 22 or 30 weeks showed not only impaired metabolic outcomes, but also significant alterations to islet architecture indicating a beta-cell compensation response. HFD mice with NAC prevention or intervention treatment can prevent or rescue this beta-cell overcompensation with significantly normalized beta-cell mass and size. This demonstrates that NAC is effective at maintaining beta-cell function during HFD-induced stress. It is agreed that transcription factor Pdx-1 plays a critical role in regulating beta-cell function by activating genes essential for beta-cell identity; loss of beta-cell identity contributes to the pathogenesis of type 2 diabetes (39). A previous study by Leenders et al. proposed under elevated oxidative stress conditions, beta-cells dedifferentiate into other islet cell types leading to reduced beta-cell identity (40). In the present study, loss of beta-cell identity and increased beta-cell oxidative stress was displayed in HFD mice, however, $HFD^{pNAC}$ and $HFD^{iNAC}$ islets showed preserved or restored beta-cell Pdx-1 nuclear localization, and reduced beta-cell oxidative stress. These findings are supported by previous reports that demonstrated NACs ability to improve Pdx-1 and insulin content in beta-cells in a genetic obesity model of T2DM (26), and to prevent glucose toxicity-induced impaired Pdx-1 binding to the insulin gene promoter in beta-cell line *in vitro* and reduce plasma 8-OHdG oxidative stress level in Zucker diabetic fatty rats (41). Although the exact mechanism of NACs action on beta-cells remains to be elucidated, it is a well-known that NAC is a biosynthetic precursor of glutathione (23). It also contains a thiol group exerting its antioxidant effects through electron donation (42)

and has recently been investigated for its potential intracellular conversion to sulfane sulfur species to scavenge oxidants (43). NAC also produces anti-inflammatory actions by indirectly inhibiting the activation of the redox-sensitive pathway NF-κB in order to prevent inflammatory responses which lead to loss of Pdx-1 expression (42). Since the present study did not evaluate inflammatory markers, it would be interesting for future studies to investigate the role of NAC on inflammatory markers in the setting of diet-induced obesity.

PaSCs in islets play a critical role in controlling ECM, growth factors and cytokine secretion. Over-active PaSCs are involved in beta-cell compensation in the early stages of T2DM progression (44). Furthermore, clinical studies have shown higher levels of αSMA and islet fibrosis in T2DM patients (45), such evidence was also observed in the current study where HFD mice showed significantly elevated intra-islet $\alpha SMA^+$ cells with excessive collagen deposition. Administration of NAC to HFD mice displayed significantly reduced intra-islet oxidative stress and intra-islet $\alpha SMA^+$, which corresponded to significantly reduced intra-islet fibrosis. This observation matches previous *in vitro* reports that NAC is capable of reducing PaSC activation and reverting cells to a quiescent state (46–48). NAC treatment results in increased vitamin A droplets indicative of quiescent PaSCs (47). It was noted that prevention NAC treated $HFD^{pNAC}$ mice showed similar PaSC activation and islet collagen staining as ND islets, suggesting that initiating NAC therapy is most beneficial to prevent PaSCs activation and intra-islet collagen deposition caused by HFD. However, intervention NAC treated islets did not show a significant improvement until 18 weeks NAC treatment, indicating PaSCs activation begin rapidly after HFD-induced stress, and reverting active PaSCs and collagen accumulation requires sufficient time with antioxidant treatment. A study on diabetic cardiac function in C57/B6 mice supports these results as they determined NAC is beneficial at improving cardiac function and reducing cardiac fibrosis, most noticeably in mice which received earlier and longer treatment (28). However, the potential mechanisms of NAC action on intra-islet PaSCs require further *in vivo* investigation.

In summary, the present study provides evidence that NAC is effective at protecting beta-cells from overcompensation and loss of beta-cell identity observed during T2DM progression in mice. The efficacy of NAC treatment in HFD-induced diabetic mice was dependent on dosage and duration of treatment. This study supports previous reports showing the ability of NAC to improve metabolic outcomes in mouse models of T2DM. Importantly, it provides first evidence of NAC's effect on the intra-islet environment where beta-cell identity was protected, and oxidative stress and PaSC activation was diminished. Ultimately, the demonstrated benefits of antioxidant NAC on diet-induced obesity and diabetes indicates that it should be further investigated as an adjuvant therapy in controlling T2DM progression in humans.

## Data availability statement

The original contributions presented in the study are included in the article/Supplementary Material. Further inquiries can be directed to the corresponding author.

## Ethics statement

The animal study was reviewed and approved by University of Western Ontario Animal User Subcommittee.

## Author contributions

MS and MW contributed to an *in vivo* mouse feeding and glucose metabolic study, data acquisition, interpretation of data, and preparation of the submitted manuscript. MB contributed to the maintenance of animals, data acquisition and preparation of the submitted manuscript. GS, MR, SZ and CS contributed to data acquisition. NB contributed interpretation of data and manuscript discussion. RW contributed to the design of experiments within this project, interpretation of data and preparation of the submitted manuscript. All authors contributed to the article and approved the submitted version.

## Funding

This study was funded by the Canadian Institutes of Health Research (grant# 152944).

## Acknowledgments

This work was supported by grants from the Canadian Institutes of Health Research.

## Conflict of interest

The authors declare that the research was conducted in the absence of any commercial or financial relationships that could be construed as a potential conflict of interest.

## Publisher's note

claim that may be made by its manufacturer, is not guaranteed or endorsed by the publisher.

## Supplementary material

The Supplementary Material for this article can be found online at: https://www.frontiersin.org/articles/10.3389/fendo.2022.938680/full#supplementary-material

SUPPLEMENTARY FIGURE 1
Experimental timeline to determine the time-dependent of NAC administration on high fat diet-induced diabetic mice. Both normal diet (ND) and high fat diet (HFD) experimental groups were established at age of 6 weeks. pNAC: preventative NAC was started at 5 weeks of age, one week prior to HFD diet start and had a total of 23 weeks of NAC treatment; iNAC: intervention NAC was given at 18 weeks of age, 12 weeks after HFD diet start and had a total of 10 weeks of NAC treatment; iNAC$^{+}$: intervention NAC was given at 18 weeks of age, 12 weeks after HFD diet start and had a total of 18 weeks of NAC treatment.

SUPPLEMENTARY FIGURE 2
10mM NAC treatment did not improve glucose metabolism in HFD-induced diabetic mice. **(A)** Body weight, **(B)** fasted blood glucose levels, **(C)** IPGTT, **(D)** area under curve (AUC) analysis of IPGTT, **(E)** IPITT and **(F)** AUC analysis of IPITT results from ND, HFD, HFD$^{pNAC}$ and HFD$^{iNAC}$ mice during 22-week experiment. Data are expressed means ± SEM (n=3-17 mice per experimental group). *p<0.05, **p<0.01, ***p<0.001 vs. ND, determined by one-way ANOVA followed by Tukey's multiple comparisons test.

SUPPLEMENTARY FIGURE 3
NAC and food intake in HFD-induced diabetic mice. **(A)** Average NAC intake for mice undergoing prevention (pNAC), intervention (iNAC) and extend intervention (iNAC+) treatment. **(B)** Food intake in ND, HFD, HFD$^{pNAC}$ and HFD$^{iNAC}$ mice and **(C)** Food intake in ND, HFD and HFD$^{iNAC+}$ mice. Data are expressed means ± SEM (*n=5-11* mice per experimental group). *p<0.05, **p<0.01, ***p<0.001 vs. ND or as indicated, determined by one-way ANOVA followed by Tukey's multiple comparisons test.

SUPPLEMENTARY FIGURE 4
Plasma lipid levels in ND, HFD, HFD$^{pNAC}$ and HFD$^{iNAC}$ mice. Fed plasma triglycerides **(A)** and cholesterol **(B)**. Data are expressed means ± SEM (*n=8-11* mice per experimental group).

SUPPLEMENTARY FIGURE 5
Correlation of desmin (green) and αSMA (red) in the islet as dash-line outlined. Lower panel displays enlarged images, arrows indicate co-staining, arrowheads label single staining. Scale bar: 50μm.

## References


1. Prentki M, Nolan CJ. Islet β cell failure in type 2 diabetes. *J Clin Invest* (2006) 116:1802–12. doi: 10.1172/JCI29103

2. Keane KN, Cruzat VF, Carlessi R, de Bittencourt PIH, Newsholme P. Molecular events linking oxidative stress and inflammation to insulin resistance and β-cell dysfunction. *Oxid Med Cell Longev* (2015) 2015:181643. doi: 10.1155/2015/181643

3. McAdam-Marx C, Mukherjee J, Bellows BK, Unni S, Ye X, Iloeje U, et al. Evaluation of the relationship between weight change and glycemic control after initiation of antidiabetic therapy in patients with type 2 diabetes using electronic medical record data. *Diabetes Res Clin Pract* (2014) 103:402–11. doi: 10.1016/j.diabres.2013.12.038

4. Temelkova-Kurktschiev T, Siegert G, Bergmann S, Henkel E, Koehler C, Jaroß W, et al. Subclinical inflammation is strongly related to insulin resistance but not to impaired insulin secretion in a high risk population for diabetes. *Metabolism* (2002) 51:743–9. doi: 10.1053/meta.2002.32804

5. Butler AE, Janson J, Bonner-Weir S, Ritzel R, Rizza RA, Butler PC. β-cell deficit and increased β-cell apoptosis in humans with type 2 diabetes. *Diabetes* (2003) 52:102–10. doi: 10.2337/diabetes.52.1.102

6. Swisa A, Glaser B, Dor Y. Metabolic stress and compromised identity of pancreatic beta cells. *Front Genet* (2017) 8:21. doi: 10.3389/fgene.2017.00021

7. Omary MB, Lugea A, Lowe AW, Pandol SJ. The pancreatic stellate cell: a star on the rise in pancreatic diseases. *J Clin Invest* (2007) 117:50–9. doi: 10.1172/JCI30082

8. Apte MV, Pirola RC, Wilson JS. Pancreatic stellate cells: a starring role in normal and diseased pancreas. *Front Physiol* (2012) 3:344. doi: 10.3389/FPHYS.2012.00344

9. Riopel M, Li J, Fellows GF, Goodyer CG, Wang R. Ultrastructural and immunohistochemical analysis of the 8-20 week human fetal pancreas. *Islets* (2014) 6(4):e982949. doi: 10.4161/19382014.2014.982949

10. Li J, Chen B, Fellows GF, Goodyer CG, Wang R. Activation of pancreatic stellate cells is beneficial for exocrine but not endocrine cell differentiation in the developing human pancreas. *Front Cell Dev Biol* (2021) 9:694276. doi: 10.3389/fcell.2021.694276

11. Sekhar RV, Mckay SV, Patel SG, Guthikonda AP, Reddy VT, Balasubramanyam A, et al. Glutathione synthesis is diminished in patients with uncontrolled diabetes and restored by dietary supplementation with cysteine and glycine. *Diabetes Care* (2011) 34:162–7. doi: 10.2337/DC10-1006

12. Rehman K, Akash MSH. Mechanism of generation of oxidative stress and pathophysiology of type 2 diabetes mellitus: How are they interlinked? *J Cell Biochem* (2017) 118:3577–85. doi: 10.1002/JCB.26097

13. Sakuraba H, Mizukami H, Yagihashi N, Wada R, Hanyu C, Yagihashi S. Reduced beta-cell mass and expression of oxidative stress-related DNA damage in the islet of Japanese type II diabetic patients. *Diabetologia* (2002) 45:85–96. doi: 10.1007/S125-002-8248-Z

14. Miki A, Ricordi C, Sakuma Y, Yamamoto T, Misawa R, Mita A, et al. Divergent antioxidant capacity of human islet cell subsets: A potential cause of beta-cell vulnerability in diabetes and islet transplantation. *PloS One* (2018) 13:e0196570. doi: 10.1371/JOURNAL.PONE.0196570

15. Kawamori D, Kajimoto Y, Kaneto H, Umayahara Y, Fujitani Y, Miyatsuka T, et al. Oxidative stress induces nucleo-cytoplasmic translocation of pancreatic transcription factor PDX-1 through activation of c-jun NH2-terminal kinase. *Diabetes* (2003) 52:2896–904. doi: 10.2337/diabetes.52.12.2896

16. Lee E, Ryu GR, Ko SH, Ahn YB, Song KH. A role of pancreatic stellate cells in islet fibrosis and β-cell dysfunction in type 2 diabetes mellitus. *Biochem Biophys Res Commun* (2017) 485:328–34. doi: 10.1016/j.bbrc.2017.02.082

17. Hong O-K, Lee S-H, Rhee M, Ko S-H, Cho J-H, Choi Y-H, et al. Hyperglycemia and hyperinsulinemia have additive effects on activation and proliferation of pancreatic stellate cells: possible explanation of islet-specific fibrosis in type 2 diabetes mellitus. *J Cell Biochem* (2007) 101:665–75. doi: 10.1002/jcb.21222

18. Hayden MR, Habibi J, Joginpally T, Karuparthi PR, Sowers JR. Ultrastructure study of transgenic Ren2 rat aorta – part 1: Endothelium and intima. *Cardiorenal Med* (2012) 2:66–82. doi: 10.1159/000335565

19. Kikuta K, Masamune A, Hamada S, Takikawa T, Nakano E, Shimosegawa T. Pancreatic stellate cells reduce insulin expression and induce apoptosis in pancreatic β-cells. *Biochem Biophys Res Commun* (2013) 433:292–7. doi: 10.1016/J.BBRC.2013.02.095

20. Ma Y, Gao M, Liu D. N-acetylcysteine protects mice from high fat diet-induced metabolic disorders. *Pharm Res* (2016) 33:2033–42. doi: 10.1007/s11095-016-1941-1

21. Falach-Malik A, Rozenfeld H, Chetboun M, Rozenberg K, Elyasiyan U, Sampson SR, et al. N-Acetyl-L-Cysteine inhibits the development of glucose intolerance and hepatic steatosis in diabetes-prone mice. *Am J Transl Res* (2016) 8:3744–56.

22. Shen F-C, Weng S-W, Tsao C-F, Lin H-Y, Chang C-S, Lin C-Y, et al. Early intervention of n-acetylcysteine better improves insulin resistance in diet-induced obesity mice. *Free Radic Res* (2018) 52:1296–310. doi: 10.1080/10715762.2018.1447670

23. Zhitkovich A. N -acetylcysteine: Antioxidant, aldehyde scavenger, and more. *Chem Res Toxicol* (2019) 32:1318–9. doi: 10.1021/acs.chemrestox.9b00152

24. Uraz S, Tahan G, Aytekin H, Tahan V. N-acetylcysteine expresses powerful anti-inflammatory and antioxidant activities resulting in complete improvement of acetic acid-induced colitis in rats. *Scand J Clin Lab Invest* (2013) 73:61–6. doi: 10.3109/00365513.2012.734859

25. Roma LP, Oliveira CAM, Carneiro EM, Albuquerque GG, Boschero AC, Souza KLA. N-acetylcysteine protects pancreatic islet against glucocorticoid toxicity. *Redox Rep* (2011) 16:173–80. doi: 10.1179/1351000211Y.0000000006

26. Kaneto H, Kajimoto Y, Miyagawa J, Matsuoka T, Fujitani Y, Umayahara Y, et al. Beneficial effects of antioxidants in diabetes: possible protection of pancreatic beta-cells against glucose toxicity. *Diabetes* (1999) 48:2398–406. doi: 10.2337/DIABETES.48.12.2398

27. Szkudlinska MA, Von Frankenberg AD, Utzschneider KM. The antioxidant n-acetylcysteine does not improve glucose tolerance or β-cell function in type 2 diabetes. *J Diabetes Complications* (2016) 30:618. doi: 10.1016/J.JDIACOMP.2016.02.003

28. Liu C, Lu XZ, Shen MZ, Xing CY, Ma J, Duan YY, et al. N-acetyl cysteine improves the diabetic cardiac function: possible role of fibrosis inhibition. *BMC Cardiovasc Disord* (2015) 15:84. doi: 10.1186/S12872-015-0076-3

29. Oakie A, Feng ZC, Li J, Silverstein J, Yee SP, Wang R. Long-term c-kit overexpression in beta cells compromises their function in ageing mice. *Diabetologia* (2019) 62:1430–44. doi: 10.1007/S00125-019-4890-5

30. Feng ZC, Riopel M, Popell A, Wang R. A survival kit for pancreatic beta cells: stem cell factor and c-kit receptor tyrosine kinase. *Diabetologia* (2015) 58:654–65. doi: 10.1007/S00125-015-3504-0

31. Yashpal NK, Li J, Wang R. Characterization of c-kit and nestin expression during islet cell development in the prenatal and postnatal rat pancreas. *Dev Dyn* (2004) 229:813–25. doi: 10.1002/DVDY.10496

32. Feng Z-C, Riopel M, Li J, Donnelly L, Wang R. Downregulation of fas activity rescues early onset of diabetes in c-kit wv/+ mice. *Am J Physiol Metab* (2013) 304:E557–65. doi: 10.1152/ajpendo.00453.2012

33. Feng ZC, Donnelly L, Li J, Krishnamurthy M, Riopel M, Wang R. Inhibition of Gsk3β activity improves β-cell function in c-KitWv/+ male mice. *Lab Invest* (2012) 92:543–55. doi: 10.1038/LABINVEST.2011.200

34. Riopel M, Krishnamurthy M, Li J, Liu S, Leask A, Wang R. Conditional β1-integrin-deficient mice display impaired pancreatic β cell function. *J Pathol* (2011) 224:45–55. doi: 10.1002/PATH.2849

35. Peters KM, Zhang R, Park C, Nong Z, Yin H, Wilson RB, et al. Vitamin d intervention does not improve vascular regeneration in diet-induced obese male mice with peripheral ischemia. *J Nutr Biochem* (2019) 70:65–74. doi: 10.1016/J.JNUTBIO.2019.04.010

36. Novelli ELB, Santos PP, Assalin HB, Souza G, Rocha K, Ebaid GX, et al. N-acetylcysteine in high-sucrose diet-induced obesity: Energy expenditure and metabolic shifting for cardiac health. *Pharmacol Res* (2009) 59:74–9. doi: 10.1016/J.PHRS.2008.10.004

37. Ress C, Kaser S. Mechanisms of intrahepatic triglyceride accumulation. *World J Gastroenterol* (2016) 22:1664–73. doi: 10.3748/WJG.V22.I4.1664

38. Samuel VT, Liu ZX, Qu X, Elder BD, Bilz S, Befroy D, et al. Mechanism of hepatic insulin resistance in non-alcoholic fatty liver disease. *J Biol Chem* (2004) 279:32345–53. doi: 10.1074/JBC.M313478200

39. Gao T, McKenna B, Li C, Reichert M, Nguyen J, Singh T, et al. Pdx1 maintains β cell identity and function by repressing an α cell program. *Cell Metab* (2014) 19:259–71. doi: 10.1016/J.CMET.2013.12.002

40. Leenders F, Groen N, de Graaf N, Engelse MA, Rabelink TJ, de Koning EJP, et al. Oxidative stress leads to β-cell dysfunction through loss of β-cell identity. *Front Immunol* (2021) 12:690379. doi: 10.3389/fimmu.2021.690379

41. Tanaka Y, Gleason CE, Tran POT, Harmon JS, Robertson RP. Prevention of glucose toxicity in HIT-T15 cells and zucker diabetic fatty rats by antioxidants. *Proc Natl Acad Sci U.S.A.* (1999) 96:10857–62. doi: 10.1073/PNAS.96.19.10857

42. Lasram MM, Dhouib IB, Annabi A, El Fazaa S, Gharbi N. A review on the possible molecular mechanism of action of n-acetylcysteine against insulin resistance and type-2 diabetes development. *Clin Biochem* (2015) 48:1200–8. doi: 10.1016/J.CLINBIOCHEM.2015.04.017

43. Pedre B, Barayeu U, Ezeriņa D, Dick TP. The mechanism of action of n-acetylcysteine (NAC): The emerging role of H2S and sulfane sulfur species. *Pharmacol Ther* (2021) 228:107916. doi: 10.1016/J.PHARMTHERA.2021.107916

44. Ryu GR, Lee E, Chun H-J, Yoon K-H, Ko S-H, Ahn Y-B, et al. Oxidative stress plays a role in high glucose-induced activation of pancreatic stellate cells. *Biochem Biophys Res Commun* (2013) 439:258–63. doi: 10.1016/j.bbrc.2013.08.046

45. Kim JW, Ko SH, Cho JH, Sun C, Hong OK, Lee SH, et al. Loss of beta-cells with fibrotic islet destruction in type 2 diabetes mellitus. *Front Biosci* (2008) 13:6022–33. doi: 10.2741/3133

46. Jesnowski R, Fürst D, Ringel J, Chen Y, Schrödel A, Kleeff J, et al. Immortalization of pancreatic stellate cells as an *in vitro* model of pancreatic fibrosis: deactivation is induced by matrigel and n-acetylcysteine. *Lab Invest* (2005) 85:1276–91. doi: 10.1038/labinvest.3700329

47. Feng H, Moriyama T, Ohuchida K, Sheng N, Iwamoto C, Shindo K, et al. N-acetyl cysteine induces quiescent-like pancreatic stellate cells from an active state and attenuates cancer-stroma interactions. *J Exp Clin Cancer Res* (2021) 40:133. doi: 10.1186/S13046-021-01939-1

48. Asaumi H, Watanabe S, Taguchi M, Tashiro M, Otsuki M. Externally applied pressure activates pancreatic stellate cells through the generation of intracellular reactive oxygen species. *Am J Physiol - Gastrointest Liver Physiol* (2007) 293:G972–8. doi: 10.1152/ajpgi.00018.2007

frontiers | Frontiers in Endocrinology

TYPE Systematic Review
PUBLISHED 02 September 2022
DOI 10.3389/fendo.2022.968481



OPEN ACCESS

EDITED BY
Alexandre Gabarra Oliveira,
São Paulo State University, Brazil

REVIEWED BY
Yingshuai Li,
Beijing University of Chinese Medicine, China
Ai Bingwei,
Jiangsu Provincial Hospital of Traditional Chinese Medicine, China

*CORRESPONDENCE
Changcai Xie
hxie114@163.com
Jiqiang Li
lijiqiangjizhen@163.com
Yu Chen
chenyu@gzucm.edu.cn

SPECIALTY SECTION
This article was submitted to Obesity, a section of the journal Frontiers in Endocrinology

RECEIVED 14 June 2022
ACCEPTED 05 August 2022
PUBLISHED 02 September 2022

CITATION
Chen J, Gu Y, Yin L, He M, Liu N, Lu Y, Xie C, Li J and Chen Y (2022) Network meta-analysis of curative efficacy of different acupuncture methods on obesity combined with insulin resistance.
*Front. Endocrinol.* 13:968481.
doi: 10.3389/fendo.2022.968481



# Network meta-analysis of curative efficacy of different acupuncture methods on obesity combined with insulin resistance

Jiankun Chen, Yingming Gu, Lihong Yin, Minyi He, Na Liu, Yue Lu, Changcai Xie*, Jiqiang Li* and Yu Chen*

State Key Laboratory of Dampness Syndrome of Chinese Medicine, The Second Affiliated Hospital of Guangzhou University of Chinese Medicine, Guangdong Provincial Hospital of Chinese Medicine, Guangzhou, China

**Objective:** This study aims to systematically evaluate the curative efficacy of different acupuncture methods in the treatment of obesity combined with insulin resistance in randomized clinical trials (RCTs) by network meta-analysis.

**Methods:** Four Chinese databases (CNKI, WanFang Data, VIP, and SinoMed) and four English databases (PubMed, Embase, the Cochrane Library, and www.clinicaltrial.gov) were electronically searched to identify qualified studies. Two reviewers independently screened the literature in accordance with the inclusion/exclusion criteria by EndNote 20 software and extracted data by ADDIS1.16.8 software, and then the risk of bias of the included studies were evaluated by the Cochrane tool. Network meta-analysis was performed by Stata 15.1 software. The primary outcomes included fasting blood glucose (FBG), fasting serum insulin (FINS), homeostasis model assessment—insulin resistance (HOMA-IR), and body mass index (BMI). The secondary outcomes included waistline, waist–hip ratio, triglyceride (TG), total cholesterol (TC), high-density lipoprotein (HDL), and low-density lipoprotein (LDL).

**Results:** Five RCTs with a total of 410 patients with obesity combined with insulin resistance were included. The results of the network meta-analysis showed that, compared with the control group, three kinds of acupuncture methods (electropuncture, acupoint catgut embedding, and acupuncture point patch) had significant efficacy in reducing FBG [electropuncture (MD = -0.44, 95% CI: -0.83, -0.05) and acupoint catgut embedding (MD = -0.36, 95% CI: -0.51, -0.21)], FINS [electropuncture (MD = -6.17, 95% CI: -9.69, -2.65), acupoint catgut embedding (MD = -5.87, 95% CI: -6.92, -4.82), and acupuncture point patch (MD = -5.86, 95% CI: -11.40, -0.32)], HOMA-IR [electropuncture (MD = -1.59, 95% CI: -2.73, -0.45) and acupoint catgut embedding (MD =-0.91, 95% CI: -1.07, -0.75)], BMI [electropuncture (MD = -1.68, 95% CI: -2.70, -0.66), acupoint catgut embedding (MD = -3.39, 95% CI: -4.38, -2.40), and acupuncture point patch [MD = -2.90, 95% CI: -4.93, -0.87)], and waistline [electropuncture (MD = -5.49, 95% CI: -8.56, -2.42)

and acupoint catgut embedding (MD = -4.91, 95% CI: -7.51, -2.31)] in obese patients with insulin resistance, suggesting that their efficacy was better than that of the western medicine group in some of the outcome indicators. For the index related to blood lipid, the efficacy of electropuncture was significantly better than behavioral therapy and western medicine. Except that acupoint catgut embedding was superior to electroacupuncture in reducing the BMI, there was no statistically significant difference in efficacy among the three acupuncture methods.

**Conclusions:** The results showed that the therapeutic effect of acupuncture methods was superior to conventional western treatment alone. Acupuncture methods could serve as an alternative or adjunctive treatment in obese patients with insulin resistance.

**Systematic Review Registration:** https://inplasy.com, identifier 202280075.

KEYWORDS

**acupuncture methods, obesity, insulin resistance, systematic review, network meta-analysis**

# Introduction

Obesity, one of the leading health risk factors worldwide, has a prevalence that is rapidly increasing worldwide (1) since 1.1 billion people are classified as overweight (2). Furthermore, obesity is associated with several health problems, including insulin resistance, cardiovascular disease, gallbladder disease, and certain malignancies (3).

Insulin resistance (IR) is the common pathological basis of metabolic diseases such as obesity and type 2 diabetes (4). Obesity and overweight are closely correlated with IR and are independent risk factors for IR (5). The pathogenesis of IR is still unclear, but some studies (6) suggested that it is caused by the interaction between nutritional overload, systemic fatty acid surplus, inflammatory response of adipose tissue, endoplasmic reticulum stress, oxidative stress, and adipose tissue hypoxia.

Acupuncture is the most rapidly growing complementary therapy that is recognized by the WHO (7). In recent years, both experimental and clinical current data concluded that acupuncture was superior to conventional medication for obesity (8) and insulin resistance (9), which can be used to improve symptoms and efficacy while reducing the side effects or adverse reactions caused by western medicine therapy. It is suggested that acupuncture exerts beneficial effects on the mechanisms of obesity and insulin resistance; however, the most effective frequency of obesity combined with insulin resistance by acupuncture remains controversial. Further prospective studies are needed to establish the effectiveness of this complementary method for obesity combined with insulin resistance treatment.

In this study, network meta-analysis was used to systematically evaluate and compare the curative efficacy of different acupuncture methods (electroacupuncture, acupoint catgut embedding, and acupuncture point patch) in the treatment of obesity combined with insulin resistance in randomized clinical trials (RCTs) so as to provide more clinical evidence for the acupuncture treatment of obesity combined with insulin resistance and to guide clinicians in sophisticated treatment options.

# Data and methods

## Criteria for considering studies for this study

### Type of studies

RCTs of different acupuncture methods in the treatment of obesity with insulin resistance, blind method, and language are not limited.

### Type of participants

The patients were diagnosed to be obese with insulin resistance. The obesity references, the Consensus of Experts on the Prevention and Treatment of Adult Obesity in China in 2011 and the Consensus of Chinese Experts on Medical Nutrition Therapy for Overweight/Obesity in 2016, were developed by the Obesity Group of the Chinese Society of Endocrinology (BMI ≥ 28). For the IR reference, according to the Expert Opinions on Insulin Resistance Evaluation published by the Chinese Diabetes

Society, HOMA-IR ≥2.68 is regarded as the standard for the diagnosis of IR, regardless of age, gender, and course of disease.

## Type of interventions

### Control group

In terms of other acupuncture treatments, drug therapy, or blank control, the experimental group consisted of those who have had any kind of acupuncture, moxibustion, acupuncture + moxibustion, warm acupuncture, electropuncture, auricular point, acupoint application, and acupoint catgut embedding. In addition to intervention measurements, other background treatment measurements were identical in both groups.

## Type of outcome measures

### Primary outcomes

These included (1) fasting blood glucose (FBG), (2) fasting serum insulin (FINS), (3) homeostasis model assessment—IR (HOMA-IR), and (4) body mass index (BMI).

### Secondary outcomes

These included (1) waistline, (2) waist–hip ratio, (3) triglyceride (TG), (3) total cholesterol (TC), (5) high-density lipoprotein (HDL), and (6) low-density lipoprotein (LDL).

## Exclusion criteria

These included (1) non-RCT research: descriptive studies, case–control studies, cohort studies, literature review, social commentary, case reports, case series analysis, *etc.*; (2) intervention measures that take a variety of therapy combination or study acupuncture and moxibustion different points, different techniques, the study of frequency; (3) animal studies, cellular or analytical studies, or systematic reviews, meta-analyses, and pooled analyses of multiple RCTs; (4) subjects who suffered from serious diseases, such as cerebrovascular diseases and tumors; and (5) others: conference abstracts, comments, guidelines, letters, amendments, and other unrelated studies where the full text is not available, and the results are incomplete.

## Literature retrieval

Cross-retrieval of the Chinese databases (CNKI, WanFang Data, VIP, and SinoMed) and the English databases (PubMed, Embase, the Cochrane Library, and www.clinicaltrial.gov) was performed by electronically searching from database construction time to March 31, 2022.

The keywords or mesh terms used were as follows: acupuncture, needle, electroacupuncture, moxibustion, fire needle, needle warming moxibustion, auricular point, point application therapy, acupoint catgut embedding, obesity, insulin resistance, controlled clinical trial, randomized controlled trial, drug therapy, groups, and placebo. Considering that there may be differences in the description of outcomes in the RCT, outcome indicators were not restricted in the retrieval to avoid omission.

## Literature management

By aggregating the studies retrieved from various archives, we used EndNote 20 software to manage the retrieved literature. After excluding the literatures duplicated between different databases, two researchers independently read the title and abstract of the literatures, screened out the obvious irrelevant literatures according to the inclusion/exclusion criteria, and screened the literatures by reading the full text if necessary. The screening results are cross-checked by two researchers, and in case of disagreement, consultation or discussion is done with a third expert.

## Literature quality evaluation and data extraction

We used Excel 2016 software to develop basic information extraction table and quality evaluation table. Two reviewers independently conducted quality evaluation and basic data extraction for each article that met the inclusion criteria. Detailed data, including basic study information (author, publication year, study type, sample size, *etc.*), intervention measures and outcome indicators, quality evaluation, *etc.*, were extracted by ADDIS1.16.8 software. Two reviewers cross-checked the results, and if there is any disagreement, it shall be decided through a discussion or consultation with a third reviewer.

## Bias risk assessment of included studies

Two reviewers assessed the risk of bias in the included studies according to the Cochrane Manual's risk of bias assessment tool for RCTs. The projects include randomization of assignment methods, assignment plan concealment, blinding of study subjects and protocol implementors, blinding of study outcome measures, integrity of outcome data, selective reporting of study results, and other sources of bias. Finally, the risk of literature bias was judged as "low", "high", and "uncertain". Two reviewers independently conducted the assessment, and then this was cross-checked, in case of disagreement, through a discussion with the third reviewer to discuss decisions, thus reaching a consensus.

## Statistical analysis

Using Stata 15.1 software and its "network" commands to draw the network diagram for comparison between intervention

measures for the evaluation of publication bias, a network meta-analysis was conducted for each outcome, and heterogeneity and inconsistency in the mesh evidence body were tested. In this study, odds ratio (OR) and 95% confidence interval (CI) were used as a way of expression for the dichotomous outcome index, while the continuous outcome index was expressed as mean difference (MD) and its 95% confidence interval.

The existence of a publication bias was identified by drawing a corrected comparison funnel plot, and the inconsistencies of the results of the mesh meta-analysis were tested by a node splitting method. If the direct comparison and the indirect comparison result in a difference of $P > 0.05$, the inconsistency is not significant, and the consistency model is adopted. At the same time, a prediction interval graph was drawn for each outcome. If the prediction interval crossed the invalid line, interstudy heterogeneity was considered, and the random effect model was selected. Efficacy ranking was based on the Surface under the Cumulative Ranking Curve (SUCRA). The larger the SUCRA is, the better the efficacy of the drug in this outcome. $P < 0.05$ was considered statistically significant.

# Results

## Literature screening process and results

A total of 627 related articles were initially detected, and 89 literatures were detected after full-text screening. Finally, 5 RCTs (10–14) were included in the network meta-analysis, including 410 patients on obesity combined with insulin resistance. The specific literature screening flow chart and results are shown in Figure 1.

## Basic characteristics of included studies

The basic characteristics of the included studies are detailed in the Open Science (Resource Services) Identifier (OSID). Five RCTs included three types of intervention (electropuncture, acupoint catgut embedding, and acupuncture point patch) and control groups (behavioral therapy, western medicine, and blank control). The mean age of the 410 patients included in this study was 33.04 ± 7.45 years, and the mean duration of disease was 4.92 ± 3.20 years. The basic characteristics of the included studies are shown in Supplementary Table S1. As shown in the table, outcomes available for network meta-analysis included FBG, FINS, HOMA-IR, BMI, waistline, waist–hip ratio, TG, TC, HDL, and LDL.

## Results of network meta-analysis

### Fasting blood glucose

Five RCTs were included in the statistical analysis of FBG, with a total sample of 410 patients. The network relationship is shown in Figure 2A; the thickness of the line segment represents the number of studies included in the comparison of each treatment method, and the circular area represents the sample size of the population using this measure. The line segments between the dots represent studies in which there was a direct comparison between the two interventions that were connected. No significant heterogeneity or inconsistency was found in the reticular body of evidence; thus we adopted the consistent fixed-effect model. The pairwise comparison results and ranking of reticular meta-analysis are shown in Figure 3 and Tables 1, 2.

Table 3 is about the pairwise comparison results of six types of interventions or controls, which showed that, compared with

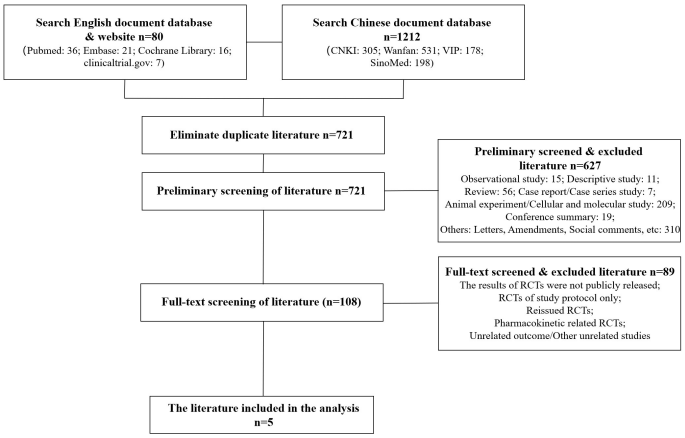


FIGURE 1
Literature screening process and results.

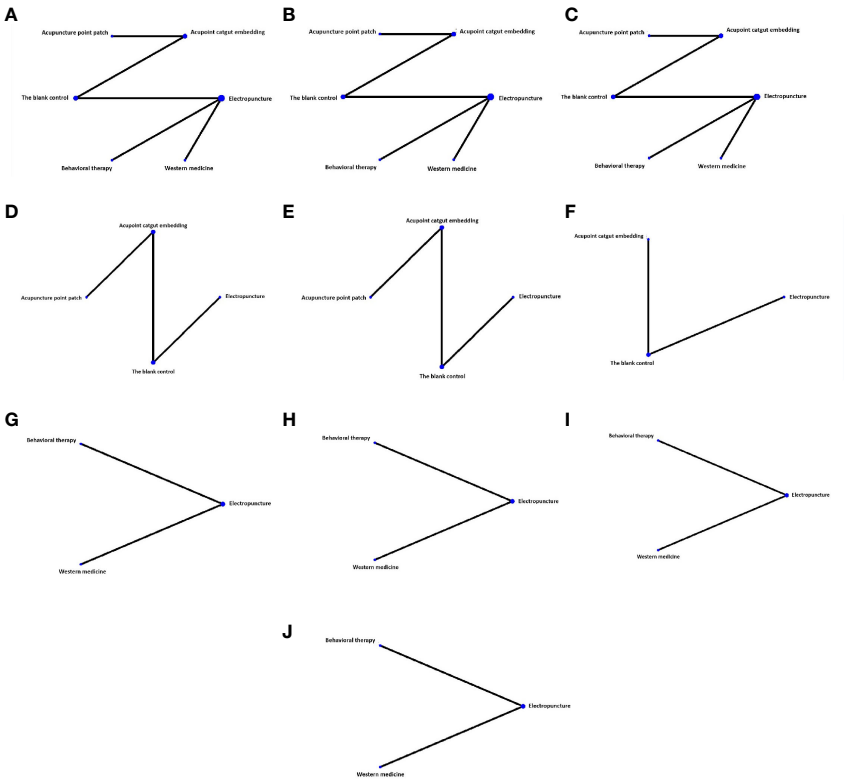


FIGURE 2
Network diagram of different indexes treated by different types of intervention. The figure shows that each intervention is indicated with a single blue dot. The size of the dot represents the cumulative total sample size of the intervention. The line segment between the dots represents the studies that have a direct comparison between the two interventions. **(A)** Fasting blood glucose, **(B)** fasting serum insulin, **(C)** homeostasis model assessment—insulin resistance, **(D)** BMI, **(E)** waistline, **(F)** waist–hip ratio, **(G)** triglyceride, **(H)** total cholesterol, **(I)** high-density lipoprotein, and **(J)** low-density lipoprotein.

the blank control, electropuncture (MD = -0.44, 95% CI: -0.83, -0.05), acupoint catgut embedding (MD = -0.36, 95% CI: -0.51, -0.21), and western medicine (MD = -0.58, 95% CI: -1.09, -0.07) groups all had reduced FBG, while no statistical differences were found in the other groups. From Figure 3 and Table 1, we found that western medicine ranked first in terms of reducing FBG in obesity combined with insulin resistance, while acupuncture point patch, electropuncture, and acupoint catgut embedding ranked second, third, and fourth, respectively.

## Fasting serum insulin

Five RCTs were included in the statistical analysis of FINS, with a total sample of 410 patients. The network relationship is shown in Figure 2B; no significant heterogeneity or inconsistency was found in the reticular body of evidence; thus, the consistent fixed effect model was adopted. The pairwise comparison results and ranking of reticular meta-analysis are shown in Figure 4 and Tables 1, 2.

Table 2 shows that, compared with the blank control, the electropuncture (MD = -6.17, 95% CI: -9.69, -2.65), acupoint catgut embedding (MD = -5.87, 95% CI: -6.92, -4.82), acupuncture point patch (MD =-5.86, 95% CI: -11.40, -0.32), and behavioral therapy (MD = -6.95, 95%CI: -10.82, -3.08) groups all caused the decrease in the FINS level. However, compared with western medicine, the electropuncture (MD = -6.87, 95% CI: -8.09, -5.65), acupoint catgut embedding (MD = -6.57, 95% CI: -10.44, -2.70), and behavioral therapy (MD = -7.65, 95% CI: -9.66, -5.64) groups all had better curative efficacy. No statistical differences were found in the other groups. From Figure 4 and Table 1, we found that behavioral therapy ranked first in terms of reducing FINS in obesity combined with insulin resistance, while electropuncture, acupuncture point patch, and acupoint catgut embedding ranked second, third, and fourth, respectively.

## Homeostasis model assessment-IR

Five RCTs were included in the statistical analysis of HOMA-IR, with a total sample of 410 patients. The network relationship is shown in Figure 2C. No significant heterogeneity or inconsistency was found in the reticular body of evidence;

thus, the consistent fixed-effect model was adopted. The pairwise comparison results and ranking of reticular meta-analysis are shown in Figure 5 and Tables 4, 5.

Table 5 shows that, compared with the blank control, the electropuncture (MD = -1.59, 95% CI: -2.73, -0.45), acupoint catgut embedding (MD = -0.91, 95% CI: -1.07, -0.75), and behavioral therapy (MD = -1.30, 95% CI: -2.54, -0.05) groups all caused the decrease in the HOMA-IR level. However, compared with western medicine, the electropuncture (MD = -2.30, 95% CI: -2.68, -1.92), acupoint catgut embedding (MD = -1.62, 95% CI: -2.83, -0.41), acupuncture point patch (MD = -1.92, 95% CI: -3.83, -0.01), and behavioral therapy (MD = -2.01, 95% CI: -2.65, -1.37) groups all had better curative efficacy. No statistical differences were found in the other groups. From Figure 5 and Table 4, we found that electropuncture ranked first in terms of reducing HOMA-IR in obesity combined with insulin resistance, while behavioral therapy, acupuncture point patch, and acupoint catgut embedding ranked second, third, and fourth, respectively.

TABLE 1 Efficacy ranking of mesh meta-analysis: fasting blood glucose and fasting serum insulin.

| Treatment | SUCRA | Rank |
|---|---|---|
| Fasting blood glucose | | |
| Western medicine | 81.1 | 1 |
| Acupuncture point patch | 62.5 | 2 |
| Electropuncture | 61.3 | 3 |
| Acupoint catgut embedding | 49.8 | 4 |
| Behavioral therapy | 40.3 | 5 |
| Blank control | 4.9 | 6 |
| Fasting serum insulin | | |
| Behavioral therapy | 83.2 | 1 |
| Electropuncture | 65.8 | 2 |
| Acupuncture point patch | 65.5 | 3 |
| Acupoint catgut embedding | 64.4 | 4 |
| Blank control | 13.2 | 5 |
| Western medicine | 7.9 | 6 |

As shown in the table, the surface under the cumulative ranking curve (SUCRA) represents the area under the curve of the cumulative probability graph of efficacy ranking. The decrease in fasting blood glucose was better, the SUCRA value was bigger, and the efficacy ranking was higher.

## Body mass index

Three RCTs were included in the statistical analysis of BMI, with a total sample of 247 patients. The network relationship is shown in Figure 2D. No significant heterogeneity or inconsistency was found in the reticular body of evidence; thus, the consistent fixed-effect model was adopted. The pairwise comparison results and ranking of reticular meta-analysis are shown in Figure 6 and Tables 4, 6.

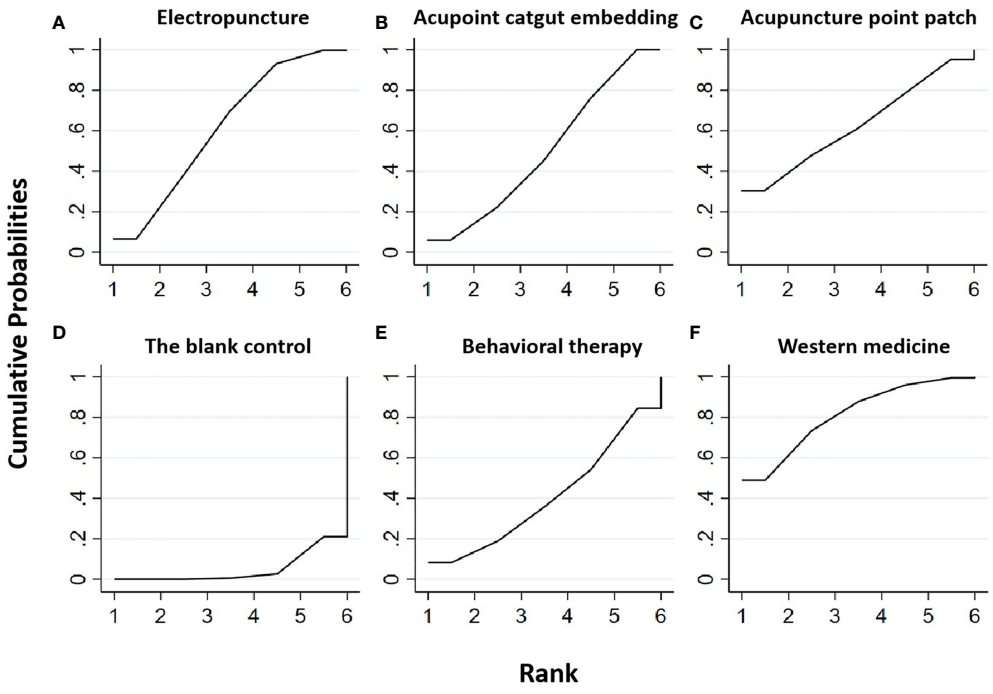


FIGURE 3
Efficacy ranking and cumulative probability graph of fasting blood glucose (FBG) treated by different types of intervention. Comparison of efficacy ranking and cumulative probability of FBG between each kind of intervention. **(A)** Electropuncture, **(B)** acupoint catgut embedding, **(C)** acupuncture point patch, **(D)** the blank control, **(E)** behavioral therapy, and **(F)** western medicine.

TABLE 2 Network meta-analysis netleague table of fasting blood glucose.

| | | | | | |
|---|---|---|---|---|---|
| **Electropuncture** | 0.08 (-0.34, 0.50) | -0.02 (-0.69, 0.65) | 0.14 (-0.28, 0.56) | -0.14 (-0.47, 0.19) | 0.44 (0.05, 0.83) |
| -0.08 (10.50, 0.34) | **Acupoint catgut embedding** | -0.10 (-0.63, 0.43) | 0.06 (-0.53, 0.66) | -0.22 (-0.76, 0.32) | 0.36 (0.21, 0.51) |
| 0.02 (-0.65, 0.69) | 0.10 (-0.43, 0.63) | **Acupuncture point patch** | 0.16 (-0.63, 0.95) | -0.12 (-087, 0.63) | 0.46 (-0.09, 1.01) |
| -0.14 (-0.56,0.28) | -0.06 (-0.66, 0.53) | -0.16 (-0.95, 0.63) | **Behavioral therapy** | -0.28 (-0.82, 0.26) | 0.30 (-0.27, 0.87) |
| 0.14 (-0.19, 0.47) | 0.22 (-0.32, 0.76) | 0.12 (-0.63, 0.87) | 0.28 (-0.26, 0.82) | **Western medicine** | 0.58 (0.07, 1.09) |
| -0.44 (-0.83, -0.05) | -0.36 (-0.51, -0.21) | -0.46 (-1.01, 0.09) | -0.30 (-0.87, 0.27) | -0.58 (-1.09, -0.07) | **The blank control** |

Bold values means the sorting tables represent the area under the curve of the cumulative probability sorting chart, the bold values are the rank of the sorting by different types of intervention in our study. While the number of the ladder table is the relative effect value and 95% CI.

Table 6 shows that, compared with blank control, the electropuncture (MD = -1.68, 95% CI: -2.70, -0.66), acupoint catgut embedding (MD = -3.39, 95% CI: -4.38, -2.40), and acupuncture point patch (MD = -2.90, 95% CI (-4.93, -0.87) groups all caused the decrease in the BMI level. However, the curative efficacy of electropuncture (MD = 1.71, 95% CI: 0.29, 3.13) was not as good as acupoint catgut embedding. No statistical differences were found in the other groups. From Figure 6 and Table 4, we found that acupoint catgut embedding ranked first in terms of reducing BMI in obesity combined with insulin resistance, while acupuncture point patch and electropuncture ranked second and third, respectively.

## Waistline

Three RCTs were included in the statistical analysis of waistline, with a total sample of 247 patients. The network relationship is shown in Figure 2E. No significant heterogeneity or inconsistency was found in the reticular body of evidence; thus, the consistent fixed-effect model was adopted. The pairwise comparison results and ranking of reticular meta-analysis are shown in Figure 7 and Tables 7, 8.

Table 8 shows that, compared with blank control, electropuncture (MD = -5.49, 95% CI: -8.56, -2.42) and acupoint catgut embedding (MD = -4.91, 95% CI: -7.51, -2.31) both caused the decrease in the waistline level. No statistical differences were found in the other groups. From Figure 7 and Table 7, we found that electropuncture ranked first in terms of reducing waistline in obesity combined with insulin resistance, while acupoint catgut embedding and acupuncture point patch ranked second and third, respectively.

## Waist–hip ratio

Two RCTs were included in the statistical analysis of the waist–hip ratio, with a total sample of 185 patients. The network relationship is shown in Figure 2F. No significant heterogeneity or inconsistency was found in the reticular body of evidence; thus, the consistent fixed-effect model was adopted. The pairwise comparison results and ranking of reticular meta-analysis are shown in Figure 8 and Tables 7, 9.

Table 9 shows that, compared with blank control, electropuncture (MD = -0.02, 95% CI: -0.03, -0.01) and acupoint catgut embedding (MD = -0.08, 95% CI: -0.11, -0.05) both caused the decrease in the waist–hip ratio level. No statistical differences were found in the other groups. From Figure 8 and Table 7, we found that acupoint catgut embedding ranked first in terms of reducing the waist–hip ratio in obesity combined with insulin resistance, while electropuncture ranked second.

## Triglyceride

Two RCTs were included in the statistical analysis of TG, with a total sample of 163 patients. The network relationship is shown in Figure 2G. No significant heterogeneity or inconsistency was found in the reticular body of evidence; thus, the consistent fixed-effect model was adopted. The pairwise comparison results and ranking of reticular meta-analysis are shown in Figure 9 and Tables 10, 11.

Table 11 shows that, compared with blank control, electropuncture, behavioral therapy, and western medicine all had no statistical differences. From Figure 9 and Table 10, we found that electropuncture ranked first in terms of reducing TG in obesity combined with insulin resistance.

TABLE 3 Network meta-analysis ladder table of fasting serum insulin.

| | | | | | |
|---|---|---|---|---|---|
| **Electropuncture** | 0.30 (-3.37, 3.97) | 0.31 (-6.26, 6.87) | -0.78 (-2.38, 0.82) | 6.87 (5.65, 8.09) | 6.17 (2.65, 9.69) |
| -0.3 (-3.97, 3.37) | **Acupoint catgut embedding** | 0.01 (-2.93, 5.08) | -1.08 (-5.08, 2.93) | 6.57 (2.70, 10.44) | 5.87 (4.82, 6.92) |
| -0.31 (-6.87, 6.26) | -0.01 (-5.45, 5.43) | **Acupuncture point patch** | -1.09 (-7.84, 5.67) | 6.56 (-0.12, 13.24) | 5.86 (0.32, 11.40) |
| 0.78 (-0.82, 2.38) | 1.08 (-2.93, 5.08) | 1.09 (-5.67, 7.84) | **Behavioral therapy** | 7.65 (5.64, 9.66) | 6.95 (3.08, 10.82) |
| -6.87 (-8.09, -5.65) | -6.57 (-10.44, -2.70) | -6.56 (-13.24, 0.12) | -7.65 (-9.66, -5.64) | **Western medicine** | -0.70 (-4.43, 3.02) |
| -6.17 (-9.69, -2.65) | -5.87 (-6.92, -4.82) | -5.86 (-11.40, -0.32) | -6.95 (-10.82, -3.08) | 0.70 (-3.02, 4.43) | **The blank control** |

Bold values means the sorting tables represent the area under the curve of the cumulative probability sorting chart, the bold values are the rank of the sorting by different types of intervention in our study. While the number of the ladder table is the relative effect value and 95% CI.

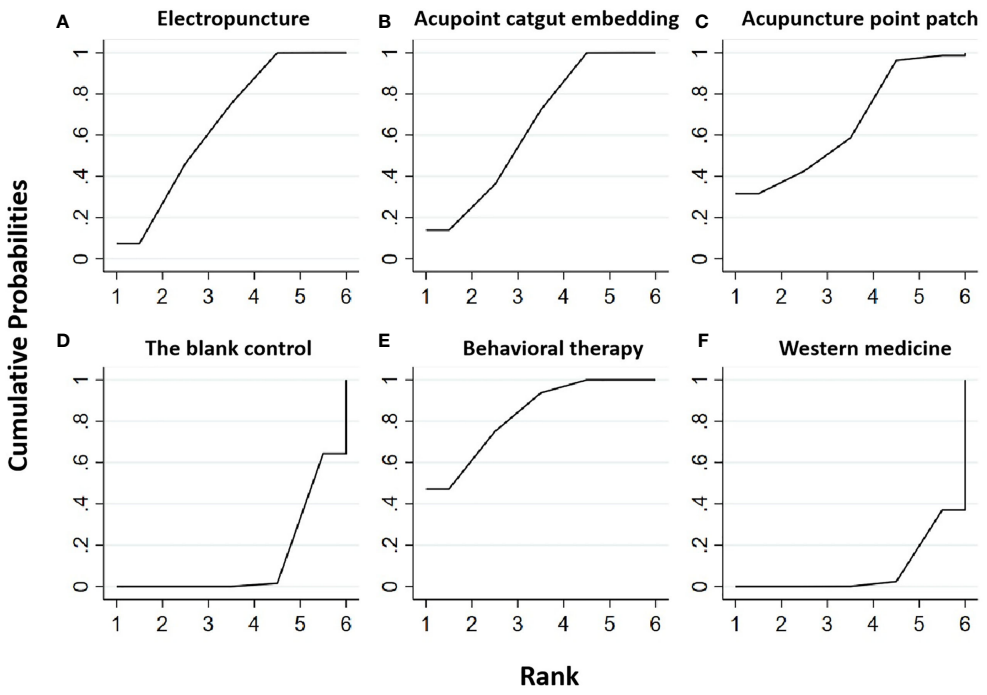


FIGURE 4
Efficacy ranking and cumulative probability graph of fasting serum insulin (FINS) treated by different types of intervention. Comparison of efficacy ranking and cumulative probability of FINS between each kind of intervention. **(A)** Electropuncture, **(B)** acupoint catgut embedding, **(C)** acupuncture point patch, **(D)** blank control, **(E)** behavioral therapy, and **(F)** western medicine.

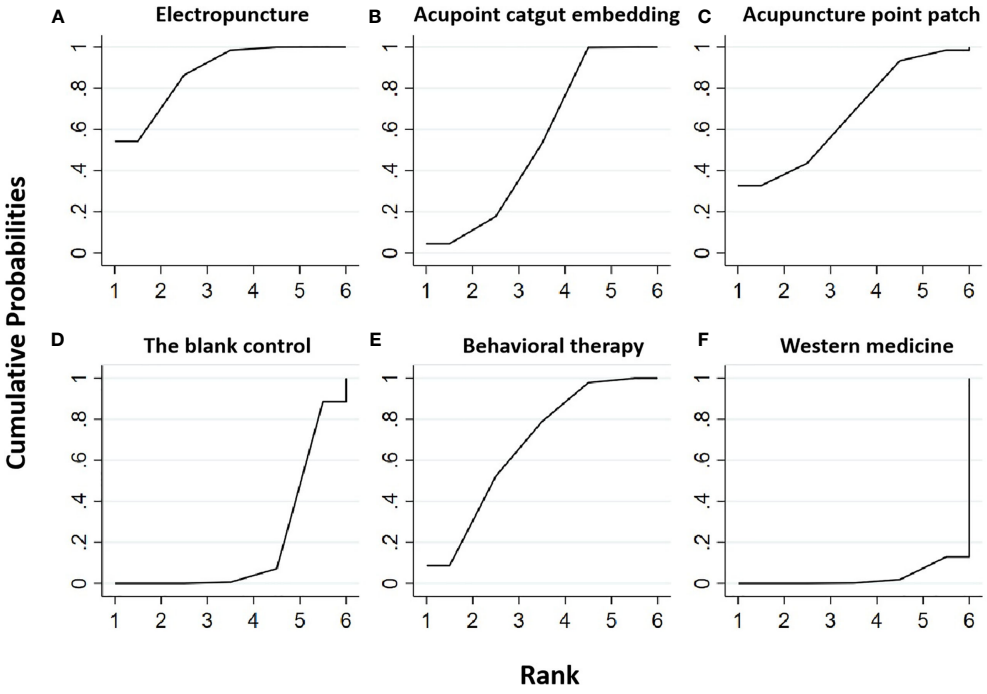


FIGURE 5
Efficacy ranking and cumulative probability graph of homeostasis model assessment—insulin resistance (HOMA-IR) treated by different types of intervention. Comparison of efficacy ranking and cumulative probability of HOMA-IR between each kind of intervention. **(A)** Electropuncture, **(B)** acupoint catgut embedding, **(C)** acupuncture point patch, **(D)** blank control, **(E)** behavioral therapy, and **(F)** western medicine.

TABLE 4 Efficacy ranking of mesh meta-analysis: homeostasis model assessment—insulin resistance (HOMA-IR) and body mass index (BMI).

| Treatment | SUCRA | Rank |
|---|---|---|
| HOMA-IR | | |
| Electropuncture | 87.8 | 1 |
| Behavioral therapy | 67.5 | 2 |
| Acupuncture point patch | 67.4 | 3 |
| Acupoint catgut embedding | 55 | 4 |
| Blank control | 19.3 | 5 |
| Western medicine | 3 | 6 |
| BMI | | |
| Acupoint catgut embedding | 89.9 | 1 |
| Acupuncture point patch | 71.5 | 2 |
| Electropuncture | 38.5 | 3 |
| Blank control | 0.1 | 4 |

As shown in the table, the surface under the cumulative ranking curve (SUCRA) represents the area under the curve of the cumulative probability graph of efficacy ranking. The decrease in fasting blood glucose is better, the SUCRA value is bigger, and the efficacy ranking is higher.

## Total cholesterol

Two RCTs were included in the statistical analysis of TG, with a total sample of 163 patients. The network relationship is shown in Figure 2H. No significant heterogeneity or inconsistency was found in the reticular body of evidence; thus, the consistent fixed-effect model was adopted. The pairwise comparison results and ranking of reticular meta-analysis are shown in Figure 10 and Tables 10, 12.

Table 12 shows that, compared with blank control, electropuncture (MD = -0.40, 95% CI: -0.74, -0.06) caused the decrease in the TC level. No statistical differences were found in the other groups. From Figure 10 and Table 10, we found that electropuncture ranked first in terms of reducing TC in obesity combined with insulin resistance.

## High-density lipoprotein

Two RCTs were included in the statistical analysis of HDL, with a total sample of 163 patients. The network relationship is shown in Figure 2I. No significant heterogeneity or inconsistency was found in the reticular body of evidence; thus, the consistent fixed-effect model was adopted. The pairwise comparison results and ranking of reticular meta-analysis are shown in Figure 11 and Tables 13, 14.

Table 14 shows that, compared with blank control, electropuncture (MD = 0.07, 95% CI: 0.01, 0.13) caused the increase in the HDL level. No statistical differences were found in the other groups. From Figure 11 and Table 13, we found that electropuncture ranked first in terms of increasing HDL in obesity combined with insulin resistance.

## Low-density lipoprotein

Two RCTs were included in the statistical analysis of LDL, with a total sample of 163 patients. The network relationship is shown in Figure 2J. No significant heterogeneity or inconsistency was found in the reticular body of evidence; thus, the consistent fixed-effect model was adopted. The pairwise comparison results and ranking of reticular meta-analysis are shown in Figure 12 and Tables 13, 15.

Table 15 shows that, compared with blank control, electropuncture (MD = -0.38, 95% CI: -0.61, -0.15) caused the decrease in the LDL level. However, the curative efficacy of behavioral therapy (MD = 0.34, 95% CI: 0.05, 0.63) was not as good as western medicine. No statistical differences were found in the other groups. From Figure 13 and Table 15, we found that electropuncture ranked first in terms of reducing LDL in obesity combined with insulin resistance.

## The assessment of literature bias risk

Five RCTs all reported the random sequence generation methods. None of them described distribution concealment, but four RCTs could be considered as having a low risk of bias. In terms of the blind method, four RCTs considered that the subjects did not achieve blinding due to significant differences in intervention measures between the experimental group and the control group. In addition, one RCT clearly described the blind method for the statistical analysis of results, while the other four RCTs did not clearly describe the blind method. Five RCTs had a low risk of bias in the proportion of lost follow-up in each group, selective reporting, and corporate funding. As a whole, except for the blind method, which is difficult to achieve, all the included studies have a low risk of bias. The specific risk of bias is shown in Figure 13.

TABLE 5 Network meta-analysis ladder table of homeostasis model assessment—insulin resistance.

| | | | | | |
|---|---|---|---|---|---|
| **Electropuncture** | 0.68 (-0.47, 1.83) | 0.38 (-1.50, 2.25) | 0.29 (-0.22, 0.80) | 2.30 (1.92, 2.68) | 1.59 (0.45, 2.73) |
| -0.68 (-1.83, 0.47) | **Acupoint catgut embedding** | -0.30 (-1.78, 1.18) | -0.39 (-1.64, 0.87) | 1.62 (0.41, 2.83) | 0.91 (0.75, 1.07) |
| -0.38 (-2.25, 1.50) | 0.30 (-1.18, 1.78) | **Acupuncture point patch** | -0.09 (-2.03, 1.85) | 1.92 (0.01, 3.83) | 1.21 (-0.28, 2.70) |
| -0.29 (-0.80. 0.22) | 0.39 (-0.87, 1.64) | 0.09 (-1.85, 2.03) | **Behavioral therapy** | 2.01 (1.37, 2.65) | 1.30 (0.05, 2.54) |
| -2.30 (-2.68, -1.92) | -1.62 (-2.83, -0.41) | -1.92 (-3.83, -0.01) | -2.01 (-2.65, -1.37) | **Western medicine** | -0.71 (-1.91, 0.49) |
| -1.59 (-2.73, -0.45) | -0.91 (-1.07, -0.75) | -1.21 (-2.70, 0.28) | -1.30 (-2.54, -0.05) | 0.71 (-0.49, 1.91) | **The blank control** |

Bold values means the sorting tables represent the area under the curve of the cumulative probability sorting chart, the bold values are the rank of the sorting by different types of intervention in our study. While the number of the ladder table is the relative effect value and 95% CI.

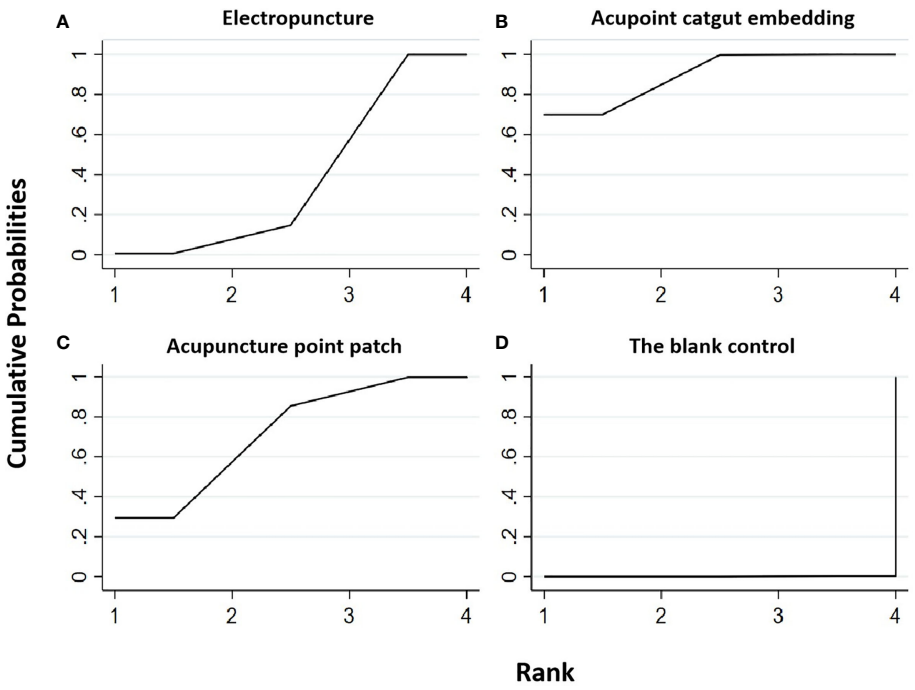


FIGURE 6
Efficacy ranking and cumulative probability graph of body mass index (BMI) treated by different types of intervention. Comparison of efficacy ranking and cumulative probability of BMI between each kind of intervention. **(A)** Electropuncture, **(B)** acupoint catgut embedding, **(C)** acupuncture point patch, and **(D)** blank control.

In summary, this study focused on three acupuncture methods in existing studies: electropuncture, acupoint catgut embedding, and acupuncture point patch. The network meta results showed that these three acupuncture methods had significant efficacy in reducing FBG, FINS, HOMA-IR, BMI, waistline, and waist–hip ratio in obesity combined with insulin resistance compared with the blank control group. Meanwhile, compared with the western medicine group, these three acupuncture methods had better efficacy in some outcome indicators. In a series of outcomes related to blood lipid, the efficacy of electropuncture was significantly better than behavioral therapy and western medicine. Except for the fact that acupoint catgut embedding was superior to electropuncture in reducing BMI, there was no statistically significant difference in efficacy among the three acupuncture methods.

## Discussion

Acupuncture, which is among the oldest healing practices in the world, was suggested as an application to a wide range of conditions including musculoskeletal diseases, neurological disorders, gynecological disorders, addictions, and dentistry by the WHO (7). It exerts its effect through the insertion of thin metallic needles at specific points on the body that can be manipulated manually or by electrical stimulation (15).

Electropuncture, consisting of stimulating specific points on the body by inserting thin metal needles into superficial structures with a tiny electrical current, is employed for removing blockages in the flow of vital energy that circulates throughout the body through a system of pathways. Acupoint catgut embedding therapy, involving persistent stimulation produced by a suture with mild irritation in subcutaneous

TABLE 6 Network meta-analysis ladder table of body mass index.

| | | | |
|---|---|---|---|
| **Electropuncture** | -1.71 (-3.13, 0.29) | -1.22 (-3.49, 1.05) | 1.68 (0.66, 2.70) |
| 1.71 (0.29,3.13) | **Acupoint catgut embedding** | 0.49 (-1.29, 2.27) | 3.39 (2.40, 4.38) |
| 1.22 (-1.05, 3.49) | -0.49 (-2.27, 1.29) | **Acupuncture point patch** | 2.90 (0.87, 4.93) |
| -1.68 (-2.70, -0.66) | -3.39 (-4.38, -2.40) | -2.90 (-4.93, -0.87) | **The blank control** |

Bold values means the sorting tables represent the area under the curve of the cumulative probability sorting chart, the bold values are the rank of the sorting by different types of intervention in our study. While the number of the ladder table is the relative effect value and 95% CI.

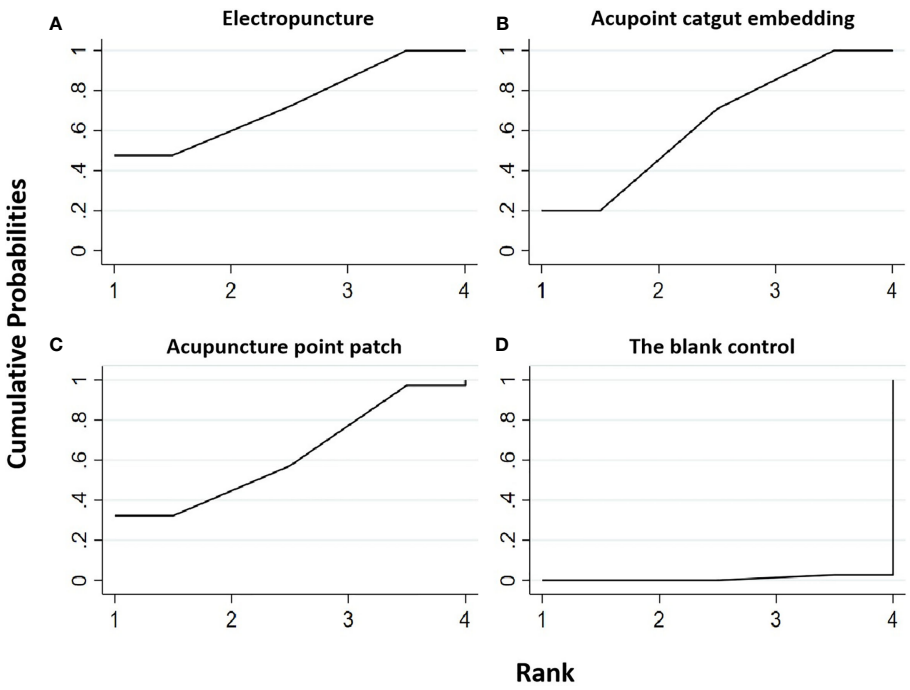


FIGURE 7
Efficacy ranking and cumulative probability graph of waistline treated by different types of intervention. Comparison of efficacy ranking and cumulative probability of waistline between each kind of intervention. **(A)** Electropuncture, **(B)** acupoint catgut embedding, **(C)** acupuncture point patch, and **(D)** blank control.

tissue, may be related to a combination of proteolytic enzymes, and macrophage action against the absorbable surgical thread may improve and extend the acupoint stimulation (16). By acupuncture point patch, which is a combination of traditional Chinese medicine, acupuncture, and channels and collaterals in applying Chinese medicine to the corresponding acupoints of the human body, diseases can be prevented and cured.

TABLE 7 Efficacy ranking of mesh meta-analysis: waistline and waist–hip ratio.

| Treatment | SUCRA | Rank |
|---|---|---|
| Waistline | | |
| Electropuncture | 73.2 | 1 |
| Acupoint catgut embedding | 63.6 | 2 |
| Acupuncture point patch | 62.3 | 3 |
| Blank control | 0.9 | 4 |
| Waist-hip ratio | | |
| Acupoint catgut embedding | 100 | 1 |
| Electropuncture | 50 | 2 |
| Blank control | 0 | 3 |

As shown in the table, the surface under the cumulative ranking curve (SUCRA) represents the area under the curve of the cumulative probability graph of efficacy ranking. The decrease in fasting blood glucose is better, the SUCRA value is bigger, and the efficacy ranking is higher.

The current conventional therapeutic strategies for obesity (*i.e.*, diet, physical exercise, drugs, and bariatric surgery) cannot achieve adequate weight control in all patients. Complementary types of treatment are therefore being tested, and in this context, acupuncture is one of the most rapidly growing complementary therapies. In the USA, the National Institutes of Health consensus panel recommends acupuncture as a useful clinical procedure.

The pathogenesis and pathological process of obesity combined with IR are complex. Currently, it is known that acupuncture can improve obesity combined with IR through multilevel, multisystem, and multitarget synergistic action, but the exact mechanism still needs to be clarified. Due to the influence of acupoint specificity, acupoint compatibility, and acupuncture stimulation parameters on the acupuncture effect and curative effect of obesity combined with insulin resistance (17), the specific internal mechanism is still not comprehensive.

We hereby critically examine major developments in the treatment of obesity combined with IR by acupuncture, which have helped shape our contemporary diagnostic and treatment strategies in obesity combined with IR. Acupuncture, in this study, involved electropuncture, acupoint catgut embedding, and acupuncture point patch, all of which were compared with other acupuncture treatments, drug therapy, or blank control. The results of this study showed that these three acupuncture

TABLE 8 Network meta-analysis ladder table of waistline.

| | | | |
|---|---|---|---|
| Electropuncture | 0.58 (-3.44, 4.60) | 0.72 (-5.06, 6.50) | 5.49 (2.42, 8.56) |
| -0.58 (-4.60, 3.44) | Acupoint catgut embedding | 0.14 (-4.01, 4.29) | 4.91 (2.31, 7.51) |
| -0.72 (-6.50, 5.06) | -0.14 (-4.29, 4.01) | Acupuncture point patch | 4.77 (-0.13, 9.67) |
| **-5.49 (-8.56, -2.42)** | **-4.91 (-7.51, -2.31)** | -4.77 (-9.67, 0.13) | Blank control |

Bold values means the sorting tables represent the area under the curve of the cumulative probability sorting chart, the bold values are the rank of the sorting by different types of intervention in our study. While the number of the ladder table is the relative effect value and 95% CI.

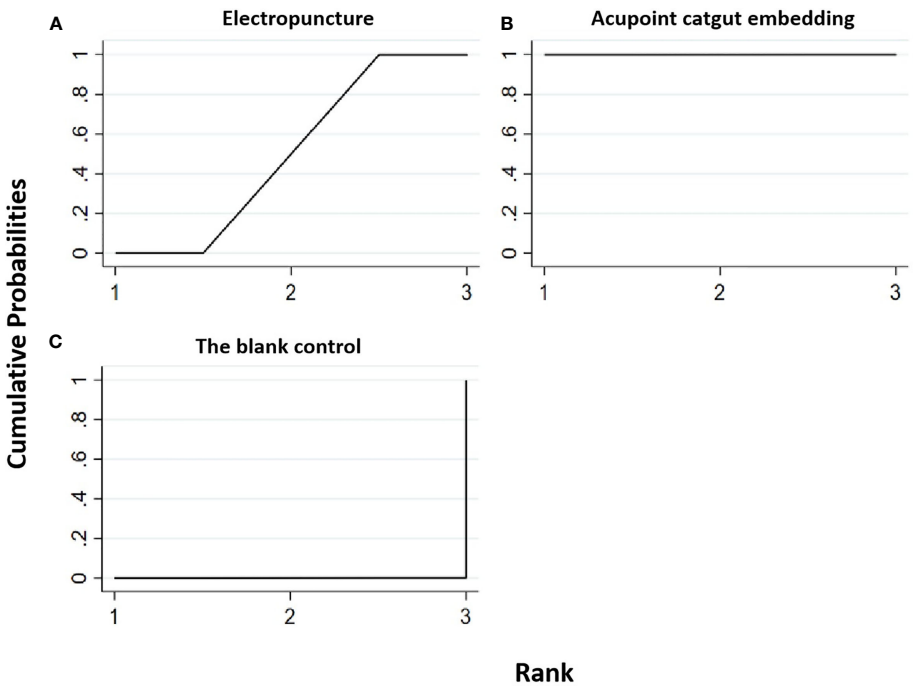


FIGURE 8
Efficacy ranking and cumulative probability graph of waist–hip ratio treated by different types of intervention. Comparison of efficacy ranking and cumulative probability of waist–hip ratio between each kind of intervention. **(A)** Electropuncture, **(B)** acupoint catgut embedding, and **(C)** blank control.

methods had significant efficacy in reducing FBG, FINS, HOMA-IR, BMI, waistline, and waist–hip ratio in obesity combined with IR compared with the control group. Meanwhile, compared with the western medicine group, these three acupuncture methods had better efficacy in some outcome indicators. In a series of outcomes related to blood lipid, the efficacy of electropuncture was significantly better than behavioral therapy and western medicine, with its respective advantages. According to the above-mentioned research results, different acupuncture methods have obvious advantages in the diagnosis and treatment of obesity combined with IR.

## Conclusion

This study has some limitations: (1) most of the included literatures did not report specific allocation concealment, blind method, and follow-up, which may lead to selection and measurement bias, and (2) the number of RCTs involved in this study was limited, and some literatures did not report safety indicators. Therefore, it is impossible to draw conclusions about the safety of different acupuncture methods. More RCTs with high-quality, multicenter, large-sample randomized controlled trials are needed to explore in depth so as to provide stronger clinical

TABLE 9 Network meta-analysis ladder table of waist–hip ratio.

| | | |
|---|---|---|
| Electropuncture | -0.06 (-0.09, -0.03) | 0.02 (0.01, 0.03) |
| 0.06 (0.03, 0.09) | Acupoint catgut embedding | 0.08 (0.05, 0.11) |
| -0.02 (-0.03, -0.01) | -0.08 (-0.11, -0.05) | Blank control |

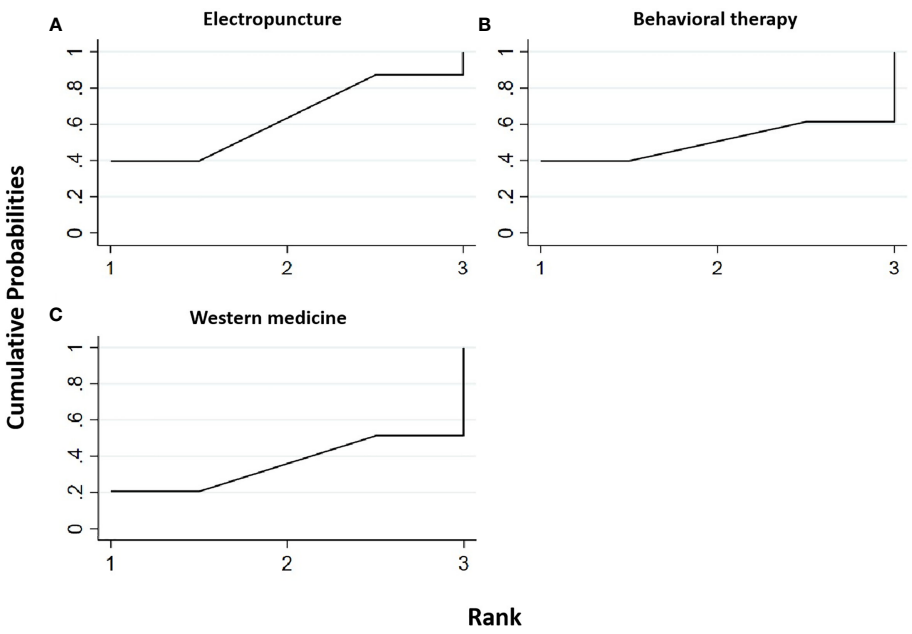


FIGURE 9
Efficacy ranking and cumulative probability graph of triglyceride (TG) treated by different types of intervention. Comparison of efficacy ranking and cumulative probability of TG between each kind of intervention. **(A)** Electropuncture, **(B)** behavioral therapy, and **(C)** western medicine.

TABLE 10 Efficacy ranking of mesh meta-analysis: triglyceride and total cholesterol.

| Treatment | SUCRA | Rank |
|---|---|---|
| Triglyceride | | |
| Electropuncture | 63.5 | 1 |
| Behavioral therapy | 50.6 | 2 |
| Western medicine | 36 | 3 |
| Total cholesterol | | |
| Electropuncture | 74.3 | 1 |
| Western medicine | 73.4 | 2 |
| Behavioral therapy | 2.3 | 3 |

As shown in the table, surface under the cumulative ranking curve (SUCRA) represents the area under the curve of the cumulative probability graph of efficacy ranking. The decrease in fasting blood glucose is better, the SUCRA value is bigger, and the efficacy ranking is higher.

TABLE 11 Network meta-analysis ladder table of triglyceride.

| | | |
|---|---|---|
| Electropuncture | 0.02 (-0.21, 0.25) | 0.04 (-0.11, 0.19) |
| -0.02 (-0.25, 0.21) | Behavioral therapy | 0.02 (-0.25, 0.29) |
| -0.04 (-0.19, 0.11) | -0.02 (-0.29, 0.25) | Western medicine |

evidence in the future. In addition, (3) at present, only the selection of acupuncture points and treatment modality have more observations on the efficacy. The timing of acupuncture for weight loss treatment is not uniformly reported clinically. Of course, the existence of different treatment durations will affect the final evaluation of efficacy. More quality literature on the duration of acupuncture treatment for obesity is expected to follow.

In summary, our study evaluated the clinical efficacy of different acupuncture methods commonly used in clinical treatment on obesity combined with IR. Different acupuncture

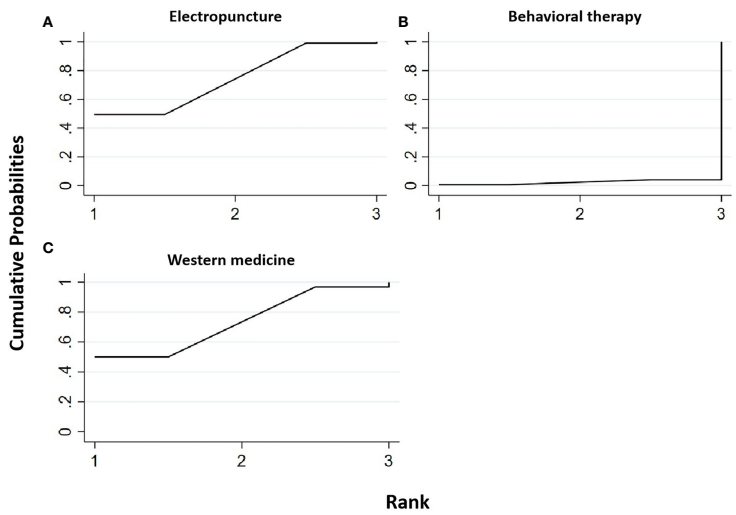


FIGURE 10
Efficacy ranking and cumulative probability graph of total cholesterol (TC) treated by different types of intervention. Comparison of efficacy ranking and cumulative probability of TC between each kind of intervention. **(A)** Electropuncture, **(B)** behavioral therapy, and **(C)** western medicine.

TABLE 12 Network meta-analysis ladder table of total cholesterol.

| | | |
|---|---|---|
| Electropuncture | 0.40 (0.06, 0.74) | 0.00 (-0.26, 0.26) |
| **-0.40 (-0.74, -0.06)** | Behavioral therapy | -0.40 (-0.83, 0.03) |
| -0.00 (-0.26, -.0.26) | 0.40 (-0.03, 0.83) | Western medicine |

Bold values means the sorting tables represent the area under the curve of the cumulative probability sorting chart, the bold values are the rank of the sorting by different types of intervention in our study. While the number of the ladder table is the relative effect value and 95% CI.

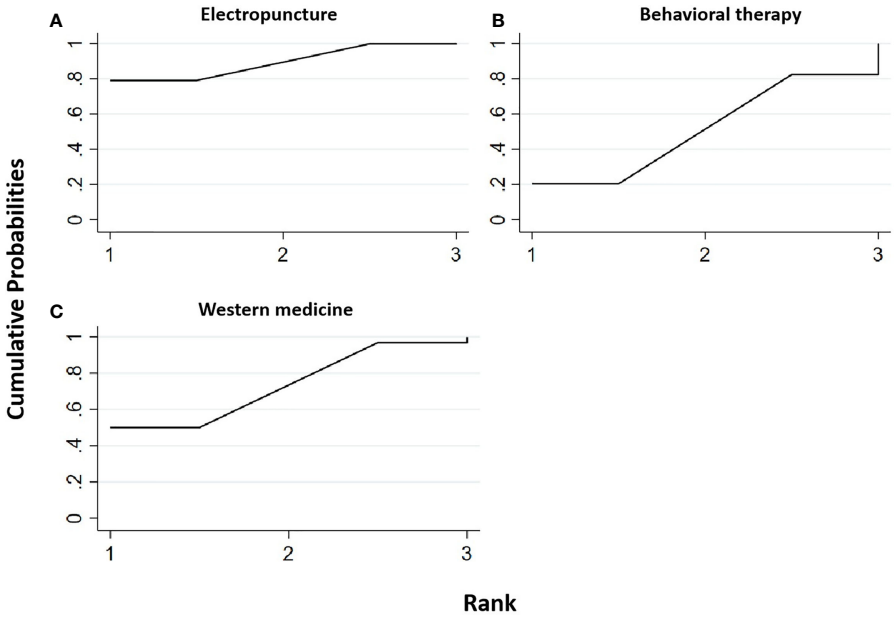


FIGURE 11
Efficacy ranking and cumulative probability graph of high-density lipoprotein (HDL) treated by different types of intervention. Comparison of efficacy ranking and cumulative probability of HDL between each kind of intervention. **(A)** Electropuncture, **(B)** behavioral therapy, and **(C)** western medicine.

TABLE 13 Efficacy ranking of mesh meta-analysis: high-density lipoprotein (HDL) and low-density lipoprotein (LDL).

| Treatment | SUCRA | Rank |
|---|---|---|
| HDL | | |
| Electropuncture | 89.5 | 1 |
| Behavioral therapy | 51.4 | 2 |
| Western medicine | 9.1 | 3 |
| LDL | | |
| Electropuncture | 83.6 | 1 |
| Western medicine | 65.9 | 2 |
| Behavioral therapy | 0.5 | 3 |

As shown in the table, the surface under the cumulative ranking curve (SUCRA) represents the area under the curve of the cumulative probability graph of efficacy ranking. The decrease in fasting blood glucose is better, the SUCRA value is bigger, and the efficacy ranking is higher.

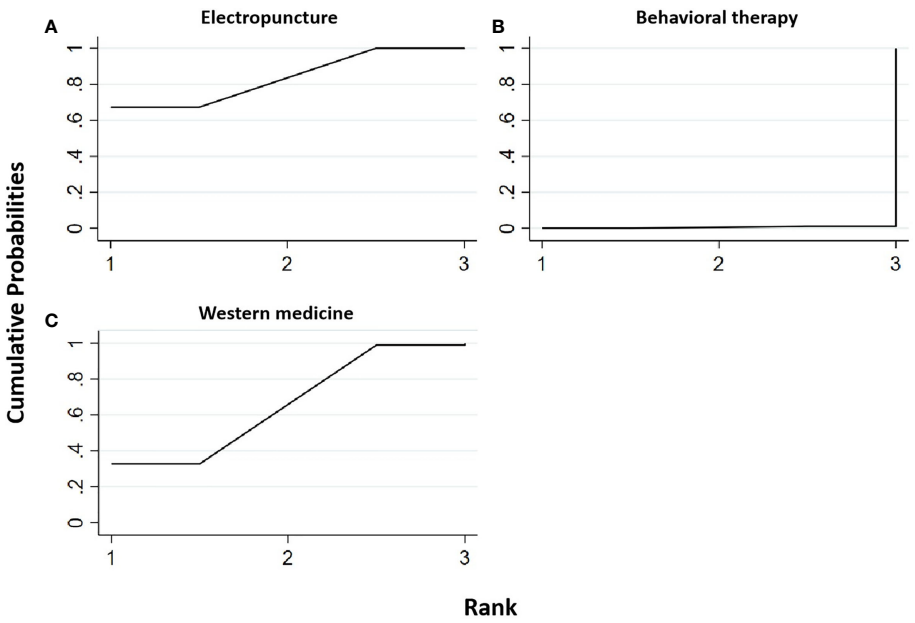


FIGURE 12
Efficacy ranking and cumulative probability graph of low-density lipoprotein (LDL) treated by different types of intervention. Comparison of efficacy ranking and cumulative probability of LDL between each kind of intervention. **(A)** Electropuncture, **(B)** behavioral therapy, and **(C)** western medicine.

TABLE 14 Network meta-analysis ladder table of high-density lipoprotein.

| | | |
|---|---|---|
| Electropuncture | -0.03 (-0.10, 0.04) | -0.07 (-0.13, -0.01) |
| 0.03 (-0.04, 0.10) | Behavioral therapy | -0.04 (-0.13, 0.05) |
| **0.07 (0.01, 0.13)** | 0.04 (-0.05, 0.13) | Western medicine |

Bold values means the sorting tables represent the area under the curve of the cumulative probability sorting chart, the bold values are the rank of the sorting by different types of intervention in our study. While the number of the ladder table is the relative effect value and 95% CI.

TABLE 15 Network meta-analysis ladder table of low-density lipoprotein.

| | | |
|---|---|---|
| Electropuncture | 0.38 (0.15, 0.61) | 0.04 (-0.13, 0.21) |
| **-0.38 (-0.61, -0.15)** | Behavioral therapy | -0.34 (-0.63, -0.05) |
| -0.04 (-0.21, 0.13) | **0.34 (0.05, 0.63)** | Western medicine |

Bold values means the sorting tables represent the area under the curve of the cumulative probability sorting chart, the bold values are the rank of the sorting by different types of intervention in our study. While the number of the ladder table is the relative effect value and 95% CI.

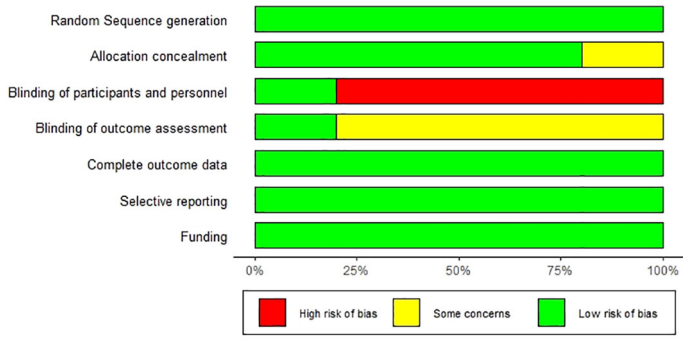


FIGURE 13
Evaluation for bias risk of the included studies.

methods have good advantages in both overall efficacy score and single index evaluation, providing strong objective evidence for obesity combined with IR in the future.

## Data availability statement

The raw data supporting the conclusions of this article will be made available by the authors, without undue reservation.

## Author contributions

CX, JL, and YC conceived and designed the experiments. JC, YG, LY, MH, NL, and YL analyzed and interpreted the data. MH, NL, and YL revised the data analysis and interpretation. JC, YG, and LY wrote the article. All authors contributed to the article and approved the submitted version.

## Funding

This work was supported by grants from State Key Laboratory of Dampness Syndrome of Chinese Medicine Special Fund (SZ2021ZZ08), Guangdong Provincial Bureau of Chinese Medicine (20225020), the Fund of Guangzhou University of Chinese Medicine (2021YJZX012, 2022YBA06), the Guangdong Provincial Hospital of Chinese Medicine Fund (YN2019ZWB01, YN2020MS02, YN2019ML01, BAQZJYJZX [2019] 007) and Research Fund for Zhaoyang Talents of Guangdong Provincial Hospital of Chinese Medicine (ZY2022KY10, ZY2022YL04).

## Conflict of interest

The authors declare that the research was conducted in the absence of any commercial or financial relationships that could be construed as a potential conflict of interest

## Publisher's note

All claims expressed in this article are solely those of the authors and do not necessarily represent those of their affiliated organizations, or those of the publisher, the editors and the reviewers. Any product that may be evaluated in this article, or claim that may be made by its manufacturer, is not guaranteed or endorsed by the publisher.

## Supplementary material

The Supplementary Material for this article can be found online at: https://www.frontiersin.org/articles/10.3389/fendo.2022.968481/full#supplementarymaterial

## References

1. Monteiro CA, Moura EC, Conde WL, Popkin BM. Socioeconomic status and obesity in adult populations of developing countries: a review. *Bull World Health Organ* (2004) 82(12):940–6. doi: 10.1590/S0042-96862004001200011

2. Haslam DW, James WP. Obesity. *Lancet* (2005) 366(9492):1197–209. doi: 10.1016/s0140-6736(05)67483-1

3. Yach D, Hawkes C, Gould CL, Hofman KJ. The global burden of chronic diseases: overcoming impediments to prevention and control. *Jama* (2004) 291 (21):2616–22. doi: 10.1001/jama.291.21.2616

4. Kim CH, Kim HK, Kim EH, Bae SJ, Choe J, Park JY. Longitudinal changes in insulin resistance, beta-cell function and glucose regulation status in prediabetes. *Am J Med Sci* (2018) 355(1):54–60. doi: 10.1016/j.amjms.2017.09.010

5. Koskinen J, Magnussen CG, Sabin MA, Kähönen M, Hutri-Kähönen N, Laitinen T, et al. Youth overweight and metabolic disturbances in predicting carotid intima-media thickness, type 2 diabetes, and metabolic syndrome in adulthood: the cardiovascular risk in young finns study. *Diabetes Care* (2014) 37 (7):1870–7. doi: 10.2337/dc14-0008

6. Regazzetti C, Peraldi P, Grémeaux T, Najem-Lendom R, Ben-Sahra I, Cormont M, et al. Hypoxia decreases insulin signaling pathways in adipocytes. *Diabetes* (2009) 58(1):95–103. doi: 10.2337/db08-0457

7. Belivani M, Dimitroula C, Katsiki N, Apostolopoulou M, Cummings M, Hatzitolios AI. Acupuncture in the treatment of obesity: a narrative review of the literature. *Acupunct Med* (2013) 31(1):88–97. doi: 10.1136/acupmed-2012-010247

8. Cho SH, Lee JS, Thabane L, Lee J. Acupuncture for obesity: a systematic review and meta-analysis. *Int J Obes (Lond)* (2009) 33(2):183–96. doi: 10.1038/ijo.2008.269

9. Martinez B, Peplow PV. Treatment of insulin resistance by acupuncture: a review of human and animal studies. *Acupunct Med* (2016) 34(4):310–9. doi: 10.1136/acupmed-2016-011074

10. Ni W, Wang P, H-j C, Liu Y, Zhang W-l, Qiu L, et al. Obesity complicated with insulin resistance treated with the electroacupuncture at the combination of back-shu and front-mu points. *World J Acupunct - Moxibustion* (2022) 32 (03):213–7. doi: 10.1016/j.wjam.2021.12.004

11. Haiyan L, Chaoyang M, Fen X. Effect of "specimen with point" electroacupuncture combined with behavioral therapy on simple obesity and its effect on insulin resistance and blood lipid level. *Chin J Tradit Chin Med* (2018) 36 (08):1848–51. doi: 10.13193/j.issn.1673-7717.2018.08.014

12. Haiyan L, Fen X, Chaoyang M. Effect of acupuncture intervention based on the theory of "specimen and acupoint" on blood lipid level and insulin resistance in patients with simple obesity. *Chin J Tradit Chin Med* (2019) 37(01):49–52. doi: 10.13193/j.issn.1673-7717.2019.01.011

13. Shan Z. *Clinical study on the treatment of simple obesity with gelatin microneedle acupoint patch*. Chengdu University of Chinese Medicine (2020). doi: 10.26988/d.cnki.gcdzu.2020.000146

14. Hong W, Shuxun Y, Zhao Y, Shengwei Z, Xian W, Meng Z. Acupoint catgut embedding in the treatment of simple obesity with gastric heat and dampness resistance: a randomized controlled study. *Chin Acupunct Moxibustion* (2022) 42 (02):137–42. doi: 10.13703/j.0255-2930.20210120-k0003

15. Lu L, Zhang Y, Tang X, Ge S, Wen H, Zeng J, et al. Evidence on acupuncture therapies is underused in clinical practice and health policy. *BMJ* (2022) 376: e067475. doi: 10.1136/bmj-2021-067475

16. Yan RH, Liu XM, Bai J, Hou BB, Yu J, Gu JS. Clinical efficacy of simple obesity treated by catgut implantation at acupoints. *Chin J Integr Med* (2015) 21 (8):594–600. doi: 10.1007/s11655-012-1215-7

17. Pi-Sunyer FX. The obesity epidemic: pathophysiology and consequences of obesity. *Obes Res* (2002) 10 Suppl 2:97s–104s. doi: 10.1038/oby.2002.202

frontiers | Frontiers in Endocrinology

TYPE Review
PUBLISHED 13 September 2022
DOI 10.3389/fendo.2022.1000739



OPEN ACCESS

EDITED BY
Bruno Melo Carvalho,
Universidade de Pernambuco, Brazil

REVIEWED BY
Monica Colitti,
University of Udine, Italy
Alisson Oliveira,
Federal University of
Pernambuco, Brazil

*CORRESPONDENCE
Yong-Yu Yang
yongyuyang@csu.edu.cn

SPECIALTY SECTION
This article was submitted to Obesity,
a section of the journal
Frontiers in Endocrinology

RECEIVED 22 July 2022
ACCEPTED 23 August 2022
PUBLISHED 13 September 2022

CITATION
Yang X-D, Ge X-C, Jiang S-Y and Yang Y-Y (2022) Potential lipolytic regulators derived from natural products as effective approaches to treat obesity.
*Front. Endocrinol.* 13:1000739.
doi: 10.3389/fendo.2022.1000739



# Potential lipolytic regulators derived from natural products as effective approaches to treat obesity

Xi-Ding Yang[1,2], Xing-Cheng Ge[3], Si-Yi Jiang[4] and Yong-Yu Yang[1,5]*

[1]Department of Pharmacy, Second Xiangya Hospital of Central South University, Changsha, China, [2]Phase I Clinical Trial Center, The Second Xiangya Hospital of Central South University, Changsha, China, [3]Xiangxing College, Hunan University of Chinese Medicine, Changsha, China, [4]Department of Pharmacy, Medical College, Yueyang Vocational Technical College, YueYang, China, [5]Hunan Provincial Engineering Research Central of Translational Medical and Innovative Drug, The Second Xiangya Hospital of Central South University, Changsha, China

Epidemic obesity is contributing to increases in the prevalence of obesity-related metabolic diseases and has, therefore, become an important public health problem. Adipose tissue is a vital energy storage organ that regulates whole-body energy metabolism. Triglyceride degradation in adipocytes is called lipolysis. It is closely tied to obesity and the metabolic disorders associated with it. Various natural products such as flavonoids, alkaloids, and terpenoids regulate lipolysis and can promote weight loss or improve obesity-related metabolic conditions. It is important to identify the specific secondary metabolites that are most effective at reducing weight and the health risks associated with obesity and lipolysis regulation. The aims of this review were to identify, categorize, and clarify the modes of action of a wide diversity of plant secondary metabolites that have demonstrated prophylactic and therapeutic efficacy against obesity by regulating lipolysis. The present review explores the regulatory mechanisms of lipolysis and summarizes the effects and modes of action of various natural products on this process. We propose that the discovery and development of natural product-based lipolysis regulators could diminish the risks associated with obesity and certain metabolic conditions.

KEYWORDS

**adipose tissue, insulin resistance, lipolysis, natural product, obesity**

# 1 Introduction

Obesity is excessive lipid accumulation in adipose tissue. It is caused by an imbalance between energy intake and energy consumption. According to the World Health Organization (WHO), more than 650 million adults over 18 years of age were obese as of 2016 (1). Obesity is a risk factor for cardiovascular disease (CVD), insulin resistance (IR), type 2 diabetes mellitus (T2DM), hypertension, dyslipidemia, and certain cancers (2). Increased adipocyte number (hyperplasia) and size (hypertrophy) are morphological manifestations of obesity (3). Adipose tissue is classified into three distinct types: white (WAT), brown (BAT), and beige (4). WAT stores excess energy in the form of triglycerides (TG), whereas BAT and beige adipose tissues catabolize TG into heat (5). Adipose tissue also functions as an endocrine organ and filler tissue and cushions, supports, and insulates the body (6).

WAT is generally considered a 'troublesome and excessive tissue'. Body weight may be lost *via* intermittent fasting, medication, exercise, or surgery (7). However, it is uncertain whether these approaches maintain weight loss or have unacceptable side effects in the long term. Exercise appears to be an effective weight loss method, although its efficacy depends largely on its duration, frequency, and intensity (8). The administration of certain drugs is promising for obesity prevention and treatment. Intermittent fasting, drugs, and exercise decompose TG faster than they are synthesized in the adipocytes. Hence, pharmacological and nutritional enhancements of this process are potential strategies for weight loss and the prevention of obesity-related metabolic syndrome.

The reservoir effect of WAT protects other tissues against the toxic effects of glycolipids associated with excess energy storage. Adipocytes have limited lipid storage capacity and can hold no additional TG when their volume expands beyond a critical point. At this stage, the adipose tissue becomes dysfunctional. This condition is observed in patients with insulin resistance, T2DM, and obesity and is manifested by decreased TG synthesis and excess free fatty acid (FFA) release (9). In cases of adipose tissue dysfunction, certain compounds improve whole-body energy metabolism by inhibiting lipolysis.

Natural products are vital sources of lead compounds and are important in drug discovery. Several natural products are widely used in obesity treatment (10). Various natural products (11–14), including flavonoids, alkaloids, and terpenoids control obesity by stimulating lipolysis, inhibiting adipogenesis and lipogenesis, and promoting energy expenditure. However, the activities and mechanisms of natural products in modulating lipolytic activity have not yet been systematically summarized. In the present review, from a lipolysis perspective, we describe the biosynthesis and metabolism of TG in adipose tissue and review the regulatory mechanisms of lipolysis. Furthermore, we summarize a wide diversity of plant secondary metabolites that have demonstrated anti-obesity effects *via* the promotion of lipolysis. We also focus on the progress of research on inhibitors of lipolysis with different mechanisms of action in adipose tissue dysfunction. This review provides insight into the precise biochemical and molecular mechanisms by which plant secondary metabolites inhibit the onset and/or progression of obesity and, by extension, its related co-morbidities. In addition, it highlights the potential of lipolysis as a therapeutic target for obesity and its complications.

# 2 Triglyceride biosynthesis and metabolism

Adipose tissue, the liver, and skeletal muscle are the mains organs responsible for the regulation of lipid metabolism. TG biosynthesis and decomposition (lipolysis) in WAT equilibrate lipid metabolism. After feeding, glucose and lipids from food are absorbed in the intestine in the form of chylomicrons and enter the bloodstream. The chylomicrons are then hydrolyzed into FFAs by lipoprotein lipase and absorbed and utilized by adipocytes and liver and muscle tissue. Insulin is secreted by β-cells in the pancreas and promotes FFA and glucose uptake, while insulin inhibits lipolysis *via* lipase inhibition. Adipocytes absorb excess FFA and glucose and produce TG as an energy storage form (15). During this process, adipogenesis and lipogenesis increase, while lipolysis, thermogenesis, and browning decrease. *De novo* lipogenesis involves TG biosynthesis and occurs in the adipocytes and liver. To maintain normal blood glucose levels, the liver converts excess glucose into glycogen and stores it in liver cells, or hepatocytes, which can also synthesize TG through the *de novo* TG synthesis pathway. TG subsequently is transported from the liver to adipose tissue by very low-density lipid (VLDL) (16). An important contributor to hepatic fat accumulation is the insufficient hepatic export of TG in the form of VLDL particles. TG synthesis and metabolism are illustrated in Figure 1.

During fasting and starvation, TG is decomposed into glycerol and FFA (17). Adipose triglyceride lipase (ATGL), hormone-sensitive lipase (HSL), and monoacylglycerol lipase (MAGL) hydrolyze TG to FFAs and glycerol. The glycerol is used to make glucose in gluconeogenesis. FFAs are then released into circulation, where they are utilized by the peripheral tissues and/or re-esterified into TG in the adipocytes. Skeletal muscle and the liver are the most important organs involved in FFA metabolism *via* β-oxidation and subsequent ATP generation. Mitochondrial-rich beige adipose tissue or BAT are the major sites responsible for non-shivering thermogenesis in mammals. Cold exposure, β-adrenergic receptor (β-AR) agonists, peroxisome proliferator-activated receptor-γ, and exercise can

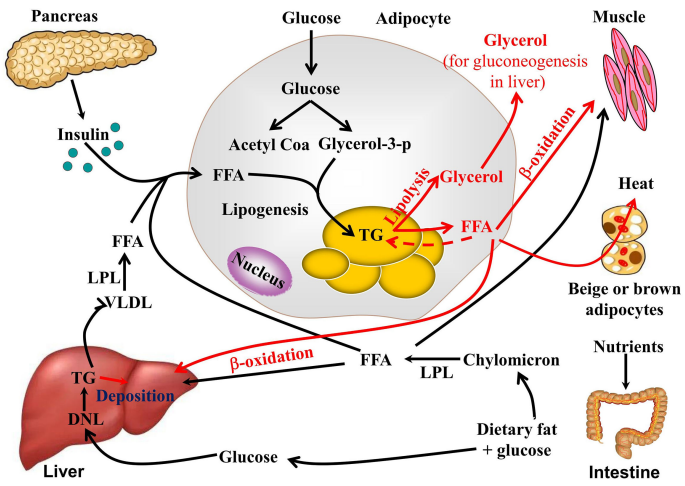


FIGURE 1
TG synthesis and metabolism.

induce the browning of WAT. FFA produced by lipolysis is also absorbed and utilized by beige adipocytes or BAT through UCP-1-dependent shiver-independent thermogenesis.

## 3 Lipolysis and its mechanisms

Lipolysis is a finely regulated process mediated by the consecutive actions of ATGL, HSL, and MAGL. ATGL or HSL first hydrolyzes TG to diglycerides and FFA. HSL then hydrolyzes diglycerides to monoglycerides and FFA. MAGL then hydrolyzes monoglycerides to glycerol and FFA (18). Lipid droplet autophagy or lipophagy is a complementary cellular lipid breakdown pathway (19). Sex, age, physical activity, fat deposit location, and genetic variation regulate basal lipolytic activity in adipocytes (20). The proinflammatory cytokines TNF-α (21), IL-6 (22), and IL-1β (23) as well as lipopolysaccharide (LPS) (24) and hypoxia (25) may induce TG lipolysis. Lipid droplet-associated proteins (LDAPs) (26), cyclic guanosine monophosphate dependent-protein kinase G (cGMP-PKG) (8), mitogen-activated protein kinase (MAPK) (27), and adenosine 5'-monophosphate (AMP)-activated protein kinase (AMPK) (28) are also implicated in TG lipolysis.

### 3.1 LDAPs

Lipid droplets (LD) are dynamic lipid storage organelles surrounded by single layers of polar and amphipathic phospholipids and structural proteins. They are now considered major fat storage, lipid secretion, and lipolysis regulators (29). The perilipins, including perilipin1, perilipin2, and perilipin5, as well as the cell death-inducing DNA fragmentation factor alpha (DFFA)-like effector (CIDE) family proteins, including Cidea, Cideb, and Cidec/Fsp27, have emerged as key lipolysis regulators (30, 31). Perilipin1 is a scaffold for organized protein-protein interactions on LD surfaces. It binds CGI-58 and suppresses HSL translocation to LD under basal conditions. During stimulatory conditions, however, phosphorylation causes perilipin to dissociate from CGI-58. The free CGI-58 then binds phosphorylated ATGL and co-activates TG hydrolysis (32). Perilipin phosphorylation recruits HSL from the cytosols to the surfaces of the LDs, and diglycerides are then hydrolyzed (26). FSP27-deficient cells exhibite increased basal lipolysis and reduced lipid storage capacity (33). The mechanisms by which perilipin1 regulates lipolysis are generally understood. However, the roles and mechanism of perilipin2, perilipin5, and the CIDE family in lipolysis remain to be elucidated.

### 3.2 cAMP-PKA pathway

*In vivo*, dynamic lipolysis processes are mainly regulated by hormones, such as catecholamines, ghrelin, adiponectin, and insulin. Under conditions of fasting, cold stress, and other compound treatment, norepinephrine is released from sympathetic nerve terminals. β-AR agonists, such as epinephrine, norepinephrine, and dopamine, upregulate cyclic AMP (cAMP) by linking various AR subtypes to the G-protein receptor complex that controls adenylate cyclase in the cell membrane. Thereafter, protein kinase A (PKA) is activated by cAMP (34). PKA phosphorylates both HSLs at Ser563, Ser659,

and Ser660, thereby activating them and promoting their translocation from the cytoplasm to the surfaces of LDs (35).

cAMP degradation is mediated by phosphodiesterase (PDE). Insulin inhibits lipolysis mainly by activating the phosphoinositide 3-kinase/protein kinase B/PDE 3B (PDE3B) pathway, which leads to p-HSL and p-perilipin dephosphorylation (36). In addition, ligands of Gi protein-coupled receptors, such as succinic acid, nicotinic acid, beta-hydroxybutyric acid, and neuropeptide Y, inhibit the formation of cAMP by binding to their receptors, thereby exerting an anti-lipolytic effect.

### 3.3 cGMP-PKG

Cyclic guanosine 3'5'-monophosphate (cGMP) is an important intracellular secondary messenger of hormone-induced lipolysis. Atrial and b-type natriuretic peptides are nitric oxide (NO) donors that stimulate lipolysis in adipocytes *via* the cGMP/PKG pathway (8). PKG phosphorylates proteins associated with lipolysis, including HSL and perilipin, thereby promoting TG breakdown (37). The cGMP is also involved in TNF-α (iNOS/NO/GC/cGMP-dependent pathway)- and endothelin-1 (GC/cGMP/$Ca^{2+}$/ERK/CaMKIII signaling pathway)-induced lipolysis in adipocytes (38–40). Few studies have reported on the involvement of cGMP/PKG in lipolysis regulation. Moreover, the roles of cGMP/PKG in lipolytic enzymes regulation and LDAPs remain to be clarified.

### 3.4 Mitogen-activated protein kinase

The mitogen-activated protein kinase (MAPK) family, which including extracellular signal-regulated kinases (ERKs), jun aminoterminal kinase (JNK), and p38 mitogen-activated protein kinases (p38) plays vital roles in adipogenesis and lipolysis. (β–AR) stimulation by catecholamine activates ERK1/2, which is sufficient to induce lipolysis by direct HSL phosphorylation at Ser600. JNK regulates lipolysis. JNK1/2 deficiency accelerates basal lipolysis in mouse adipocytes (41). The MEK1/2-ERK1/2 pathway controls TNF-α-stimulated lipolysis in human adipocytes (42).

### 3.5 AMPK pathway

AMPK is a Ser/Thr protein and an important regulatory sensor of cellular energy metabolism. Activated AMPK inhibits sterol regulatory element binding protein-1, CCAAT/enhancer binding protein alpha, peroxisome proliferator activated receptor gamma, and acetyl-CoA carboxylase (ACC). Hence, AMPK suppresses adipocyte differentiation (43). AMPK also phosphorylates ATGL Ser406, which promotes TG decomposition (44). However, the roles of AMPK in regulating TG lipolysis in adipocytes are controversial. AMPK may phosphorylate HSL at Ser565 to inhibit phosphorylation at HSL Ser660 and Ser563. In this manner, it reduces HSL activity and suppresses lipolysis (45). AMPK is implicated in chaperone-mediated autophagy which selectively degrades perilipins and initiates lipolysis (46). Therefore, proteins and signaling pathways that modulate AMPK expression and activity, such as SIRT (47) and SIRT3 (48), mobilize TG in adipocytes.

Protein kinase C (49), $Ca^{2+}$ (50), inositol hexakisphosphate kinase-1 (51), transient receptor potential vanilloid channels (38, 52), and endoplasmic reticulum (ER) stress (53) regulate lipolysis in adipocytes either alone or by interacting with the aforementioned signaling pathways (Figure 2).

## 4 Natural products involved in lipolysis

The structural diversity of natural products determines their wide range of pharmacological activity. Natural products may be used to treat obesity and its associated metabolic diseases. Traditional and complementary medicines including various herbs and extracts have been widely used to prevent and treat metabolic disorders (54, 55). Flavonoids (56), alkaloids (57), terpenoids (58), and polyphenols (59) stimulate lipolysis in adipocytes, thereby causing weight loss and improving metabolic status. Their modes of action involve the PKA-HSL, PKC, AMPK, MAPK, and other signaling pathways.

### 4.1 Natural products promote lipolysis

#### 4.1.1 Flavonoids

Flavonoids comprise a large family of natural substances sharing a molecular structure characterized by at least one phenolic ring. Flavonoids are reputed for their health benefits. Epigallocatechin-3-gallate (EGCG) is a polyphenolic catechin in green tea that improves the lipid prolife and reduces body weight (60). EGCG inhibits adipogenesis and adipocyte differentiation, reduces energy intake, and increases energy expenditure and lipolysis (61, 62). EGCG-stimulated lipolysis is mediated by activating HSL (63), ERK1/2 (64), and p-AMPK (65). Lipophagy is also associated with EGCG-induced lipolysis. Rab7 knockdown attenuates EGCG-dependent lipid reduction (65). However, a clinical trial demonstrated no effect of EGCG on obesity reduction, lipolysis, or white adipocyte browning in humans (66).

Kaempferol (67), apigenin (68), genistein (69), morusin (70), medicarpin (71), and myricetin (72) commonly occur in fruits, vegetables, and tea. These flavonoids have anti-obesity and pro-lipolysis efficacy. Elevated lipolysis upregulates thermogenic

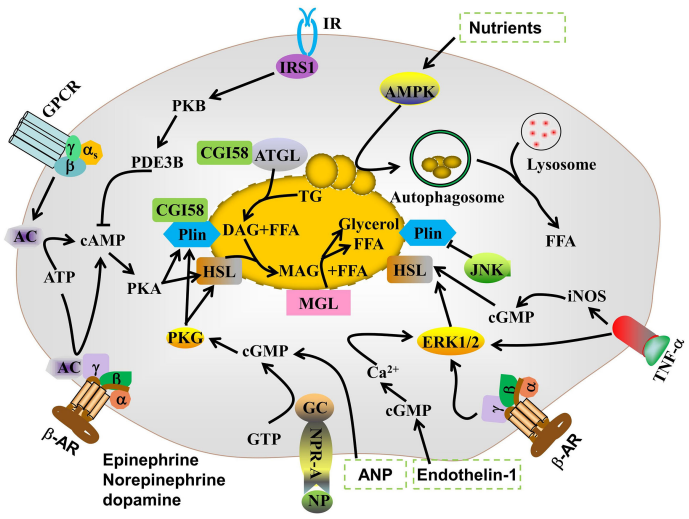


FIGURE 2
Signaling pathways regulating lipolysis in adipocytes.

genes and increases mitochondrial biogenesis by supplying FFAs for mitochondrial β-oxidation. Apigenin activates lipolysis *via* the ATGL/FOXO1/SIRT1 pathway and increases FFA consumption by upregulating fatty acid oxidation (FAO) (AMPK/ACC), thermogenesis, and browning (UCP-1, PGC-1α) (68). Lipolysis is also associated with activated BAT or beiging which is regarded as an alternative strategy against diet-induced obesity. Xanthohumol (73), apigenin (68), and EGCG (65) inhibit adipogenesis, stimulate adipocyte lipolysis, and may act as browning or beiging agents because they upregulate the thermogenic protein UCP1 (Table 1).

### 4.1.2 Alkaloids

Consumption of coffee, ephedrine, or capsaicin increases lipolytic responses, raise metabolic rates, and increase energy expenditure and weight loss (74, 75). Caffeine is the main

TABLE 1 Lipolytic effects and modes of action of flavonoids.

| Compound | Model | Concentration | Effect | Mechanism | Reference |
|---|---|---|---|---|---|
| EGCG | 3T3-L1 adipocytes; C3H10T1/2 cells | 10 μM | Adipogenesis inhibition<br>Lipophagy activation and adipocyte browning | Increasing p-AMPK<br>Lipophagy mediates EGCG-induced lipolysis | Kim et al. (65) |
| | 3T3-L1 adipocytes | 10 μM | Lipolysis promotion | Increasing HSL | Lee et al. (63) |
| | Rat primary adipocytes | 2.79 μM | Lipolysis promotion | Increasing p-ERK1/2 | Ogasawara et al. (64) |
| Kaempferol | 3T3-L1 adipocytes | 60 μM | Lipolysis promotion<br>Adipogenesis inhibition | Increasing ATGL and HSL | Torres-Villarreal et al. (67) |
| Apigenin | HFD-Fed mice | 0.04% | Increasing lipolysis, thermogenesis, and browning | Increasing ATGL, SIRT1, and p-AMPK | Sun et al. (68) |
| Myricetin | 3T3-L1 adipocytes | 50 and 100 μM | Increasing lipolysis | Decreasing perilipin1<br>Increasing p-p38 and p-JNK | Wang et al. (72) |
| Genistein | Primary rat adipocytes | 0.1 and 1 mM | Increasing lipolysis | PKA-mediates, genistein-induced lipolysis | Szkudelska et al. (69) |
| Morusin | 3T3-L1 and primary adipocytes | 5, 10 and 20 μM | Lipolysis promotion<br>Adipogenesis inhibition | Increasing HSL, ATGL, and p-perilipin expression | Lee et al. (70) |
| Medicarpin | BAT cells | (10 μM) | Lipolysis promotion | PKA-mediates, medicarpin-induced lipolysis | Imran et al. (71) |
| Xanthohumol | 3T3-L1 and primary human adipocytes. | 25 μM | Adipogenesis suppression<br>Increasing lipolysis and white adipocyte beiging | AMPK signaling pathway mediates lipolysis | Samuels et al. (73) |

alkaloid in tea, coffee, and cacao. It decreases body fat, improves glucose tolerance and insulin sensitivity (76), and increases lipolysis by raising cAMP levels and upregulating lipolytic enzymes (77). Ephedrine is an α- and β-adrenergic receptor agonist with efficacy as a bronchodilator. It also activates the β-adrenergic receptors, contributing to lipolysis (78). Capsaicin analogs significantly increase cAMP levels and PKA activity in BAT (79). While ephedrine, caffeine, capsaicin, and synephrine strongly induce lipolysis, they are also associated with various cardiovascular and gastrointestinal side effects when they are administered for weight loss (80). Therefore, novel lipolytic compounds with minimal adverse reactions merit further investigation.

Berberine (BBR) is an isoquinoline alkaloid derived from the Chinese herb *Coptis chinensis*. It has anti-obesity, anti-diabetic, and anti-hyperlipidemic efficacy. BBR stimulates basal lipolysis in 3T3–L1 adipocytes by upregulating ATGL *via* the AMPK pathway (81, 82). However, Zhou et al. found that BBR attenuates isoprenaline-stimulated lipolysis in 3T3–L1 adipocytes by reducing phosphodiesterase-3B and -4 inhibition, thereby decreasing cAMP production and inhibiting HSL activation (83). Trigonelline (*N*-methylnicotinic acid) is a pyridine derivative that increases brown and beige fat-specific markers as well as mitochondrial biogenesis in 3T3-L1 adipocytes (57). Trigonelline as well as cordycepin from *Cordyceps militaris* promotes white adipocytes beiging and browning and increases lipolysis by various mechanisms (57, 84) (Table 2).

### 4.1.3 Terpenoids

Terpenoids comprise five-carbon isoprene units and have diverse effects on obesity and its associated metabolic diseases. Triterpenoids include 18β-glycyrrhetinic acid (18β-GA) (88), ursolic acid (89), acetyl-keto-β-boswellic acid (AKBA) (90), alisol A 24-acetate (AA-24-a) (91), celastrol (92), and betulinic acid (93). All of these reduce neutral lipids in the cytosol and increase FFA release. Madecassoside (94), tanshinone 1 (95), triptolide (58), crocin (96), guggulsterone (97), bilobalide (98), α-cubebenoate (99, 100), betulinic acid (93), fucoxanthinol (101), widdrol (102), ginkgolide C (103), and illudins C2 and C3 (104) could all potentially treat obesity either by inhibiting adipocyte differentiation and lipogenesis or by increasing lipolysis. The LDAP (88–90), PKA (89, 90), AMPK (96, 98), and PKC-MEK-ERK (102) pathways are involved in the lipolytic mechanisms induced by these compounds (Table 3).

Celastrol and triptolide are the main bioactive constituents in the root of *Tripterygium wilfordii*. The administration of celastrol and triptolide reduces body and fat weight, suppresses lipogenesis (58, 92), increases heat production in BAT, and enhances lipolysis (58). Celastrol rapidly lowers body weight by covalently inhibiting GRP78 chaperone activity and disconnecting ER stress signal transduction (92). Elevated lipolysis induced by triptolide is mediated by p53 which directly binds and promotes the transcription of the ATGL promoter (58). Although triptolide and celastrol have good anti-obesity efficacy, their potential toxicity must be established.

TABLE 2 Lipolytic effects and modes of action of alkaloids.

| Compound | Animal or cell model | Concentration | Effect | Mechanism | Reference |
|---|---|---|---|---|---|
| BBR | Differentiated porcine adipocytes | 10-40 μM | Lipolysis and FFA oxidation promotion | Increasing p-ATGL<br>Decreasing perilipin<br>AMPK mediates BBR-induced lipolysis | Yang et al. (82) |
| Trigonelline | 3T3-L1 cells | 75 μM | Promoting lipolysis, browning, and FFA oxidation<br>Decreasing adipogenesis and lipogenesis | β3-AR/PKA activation<br>PDE4 inactivation | Choi et al. (57) |
| Capsaicin | 3T3-L1 cells | 10 μM | Promoting lipolysis | Increasing HSL and UCP2 | Lee, et al. (85) |
| | HFD-Fed transient receptor potential vanilloid 1 deficient ($TRPV1^{-/-}$) mice<br>3T3-L1 cells | Animal: chow plus 0.01% capsaicin<br>Cell: 1 μmol/L | Promoting lipolysis | TRPV1 mediates capsaicin-induced lipolysis | Chen, et al. (86) |
| Caffeine | SD rats | 5 mg/kg | Promoting lipolysis | N.A. | Kobayashi-Hattori et al. (87) |
| Cordycepin | Animal: S-D rats<br>Cell: 3T3-L1 cells | Animal: 12.5, 25, and 50 mg/kg<br>Cell: 1.563-25 μg/mL | White adipocyte beiging and browning<br>Blocking lipid droplet formation and promoting lipid droplet degradation | Decreasing Fsp27, perilipin 3, perilipin 2, Rab5, Rab11, CGI-58 and perilipin 1<br>Increasing ATGL | Xu et al. (84) |

HFD, high-fat diet; N.A., not available.

TABLE 3 Lipolytic effects and modes of action of terpenoids.

| Compound | Animal or cell model | Concentration | Effect | Mechanism | Reference |
|---|---|---|---|---|---|
| 18β-GA | 3T3-L1 cells | 40 μM | Inhibiting adipogenic differentiation<br>Increasing lipolysis | Increasing HSL, ATGL, perilipin and p-HSL expression | Moon et al. (88) |
| Ursolic acid | Primary rat adipocytes | 25 and 50 μM | Increasing lipolysis | Increasing HSL translocation and ATGL expression<br>Decreasing perilipin1<br>PKA participates in lipolytic action of UA | Li et al. (89). |
| AKBA | 3T3-L1 adipocytes | 30 μM | Increasing lipolysis | Increasing ATGL and HSL<br>Decreasing perilipin | Liu et al. (90) |
| Betulinic acid | Rat adipocytes | 10 and 25 μM | Increasing lipolysis | Decreasing PDE activity | Kim et al. (93) |
| AA-24-a | 3 T3-L1 cells | 30, 40 and 50 μM | Increasing lipolysis | PKA- and ERK- mediated AA-24-A-promote lipolysis | Lou et al. (91) |
| Celastrol | C57BL/6N mice fed HFD | 7.5 mg/kg/d for 21 d | Inhibiting lipogenesis<br>Increasing lipolysis and thermogenesis | Inhibiting endoplasmic reticulum (ER) stress | Luo et al. (92) |
| | 3T3-L1 adipocytes | 400 nM | Inhibiting adipocyte differentiation and adipogenesis | N.A. | Choi et al. (105) |
| Tanshinone 1 | Immortalized brown adipocytes (iBAs) and differentiated C3H10T1/2 cells | 15 μM | Reducing HFD-induced obesity<br>Activating brown adipocytes<br>Increasing lipolysis and browning | Increasing HSL and p-AMPK | Jung et al. (95) |
| *Cis*-Guggul-sterone | 3T3-L1 adipocytes | 25 and 50 μM | Inhibiting lipid content<br>Increasing lipolysis | Increasing p-ERK1/2 | Yang et al. (97) |
| Madecas-soside | KKay/TaJcl obese diabetic mice | 40 mg/kg/d | Inhibiting lipogenesis.<br>Promoting lipolysis and thermogenesis | Increasing p-HSL, p-AMPK | Sun et al. (94) |
| Triptolide | Cell: 3T3-L1 and porcine adipocytes<br>Animal: C57BL/6J fed HFD | Cell: 10 nM Animal: 0.2 mg/kg for 7 wks | Reducing fat tissue accumulation<br>Increasing heat production<br>Increasing lipolysis | P53-mediated ATGL transcription responsible for triptolide-induced lipolysis | Wang et al. (58) |
| Crocin | Cell: 3T3-L1 adipocytes Animal: db/db mice | Cell: 20 μM<br>Animal: 20 mg/kg/d | Increasing lipolysis<br>Inhibiting preadipocyte differentiation and adipogenesis | AMPK mediates crocin-trigged lipolysis | Gu et al. (96) |
| Bilobalide | 3T3-L1 adipocytes | 25 and 100 μM | Inhibiting preadipocyte differentiation and adipogenesis<br>Increasing lipolysis | Increasing ATGL, pHSL, pACC1/ACC1, and pAMPK/AMPK | Bu et al. (98) |
| α-Cubebe-noate | Primary adipocytes and 3T3-L1 adipocytes | 10, 20, and 30 μg/mL | Inhibiting adipogenesis and lipogenesis<br>Increasing lipolysis | Increasing pHSL, ATGL, and p-perilipin | Bae et al. (99) |
| α-Cubebenol | 3T3-L1 adipocytes | 7.5, 15, and 30 μg/mL | Inhibiting adipogenesis<br>Increasing lipolysis | Increasing cAMP, ATGL, p-perilipin, and p-HSL<br>Decreasing perilipins and PDE4 | Lee et al. (100) |
| Illudins C2 and C3 | 3T3-L1 adipocytes | 5 and 10 μM | Suppressing adipogenesis<br>Increasing lipolysis | PKA and ERK mediate illudins C2 and C3-stimulated lipolysis | Kim et al. (104) |
| Fuco-xanthinol | 3T3-L1 adipocytes | 5 and 10 μM | Decreasing TG content<br>Increasing lipolysis | Increasing ATGL, pHSL, pACC1/ACC1, and pAMPK/AMPK<br>Decreasing CGI-58, ATGL, p-HSL, and perilipin | Yoshikawa et al. (101) |
| Widdrol | 3T3-L1 adipocytes | 10-25 μg/mL | Increasing lipolysis | PKC and MEK/ERK pathway mediated Widdrol-induced lipolysis | Jeong et al. (102) |
| Ginkgolide C | 3T3-L1 adipocytes | 10, 30 and 100 μM | Suppressing adipogenesis and promoting lipolysis | Increasing ATGL, p-HSL, and p-AMPK | Liou et al. (103) |

N.A., not available.

### 4.1.4 Other compounds

Resveratrol (RSV) (106), 2,4,5-trimethoxybenzaldehyde (2,4,5-TMBA) (11), raspberry ketone (RK) (107), cinnamaldehyde (108), lipoic acid (109), syringic acid (110), 6'-O-acetyl mangiferin (111), ferulic acid (112), and magnolol (113) have all demonstrated potential prophylactic and therapeutic efficacy against obesity. RSV directly affectes isoprenaline-stimulated lipolysis *in vitro* in fac cells from overweight humans (114). It also increases FFA and glycerol content in high-fat diet (HFD)-fed mice or 3T3-L1 adipocytes (106). Arrate et al. showed ATGL-mediated, RSV-induced lipolysis *in vivo* (115). However, a randomized, double-blind, crossover study revealed that RSV improved adipose tissue lipolysis and decreased plasma FFA and glycerol levels (116). This apparent contradiction in the anti-obesity effects of RSV in rodents and humans necessitates the re-evaluation of RSV as a putative anti-obesity drug.

RK has a structure resembling those of capsaicin and synephrine and can prevent HFD-induced obesity (117). 3T3-L1 adipocytes treated with 10 μM RK presented with elevated FAO and inhibition of lipid accumulation (118). Magnolol is the main bioactive compound in *Magnolia officinalis*. Its lipolytic effect is mediated by the calcium/calmodulin-dependent protein kinase (CaMK)/ERK1/2 signaling pathway and not by PKA (119). Magnolol may cause browning in white adipocytes and augment thermogenesis (113) (Table 4). Further research in the form of animal models is required to validate the lipolytic potential and clinical value of the foregoing compounds.

The lipolytic effects of the compounds above have already been established in *in vivo* or *in vitro* experiments. For

TABLE 4 Lipolytic effects and modes of action of other compounds.

| Compound | Animal or cell model | Concentration | Effect | Mechanism | Reference |
|---|---|---|---|---|---|
| 2,4,5-TMBA | 3T3-L1 adipocytes | 100 μg/mL | Suppressing differentiation and adipogenesis<br>Increasing lipolysis | Reducing perilipin<br>Increasing HSL | Wu et al. (11) |
| Raspberry ketone | Animal: ICR mice +HFD<br>Cell: Primary adipocytes | Animal: 1) HFD including 0.5, 1, or 2% RK<br>2) HFD containing 1% RK<br>Cell: $10^{-3}$ μM and $10^{-4}$ μM | Preventing obesity<br>Increasing norepinephrine-induced lipolysis | Increasing HSL protein translocation | Morimoto (117). |
| | 3T3-L1 adipocytes | 10 μM | Increasing FAO and lipolysis<br>Suppressing lipid accumulation | N.A. | Park et al. (118) |
| | 3T3-L1 adipocytes | 10, 20, and 50 μM | Inhibiting adipogenic and lipogenesis<br>Increasing lipolysis | Increasing ATGL and HSL | Park et al. (120) |
| RSV | Human adipocytes | 100 μM | Increasing isoprenaline-induced lipolysis<br>Impairing insulin-mediated anti-lipolysis | N.A. | Gomez-Zorita et al. (114) |
| | Animal: C57BL/6J mice +HFD<br>Cell: 3T3-L1 adipocytes | Animal: 15 mg/kg<br>Cell: 20 μM | Promoting lipolysis<br>Improving metabolic abnormalities | N.A. | Gong et al. (106) |
| | Cell: 3T3-L1 adipocytes, human SGBS adipocytes<br>Tissue: fat pads from wild-type, $ATGL^{-/-}$ and $HSL^{-/-}$ mice | 100 μM | Increasing basal-, isoproterenol-, and isoproterenol-stimulated lipolysis | ATGL mediates RVS-induced lipolysis | Lasa et al. (115) |
| Lipoic acid | 3T3-L1 adipocytes | 250 μM | Increasing lipolysis | cAMP-PKA mediates LA-induced lipolysis | Fernández-Galilea et al. (109) |
| Cinnamal-dehyde | Animal: Swiss albino mice fed HFD.<br>Cell: 3T3-L1 adipocytes | Animal: 10 mg/kg/d for 14 wks<br>Cells: 20 μM and 40 μM | Inhibiting preadipocyte differentiation and lipid accumulation in adipocytes<br>Increasing lipolysis and browning | Increasing HSL<br>Decreasing Plin1 | Khare et al. (108) |
| Magnolol | Sterol ester (SE)-loaded 3T3-L1 preadipocytes | 5-60 μM | Promoting lipolysis | CaMK/ERK mediate magnolol-induced lipolysis | Huang et al. (119) |
| | 3T3-L1 adipocytes | | Promoting lipolysis, browning, and thermogenesis | Increasing p-HSL, PKA, p-AMPK, Plin1 | Parray, et al. (113) |
| Syringic acid | 3T3-L1 adipocytes | 1000 μmol/mL | Promoting lipolysis | N.A. | John et al. (110) |
| 6'-O-acetyl mangiferin | 3T3-L1 adipocytes | 12.5, 25, and 50 μM | Promoting lipolysis | Increasing p-HSL, ATGL, and p-AMPK | Sim et al. (111) |
| Ferulic acid | 3T3-L1 adipocytes | 10 μM | Inhibiting lipogenesis and promoting lipolysis | Increasing p-perilipin, p-HSL | Kuppusamy et al. (112) |

N.A., not available.

TABLE 5 Anti-lipolytic effects and mechanisms of various compounds.

| Compound | Animal or cell model | Concentration | Effect | Mechanism | Reference |
|---|---|---|---|---|---|
| RA | 3T3-L1 adipocytes | 50 μM | Inhibiting adipogenesis and lipolysis | Decreasing p-HSL-ser660 and p-perilipin A | Rui et al. (136) |
| AS-IV | Animal: ICR mice fed HFD | Animal: 50 and 100 mg/kg | Inhibiting lipolysis and hepatic lipid deposition<br>Improving glucose tolerance | Decreasing cAMP<br>Increasing PDE3B, AMP, and Akt | Du et al. (126) |
| | 3T3-L1 adipocytes | 50, 100, and 200 μM | Inhibiting TNF-α-induced lipolysis and improving IR | Increasing perilipin<br>Decreasing p-ERK1/2 | Jiang et al. (131) |
| Curcumin | Adipose tissue<br>Cells: 3T3-L1 adipocytes | 0.1, 1, and 10 μM | Inhibiting lipolysis<br>Reducing lipid deposition and IR in liver | Decreasing cAMP, p-HSL and ER stress<br>Increasing AMP and PDE3B | Wang et al. (125) |
| | 3T3-L1 adipocytes | 20 μM | Inhibiting TNF-α or catecholamine-induced lipolysis | Decreasing p-ERK1/2, p-perilipin, and HSL translocation | Xie et al. (132) |
| Ilexgenin A | Adipose tissue | 20 or 50 mg/kg | Inhibiting lipolysis and hepatic IR | Decreasing cAMP, pSer-660-HSL and ER stress<br>Increasing AMP, PDE3B, pSer-565-HSL, and p-AMPK | Li et al. (127) |
| BBR | 3T3-L1 adipocytes | 10 μM | BBR-decreased isoprenaline- and noradrenaline-induced lipolysis | Reducing PDE inhibition | Zhou et al. (83) |
| RSV | Obese human | 150 mg/d for 30 d | Inhibiting lipolysis<br>Increasing muscle and decreasing hepatic lipid content | N.A. | Timmers et al. (116) |
| Piceatannol | 3T3-L1 adipocytes, brown adipocyte, and WAT | 25 and 50 μM | Inhibiting basal and isoprenaline-stimulated lipolysis | Autophagy mediated ATGL, CGI-58, and perilipin1 downregulation induced by piceatannol | Kwon et al. (140) |
| EPA | Primary rat adipocytes, 3T3-L1 adipocytes, and rat adipose tissue | 100 and 200 μM | Inhibiting IL-6- and TNF-α-induced lipolysis | Increasing pSer565 HSL<br>Decreasing ATGL | Lorente-Cebrián et al. (134) |
| C3G | 3T3-L1 adipocytes | 50 μM | Inhibiting high glucose-induced lipolysis | Increasing AMPK activity<br>Decreasing FoxO1-mediated ATGL transcription | Guo et al. (138) |
| Emodin | 3T3-L1 adipocytes | 50 μM | Increasing glucose metabolism<br>Decreasing TNF-α-induced lipolysis | Decreasing p-perilipin and p-ERK1/2 | Zhang et al. (133) |
| DDE | 3T3-L1 adipocytes or human subcutaneous adipocytes | 1 and 10 μM | Inhibiting basal- and TNF-α-induced lipolysis | N.A. | Nehrenheim et al. (139) |
| Phillyrin | 3T3-L1 adipocytes | 20, 40, 80 μM | Increase in glucose uptake and decrease in TNF-α-induced lipolysis | Decreasing p-ERK1/2<br>Increasing perilipin | Kong et al. (135) |
| Rg5 | Animal: ICR mice fed HFD<br>Cells: 3T3-L1 adipocytes | Animal: 50 mg/kg<br>Cells: 0.1, 1, 10 μM | Inhibiting lipolysis in adipocytes and IR in muscle | Decreasing cAMP and p-PKA<br>Increasing PDE3B and AMP | Xiao et al. (128) |
| Carnosic acid | Human multipotent, adipose-derived stem cells | 10 μM | Inhibiting isoprenaline-induced lipolysis | N.A. | Colson et al. (137) |

N.A., not available.

compounds with pro-lipolytic activity tested only *in vivo*, preclinical pharmacodynamics and safety evaluations are required. In pharmacodynamics experiments, primary outcome measures, such as change in body weight, food intake, resting metabolic rate, blood lipids, and biochemistry, need to be tested. In addition to general and specific toxicities of drugs, the safety evaluation should pay special attention to liver and kidney toxicity caused by long-term use of lipolysis agonists, as well as pancreatic damage, insulin resistance, and cardiovascular events that may be caused by elevated FFA.

## 4.2 Natural products that inhibit lipolysis

Adipose tissue dysfunction increases circulating FFA levels. Elevated FFAs are often observed in patients with IR and T2DM (9). Impaired lipogenic capacity driven by insulin signaling and re-esterification of FFA with adipocytes results in impaired buffering capacity for FFA and high concentrations of circulating FFA (26). Long-term over-activation of lipolysis may promote lipid 'overflow' into the muscle, liver, endothelium, heart, and β-cells, thereby causing muscular/

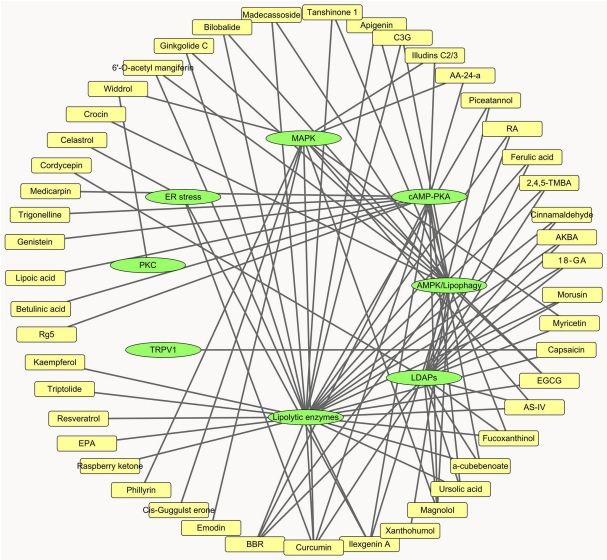


FIGURE 3
Network analysis of natural products and lipolytic pathways.

hepatic IR, CVD, and impaired insulin secretion (121). For example, adipocyte-derived FFA is involved in regulating hepatic energy metabolism (122). FFA impairs the insulin signaling pathway by forming diacylglycerol and ceramides and increases gluconeogenesis *via* the hepatic acetyl-CoA pathway in liver during diseased states (26, 123), which leads to TG accumulation in the liver. In patients with adipose tissue dysfunction, then, the inhibition of lipolysis may ameliorate IR- and obesity-associated metabolic diseases. Thiazolidinedione antidiabetic drugs improve insulin sensitivity and reduce circulating FFA levels by attenuating lipolysis and FFA release (124).

Curcumin (125), astragaloside IV (AS-IV) (126), and ilexgenin A (127) attenuate lipolysis by modulating the cAMP/PKA/HSL pathway. The inhibition of lipolysis in adipose tissue may improve hepatic insulin sensitivity (125, 126). Ginsenoside Rg5 (Rg5) suppresses lipolysis and inhibited IR in muscle (128). The foregoing findings suggest that a decrease in adipose tissue lipolysis mediated by natural bioactive components is a potentially efficacious therapy for hepatic IR and related disorders.

TNF-α is a proinflammatory cytokine expressed in adipose tissue that might link obesity and IR (129) and increases plasma FFA levels in obesity and T2DM (130). AS-IV (131), curcumin (132), emodin (133), eicosapentaenoic acid (EPA) (134), and phillyrin (135) attenuates TNF-α-induced lipolysis by suppressing p-ERK1/2 and reversing perilipin or p-perilipin downregulation. Rosmarinic acid (RA) (136, 137), RSV (116), BBR (83), cyanidin-3-O-β-glucoside (C3G) (138), dihydrodehydrodiisoeugenol (DDE) (139), carnosic acid (137), and piceatannol (140) may also inhibit lipolysis. The effects and mechanisms of these compounds are summarized in Table 5.

## 5 Conclusions and perspectives

In the present review, we summarized the effect and modes of action of a wide range of natural products on lipolysis. Overall, these compounds individually or synergistically affect lipolytic enzymes, LDAPs, ER stress, and the cAMP-PKA, MAPK, AMPK, and PKC signaling pathways (Figure 3). The lipolytic effects of certain compounds have already been established. Nevertheless, their influences and mechanisms in fat synthesis and metabolism, their toxicity, and their effects on whole-body phenotypes, appetite, energy expenditure, and thermogenesis remain to be determined. About half the compounds evaluated herein affect lipolytic enzyme expression. However, *in vitro* enzyme activity assay and compound-enzyme interaction data were lacking for them. These experiments may help identify novel lipolysis inhibitors and agonists.

Our understanding of adipocyte lipolysis has progressed from basic knowledge of its associated enzymatic processes to elucidtation of the dynamic and complex regulatory mechanisms involved. Lipolysis interacts with other related processes, including thermogenesis, adipocyte browning, and lipogenesis. Clarification of the mechanisms of lipolysis and the changes it causes in whole-body energy metabolism has positive

clinical value and socioeconomic benefits in that it may help develop modalities to prevent and treat obesity and its associated metabolic disorders. Lipolysis regulates TG metabolism and weight loss. Certain compounds with lipolytic activity, such as celastrol (141), apigenin (142), cordycepin (84), and BBR (143), have demonstrated anti-obesity efficacy. Theoretically, activating lipolysis may be a rational therapeutic approach for obesity. Thus far, however, no anti-obesity drugs targeting lipolytic enzymes or its related targets have been marketed.

The pathologies of obesity and its related metabolic conditions are highly complex. Simply targeting lipolysis can achieve weight loss. From the perspective of energy metabolism, however, weight loss is the result of multiple factors, including dietary restrictions and increases in lipolysis and energy utilization. It remains to be established whether lipolysis triggered by lipolytic agonists may damage certain cells, tissues, and organs or cause complications. The ideal anti-obesity drug should safely suppress appetite, increase lipolysis, and activate energy expenditure. Finally, the physiological functions of adipocytes should be rationally exploited, and their roles during metabolic disease should be identified. For patients with adipose dysfunction, the dynamic regulation of lipolysis and the amelioration of adipocyte dysfunction could improve obesity-associated metabolic conditions. For example, AS-IV and curcumin inhibit adipose lipolysis and thus prevent hepatic IR, which demonstrates their potential as treatments for metabolic-associated fatty liver disease through the regulation of lipolysis in adipose tissue during diseased states.

## Author contributions

X-DY and Y-YY wrote the manuscript. X-CG and S-YJ collected and checked the data. Y-YY contributions to design of the work and revised the work. All authors contributed to the article and approved the submitted version.

## Funding

This study was supported by the National Natural Science Foundation (No. 81603171) and the Natural Science Foundation of Hunan Province (2022JJ30860 and 2022JJ30862).

## Conflict of interest

The authors declare that the research was conducted in the absence of any commercial or financial relationships that could be construed as a potential conflict of interest.

## Publisher's note



## References

1. WHO. Obesity and overweight (2016). Available at: https://www.who.int/news-room/fact-sheets/detail/obesity-and-overweight.

2. Mili N, Paschou SA, Goulis DG, Dimopoulos MA, Lambrinoudaki I, Psaltopoulou T. Obesity, metabolic syndrome, and cancer: Pathophysiological and therapeutic associations. *Endocrine* (2021) 74:478–97. doi: 10.1007/s12020-021-02884-x

3. Drolet R, Richard C, Sniderman AD, Mailloux J, Fortier M, Huot C, et al. Hypertrophy and hyperplasia of abdominal adipose tissues in women. *Int J Obes (Lond)* (2008) 32:283–91. doi: 10.1038/sj.ijo.0803708

4. Wu J, Bostrom P, Sparks LM, Ye L, Choi JH, Giang AH, et al. Beige adipocytes are a distinct type of thermogenic fat cell in mouse and human. *Cell* (2012) 150:366–76. doi: 10.1016/j.cell.2012.05.016

5. Giralt M, Villarroya F. White, brown, beige/brite: Different adipose cells for different functions? *Endocrinology* (2013) 154:2992–3000. doi: 10.1210/en.2013-1403

6. Tanaka K, Fukuda D, Sata M. Roles of epicardial adipose tissue in the pathogenesis of coronary atherosclerosis - an update on recent findings. *Circ J* (2020) 85:2–8. doi: 10.1253/circj.CJ-20-0935

7. Obert J, Pearlman M, Obert L, Chapin S. Popular weight loss strategies: A review of four weight loss techniques. *Curr Gastroenterol Rep* (2017) 19:61. doi: 10.1007/s11894-017-0603-8

8. Ceddia RP, Collins S. A compendium of G-protein-coupled receptors and cyclic nucleotide regulation of adipose tissue metabolism and energy expenditure. *Clin Sci (Lond)* (2020) 134:473–512. doi: 10.1042/cs20190579

9. Guilherme A, Virbasius JV, Puri V, Czech MP. Adipocyte dysfunctions linking obesity to insulin resistance and type 2 diabetes. *Nat Rev Mol Cell Biol* (2008) 9:367–77. doi: 10.1038/nrm2391

10. Negi H, Gupta M, Walia R, Khataibeh M, Sarwat M. Medicinal plants and natural products: More effective and safer pharmacological treatment for the management of obesity. *Curr Drug Metab* (2021) 22:918–30. doi: 10.2174/1389200222666210729114456

11. Wu MR, Hou MH, Lin YL, Kuo CF. 2,4,5-TMBA, a natural inhibitor of cyclooxygenase-2, suppresses adipogenesis and promotes lipolysis in 3T3-L1 adipocytes. *J Agric Food Chem* (2012) 60:7262–9. doi: 10.1021/jf302285k

12. Martín M, Ramos SA-O. Dietary flavonoids and insulin signaling in diabetes and obesity. *Cells* (2021) 10:1474. doi: 10.3390/cells10061474

13. Islam MA-O, Ali ES, Mubarak MA-O. Anti-obesity effect of plant diterpenes and their derivatives: A review. *Phytother Res* (2020) 34:1216–25. doi: 10.1002/ptr.6602

14. Li R, Lan YA-O, Chen CA-OX, Cao Y, Huang QA-O, Ho CA-O, et al. Anti-obesity effects of capsaicin and the underlying mechanisms: A review. *Food Funct* (2020) 11:7356–70. doi: 10.1039/d0fo01467b

15. Sakers A, De Siqueira MK, Seale P, Villanueva CJ. Adipose-tissue plasticity in health and disease. *Cell* (2022) 185:419–46. doi: 10.1016/j.cell.2021.12.016

16. Sanders FW, Griffin JL. *De novo* lipogenesis in the liver in health and disease: More than just a shunting yard for glucose. *Biol Rev Camb Philos Soc* (2016) 91:452–68. doi: 10.1111/brv.12178

17. Sethi JK, Vidal-Puig AJ. Thematic review series: Adipocyte biology. *Adipose Tissue Funct Plasticity Orchestrate Nutr Adapt J Lipid Res* (2007) 48:1253–62. doi: 10.1194/jlr.R700005-JLR200

18. Taschler U, Radner FP, Heier C, Schreiber R, Schweiger M, Schoiswohl G, et al. Monoglyceride lipase deficiency in mice impairs lipolysis and attenuates diet-induced insulin resistance. *J Biol Chem* (2011) 286:17467–77. doi: 10.1074/jbc.M110.215434

19. Kaushik S, Cuervo AM. Degradation of lipid droplet-associated proteins by chaperone-mediated autophagy facilitates lipolysis. *Nat Cell Biol* (2015) 17:759–70. doi: 10.1038/ncb3166

20. Fruhbeck G, Mendez-Gimenez L, Fernandez-Formoso JA, Fernandez S, Rodriguez A. Regulation of adipocyte lipolysis. *Nutr Res Rev* (2014) 27:63–93. doi: 10.1017/S095442241400002X

21. Jin D, Sun J, Huang J, He Y, Yu A, Yu X, et al. TNF-alpha reduces g0s2 expression and stimulates lipolysis through PPAR-gamma inhibition in 3T3-L1 adipocytes. *Cytokine* (2014) 69:196–205. doi: 10.1016/j.cyto.2014.06.005

22. Morisset AS, Huot C, Legare D, Tchernof A. Circulating IL-6 concentrations and abdominal adipocyte isoproterenol-stimulated lipolysis in women. *Obes (Silver Spring)* (2008) 16:1487–92. doi: 10.1038/oby.2008.242

23. Feingold KR, Doerrler W, Dinarello CA, Fiers W, Grunfeld C. Stimulation of lipolysis in cultured fat cells by tumor necrosis factor, interleukin-1, and the interferons is blocked by inhibition of prostaglandin synthesis. *Endocrinology* (1992) 130:10–6. doi: 10.1210/endo.130.1.1370149

24. Hoch M, Eberle AN, Peterli R, Peters T, Seboek D, Keller U, et al. LPS induces interleukin-6 and interleukin-8 but not tumor necrosis factor-alpha in human adipocytes. *Cytokine* (2008) 41:29–37. doi: 10.1016/j.cyto.2007.10.008

25. Musutova M, Weiszenstein M, Koc M, Polak J. Intermittent hypoxia stimulates lipolysis, but inhibits differentiation and *De novo* lipogenesis in 3T3-L1 cells. *Metab Syndr Relat Disord* (2020) 18:146–53. doi: 10.1089/met.2019.0112

26. Yang A, Mottillo EP. Adipocyte lipolysis: from molecular mechanisms of regulation to disease and therapeutics. *Biochem J* (2020) 477:985–1008. doi: 10.1042/BCJ20190468

27. Mottillo EP, Shen XJ, Granneman JG. beta3-adrenergic receptor induction of adipocyte inflammation requires lipolytic activation of stress kinases p38 and JNK. *Biochim Biophys Acta* (2010) 1801:1048–55. doi: 10.1016/j.bbalip.2010.04.012

28. Boone-Villa DA-O, Ventura-Sobrevilla JA-O, Aguilera-Méndez AA-O, Jiménez-Villarreal JA-O. The effect of adenosine monophosphate-activated protein kinase on lipolysis in adipose tissue: An historical and comprehensive review. *Arch Physiol Biochem* (2022) 128:7–23. doi: 10.1080/13813455.2019.1661495

29. Klug YA, Deme JC, Corey RA, Renne MF, Stansfeld PJ, Lea SM, et al. Mechanism of lipid droplet formation by the yeast Sei1/Ldb16 seipin complex. *Nat Commun* (2021) 12:5892. doi: 10.1038/s41467-021-26162-6

30. Chen FJ, Yin Y, Chua BT, Li P. CIDE family proteins control lipid homeostasis and the development of metabolic diseases. *Traffic* (2020) 21:94–105. doi: 10.1111/tra.12717

31. Sztalryd C, Brasaemle DL. The perilipin family of lipid droplet proteins: Gatekeepers of intracellular lipolysis. *Biochim Biophys Acta Mol Cell Biol Lipids* (2017) 1862:1221–32. doi: 10.1016/j.bbalip.2017.07.009

32. Yu L, Li Y, Grisé A, Wang H. CGI-58: Versatile regulator of intracellular lipid droplet homeostasis. *Adv Exp Med Biol* (2020) 1276:197–222. doi: 10.1007/978-981-15-6082-8_13

33. Nishino N, Tamori Y, Tateya S, Kawaguchi T, Shibakusa T, Mizunoya W, et al. FSP27 contributes to efficient energy storage in murine white adipocytes by promoting the formation of unilocular lipid droplets. *J Clin Invest* (2008) 118:2808–21. doi: 10.1172/JCI34090

34. Corbin JD, Reimann EM, Walsh DA, Krebs EG. Activation of adipose tissue lipase by skeletal muscle cyclic adenosine 3',5'- monophosphate-stimulated protein kinase. *J Biol Chem* (1970) 245:4849–51. doi: 10.1016/S0021-9258(18)62871-6

35. Langin D. Control of fatty acid and glycerol release in adipose tissue lipolysis. *C R Biol* (2006) 329:598–607. doi: 10.1016/j.crvi.2005.10.008

36. Ahmadian M, Wang Y, Sul HS. Lipolysis in adipocytes. *Int J Biochem Cell Biol* (2010) 42:555–9. doi: 10.1016/j.biocel.2009.12.009

37. Lafontan M, Moro C, Berlan M, Crampes F, Sengenes C, Galitzky J. Control of lipolysis by natriuretic peptides and cyclic GMP. *Trends Endocrinol Metab* (2008) 19:130–7. doi: 10.1016/j.tem.2007.11.006

38. Lien CC, Yin WH, Yang DM, Chen LK, Chen CW, Liu SY, et al. Endothelin-1 induces lipolysis through activation of the GC/cGMP/Ca(2+)/ERK/CaMKIII pathway in 3T3-L1 adipocytes. *Biochim Biophys Acta Mol Cell Biol Lipids* (2022) 1867:159071. doi: 10.1016/j.bbalip.2021.159071

39. Chin CH, Tsai Fc Fau - Chen S-P, Chen Sp Fau - Wang K-C, Wang Kc Fau - Chang C-C, Chang Cc Fau - Pai M-H, Pai Mh Fau - Fong T-H, et al. YC-1, a potent antithrombotic agent, induces lipolysis through the PKA pathway in rat visceral fat cells. *Eur J Pharmacol* (2012) 689:1–7. doi: 10.1016/j.ejphar.2012.05.013

40. Lien CC, Au Lc Fau - Tsai Y-L, Tsai Yl Fau - Ho L-T, Ho Lt Fau - Juan C-C, Juan CC. Short-term regulation of tumor necrosis factor-alpha-induced lipolysis in 3T3-L1 adipocytes is mediated through the inducible nitric oxide synthase/nitric oxide-dependent pathway. *Endocrinology* (2009) 150:4892–900. doi: 10.1210/en.2009-0403

41. Rozo AV, Vijayvargia R, Weiss HR, Ruan H. Silencing Jnk1 and Jnk2 accelerates basal lipolysis and promotes fatty acid re-esterification in mouse adipocytes. *Diabetologia* (2008) 51:1493–504. doi: 10.1007/s00125-008-1036-6

42. Zhang HH, Halbleib M, Ahmad F, Manganiello VC, Greenberg AS. Tumor necrosis factor-alpha stimulates lipolysis in differentiated human adipocytes through activation of extracellular signal-related kinase and elevation of intracellular cAMP. *Diabetes* (2002) 51:2929–35. doi: 10.2337/diabetes.51.10.2929

43. Wang Q, Liu S, Zhai A, Zhang B, Tian G. AMPK-mediated regulation of lipid metabolism by phosphorylation. *Biol Pharm Bull* (2018) 41:985–93. doi: 10.1248/bpb.b17-00724

44. Ahmadian M, Abbott MJ, Tang T, Hudak CS, Kim Y, Bruss M, et al. Desnutrin/ATGL is regulated by AMPK and is required for a brown adipose phenotype. *Cell Metab* (2011) 13:739–48. doi: 10.1016/j.cmet.2011.05.002

45. Anthony NM, Gaidhu MP, Ceddia RB. Regulation of visceral and subcutaneous adipocyte lipolysis by acute AICAR-induced AMPK activation. *Obesity* (2009) 17:1312–7. doi: 10.1038/oby.2008.645

46. Kaushik S, Cuervo AM. AMPK-dependent phosphorylation of lipid droplet protein PLIN2 triggers its degradation by CMA. *Autophagy* (2016) 12:432–8. doi: 10.1080/15548627.2015.1124226

47. Chakrabarti P, English T Fau - Karki S, Karki S Fau - Qiang L, Qiang L Fau - Tao R, Tao R Fau - Kim J, Kim J Fau - Luo Z, et al. SIRT1 controls lipolysis in adipocytes *via* FOXO1-mediated expression of ATGL. *J Lipid Res* (2011) 52:1693–701. doi: 10.1194/jlr.M014647

48. Zhang T, Liu J, Tong Q, Lin L. SIRT3 acts as a positive autophagy regulator to promote lipid mobilization in adipocytes *via* activating AMPK. *Int J Mol Sci* (2020) 21:372. doi: 10.3390/ijms21020372

49. Gorin E, Tai LR, Honeyman TW, Goodman HM. Evidence for a role of protein kinase c in the stimulation of lipolysis by growth hormone and isoproterenol. *Endocrinology* (1990) 126:2973–82. doi: 10.1210/endo-126-6-2973

50. Turovsky EA-O, Varlamova EA-O, Turovskaya MV. Activation of Cx43 hemichannels induces the generation of Ca(2+) oscillations in white adipocytes and stimulates lipolysis. *Int J Mol Sci* (2021) 22:8095. doi: 10.3390/ijms22158095

51. Ghoshal S, Tyagi R, Zhu Q, Chakraborty A. Inositol hexakisphosphate kinase-1 interacts with perilipin1 to modulate lipolysis. *Int J Biochem Cell Biol* (2016) 78:149–55. doi: 10.1016/j.biocel.2016.06.018

52. Sánchez JC, Valencia-Vásquez A, García AM. Role of TRPV4 channel in human white adipocytes metabolic activity. *Endocrinol Metab (Seoul)* (2021) 36:997–1006. doi: 10.3803/EnM.2021.1167

53. Bogdanovic E, Kraus N, Patsouris D, Patsouris D, Diao L, Diao L, et al. Endoplasmic reticulum stress in adipose tissue augments lipolysis. *J Cell Mol Med* (2015) 19:82–91. doi: 10.1111/jcmm.12384

54. Li J, Bai L, Wei F, Zhao J, Wang D, Xiao Y, et al. Therapeutic mechanisms of herbal medicines against insulin resistance: A review. *Front Pharmacol* (2019) 10:661. doi: 10.3389/fphar.2019.00661

55. Bahmani M, Eftekhari Z, Saki K, Fazeli-Moghadam E, Jelodari M, Rafieian-Kopaei M. Obesity phytotherapy: Review of native herbs used in traditional medicine for obesity. *J Evidence-Based Complement Altern Med* (2016) 21:228–34. doi: 10.1177/2156587215599105

56. Carrasco-Pozo C, Cires MJ, Gotteland M. Quercetin and epigallocatechin gallate in the prevention and treatment of obesity: From molecular to clinical studies. *J Med Food* (2019) 22:753–70. doi: 10.1089/jmf.2018.0193

57. Choi M, Mukherjee S, Yun JW. Trigonelline induces browning in 3T3-L1 white adipocytes. *Phytother Res* (2021) 35:1113–24. doi: 10.1002/ptr.6892

58. Wang X, Xu M, Peng Y, Naren Q, Xu Y, Wang X, et al. Triptolide enhances lipolysis of adipocytes by enhancing ATGL transcription *via* upregulation of p53. *Phytother Res* (2020) 34:3298–310. doi: 10.1002/ptr.6779

59. Pan H, Gao Y, Tu Y. Mechanisms of body weight reduction by black tea polyphenols. *Molecules* (2016) 21:1659. doi: 10.3390/molecules21121659

60. Li F, Gao C, Yan P, Zhang M, Wang Y, Hu Y, et al. EGCG reduces obesity and white adipose tissue gain partly through AMPK activation in mice. *Front Pharmacol* (2018) 9:1366. doi: 10.3389/fphar.2018.01366

61. Lee MS, Kim CT, Kim Y. Green tea (-)-epigallocatechin-3-gallate reduces body weight with regulation of multiple genes expression in adipose tissue of diet-induced obese mice. *Ann Nutr Metab* (2009) 54:151–7. doi: 10.1159/000214834

62. Moon HS, Chung CS, Lee HG, Kim TG, Choi YJ, Cho CS. Inhibitory effect of (-)-epigallocatechin-3-gallate on lipid accumulation of 3T3-L1 cells. *Obes (Silver Spring)* (2007) 15:2571–82. doi: 10.1038/oby.2007.309

63. Lee MS, Kim CT, Kim IH, Kim Y. Inhibitory effects of green tea catechin on the lipid accumulation in 3T3-L1 adipocytes. *Phytother Res* (2009) 23:1088–91. doi: 10.1002/ptr.2737

64. Ogasawara J, Kitadate K, Nishioka H, Fujii H, Sakurai T, Kizaki T, et al. Comparison of the effect of oligonol, a new lychee fruit-derived low molecular form of polyphenol, and epigallocatechin-3-gallate on lipolysis in rat primary adipocytes. *Phytother Res* (2011) 25:467–71. doi: 10.1002/ptr.3296

65. Kim SN, Kwon HJ, Akindehin S, Jeong HW, Lee YH. Effects of epigallocatechin-3-Gallate on autophagic lipolysis in adipocytes. *Nutrients* (2017) 9:680. doi: 10.3390/nu9070680

66. Chatree S, Sitticharoon C, Maikaew P, Pongwattanapakin K, Keadkraichaiwat I, Churintaraphan M, et al. Epigallocatechin gallate decreases plasma triglyceride, blood pressure, and serum kisspeptin in obese human subjects. *Exp Biol Med (Maywood)* (2021) 246:163–76. doi: 10.1177/1535370220962708

67. Torres-Villarreal D, Camacho A, Castro H, Ortiz-Lopez R, de la Garza AL. Anti-obesity effects of kaempferol by inhibiting adipogenesis and increasing lipolysis in 3T3-L1 cells. *J Physiol Biochem* (2019) 75:83–8. doi: 10.1007/s13105-018-0659-4

68. Sun YS, Qu W. Dietary apigenin promotes lipid catabolism, thermogenesis, and browning in adipose tissues of HFD-fed mice. *Food Chem Toxicol* (2019) 133:110780. doi: 10.1016/j.fct.2019.110780

69. Szkudelska K, Nogowski L, Szkudelski T. Genistein affects lipogenesis and lipolysis in isolated rat adipocytes. *J Steroid Biochem Mol Biol* (2000) 75:265–71. doi: 10.1016/s0960-0760(00)00172-2

70. Lee MR, Kim JE, Choi JY, Park JJ, Kim HR, Song BR, et al. Morusin functions as a lipogenesis inhibitor as well as a lipolysis stimulator in differentiated 3T3-L1 and primary adipocytes. *Molecules* (2018) 23: 2004. doi: 10.3390/molecules23082004

71. Imran KM, Yoon D, Lee TJ, Kim YS. Medicarpin induces lipolysis *via* activation of protein kinase a in brown adipocytes. *BMB Rep* (2018) 51:249–54. doi: 10.5483/bmbrep.2018.51.5.228

72. Wang Q, Wang ST, Yang X, You PP, Zhang W. Myricetin suppresses differentiation of 3 T3-L1 preadipocytes and enhances lipolysis in adipocytes. *Nutr Res* (2015) 35:317–27. doi: 10.1016/j.nutres.2014.12.009

73. Samuels JS, Shashidharamurthy R, Rayalam S. Novel anti-obesity effects of beer hops compound xanthohumol: Role of AMPK signaling pathway. *Nutr Metab (Lond)* (2018) 15:42. doi: 10.1186/s12986-018-0277-8

74. Mougios V, Ring S, Petridou A, Nikolaidis MG. Duration of coffee- and exercise-induced changes in the fatty acid profile of human serum. *J Appl Physiol (1985)* (2003) 94:476–84. doi: 10.1152/japplphysiol.00624.2002

75. Diepvens K, Westerterp KR, Westerterp-Plantenga MS. Obesity and thermogenesis related to the consumption of caffeine, ephedrine, capsaicin, and green tea. *Am J Physiol Regul Integr Comp Physiol* (2007) 292:R77–85. doi: 10.1152/ajpregu.00832.2005

76. Panchal SK, Wong WY, Kauter K, Ward LC, Brown L. Caffeine attenuates metabolic syndrome in diet-induced obese rats. *Nutrition* (2012) 28:1055–62. doi: 10.1016/j.nut.2012.02.013

77. Han LK, Takaku T, Li J, Kimura Y, Okuda H. Anti-obesity action of oolong tea. *Int J Obes Relat Metab Disord* (1999) 23:98–105. doi: 10.1038/sj.ijo.0800766

78. De Matteis R, Arch JR, Petroni ML, Ferrari D, Cinti S, Stock MJ. Immunohistochemical identification of the beta(3)-adrenoceptor in intact human adipocytes and ventricular myocardium: Effect of obesity and treatment with ephedrine and caffeine. *Int J Obes Relat Metab Disord* (2002) 26:1442–50. doi: 10.1038/sj.ijo.0802148

79. Ohyama K, Nogusa Y, Suzuki K, Shinoda K, Kajimura S, Bannai M. A combination of exercise and capsinoid supplementation additively suppresses diet-induced obesity by increasing energy expenditure in mice. *Am J Physiol Endocrinol Metab* (2015) 308:E315–23. doi: 10.1152/ajpendo.00354.2014

80. Perova IB, Eller KI, Musatov AV, Tymolskaya EV. Synephrine in dietary supplements and specialized foodstuffs: Biological activity, safety and methods of analysis]. *Vopr Pitan* (2021) 90:101–13. doi: 10.33029/0042-8833-2021-90-6-101-113

81. Jiang D, Wang D, Zhuang X, Wang Z, Ni Y, Chen S, et al. Berberine increases adipose triglyceride lipase in 3T3-L1 adipocytes through the AMPK pathway. *Lipids Health Dis* (2016) 15:214. doi: 10.1186/s12944-016-0383-4

82. Yang Y, Lu R, Gao F, Zhang J, Liu F. Berberine induces lipolysis in porcine adipocytes by activating the AMPactivated protein kinase pathway. *Mol Med Rep* (2020) 21:2603–14. doi: 10.3892/mmr.2020.11070

83. Zhou L, Wang X, Yang Y, Wu L, Li F, Zhang R, et al. Berberine attenuates cAMP-induced lipolysis *via* reducing the inhibition of phosphodiesterase in 3T3-L1 adipocytes. *Biochim Biophys Acta* (2011) 1812:527–35. doi: 10.1016/j.bbadis.2010.10.001

84. Xu H, Wu B, Wang X, Ma F, Li Y, An Y, et al. Cordycepin regulates body weight by inhibiting lipid droplet formation, promoting lipolysis and recruiting beige adipocytes. *J Pharm Pharmacol* (2019) 71:1429–39. doi: 10.1111/jphp.13127

85. Lee MS, Kim CT, Kim IH, Kim Y. Effects of capsaicin on lipid catabolism in 3T3-L1 adipocytes. *Phytother Res* (2011) 25:935–9. doi: 10.1002/ptr.3339

86. Chen J, Li L, Li Y, Liang X, Sun Q, Yu H, et al. Activation of TRPV1 channel by dietary capsaicin improves visceral fat remodeling through connexin43-mediated Ca2+ influx. *Cardiovasc Diabetol* (2015) 14:22. doi: 10.1186/s12933-015-0183-6

87. Kobayashi-Hattori K, Mogi A, Matsumoto Y, Takita T. Effect of caffeine on the body fat and lipid metabolism of rats fed on a high-fat diet. *Biosci Biotechnol Biochem* (2005) 69:2219–23. doi: 10.1271/bbb.69.2219

88. Moon MH, Jeong JK, Lee YJ, Seol JW, Ahn DC, Kim IS, et al. 18beta-glycyrrhetinic acid inhibits adipogenic differentiation and stimulates lipolysis. *Biochem Biophys Res Commun* (2012) 420:805–10. doi: 10.1016/j.bbrc.2012.03.078

89. Li Y, Kang Z, Li S, Kong T, Liu X, Sun C. Ursolic acid stimulates lipolysis in primary-cultured rat adipocytes. *Mol Nutr Food Res* (2010) 54:1609–17. doi: 10.1002/mnfr.200900564

90. Liu JJ, Toy WC, Liu S, Cheng A, Lim BK, Subramaniam T, et al. Acetyl-keto-beta-boswellic acid induces lipolysis in mature adipocytes. *Biochem Biophys Res Commun* (2013) 431:192–6. doi: 10.1016/j.bbrc.2012.12.136

91. Lou HX, Fu WC, Chen JX, Li TT, Jiang YY, Liu CH, et al. Alisol a 24-acetate stimulates lipolysis in 3 T3-L1 adipocytes. *BMC Complement Med Ther* (2021) 21:128. doi: 10.1186/s12906-021-03296-0

92. Luo D, Fan N, Zhang X, Ngo FY, Zhao J, Zhao W, et al. Covalent inhibition of endoplasmic reticulum chaperone GRP78 disconnects the transduction of ER stress signals to inflammation and lipid accumulation in diet-induced obese mice. *Elife* (2022) 11:e72182. doi: 10.7554/eLife.72182

93. Kim J, Lee YS, Kim CS, Kim JS. Betulinic acid has an inhibitory effect on pancreatic lipase and induces adipocyte lipolysis. *Phytother Res* (2012) 26:1103–6. doi: 10.1002/ptr.3672

94. Sun B, Hayashi M, Kudo M, Wu L, Qin L, Gao M, et al. Madecassoside inhibits body weight gain *via* modulating SIRT1-AMPK signaling pathway and activating genes related to thermogenesis. *Front Endocrinol (Lausanne)* (2021) 12:627950. doi: 10.3389/fendo.2021.627950

95. Jung DY, Suh N, Jung MH. Tanshinone 1 prevents high fat diet-induced obesity through activation of brown adipocytes and induction of browning in white adipocytes. *Life Sci* (2022) 298:120488. doi: 10.1016/j.lfs.2022.120488

96. Gu M, Luo L, Fang K. Crocin inhibits obesity *via* AMPK-dependent inhibition of adipocyte differentiation and promotion of lipolysis. *Biosci Trends* (2018) 12:587–94. doi: 10.5582/bst.2018.01240

97. Yang JY, Della-Fera MA, Baile CA. Guggulsterone inhibits adipocyte differentiation and induces apoptosis in 3T3-L1 cells. *Obes (Silver Spring)* (2008) 16:16–22. doi: 10.1038/oby.2007.24

98. Bu S, Yuan CY, Xue Q, Chen Y, Cao F. Bilobalide suppresses adipogenesis in 3T3-L1 adipocytes *via* the AMPK signaling pathway. *Molecules* (2019) 24:3503. doi: 10.3390/molecules24193503

99. Bae SJ, Kim JE, Choi YJ, Lee SJ, Gong JE, Choi YW, et al. Novel function of alpha-cubebenoate derived from schisandra chinensis as lipogenesis inhibitor, lipolysis stimulator and inflammasome suppressor. *Molecules* (2020) 25:4495. doi: 10.3390/molecules25214995

100. Lee SJ, Kim JE, Choi YJ, Gong JE, Jin YJ, Lee DW, et al. Anti-obesity effect of α-cubebenol isolated from schisandra chinensis in 3T3-L1 adipocytes. *Biomolecules* (2021) 11:1650. doi: 10.3390/biom11111650

101. Yoshikawa M, Hosokawa M, Miyashita K, Fujita T, Nishino H, Hashimoto T. Fucoxanthinol attenuates oxidative stress-induced atrophy and loss in myotubes and reduces the triacylglycerol content in mature adipocytes. *Mol Biol Rep* (2020) 47:2703–11. doi: 10.1007/s11033-020-05369-8

102. Jeong HY, Yun HJ, Kim BW, Lee EW, Kwon HJ. Widdrol-induced lipolysis is mediated by PKC and MEK/ERK in 3T3-L1 adipocytes. *Mol Cell Biochem* (2015) 410:247–54. doi: 10.1007/s11010-015-2558-0

103. Liou CJ, Lai XY, Chen YL, Wang CL, Wei CH, Huang WC. Ginkgolide c suppresses adipogenesis in 3T3-L1 adipocytes *via* the AMPK signaling pathway. *Evid Based Complement Alternat Med* (2015) 2015:298635. doi: 10.1155/2015/298635

104. Kim SO, Sakchaisri K, Asami Y, Ryoo IJ, Choo SJ, Yoo ID, et al. Illudins C2 and C3 stimulate lipolysis in 3T3-L1 adipocytes and suppress adipogenesis in 3T3-L1 preadipocytes. *J Nat Prod* (2014) 77:744–50. doi: 10.1021/np400520a

105. Choi SK, Park S, Jang S, Cho HH, Lee S, You S, et al. Cascade regulation of PPARgamma(2) and C/EBPalpha signaling pathways by celastrol impairs adipocyte differentiation and stimulates lipolysis in 3T3-L1 adipocytes. *Metabolism* (2016) 65:646–54. doi: 10.1016/j.metabol.2016.01.009

106. Gong L, Guo S, Zou Z. Resveratrol ameliorates metabolic disorders and insulin resistance in high-fat diet-fed mice. *Life Sci* (2020) 242:117212. doi: 10.1016/j.lfs.2019.117212

107. Mehanna ET, Barakat BM, ElSayed MH, Tawfik MK. An optimized dose of raspberry ketones controls hyperlipidemia and insulin resistance in male obese rats: Effect on adipose tissue expression of adipocytokines and aquaporin 7. *Eur J Pharmacol* (2018) 832:81–9. doi: 10.1016/j.ejphar.2018.05.028

108. Khare P, Jagtap S, Jain Y, Baboota RK, Mangal P, Boparai RK, et al. Cinnamaldehyde supplementation prevents fasting-induced hyperphagia, lipid accumulation, and inflammation in high-fat diet-fed mice. *Biofactors* (2016) 42:201–11. doi: 10.1002/biof.1265

109. Fernandez-Galilea M, Perez-Matute P, Prieto-Hontoria PL, Martinez JA, Moreno-Aliaga MJ. Effects of lipoic acid on lipolysis in 3T3-L1 adipocytes. *J Lipid Res* (2012) 53:2296–306. doi: 10.1194/jlr.M027086

110. John CM, Arockiasamy S. Syringic acid (4-hydroxy-3,5-dimethoxybenzoic acid) inhibits adipogenesis and promotes lipolysis in 3T3-L1 adipocytes. *Nat Prod Res* (2020) 34:3432–36. doi: 10.1080/14786419.2019.1573820

111. Sim MO, Lee HJ, Jeong DE, Jang JH, Jung HK, Cho HW. 6'-o-acetyl mangiferin from iris rossii baker inhibits lipid accumulation partly *via* AMPK activation in adipogenesis. *Chem Biol Interact* (2019) 311:108755. doi: 10.1016/j.cbi.2019.108755

112. Kuppusamy P, Ilavenil S, Hwang IH, Kim D, Choi KA-O. Ferulic acid stimulates adipocyte-specific secretory proteins to regulate adipose homeostasis in 3T3-L1 adipocytes. *Molecules* (2021) 26:1984. doi: 10.3390/molecules26071984

113. Parray HA, Lone J, Park JP, Choi JW, Yun JW. Magnolol promotes thermogenesis and attenuates oxidative stress in 3T3-L1 adipocytes. *Nutrition* (2018) 50:82–90. doi: 10.1016/j.nut.2018.01.017

114. Gomez-Zorita S, Treguer K, Mercader J, Carpene C. Resveratrol directly affects *in vitro* lipolysis and glucose transport in human fat cells. *J Physiol Biochem* (2013) 69:585–93. doi: 10.1007/s13105-012-0229-0

115. Lasa A, Schweiger M, Kotzbeck P, Churruca I, Simon E, Zechner R, et al. Resveratrol regulates lipolysis *via* adipose triglyceride lipase. *J Nutr Biochem* (2012) 23:379–84. doi: 10.1016/j.jnutbio.2010.12.014

116. Timmers S, Konings E, Bilet L, Houtkooper RH, van de Weijer T, Goossens GH, et al. Calorie restriction-like effects of 30 days of resveratrol supplementation on energy metabolism and metabolic profile in obese humans. *Cell Metab* (2011) 14:612–22. doi: 10.1016/j.cmet.2011.10.002

117. Morimoto C, Satoh Y, Hara M, Inoue S, Tsujita T, Okuda H. Anti-obese action of raspberry ketone. *Life Sci* (2005) 77:194–204. doi: 10.1016/j.lfs.2004.12.029

118. Park KS. Raspberry ketone increases both lipolysis and fatty acid oxidation in 3T3-L1 adipocytes. *Planta Med* (2010) 76:1654–8. doi: 10.1055/s-0030-1249860

119. Huang SH, Shen WJ, Yeo HL, Wang SM. Signaling pathway of magnolol-stimulated lipolysis in sterol ester-loaded 3T3-L1 preadipocyes. *J Cell Biochem* (2004) 91:1021–9. doi: 10.1002/jcb.10788

120. Park KS. Raspberry ketone, a naturally occurring phenolic compound, inhibits adipogenic and lipogenic gene expression in 3T3-L1 adipocytes. *Pharm Biol* (2015) 53:870–5. doi: 10.3109/13880209.2014.946059

121. Ahmed B, Sultana R, Greene MW. Adipose tissue and insulin resistance in obese. *BioMed Pharmacother* (2021) 137:111315. doi: 10.1016/j.biopha.2021.111315

122. Duwaerts CC, Maher JJ. Macronutrients and the adipose-liver axis in obesity and fatty liver. *Cell Mol Gastroenterol Hepatol* (2019) 7:749–61. doi: 10.1016/j.jcmgh.2019.02.001

123. Roden M, Stingl H, Chandramouli V, Schumann WC, Hofer A, Landau BR, et al. Effects of free fatty acid elevation on postabsorptive endogenous glucose production and gluconeogenesis in humans. *Diabetes* (2000) 49:701–7. doi: 10.2337/diabetes.49.5.701

124. He J, Xu C, Kuang J, Liu Q, Jiang H, Mo L, et al. Thiazolidinediones attenuate lipolysis and ameliorate dexamethasone-induced insulin resistance. *Metabolism* (2015) 64:826–36. doi: 10.1016/j.metabol.2015.02.005

125. Wang L, Zhang B, Huang F, Liu B, Xie Y. Curcumin inhibits lipolysis *via* suppression of ER stress in adipose tissue and prevents hepatic insulin resistance. *J Lipid Res* (2016) 57:1243–55. doi: 10.1194/jlr.M067397

126. Du Q, Zhang S, Li A, Mohammad IS, Liu B, Li Y. Astragaloside IV inhibits adipose lipolysis and reduces hepatic glucose production *via* akt dependent PDE3B expression in HFD-fed mice. *Front Physiol* (2018) 9:15. doi: 10.3389/fphys.2018.00015

127. Li LZ, Zhang T, Yang L, Zhang L, Wang L, Liu B, et al. Inhibition of lipolysis by ilexgenin a *via* AMPK activation contributes to the prevention of hepatic insulin resistance. *Eur J Pharmacol* (2017) 813:84–93. doi: 10.1016/j.ejphar.2017.07.038

128. Xiao N, Yang LL, Yang YL, Liu LW, Li J, Liu B, et al. Ginsenoside Rg5 inhibits succinate-associated lipolysis in adipose tissue and prevents muscle insulin resistance. *Front Pharmacol* (2017) 8:43. doi: 10.3389/fphar.2017.00043

129. Stagakis I, Bertsias G, Karvounaris S, Kavousanaki M, Virla D, Raptopoulou A, et al. Anti-tumor necrosis factor therapy improves insulin resistance, beta cell function and insulin signaling in active rheumatoid arthritis patients with high insulin resistance. *Arthritis Res Ther* (2012) 14:R141. doi: 10.1186/ar3874

130. Hotamisligil GS, Shargill NS, Spiegelman BM. Adipose expression of tumor necrosis factor-alpha: direct role in obesity-linked insulin resistance. *Science* (1993) 259:87–91. doi: 10.1126/science.7678183

131. Jiang B, Yang Y, Jin H, Shang W, Zhou L, Qian L, et al. Astragaloside IV attenuates lipolysis and improves insulin resistance induced by TNFalpha in 3T3-L1 adipocytes. *Phytother Res* (2008) 22:1434–9. doi: 10.1002/ptr.2434

132. Xie XY, Kong PR, WU JF, Li Y, Li YX. Curcumin attenuates lipolysis stimulated by tumor necrosis factor-α or isoproterenol in 3T3-L1 adipocytes. *Phytomedicine* (2012) 20:3–8. doi: 10.1016/j.phymed.2012.09.003

133. Zhang X, Zhang R, Lv P, Yang J, Deng Y, Xu J, et al. Emodin up-regulates glucose metabolism, decreases lipolysis, and attenuates inflammation. *Vitro J Diabetes* (2015) 7:360–8. doi: 10.1111/1753-0407.12190

134. Lorente-Cebrián S, Bustos M, Marti A, Fernández-Galilea M, Martinez JA, Moreno-Aliaga JM. Eicosapentaenoic acid inhibits tumour necrosis factor-α-induced lipolysis in murine cultured adipocytes. *J Nutr Biochem* (2012) 23:218–27. doi: 10.1016/j.jnutbio.2010.11.018

135. Kong P, Zhang L, Guo Y, Lu Y, Lin D. Phillyrin, a natural lignan, attenuates tumor necrosis factor α-mediated insulin resistance and lipolytic acceleration in 3T3-L1 adipocytes. *Planta Med* (2014) 80:880–6. doi: 10.1055/s-0034-1368614

136. Rui Y, Tong L, Cheng J, Wang G, Qin L, Wan Z. Rosmarinic acid suppresses adipogenesis, lipolysis in 3T3-L1 adipocytes, lipopolysaccharide-stimulated tumor necrosis factor-alpha secretion in macrophages, and inflammatory mediators in 3T3-L1 adipocytes. *Food Nutr Res* (2017) 61:1330096. doi: 10.1080/16546628.2017.1330096

137. Colson C, Batrow PL, Gautier N, Rochet N, Ailhaud G, Peiretti F, et al. The rosmarinus bioactive compound carnosic acid is a novel PPAR antagonist that inhibits the browning of white adipocytes. *Cells* (2020) 9:2433. doi: 10.3390/cells9112433

138. Guo H, Guo J, Jiang X, Li Z, Ling W. Cyanidin-3-O-beta-glucoside, a typical anthocyanin, exhibits antilipolytic effects in 3T3-L1 adipocytes during hyperglycemia: involvement of FoxO1-mediated transcription of adipose triglyceride lipase. *Food Chem Toxicol* (2012) 50:3040–7. doi: 10.1016/j.fct.2012.06.015

139. Nehrenheim K, Meyer I, Brenden H, Vielhaber G, Krutmann J, Grether-Beck S. Dihydrodehydrodiisoeugenol enhances adipocyte differentiation and decreases lipolysis in murine and human cells. *Exp Dermatol* (2013) 22:638–43. doi: 10.1111/exd.12218

140. Kwon JY, Kershaw J, Chen CY, Komanetsky SM, Zhu Y, Guo X, et al. Piceatannol antagonizes lipolysis by promoting autophagy-lysosome-dependent degradation of lipolytic protein clusters in adipocytes. *J Nutr Biochem* (2022) 105:108998. doi: 10.1016/j.jnutbio.2022.108998

141. Wang B, Yang X, Zhao M, Su Z, Hu Z, Zhang C, et al. Celastrol prevents high-fat diet-induced obesity by promoting white adipose tissue browning. *Clin Transl Med* (2021) 11:e641. doi: 10.1002/ctm2.641

142. Su T, Huang C, Yang C, Jiang T, Su J, Chen M, et al. Apigenin inhibits STAT3/CD36 signaling axis and reduces visceral obesity. *Pharmacol Res* (2020) 152:104586. doi: 10.1016/j.phrs.2019.104586

143. Ilyas Z, Perna S, Al-Thawadi S, Alalwan TA, Riva A, Petrangolini G, et al. The effect of berberine on weight loss in order to prevent obesity: A systematic review. *BioMed Pharmacother* (2020) 127:110137. doi: 10.1016/j.biopha.2020.110137

frontiers | Frontiers in Endocrinology

TYPE Original Research
PUBLISHED 02 December 2022
DOI 10.3389/fendo.2022.1015614



OPEN ACCESS

EDITED BY
Guilherme Zweig Rocha,
State University of Campinas, Brazil

REVIEWED BY
Roberto Codella,
University of Milan, Italy
Bart Van Der Schueren,
KU Leuven, Belgium
Conxa Castell,
Public Health Agency of Catalonia, Spain

*CORRESPONDENCE
Didac Mauricio
didacmauricio@gmail.com

SPECIALTY SECTION
This article was submitted to Obesity, a section of the journal Frontiers in Endocrinology

RECEIVED 09 August 2022
ACCEPTED 16 November 2022
PUBLISHED 02 December 2022

CITATION
Genua I, Franch-Nadal J, Navas E, Mata-Cases M, Giménez-Pérez G, Vlacho B, Mauricio D and Goday A (2022) Obesity and related comorbidities in a large population-based cohort of subjects with type 1 diabetes in Catalonia. *Front. Endocrinol.* 13:1015614. doi: 10.3389/fendo.2022.1015614



# Obesity and related comorbidities in a large population-based cohort of subjects with type 1 diabetes in Catalonia

Idoia Genua[1,2,3], Josep Franch-Nadal[4,5,6], Elena Navas[7], Manel Mata-Cases[4,6,8], Gabriel Giménez-Pérez[9,10], Bogdan Vlacho[3,4,6], Didac Mauricio[1,4,6,11]* and Albert Goday[2,12,13]

[1]Department of Endocrinology and Nutrition, Hospital de la Santa Creu i Sant Pau, Barcelona, Spain, [2]Department of Medicine, Autonomous University of Barcelona, Barcelona, Spain, [3]Institut d'Investigació Biomèdica Sant Pau (IIB SANT PAU), Barcelona, Spain, [4]Diabetis en Atenció Primaria-Catalunya (DAP-Cat) group, Unitat de Suport a la Recerca Barcelona, Fundació Institut Universitari per a la recerca a l'Atenció Primària de Salut Jordi Gol i Gurina (IDIAPJGol), Barcelona, Spain, [5]Primary Health Care Center Raval Sud, Gerència d'Atenció Primaria, Institut Català de la Salut, Barcelona, Spain, [6]Centro de Investigación Biomédica en Red (CIBER) of Diabetes and Associated Metabolic Diseases (CIBERDEM), Instituto de Salud Carlos III (ISCIII), Barcelona, Spain, [7]Unitat de Suport a la Recerca|, Barcelona, Spain, [8]Primary Health Care Center La Mina, Gerència d'Atenció Primària Barcelona Ciutat, Institut Català de la Salut, Sant Adrià de Besòs, Spain, [9]Endocrinology Section, Department of Medicine, Hospital General de Granollers, Granollers, Spain, [10]School of Medicine and Health Sciences, Universitat Internacional de Catalunya, Sant Cugat del Vallès, Spain, [11]Department of Medicine, Universitat de Vic - Universitat Central de Catalunya, Barcelona, Spain, [12]Deparment of Endocrinology & Nutrition, Hospital del Mar, IMIM Institut Mar d'Investigacions Mediques. Parc de Salut Mar, Barcelona, Spain, [13]CIBERobn, Instituto de Salud Carlos III (ISCIII), Madrid, Spain

**Introduction:** Obesity, an increasing global health problem, can affect people with other disease conditions. The prevalence of obesity in people with type 1 diabetes (T1D) is not well known. The aim of this study was to describe extensively the characteristics and prevalence of different classes of obesity according to BMI (body mass index) categories in a large cohort of patients with T1D.

**Material and methods:** This was a retrospective, cross-sectional study in Catalonia. We reviewed all patients with T1D diagnosis, ≥ 18 years old and with BMI data from the SIDIAP database. Sociodemographic and clinical data, cardiovascular risk factors, laboratory parameters and concomitant medications were collected.

**Results:** A total of 6,068 patients with T1D were analyzed. The prevalence of obesity in the total sample was 18% (13.8% with class 1 obesity [BMI 30-34.9 kg/m2]). Patients with obesity had a higher prevalence of other cardiovascular risk factors (i.e. hypertension was 61.4% vs. 37.5%; dyslipidemia 63.6% vs 44%, and chronic kidney disease 38.4% vs. 24.4%; p<0.001 in all cases) and poorer

control of them. The higher prevalence was regardless of sex, age and duration of diabetes. The increase in these comorbidities was noticeable from a BMI > 25 kg/m2. Patients with obesity did not have poorer glycemic control.

**Conclusion:** The presence of obesity in people with T1D is frequent and cardiovascular risk factors are more common and more poorly controlled in T1D patients with obesity.

KEYWORDS

Obesity, type 1 diabetes, cardiovascular risk factors, metabolic syndrome, comorbidities

# Introduction

While it is well-known that obesity is commonly linked to type 2 diabetes (T2D), obesity may also be associated with type 1 diabetes (T1D) in a bidirectional way (1). With the ongoing obesity epidemic and the improvement in T1D treatments, the concern about possible consequences of this relationship has increased in the recent years.

The prevalence of obesity in patients with T1D is not well known. Furthermore, it differs widely among the available studies, varying from 8.9% to 28.4% across large cohort studies made in the USA and west and northern European countries (2–7), and reported to be only 2% in a smaller cohort in an Asian population (8). These variations can probably be explained because the incidence and prevalence of both conditions in the general population vary by country and by regions and, also, the fact that the prevalence of both T1D and obesity has increased in the last decades in the general population (9–11). It is therefore important to have current, region-specific data. Overall, the association between obesity and T1D appears to be frequent and the current prevalence of different classes of obesity in T1D and its characteristics need to be further studied.

The deleterious effect of obesity in the general population is well described (12). Nevertheless, data about the characteristics and consequences in patients with T1D are scarce. The association of obesity in people with T1D may entail additional problems such as poor metabolic control, increased cardiovascular (CV) risk factors and a consequent increase in related complications (13).

In a previous study (14), we described the clinical characteristics of a large cohort of patients with T1D in Catalonia, finding a high prevalence of obesity (16.5%). However, the different degrees of obesity, its characteristics and its implications were not addressed in that initial study. Considering its prevalence and its possible implications, we strongly felt that a more comprehensive analysis was needed; this led us to plan the current sub-study.

The aim of this study was to describe extensively the characteristics and prevalence of obesity (including according to different degrees of obesity) in a large population-based cohort of patients with T1D living in a Mediterranean area, i.e. Catalonia, with a high prevalence of obesity in the general population, and to analyze the impact of the obesity on metabolic control and other CV risk factors.

# Material and methods

We performed a cross-sectional analysis of retrospective routinely collected pseudo-anonymized health data from people who attended primary healthcare centers from the leading public healthcare provider (Institut Català de la Salut, ICS) in Catalonia (Spain). This pseudo-anonymized health data was obtained from the SIDIAP database (*Sistema d'Informació per al desenvolupament de la Investigació en Atenció Primària*, https://www.sidiap.org/), which is a well validated primary healthcare database used in diabetes epidemiological research (14). The SIDIAP database collects healthcare data from more than 74% (5,564,292 persons) of the Catalonian population. The cross-sectional analysis was performed on the cut-off date (December 31st, 2016) for 12 months (from January 1st, 2016).

## Study participants

For our analysis, we included all of the subjects in the database with a diagnosis of T1D, defined as the presence of the diagnostic ICD-10 (International Classification of Diseases 10) code E10 and sub-codes, as described in the previous study (14). Only patients ≥18 years old and with body mass index (BMI) data (directly measured and recorded by a healthcare professional) were considered for the analysis. Those with an E10 diagnosis treated with any glucose-lowering agents other than insulin and those who had not been treated with short-

acting insulins for more than two years after the recorded date of diagnosis were excluded, as described previously (14).

No formal sample size calculation was done, as the current study is a sub-analysis of the initial study on the characteristics of type 1 diabetes in Catalonia (14).

## Study variables

On the cut-off date, we collected different sociodemographic data (age, sex), clinical data (BMI, blood pressure, age at T1D diagnosis, duration of T1D), CV risk factors (hypertension, dyslipidemia, smoking, and obesity), laboratory parameters (HbA1c, blood lipids, estimated glomerular filtration rate (GFR; using the CKD-EPI formula) and insulin therapy and other concomitant medications related to CV risk factors. Dyslipidemia and hypertension were defined by the ICD-10 diagnostic code and/or a record of lipid-lowering or antihypertensive drugs, respectively. Chronic kidney disease (CKD) was defined by the ICD-10 diagnostic code and/or GFR <60 or urine albumin to creatinine ratio (ACR) >30 mg/g. Diagnostic codes and proxies used to define the study variables are presented in Supplementary Appendix 1 (code list). Objectives for CV prevention were established according to the European Society of Cardiology guidelines (15) (HbA1c <7% and blood pressure <140/90 mmHg and low-density lipoprotein cholesterol (LDLc) <100 mg/dl for primary prevention and HbA1c <7% and blood pressure <140/90mmHg and LDLc <70mg/dl for secondary prevention).

A complete-case analysis was performed.

## Statistical analysis

Descriptive statistics were calculated to summarize the sociodemographic characteristics, as well as the study variables (clinics and treatments). Continuous variables were expressed as means and standard deviations or medians and interquartile range, and categorical variables were expressed as frequencies and percentages. Descriptive analyses were conducted for the overall population, and stratified by sex and BMI groups (<30, 30 – 34.9, 35 – 39.9 and ≥40 kg/m$^2$) for all the study variables. In addition, for the clinical variables, analyses were stratified by sex, age groups (<40 and ≥40 years) and diabetes duration (<10, 10–19 and >19 years). To evaluate the differences between the characteristics (variables) according to the generated groups, the Chi-square test and the F-Fisher test were used when appropriate. To analyze continuous variables, the tests used were the T-Student test or analysis of variance (Anova). Additionally, the Bonferroni test was performed for multiple comparisons. To obtain the optimal cut-off points of the BMI in the ROC analysis, the "Concordance Probability Method (CZ)" was used. Statistical analysis was performed using R software for Windows version 3.6.1, Vienna, Austria.

# Results

A description of the whole cohort of patients with T1D in Catalonia has been published previously by this group elsewhere (14). From the overall number of subjects with T1D (15,008), we included those older than 18 years old (13,547) who had BMI data available (6,610). A total of 6,068 patients with T1D were analyzed in the current study. The sociodemographic and clinical characteristics of the studied population according to sex are shown in Table 1. The mean age of the entire cohort was 48.7 ± 15.9 years old with mean glycosylated hemoglobin (HbA1c) value of 8.0 ± 1.4%. The mean age at T1D diagnosis was 35.0 years, and 54.6% were men. Only 8.3% of the patients achieved all 3 risk factor target level for primary prevention for cardiovascular diseases (HbA1c <7%, BP<140/90 and LDLc <100 mg/dl).

The mean BMI was 26.2 ± 4.5 kg/m$^2$, with a prevalence of obesity (BMI ≥30 kg/m$^2$) of 18%. There were no statistically significant differences between sexes (20.1% in women and 16.2% in men). Regarding different degrees of obesity, 13.7% of patients with T1D had class 1 obesity (BMI between 30-34.9 kg/m$^2$), 3.3% had class 2 obesity (BMI between 35-39.9 kg/m$^2$) and only 1% had class 3 obesity (BMI ≥40 kg/m$^2$) (Table 2).

Compared to patients with T1D without obesity, those with obesity were older at the time of the study (53.6 ± 15.8 vs 47.7 ± 15.7 years old; p<0.001), and also at the time of T1D diagnosis (39.4 ± 18.7 vs 34.1 ± 17.2 years old; p<0.001), but there was no difference in the duration of T1D from diagnosis (14.8 vs 14.2 years). The prevalence of obesity gradually increased with age (6.2% in ≤20 years old, 9.7% in 21-30 years old, 14.6% in 31-40 years old, 16.1% in 41-50 years old, 20.9% in 51-60 years old, 21.8% in 61-70 years old and 29.6% in >70 years old; p<0.001). Patients with obesity were more likely to be non-smokers.

Concerning glycemic control, patients with obesity did not have a poorer control compared to those without obesity (mean HbA1c 8.0 ± 1.3 vs 8.0 ± 1.5, respectively; p=0.233). Moreover, having obesity did not make it less likely to have glycemic control within the optimal range (defined as HbA1c <7%), with 21.9% of patients with obesity and 21.5% without obesity having HbA1c < 7%.

Table 2 shows the clinical characteristics of patients with T1D according to different degrees of obesity. Compared to non-obese patients, a higher proportion of those with obesity had CV risk factors (hypertension was 61.4% vs. 37.5%; dyslipidemia 63.6% vs 44%, and chronic kidney disease 38.4% vs. 24.4%; p<0.001 in all cases). Furthermore, obesity was associated with poorer control of some CV risk factors; fewer patients with obesity than those without had fair blood pressure control

10.3389/fendo.2022.1015614

TABLE 1 Characteristics of the whole study population and also according to sex.

| | Total population | Women | Men | p-value |
|---|---|---|---|---|
| N | 6068 (100.0%) | 2756 (45.4%) | 3312 (54.6%) | |
| Current age (years) | 48.7 (15.9) | 49.3 (16.8) | 48.3 (15.1) | 0.272 |
| Age at diagnosis (years) | 35.0 (17.6) | 35.3 (18.9) | 34.8 (16.4) | >0.999 |
| **Diabetes duration (years)** | | | | >0.999 |
| <10 years | 2084 (34.3%) | 925 (33.6%) | 1159 (35.0%) | |
| 10 – 19 years | 2703 (44.5%) | 1227 (44.5%) | 1476 (44.6%) | |
| >19 years | 1281 (21.1%) | 604 (21.9%) | 677 (20.4%) | |
| HbA1c % (n = 4249) | 8.0 (1.4) | 8.0 (1.4) | 8.0 (1.4) | >0.999 |
| **BMI (kg/m$^2$)** (n= 6068) | 26.2 (4.5) | 26.1 (5.0) | 26.2 (4.1) | **0.003** |
| Non obesity (BMI < 30 kg/m$^2$) | 4976 (82.0%) | 2202 (79.9%) | 2774 (83.8%) | |
| Obesity (BMI ≥ 30 kg/m$^2$) | 1092 (18.0%) | 554 (20.1%) | 538 (16.2%) | |
| **Smoking status**: | | | | **<0.001** |
| Non-smoker | 2885 (47.5%) | 1598 (58.0%) | 1287 (38.9%) | |
| Ex-smoker | 1638 (27.0%) | 625 (22.7%) | 1013 (30.6%) | |
| Smoker | 1545 (25.5%) | 533 (19.3%) | 1012 (30.6%) | |
| **BP** | | | | |
| Systolic BP (mmHg) (n= 5711) | 127 (14.0) | 125 (14.7) | 129 (13.0) | **<0.001** |
| Diastolic BP (mmHg) (n= 5711) | 73.6 (9.1) | 72.4 (8.8) | 74.6 (9.2) | **<0.001** |
| Total cholesterol (mg/dl) (n=4331) | 182 (37.9) | 187 (36.4) | 178 (38.7) | **<0.001** |
| HDLc (mg/dl) (n= 4145) | 59.1 (17.3) | 65.4 (17.2) | 53.7 (15.5) | **<0.001** |
| LDLc (mg/dl) (n= 3933) | 103 (30.2) | 103 (29.0) | 102 (31.2) | >0.999 |
| Triglycerides (mg/dl) (n= 4005) | 111 (91.3) | 100 (64.3) | 120 (108.0) | **<0.001** |
| Microalbuminuria (n= 3252) | 68.2 (275) | 61.5 (278) | 74.0 (272) | >0.999 |
| Estimated GFR (CKDEPI) (n= 3632) | 79.2 (22.4) | 78.4 (22.3) | 79.9 (22.4) | 0.929 |
| **Other variables** | | | | |
| Chronic kidney disease (n= 2962) | 805 (27.2%) | 366 (26.9%) | 439 (27.4%) | >0.999 |
| Dyslipidemia (%), (n= 6068) | 2881 (47.5%) | 1225 (44.4%) | 1656 (50.0%) | **<0.001** |
| Hypertension (%), (n= 6068) | 2534 (41.8%) | 1082 (39.3%) | 1452 (43.8%) | **0.009** |
| **Cardiovascular prevention** | | | | |
| Primary (%), (n = 4434) | 368 (8.3%) | 170 (8.5%) | 198 (8.2%) | >0.999 |
| Secondary (%), (n = 4434) | 114 (2.5%) | 38 (1.8%) | 76 (3.1%) | 0.256 |
| **More treatments** | | | | |
| BP lowering (%) | 2366 (39.0%) | 1005 (36.5%) | 1361 (41.1%) | **0.006** |
| Antithrombotic (%) | 1675 (27.6%) | 673 (24.4%) | 1002 (30.3%) | **<0.001** |
| Lipid-lowering (%) | 2500 (41.2%) | 1055 (38.3%) | 1445 (43.6%) | **<0.001** |
| **Insulin therapy** | | | | |
| Short-acting insulin (%) | 5603 (92.3%) | 2576 (93.5%) | 3027 (91.4%) | 0.068 |
| Long-acting insulin (%) | 5093 (83.9%) | 2275 (82.5%) | 2818 (85.1%) | 0.198 |
| Mixed insulin (%) | 873 (14.4%) | 378 (13.7%) | 495 (14.9%) | >0.999 |
| Intermediate-acting insulin (%) | 316 (5.2%) | 135 (4.9%) | 181 (5.4%) | >0.999 |

P-value<0.05 is considered to be statistically significant. Data are mean (SD) or n(%). Where indicated, the n value denotes the number of study patients with available data during the study period. BMI, body mass index; BP, blood pressure; HDLc, HDL-cholesterol; LDLc, LDL-cholesterol; GFR, glomerular filtration rate. Primary prevention includes the composite target achievement of HbA1c<7%, blood pressure <140/90 and LDL-C<100. Secondary prevention includes the composite target achievement of HbA1c<7%, blood pressure <140/90 and LDL-C<70.
Bold values correspond to statistically significant p-values.

(defined as <140/90 mmHg) (75% vs. 84% (p <0.001), triglyceride levels were higher in the obese group (134 ± 113 vs 106 ± 84.3 mg/dl; p<0.001), and high density lipoprotein cholesterol (HDLc) levels were lower in the obese group (53.1 ± 15.2 vs 60.5 ± 17.5 mg/dl; p<0.001). No differences were found in total cholesterol or LDLc levels. We have also compared CV risk factors of patients with T1D according to the different obesity categories, and the same differences were observed, as shown in Table 2.

No differences were found in the percentage of patients that met the established targets for primary (HbA1c <7% and blood pressure <140/90 and LDLc <100 mg/dl) and secondary

10.3389/fendo.2022.1015614

TABLE 2 Characteristics of T1D according to the different categories of body mass index.

| | No Obesity < 30kg/m$^2$ | Obesity Class 1 30-34.9 kg/m$^2$ | Obesity Class 2 35-39.9 kg/m$^2$ | Obesity Class 3 ≥ 40 kg/m$^2$ | p-value |
|---|---|---|---|---|---|
| N (%) | 4976 (82.0%) | 830 (13.8%) | 199 (3.2%) | 63 (1.0%) | |
| Current age (years) | 47.7 (15.7) | 53.0 (15.7) | 55.9 (15.9) | 53.7 (16.6) | **<0.001** |
| Age at diagnosis (years) | 34.1 (17.2) | 38.4 (18.4) | 42.5 (19.6) | 41.9 (19.1) | **<0.001** |
| **Diabetes duration (years)** | | | | | >0.999 |
| <10 years | 1722 (34.6%) | 258 (31.1%) | 80 (40.2%) | 24 (38.1%) | |
| 10 – 19 years | 2221 (44.6%) | 380 (45.8%) | 73 (36.7%) | 29 (46.0%) | |
| >19 years | 1033 (20.8%) | 192 (23.1%) | 46 (23.1%) | 10 (15.9%) | |
| HbA1c % (n = 4249) | 8.0 (1.5) | 7.9 (1.3) | 8.1 (1.3) | 8.1 (1.6) | >0.999 |
| BMI (kg/m$^2$) (n= 6068) | 24.6 (2.9) | 31.9 (1.3) | 36.9 (1.4) | 43.3 (3.2) | **<0.001** |
| **Smoking status** | | | | | **<0.001** |
| Non smoker | 2321 (46.6%) | 422 (50.8%) | 105 (52.8%) | 37 (58.7%) | |
| Former Smoker | 1209 (24.3%) | 252 (30.4%) | 68 (34.2%) | 16 (25.4%) | |
| Smoker | 1446 (29.1%) | 156 (18.8%) | 26 (13.1%) | 10 (15.9%) | |
| **BP** | | | | | |
| Systolic BP (mmHg) (n= 5711) | 126 (13.9) | 131 (13.3) | 131 (12.4) | 132 (16.6) | **<0.001** |
| Diastolic BP (mmHg) (n= 5711) | 73.2 (9.0) | 75.3 (9.2) | 75.5 (9.2) | 74.2 (12.0) | **<0.001** |
| Total cholesterol (mg/dl) (n=4331) | 183 (37.6) | 180 (38.0) | 179 (41.0) | 194 (48.0) | 0.709 |
| HDLc (mg/dl) (n= 4145) | 60.5 (17.5) | 53.6 (15.3) | 51.2 (15.1) | 51.8 (13.5) | **<0.001** |
| LDLc (mg/dl) (n= 3933) | 103 (30.1) | 102 (31.4) | 98.8 (30.6) | 103 (25.2) | >0.999 |
| Triglycerides (mg/dl) (n= 4005) | 106 (84.3) | 129 (119) | 141 (82.9) | 164 (122) | **<0.001** |
| Microalbuminuria (n= 3252) | 64.7 (273) | 64.5 (251) | 108 (301) | 224 (452) | **0.024** |
| Estimated GFR (CKDEPI) (n= 3632) | 80.4 (21.7) | 76.4 (23.3) | 69.1 (24.3) | 62.9 (28.8) | **<0.001** |
| **Other variables** | | | | | |
| Chronic kidney disease (n= 2962) | 577 (24.4%) | 155 (34.9%) | 51 (46.8%) | 22 (53.7%) | **<0.001** |
| Dyslipidemia (%), (n= 6068) | 2187 (44.0%) | 519 (62.5%) | 135 (67.8%) | 40 (63.5%) | **<0.001** |
| Hypertension (%), (n= 6068) | 1864 (37.5%) | 485 (58.4%) | 139 (69.8%) | 46 (73.0%) | **<0.001** |
| **Cardiovascular Prevention** | | | | | |
| Primary (%), (n = 4434) | 303 (8.5%) | 54 (8.3%) | 9 (5.9%) | 2 (3.9%) | >0.999 |
| Secondary (%), (n = 4434) | 86 (2.4%) | 24 (3.7%) | 4 (2.6%) | 0 (0.0%) | >0.999 |
| **More treatments** | | | | | |
| BP lowering (%) | 1735 (34.9%) | 455 (54.8%) | 132 (66.3%) | 44 (69.8%) | **<0.001** |
| Antithrombotic (%) | 1259 (25.3%) | 307 (37.0%) | 80 (40.2%) | 29 (46.0%) | **<0.001** |
| Lipid-lowering (%) | 1868 (37.5%) | 472 (56.9%) | 124 (62.3%) | 36 (57.1%) | **<0.001** |
| **Insulin therapy** | | | | | |
| Short-acting insulin (%) | 4626 (93.0%) | 747 (90.0%) | 176 (88.4%) | 54 (85.7%) | **0.016** |
| Long-acting insulin (%) | 4220 (84.8%) | 672 (81.0%) | 155 (77.9%) | 46 (73.0%) | **0.008** |
| Mixed insulin (%) | 673 (13.5%) | 144 (17.3%) | 37 (18.6%) | 19 (30.2%) | **0.001** |
| Intermediate-acting insulin (%) | 258 (5.1%) | 42 (5.0%) | 12 (6.0%) | 4 (6.3%) | >0.999 |

P-value<0.05 is considered to be statistically significant. Data are mean (SD) or n(%). Where indicated, the n value denotes the number of study patients with available data during the study period. BMI, body mass index; BP, blood pressure; GFR, glomerular filtration rate; HDLc, HDL-cholesterol; LDLc, LDL-cholesterol. Primary prevention includes the composite target achievement of HbA1c<7%, blood pressure <140/90 and LDL-C<100. Secondary prevention includes the composite target achievement of HbA1c<7%, blood pressure <140/90 and LDL-C<70.
Bold values correspond to statistically significant p-values.

(HbA1c <7% and blood pressure <140/90 and LDLc <70 mg/dl) CV prevention when comparing distinct BMI categories.

The prevalence of obesity and clinical characteristics according to gender, current age and diabetes duration are presented in Tables 3A–C. The higher prevalence of hypertension and dyslipidemia in the obesity group was maintained irrespective of sex, age and duration of diabetes.

Table 4 represents the relation between BMI, as a continuous variable, and the degree of control of CV risk factors showing a progressive worsening in their control from a BMI of >25 kg/m$^2$. The BMI cut-off values at which the progressive worsening occurred were 25.6, 25.6, 25.4, 26.6, 25.2 and 26.5 kg/m$^2$ for systolic and diastolic blood pressure, total cholesterol, HDLc, LDLc and triglycerides, respectively.

## Discussion

The present study confirms a high prevalence of obesity in people with T1D, with a concomitant higher prevalence and poorer control of other CV risk factors. The prevalence of T1D in Spain is medium-high, being around 15 cases per 1,000 in people under 19 years old (16) and 0.3% in the working population (17). The estimated prevalence of obesity in Spain is also medium-high at around 23% (18). With the prevalence of both conditions being medium-high in our area, it is relevant to explore the association between both diseases. To our knowledge, this is the largest cohort that describes extensively the prevalence and clinical characteristics of obesity, including different degrees of obesity, in adults with T1D.

The prevalence of obesity observed in patients with T1D (18%, mainly class 1 obesity) is similar or a bit lower than the prevalence of obesity in the general population in Spain (23%) (18). Both epidemiological data are based on BMI according to the direct measurement of weight and height, and therefore are methodologically homogeneous. These data are more accurate than data on self-declaration of weight and height, as obtained in national health surveys. The prevalence found in our cohort is in line with another recently published European study in Belgium in a cohort of 32,809 patients (between 2017 and 2018) with T1D that reported a prevalence of obesity of around 17%, similar to that in the Belgium general population (4). Another recent large European cohort study found a prevalence of obesity of 15.3% in T1D (3). As mentioned in a recent review (1), the prevalence found in the current study is close to the prevalence of obesity seen in the general population. On the other hand, other recent studies in large cohorts from non-European countries with a higher prevalence of obesity in the general population, observed a markedly lower prevalence of obesity in T1D (2, 19). Despite these differences, it is definitely clear that obesity in people with T1D is a prevalent comorbidity that we cannot disregard.

As expected, considering the general population, patients with obesity were older (18). Unlike in the general population, few studies have evaluated the association of obesity with other CV risk factors in people with T1D. A study that assessed this in 11,348 children in the USA, with a 14% prevalence of obesity, also found a higher prevalence of hypertension and dyslipidemia in the obese group, with no differences in HbA1c values (20). In contrast, a Swedish study in 26,125 people with T1D, found higher HbA1c levels in patients with obesity at baseline, as well as higher mean systolic blood pressure (21). Considering that the main cause of mortality in T1D is CV disease, having an increase and poorer control of CV risk factors in those with obesity is a relevant finding. Further, a study found higher major complication outcomes (an aggregate of mortality, coronary artery disease, and renal failure) in T1D patients with metabolic syndrome (22). Interestingly, patients with obesity were more frequently non-smokers, a fact that is favorable and does not further increase the adverse CV risk profile of these subjects.

Whether people with T1D and obesity have poorer glycemic control remains unclear. We did not find differences in chronic glycemic control (HbA1c). The T1D exchange clinic registry (23) found that adolescents who had better metabolic control were at higher risk of obesity. However, a study of the SWEET registry in children and adolescents found that underweight and obese children had significantly higher HbA1c (24). Although these studies were conducted in pediatric populations that might not be comparable to adults, results from the few studies in adult populations are also inconsistent (21, 25). The fact that a more intensive insulin therapy is related to weight gain could go some way to explaining why obesity does not clearly worsen metabolic control (26).

The established cut-off points by WHO for overweight and obesity in the general population are based on the relationship between BMI and morbidity and mortality. However, it is well known that these cut-offs are inaccurate for some groups (27). Nevertheless, we found a good correlation between the classic BMI cut-off points and the risk of comorbidities in this specific subgroup of patients. We acknowledge that obtained AUC, sensitivity and specificity are not very discriminant. However, we did not aim at building a screening tool, but at exploring the threshold upon which the overweight-related risk factor profile was unfavorable. The major strengths of the study are the extensive description of patients and the large cohort used for the analysis. Data are representative and robust, encompassing a large proportion of the Catalonian population, with the SIDIAP database having been used in several other diabetes studies (14, 28, 29). The restrictive criteria used to define the diagnosis of T1D ensured the correct diagnosis of T1D.

The study has some limitations. First, due to the cross-sectional retrospective nature of the study, inherent limitations of this type of study are presented. We cannot establish tendencies or causality. In addition, obesity was frequently not well documented compared to other diseases, and BMI was probably more often recorded in more complicated and older

TABLE 3A Prevalence of obesity and clinical characteristics according to sex.

| Sex | Women (n = 2756) | | | Men (n = 3312) | | |
|---|---|---|---|---|---|---|
| | <30kg/m$^2$ | ≥30kg/m$^2$ | p-value | <30kg/m$^2$ | ≥30kg/m$^2$ | p-value |
| n (%) | 2,202 (79.8%) | 554 (20.2%) | | 2774 (83.7%) | 538 (16.2%) | |
| Systolic BP, mmHg | 123 (14.5) | 130 (14.1) | **<0.001** | 129 (13.0) | 132 (12.4) | **<0.001** |
| Diastolic BP, mmHg | 72.0 (8.7) | 73.7 (9.4) | **<0.001** | 74.1 (9.2) | 76.8 (9.1) | **<0.001** |
| Total cholesterol (mg/dl) | 188 (36.2) | 185 (37.1) | >0.999 | 178 (38.2) | 176 (41.2) | >0.999 |
| HDLc (mg/dl) | 67.4 (17.2) | 58.0 (15.0) | **<0.001** | 54.9 (15.6) | 47.8 (13.5) | **<0.001** |
| LDLc (mg/dl) | 103 (28.8) | 103 (29.8) | >0.999 | 103 (31.1) | 99.9 (32.0) | >0.999 |
| Triglycerides (mg/dl) | 94.7 (60.5) | 120 (72.9) | **<0.001** | 114 (98.2) | 148 (143) | **<0.001** |
| HbA1c % | 8.0 (1.5) | 8.0 (1.3) | >0.999 | 8.0 (1.5) | 7.9 (1.3) | >0.999 |
| Dyslipidemia | 903 (41.0%) | 322 (58.1%) | **<0.001** | 1284 (46.3%) | 372 (69.1%) | **<0.001** |
| Hypertension | 756 (34.3%) | 326 (58.8%) | **<0.001** | 1108 (39.9%) | 344 (63.9%) | **<0.001** |
| Chronic kidney disease | 239 (22.7%) | 127 (41.5%) | **<0.001** | 338 (25.7%) | 101 (35.1%) | **0.018** |

BP, blood pressure, HbA1c, glycosylate haemoglobin; HDLc, HDL-cholesterol; LDLc, LDL-cholesterol. P-value<0.05 is considered to be statistically significant.
Bold values correspond to statistically significant p-values.

TABLE 3B Prevalence of obesity and clinical characteristics according to current age.

| Current age (years) | <40 years (n = 1843) | | | ≥40 years (n = 4225) | | |
|---|---|---|---|---|---|---|
| | <30kg/m$^2$ | ≥30kg/m$^2$ | p-value | <30kg/m$^2$ | ≥30kg/m$^2$ | p-value |
| N (%) | 1618 (87.8%) | 225 (12.2%) | | 3358 (79.4%) | 867 (20.6%) | |
| Systolic BP, mmHg | 121 (12.6) | 125 (12.0) | **<0.001** | 129 (13.8) | 133 (13.2) | **<0.001** |
| Diastolic BP, mmHg | 72.9 (8.6) | 77.9 (7.3) | **<0.001** | 73.4 (9.2) | 74.6 (9.7) | **0.007** |
| Total cholesterol (mg/dl) | 184 (39.1) | 183 (36.8) | >0.999 | 182 (36.9) | 180 (40.0) | >0.999 |
| HDLc (mg/dl) | 59.4 (15.3) | 51.3 (13.6) | **<0.001** | 61.0 (18.3) | 53.5 (15.5) | **<0.001** |
| LDLc (mg/dl) | 105 (30.5) | 108 (30.1) | >0.999 | 102 (29.9) | 99.9 (30.9) | >0.999 |
| Triglycerides (mg/dl) | 104 (88.2) | 133 (187) | 0.618 | 106 (82.5) | 132 (86.6) | **<0.001** |
| HbA1c % | 8.2 (1.7) | 7.9 (1.3) | **0.028** | 8.0 (1.3) | 8.0 (1.3) | >0.999 |
| Dyslipidemia | 200 (12.4%) | 53 (23.6%) | **<0.001** | 1987 (59.2%) | 641 (73.9%) | **<0.001** |
| Hypertension | 154 (9.5%) | 45 (20.0%) | **<0.001** | 1710 (50.9%) | 625 (72.1%) | **<0.001** |
| Chronic kidney disease | 87 (12.7%) | 18 (17.1%) | >0.999 | 490 (29.1%) | 210 (42.9%) | **<0.001** |

BP, blood pressure; HbA1c, glycosylate haemoglobin; HDLc, HDL-cholesterol; LDLc, LDL-cholesterol. P-value<0.05 is considered to be statistically significant.
Bold values correspond to statistically significant p-values.

TABLE 3C Prevalence of obesity and clinical characteristics according to diabetes duration.

| Diabetes duration (years) | <10 years (n = 2084) | | | 10 – 19 years (n = 2703) | | | >19 years (n = 1281) | | |
|---|---|---|---|---|---|---|---|---|---|
| | <30kg/m$^2$ | ≥30kg/m$^2$ | p-value | <30kg/m$^2$ | ≥30kg/m$^2$ | p-value | <30kg/m$^2$ | ≥30kg/m$^2$ | p-value |
| N(%) | 1722 (82.7%) | 362 (17.3%) | | 2221 (82.1%) | 482 (17.9%) | | 1033 (80.6%) | 248 (19.4%) | |
| Systolic BP, mmHg | 125 (14.6) | 131 (14.4) | **<0.001** | 127 (13.7) | 132 (12.6) | **<0.001** | 128 (13.1) | 131 (13.2) | **0.036** |
| Diastolic BP, mmHg | 72.8 (9.0) | 75.7 (9.3) | **<0.001** | 73.6 (8.9) | 75.5 (9.5) | **<0.001** | 73.0 (9.3) | 74.2 (9.2) | >0.999 |
| Total cholesterol (mg/dl) | 183 (39.2) | 181 (41.0) | >0.999 | 183 (36.6) | 182 (38.1) | >0.999 | 181 (36.9) | 179 (39.4) | >0.999 |
| HDLc (mg/dl) | 58.7 (17.6) | 50.2 (14.3) | **<0.001** | 61.3 (17.2) | 53.7 (15.1) | **<0.001** | 62.0 (17.7) | 56.3 (15.9) | **<0.001** |
| LDLc (mg/dl) | 103 (31.4) | 103 (30.7) | >0.999 | 103 (29.7) | 103 (31.3) | >0.999 | 100 (28.4) | 95.3 (29.8) | 0.725 |
| Triglycerides (mg/dl) | 114 (108) | 154 (157) | **<0.001** | 102 (69.7) | 123 (76.1) | **<0.001** | 99.0 (60.5) | 123 (85.3) | **0.008** |
| HbA1c % | 8.0 (1.7) | 7.8 (1.5) | 0.405 | 8.1 (1.3) | 8.1 (1.3) | >0.999 | 8.0 (1.3) | 7.9 (1.2) | >0.999 |

*(Continued)*

TABLE 3C Continued

| Diabetes duration (years) | <10 years (n = 2084) | | | 10 – 19 years (n = 2703) | | | >19 years (n = 1281) | | |
|---|---|---|---|---|---|---|---|---|---|
| | <30kg/m$^2$ | ≥30kg/m$^2$ | p-value | <30kg/m$^2$ | ≥30kg/m$^2$ | p-value | <30kg/m$^2$ | ≥30kg/m$^2$ | p-value |
| Dyslipidemia | 640 (37.2%) | 211 (58.3%) | **<0.001** | 980 (44.1%) | 301 (62.4%) | **<0.001** | 567 (54.9%) | 182 (73.4%) | **<0.001** |
| Hypertension | 528 (30.7%) | 216 (59.7%) | **<0.001** | 808 (36.4%) | 277 (57.5%) | **<0.001** | 528 (51.1%) | 177 (71.4%) | **<0.001** |
| Chronic kidney disease | 201 (23.9%) | 102 (48.1%) | **<0.001** | 234 (23.6%) | 75 (29.4%) | 0.675 | 142 (26.5%) | 51 (40.2%) | **0.036** |

P-value<0.05 is considered to be statistically significant. BP, blood pressure; HDLc, HDL-cholesterol; LDLc, LDL-cholesterol.
Bold values correspond to statistically significant p-values.

TABLE 4 Cut-off points of the body mass index that show optimal or suboptimal control according to clinical variables.

| Variables | Suboptimal control | Patients with suboptimal control N (%) | Optimal control | Patients with optimal control N (%) | BMI cut-off points | AUC (95% CI) | Sensitivity or True Positive Rate | Specificity or True Negative Rate |
|---|---|---|---|---|---|---|---|---|
| Systolic BP, mmHg | ≥130 mmHg | 2709 (47.4%) | <130 mmHg | 3002 (52.5%) | 25.6 kg/m$^2$ | 0.62 (0.60; 0.63) | 60.1% | 57.4% |
| Diastolic BP, mmHg | ≥80 mmHg | 1570 (27.4%) | <80 mmHg | 4141 (72.5%) | 25.6 kg/m$^2$ | 0.58 (0.56; 0.59) | 60.3% | 52.6% |
| Total cholesterol (mg/dl) | ≥240 mg/dl | 307 (7.1%) | <240 mg/dl | 4024 (92.9%) | 25.4 kg/m$^2$ | 0.50 (0.46; 0.53) | 56.4% | 46.3% |
| HDLc (mg/dl) | | | | | | | | |
| Men | <40 mg/dl | 351 (15.6%) | ≥40 mg/dl | 1891 (84.3%) | 26.6 kg/m$^2$ | 0.61 (0.57; 0.64) | 59.8% | 57.9% |
| Women | <50 mg/dl | 329 (17.2%) | ≥50 mg/dl | 1574 (82.7%) | 26.1 kg/m$^2$ | 0.67 (0.63; 0.70) | 69.9% | 59.4% |
| LDLc (mg/dl) | ≥100 mg/dl | 1987 (50.5%) | <100 mg/dl | 1946 (49.4%) | 25.2 kg/m$^2$ | 0.51 (0.49; 0.53) | 57.9% | 46.8% |
| Triglycerides (mg/dl) | ≥150 mg/dl | 662 (16.5%) | <150 mg/dl | 3343 (84.4%) | 26.5 kg/m$^2$ | 0.60 (0.58; 0.62) | 59.8% | 57.7% |
| Glomerular Filtration (mg/dL) | <60 mg/dL | 471 (12.9%) | ≥60 mg/dL | 3161 (87.0%) | 27.6 kg/m$^2$ | 0.60 (0.57; 0.63) | 51.6% | 66.4% |
| Microalbuminuria | >30 mg | 542 (16.6%) | ≤30 mg | 2710 (83.3%) | 27.2 kg/m$^2$ | 0.53 (0.51; 0.56) | 45.8% | 62.1% |

AUC, area under the curve; BP, blood pressure; CI, confidence interval; HDLc, high-density lipoprotein cholesterol; LDLc, low-density lipoprotein cholesterol; BMI, body mass index.

patients. The study relied on the recorded codes without external validation and because of the restrictive definition criteria we may have excluded a few subjects with T1D who were also treated with glucose-lowering agents other than insulin.

In conclusion, the prevalence of obesity in T1D is relevant and is associated with a higher risk of having other CV risk factors with a suboptimal control of them. It seems that glycemic control is not related to the degree of obesity.

## Data availability statement

Restrictions apply to the availability of some or all data generated or analyzed during this study because they were used under license. Requests to access these datasets should be directed to DM, didacmauricio@gmail.com.

## Ethics statement

The studies involving human participants were reviewed and approved by Primary Health Care University Research Institute Jordi Gol (number P17/115). Written informed consent for participation was not required for this study in accordance with the national legislation and the institutional requirements.

## Author contributions

Conceptualization: AG, JF-N and DM; formal analysis: EN; resources and data curation, EN; writing—original draft preparation IG; writing—review and editing: BV, IG, AG, EN, JF-N, GG-P, MM-C and DM; supervision: DM, AG, and JF-N; project administration: JF-N. All authors contributed to the article and approved the submitted version.

## Funding

This research was partially funded by an unrestricted grant by Lilly S.A. The funder was not involved in the study design, collection, analysis, interpretation of data, the writing of this article or the decision to submit it for publication. This research was supported by CIBER-Consorcio Centro de Investigación Biomédica en Red (leading group: CIBERDEM - CB15/00071), Instituto de Salud Carlos III, Ministerio de Ciencia e Innovación and Unión Europea – European Regional Development Fund.

## Acknowledgments

We thank Amanda Prowse for her support in linguistics.

## Conflict of interest

IG received support for attending meetings form Boehringer Ingelheim, Lilly, MSD, Novo-Nordisk and Sanofi. JF-N received advisory and/or speaking fees from Astra-Zeneca, Ascensia, Boehringer Ingelheim, GSK, Lilly, MSD, Novartis, Novo Nordisk and Sanofi. Received research grants to the institution from Astra-Zeneca. GSK, Lilly, MSD, Novartis, Novo Nordisk, Sanofi and Boehringer. DM has received advisory and/or speaking fees from Almirall, Esteve, Ferrer, Janssen, Lilly, Menarini, MSD, NovoNordisk and Sanofi. GG-P has received speaking fees from Lilly and Astra-Zeneca. MM-C has received advisory honorarium from for Astra-Zeneca, Bayer, Boehringer Ingelheim, GSK, Lilly, MSD, NOVARTIS, NovoNordisk, Sanofi; speaker honorarium from Astra- Zeneca, Bayer, Boehringer Ingelheim, GSK, Lilly, Menarini, MSD, Novartis, NovoNordisk, and Sanofi; and research grants to institution from Astra-Zeneca, GSK, Lilly, MSD, Novartis, NovoNordisk, and Sanofi.

The remaining authors declare that the research was conducted in the absence of any commercial or financial relationships that could be construed as a potential conflict of interest.

## Publisher's note



## Supplementary material

The Supplementary Material for this article can be found online at: https://www.frontiersin.org/articles/10.3389/fendo.2022.1015614/full#supplementary-material

## References

1. van der Schueren B, Ellis D, Faradji RN, Al-Ozairi E, Rosen J, Mathieu C. Obesity in people living with type 1 diabetes. *Lancet Diabetes Endocrinol* (2021) 9:776–85. doi: 10.1016/S2213-8587(21)00246-1

2. Foster NC, Beck RW, Miller KM, Clements MA, Rickels MR, Dimeglio LA, et al. State of type 1 diabetes management and outcomes from the T1D exchange in 2016-2018. *Diabetes Technol Ther* (2019) 21:66–72. doi: 10.1089/dia.2018.0384

3. van Mark G, Lanzinger S, Barion R, Degenhardt M, Badis S, Noll H, et al. Patient and disease characteristics of adult patients with type 1 diabetes in Germany: An analysis of the DPV and DIVE databases. *Ther Adv Endocrinol Metab* (2019) 10:1–12. doi: 10.1177/2042018819830867

4. Lavens A, Nobels F, de Block C, Oriot P, Verhaegen A, Chao S, et al. Effect of an integrated, multidisciplinary nationwide approach to type 1 diabetes care on

metabolic outcomes: An observational real-world study. *Diabetes Technol Ther* (2021) 23(8):565–76. doi: 10.1089/dia.2021.0003

5. Vestberg D, Rosengren A, Olsson M, Gudbjörnsdottir S, Svensson AM, Lind M. Relationship between overweight and obesity with hospitalization for heart failure in 20,985 patients with type 1 diabetes: A population-based study from the Swedish national diabetes registry. *Diabetes Care* (2013) 36(9):2857–61. doi: 10.2337/dc12-2007

6. Hill CJ, Cardwell CR, Maxwell AP, Young RJ, Matthews B, O'Donoghue DJ, et al. Obesity and kidney disease in type 1 and 2 diabetes: An analysis of the national diabetes audit. *QJM* (2013) 106(10):933–42. doi: 10.1093/qjmed/hct123

7. Dahlström EH, Sandholm N, Forsblom CM, Thorn LM, Jansson FJ, Harjutsalo V, et al. Body mass index and mortality in individuals with type 1 diabetes. *J Clin Endocrinol Metab* (2019) 104(11):5195–204. doi: 10.1210/jc.2019-00042

8. Arai K, Yokoyama H, Okuguchi F, Yamazaki K, Takagi H, Hirao K, et al. Association between body mass index and core components of metabolic syndrome in 1486 patients with type 1 diabetes mellitus in Japan (JDDM 13). *Endoc J* (2008) 55(6):1025-1032. doi: 10.1507/endocrj.K08E-167

9. DiMeglio LA, Evans-Molina C, Oram RA. Type 1 diabetes. *Lancet* (2018) 391:2449–62. doi: 10.1016/S0140-6736(18)31320-5

10. Chooi YC, Ding C, Magkos F. The epidemiology of obesity. *Metabol: Clin Exp* (2019) 92:6–10. doi: 10.1016/j.metabol.2018.09.005

11. Hernáez Á, Zomeño MD, Dégano IR, Pérez-Fernández S, Goday A, Vila J, et al. Excess weight in Spain: Current situation, projections for 2030, and estimated direct extra cost for the Spanish health system. *Rev Española Cardiol (English Edition)* (2019) 72(11):916–24. doi: 10.1016/j.rec.2018.10.010

12. Haslam DW, James PT. (2005). Watton Place Clinic: National Obesity Forum. Available at: www.thelancet.com.

13. Corbin KD, Driscoll KA, Pratley RE, Smith SR, Maahs DM, Mayer-Davis EJ. Obesity in type 1 diabetes: Pathophysiology, clinical impact, and mechanisms. *Endoc Rev* (2018) 39:629–63. doi: 10.1210/er.2017-00191

14. Gimenez-Perez G, Franch-Nadal J, Ortega E, Mata-Cases M, Goday A, Real J, et al. Clinical characteristics and degree of glycemic and cardiovascular risk factor control in patients with type 1 diabetes in catalonia (Spain). *J Clin Med* (2021) 10 (7):1536. doi: 10.3390/jcm10071536

15. Catapano AL, Graham I, de Backer G, Wiklund O, Chapman MJ, Drexel H, et al. ESC/EAS guidelines for the management of dyslipidaemias. *Eur Heart J* (2016) 37(39):2999–3058. doi: 10.1093/eurheartj/ehw272

16. Patterson CC, Karuranga S, Salpea P, Saeedi P, Dahlquist G, Soltesz G, et al. Worldwide estimates of incidence, prevalence and mortality of type 1 diabetes in children and adolescents: Results from the international diabetes federation diabetes atlas, 9th edition. *Diabetes Res Clin Pract* (2019) 157:107842. doi: 10.1016/j.diabres.2019.107842

17. Reviriego J, Vázquez LA, Goday A, Cabrera M, García-Margallo MT, Calvo E. Prevalence of impaired fasting glucose and type 1 and 2 diabetes mellitus in a large nationwide working population in Spain. *Endocrinol y Nutricion* (2016) 63 (4):157–63. doi: 10.1016/j.endonu.2015.12.006

18. Gutiérrez-Fisac JL, Guallar-Castillón P, León-Muñoz LM, Graciani A, Banegas JR, Rodríguez-Artalejo F. Prevalence of general and abdominal obesity in the adult population of Spain, 2008-2010: The ENRICA study. *Obes Rev* (2012) 13(4):388–92. doi: 10.1111/j.1467-789X.2011.00964.x

19. Faradji-Hazán RN, Valenzuela-Lara M, Díaz-Barriga Menchaca AP, Almeda-Valdes P, Antonio-Villa NE, Vidrio-Velázquez M, et al. Type 1 diabetes care in Mexico: An analysis of the RENACED-DT1 national registry. *Rev investigacion clinica organo del Hosp Enfermedades la Nutricion* (2021) 73 (4):222–30. doi: 10.24875/RIC.20000498

20. Redondo MJ, Foster NC, Libman IM, Mehta SN, Hathway JM, Bethin KE, et al. Prevalence of cardiovascular risk factors in youth with type 1 diabetes and elevated body mass index. *Acta Diabetol* (2016) 53(2):271–7. doi: 10.1007/s00592-015-0785-1

21. Edqvist J, Rawshani A, Adiels M, Björck L, Lind M, Svensson AM, et al. BMI, mortality, and cardiovascular outcomes in type 1 diabetes: Findings against an obesity paradox. *Diabetes Care* (2019) 42(7):1297–304. doi: 10.2337/dc18-1446

22. Pambianco G, Costacou T, Orchard TJ. *The prediction of major outcomes of type 1 diabetes: a 12-year prospective evaluation of three separate definitions of the metabolic syndrome and their components and estimated glucose disposal rate the Pittsburgh epidemiology of diabetes complications study experience* (2007). Available at: http://diabetesjournals.org/care/article-pdf/30/5/1248/596117/zdc00507001248.pdf.

23. Minges KE, Whittemore R, Weinzimer SA, Irwin ML, Redeker NS, Grey M. Correlates of overweight and obesity in 5529 adolescents with type 1 diabetes: The T1D exchange clinic registry. *Diabetes Res Clin Pract* (2017) 126:68–78. doi: 10.1016/j.diabres.2017.01.012

24. Maffeis C, Birkebaek NH, Konstantinova M, Schwandt A, Vazeou A, Casteels K, et al. Prevalence of underweight, overweight, and obesity in children and adolescents with type 1 diabetes: Data from the international SWEET registry. *Pediatr Diabetes* (2018) 19(7):1211–20. doi: 10.1111/pedi.12730

25. Price SA, Gorelik A, Fourlanos S, Colman PG, Wentworth JM. Obesity is associated with retinopathy and macrovascular disease in type 1 diabetes. *Obes Res Clin Pract* (2014) 8(2):e178–82. doi: 10.1016/j.orcp.2013.03.007

26. *Weight gain associated with intensive therapy in the diabetes contraband complications trial* . Available at: http://diabetesjournals.org/care/article-pdf/11/7/567/438558/11-7-567.pdf.

27. Caleyachetty R, Barber TM, Mohammed NI, Cappuccio FP, Hardy R, Mathur R, et al. Ethnicity-specific BMI cutoffs for obesity based on type 2 diabetes risk in England: A population-based cohort study. *Lancet Diabetes Endocrinol* (2021) 9(7):419–26. doi: 10.1016/S2213-8587(21)00088-7

28. Mata-Cases M, Franch-Nadal J, Real J, Mauricio D. Glycaemic control and antidiabetic treatment trends in primary care centres in patients with type 2 diabetes mellitus during 2007–2013 in Catalonia: a population-based study. *BMJ Open* (2016) 6(10):e012463. doi: 10.1136/bmjopen-2016-012463

29. Vinagre I, Mata-Cases M, Hermosilla E, Morros R, Fina F, Rosell M, et al. Control of glycemia and cardiovascular risk factors in patients with type 2 diabetes in primary care in Catalonia (Spain). *Diabetes Care* (2012) 35(4):774–9. doi: 10.2337/dc11-1679

frontiers | Frontiers in Endocrinology

TYPE Original Research
PUBLISHED 05 December 2022
DOI 10.3389/fendo.2022.1064532



OPEN ACCESS

EDITED BY
Alexandre Gabarra Oliveira,
São Paulo State University, Brazil

REVIEWED BY
Sudhanshu Kumar Bharti,
Patna University, India
Gopal L. Khatik,
National Institute of Pharmaceutical Education and Research, India

*CORRESPONDENCE
Anurag Varshney
anurag@patanjali.res.in

SPECIALTY SECTION
This article was submitted to Obesity, a section of the journal Frontiers in Endocrinology

RECEIVED 08 October 2022
ACCEPTED 18 November 2022
PUBLISHED 05 December 2022

CITATION
Balkrishna A, Gohel V, Pathak N, Tomer M, Rawat M, Dev R and Varshney A (2022) Anti-hyperglycemic contours of Madhugrit are robustly translated in the *Caenorhabditis elegans* model of lipid accumulation by regulating oxidative stress and inflammatory response. *Front. Endocrinol.* 13:1064532. doi: 10.3389/fendo.2022.1064532



# Anti-hyperglycemic contours of Madhugrit are robustly translated in the *Caenorhabditis elegans* model of lipid accumulation by regulating oxidative stress and inflammatory response

Acharya Balkrishna[1,2,3], Vivek Gohel[1], Nishit Pathak[1], Meenu Tomer[1], Malini Rawat[1], Rishabh Dev[1] and Anurag Varshney[1,2,4]*

[1]Drug Discovery and Development Division, Patanjali Research Institute, Governed by Patanjali Research Foundation Trust, Haridwar, Uttarakhand, India, [2]Department of Allied and Applied Sciences, University of Patanjali, Haridwar, Uttarakhand, India, [3]Patanjali Yog Peeth (UK) Trust, Glasgow, United Kingdom, [4]Special Centre for Systems Medicine, Jawaharlal Nehru University, New Delhi, India

**Background:** The prevalence of diabetes has considerably increased in recent years. In the long run, use of dual therapy of anti-diabetic agents becomes mandatory to attain euglycemia. Also, the incidences of diabetes-related co-morbidities have warranted the search for new therapeutic approaches for the management of the disease. Traditional herbo-mineral, anti-diabetic agents like Madhugrit are often prescribed to mitigate diabetes and related complications. The present study aimed to thoroughly characterize the pharmacological applications of Madhugrit.

**Methods:** Phytometabolite characterization of Madhugrit was performed by ultra-high performance liquid chromatography. Evaluation of cell viability, α-amylase inhibition, glucose uptake, inflammation, and wound healing was performed by *in vitro* model systems using AR42J, L6, THP1, HaCaT cells, and reporter cell lines namely NF-κB, TNF-α, and IL-1β. The formation of advanced glycation end products was determined by cell-free assay. In addition, the therapeutic potential of Madhugrit was also analyzed in the *in vivo Caenorhabditis elegans* model system. Parameters like brood size, % curling, glucose and triglyceride accumulation, lipid deposition, ROS generation, and lipid peroxidation were determined under hyperglycemic conditions induced by the addition of supraphysiological glucose levels.

**Results:** Madhugrit treatment significantly reduced the α-amylase release, enhanced glucose uptake, decreased AGEs formation, reduced differentiation of monocyte to macrophage, lowered the pro-inflammatory cytokine release,

and enhanced wound healing in the *in vitro* hyperglycemic (glucose; 25 mM) conditions. In *C. elegans* stimulated with 100 mM glucose, Madhugrit (30 µg/ml) treatment normalized brood size, reduced curling behavior, decreased accumulation of glucose, triglycerides, and lowered oxidative stress.

**Conclusions:** Madhugrit showed multimodal approaches in combating hyperglycemia and related complications due to the presence of anti-diabetic, anti-inflammatory, anti-oxidant, wound healing, and lipid-lowering phytoconstituents in its arsenal. The study warrants the translational use of Madhugrit as an effective medicine for diabetes and associated co-morbidities.

KEYWORDS

**Madhugrit, ayurveda, diabetes, inflammation, wound healing, lipid accumulation, oxidative stress**

## Introduction

Diabetes is a fast-growing chronic metabolic disorder of global concern. Currently, about 463 million people have diabetes which has been estimated to increase to 700 million by the year 2045 (1, 2). The sub-optimal glycemic control in diabetes has been linked to persistent systemic inflammation, immune cell dysfunction, and poor wound healing (3). An effective therapeutic approach to manage diabetes must include control of postprandial hyperglycemia, utilization of excess glucose, minimization of protein glycation, oxidative stress, and inflammation (4–6). The current therapeutic agents can only address one part of the pathologic manifestations, leaving a considerable portion of diabetic complications unchecked. Since multiple problems are associated with the pathophysiology and treatment of diabetes, the use of monotherapy is not sufficient (6, 7). The long-term use of pharmacological agents for the treatment of diabetes can also incur adverse effects and treatment resistance, mandating dose titration and inclusion of additional drugs (7–9).

The α-amylase, a calcium metalloenzyme, causes postprandial hyperglycemia by increasing the digestion of ingested carbohydrates (10, 11). A sustained increase in glucose levels leads to the development of oxidative stress which is reported to be responsible for inflammation, impaired glucose utilization in peripheral tissues, and delayed wound healing (4, 7, 12, 13). During diabetes, an alteration occurs in the gut microbiota which leads to the release of microbial products like lipopolysaccharide (LPS). These events are believed to cause low-grade inflammation, mediated by the induction of inflammatory cytokines by gut immune cells (14). Hence, an effective therapeutic agent for diabetes must be able to subside hyperglycemia, oxidative stress, and inflammation to control diabetes and related symptoms.

The phytopharmaceutical product Madhugrit is routinely prescribed to diabetic individuals for the maintenance of euglycemia. Madhugrit is composed of Chandraprabha Vati (classical Ayurvedic medicine) (15), supplemented with Giloy (*Tinospora cordifolia*), Indrayana (*Citrullus colocynthis*), Karela (*Momordica charantia*), Chirayata (*Swertia chirata*), Shatavar (*Asparagus racemosus*), Ashwagandha (*Withania somnifera*) and Shuddh Shilajit (*Asphaltum punjabianum*) (Supplementary Tables 1, 2). Due to the presence of these anti-diabetic (16–18), anti-oxidant (19–21), and anti-inflammatory (22) components, Madhugrit might be able to maintain glucose levels efficiently and manage other diabetes related complications.

At present, the pre-clinical evaluation of anti-diabetic agents is carried out by chemical, surgical, and genetic manipulations on rodents (23). A disadvantage of such models is that they are time-consuming, expensive, and require comprehensive regulatory approvals (24). The nematode *Caenorhabditis elegans* is being increasingly used as an acceptable *in vivo* model of human diseases. This model of the multiorgan eukaryotic organism has several benefits like small size (~1 mm length of an adult), substantial progeny (~300 by parthenogenesis), and a short lifespan (~21 days). Furthermore, research using *C. elegans* does not need extensive regulatory approvals. *C. elegans* has been substantially used in studies of glucose-induced toxicity (24,

**Abbreviations:** UHPLC, Ultra-High Performance Liquid Chromatography; NF-κB, Nuclear factor kappa-light-chain-enhancer of activated B cells; TNF-α, Tumour Necrosis Factor alpha; IL-1β, Interleukin 1 beta; IL-6, Interleukin 6; ROS, Reactive oxygen species; AGEs, Advanced glycation end products; LPS, Lipopolysaccharide; NGM, Nematode growth medium; MDA, Malondialdehyde; TBA, Thiobarbituric acid; TCA, Trichloroacetic acid; Met, Metformin.

25). Consequently, *C. elegans* model could also be used to screen anti-diabetic test articles (26).

The present study investigated the effect of Madhugrit on alleviating diabetic complications induced by hyperglycemic conditions. Extensive phytochemical profiling of Madhugrit was carried out by HPLC analysis and subsequently, its pharmacological activity was explored. The therapeutic potential of Madhugrit was evaluated by *in vitro* analysis of parameters such as cell viability, modulations in α-amylase release, glucose uptake, inflammation, wound healing, and formation of advanced glycation end products (AGEs). These *in vitro* experiments were followed by *in vivo* analysis in *C. elegans* by measuring brood size, % curling, glucose levels, triglyceride accumulation, lipid deposition, ROS generation and lipid peroxidation. The biguanide anti-hyperglycemic drug, Metformin, was used as the method control (27–30), in parallel.

# Materials and methods

## Reagents

Madhugrit (batch #1MDT-210081) was sourced from Divya Pharmacy, India. The standards for HPLC analysis namely gallic acid, magnoflorine, piperine, rutin, ellagic acid, coumarin, cinnamic acid, and palmatine were obtained from Sigma-Aldrich, USA; protocatechuic acid, corilagin from Natural remedies, India, and methyl gallate from TCI chemicals, India. Reagents namely RPMI 1640 (no glucose), DMEM (low glucose), DPBS, antibiotic-antimycotic solution, starch, Malondialdehyde (MDA), Trichloroacetic acid (TCA), LPS, and 2′,7′-Dichlorofluorescin diacetate ($H_2$DCFDA) were procured from Sigma-Aldrich, USA. Heat-inactivated FBS, TPVG, Bovine serum albumin (BSA), Nile red, and Alamar blue were obtained from HiMedia, India. Horse serum was bought from Gibco, USA. Chemicals, 2-thiobarbituric acid (TBA), D-glucose, Metformin, and dexamethasone were obtained from TCI chemicals, India. Phorbol 12-myristate 13-acetate (PMA) was purchased from Alfa Aesar, UK. Mitomycin C was obtained from Roche, Germany. Pierce BCA protein assay kit and sodium azide were obtained from Thermo Fisher Scientific, USA. Human TNF-α and IL-6 ELISA kits were obtained from BD Biosciences, USA. QUANTI-Blue reagent was purchased from InvivoGen, USA.

## Phytochemical analysis of Madhugrit on UHPLC platform

Madhugrit powder(500 mg) was diluted with 10 ml water: methanol (50:50), sonicated for 30 min, centrifuged at 10,000×g for 5 min, and filtered by a 0.45 µm nylon filter. This solution was further used for the metabolite analysis. Prominence-XR UHPLC system (Shimadzu, Japan) equipped with a Quaternary pump (Nexera XR LC-20AD XR), DAD detector (SPD-M20 A), auto-sampler (Nexera XR SIL-20 AC XR), degassing unit (DGU-20A 5R) and column oven (CTO-10 AS VP) were used for analysis. Separation was achieved using a Shodex C18-4E (5µm, 4.6 X 250 mm) column subjected to binary gradient elution. The two solvents used for the analysis were: (A) water containing 0.1% orthophosphoric acid (pH 2.5) and (B) 0.1% orthophosphoric acid in a mixture of acetonitrile and water (88:12). Gradient programming of the solvent system: 5% B for 0-5 min, 5-10% B from 5-20 min, 10% B from 20-30 min, 10-20% B from 30-40 min, 20-35% B from 40-50 min, 35-60% B from 50-65 min, 60-85% B from 65-70 min, 85-5% B from 70-71 min and 5% B from 71-75 min with a flow rate of 1 ml/min. A 10 µl of standard and test solution was injected and the column temperature was maintained at 30°C. Wavelength of 270 nm was used for gallic acid, methyl gallate, protocatechuic acid, magnoflorine, corilagin, coumarin, cinnamic acid, piperine, and palmatine; 250 nm for ellagic acid and 350 nm for rutin. The obtained chromatograms of standards and sample were overlayed and the phytometabolites were quantified respectively at different retention times (RT).

## Cell culture maintenance

The rat pancreatic cell line AR42J; rat myoblast cells L6; human monocytic cells THP-1 were procured from the ATCC licensed repository, National Centre for Cell Science, India. The human keratinocyte cells HaCaT were purchased from Krishgen Biosystems, India. The reporter cell lines namely HEK-Blue TNF-α, HEK-Blue IL-1β, and THP1-Blue NF-κB were obtained from *In vivo*Gen, USA. AR42J, L6, and HaCaT were propagated in normal glucose (NG, 5.5 mM) DMEM supplemented with 10% FBS and 1% antibiotic-antimycotic solution. THP-1 cells were cultured in normal NG (5.5 mM) RPMI 1640 supplemented with 10% FBS and 1% antibiotic-antimycotic solution. The reporter cell lines were cultured as per the manufacturer's instructions. The cultured cells were maintained at 37°C and 5% $CO_2$ in a humidified incubator and used within 5 passages after revival.

## Cell viability

The effect of Madhugrit on the viability of AR42J, L6, THP-1 monocytes, THP1 macrophages, and HaCaT, were evaluated by Alamar blue dye (15 µg/ml). Madhugrit (10, 30, 100 µg/ml) was added during differentiation of AR42J into amylase-secreting exocrine cells by 100 nM dexamethasone and incubated for 72 hr (31–33). The L6 cells were differentiated with 2% Horse serum containing media for 72 hr post which the cells were incubated

with Madhugrit (10-100 µg/ml) for 24 hr. THP1 monocytes and macrophages were incubated with Madhugrit (10-100 µg/ml) for 48 hr. HaCaT cells were also treated for 48 hr with Madhugrit (10-100 µg/ml). Following incubation with Alamar blue dye, the plates were read at Ex. 560/Em.590 nm by Envision multimode plate reader (PerkinElmer, USA). All treatments were performed with NG (5.5 mM) culture media. Data were presented as mean ± SEM (n=3).

## Assessment of α-amylase inhibition in AR42J cells

AR42J cells were plated at a density of $1\times10^6$ cells per well in a 6-well plate. Post 72 hr treatment, as described earlier, cells were washed with DPBS and induced with 1% (w/v) starch for 1 hr after which the supernatant was collected and α-amylase (U/L) levels were analyzed by Architect ci8200 biochemical analyzer (Abbott Diagnostics, USA), at an external laboratory. Undifferentiated cells (UDC) were used as normal control. Data were presented as mean ± SEM (n=3).

## Assessment of glucose uptake in L6 cells

L6 cells were seeded at a density of $2\times10^5$ cells per well in 12-well plate. After differentiation, cells were treated with Madhugrit (10, 30, and 100 µg/ml) or Metformin (2 mM) in serum-free NG (5.5 mM) culture media. After 24 hr the cells were washed with DPBS and stimulated with 100 µM 2-NBDG dye for 1 hr in DPBS, thereafter cells were washed twice with DPBS and lysed by 2 phased freeze-thaw process. The cell lysate was collected, centrifuged at 12,000×g for 10 min and 100 µl of the supernatant was pipetted in 96-well black plate and read at Ex.475/Em.529 nm by Envision multimode plate reader (PerkinElmer, USA). Data were presented as mean ± SEM (n=3).

## Advanced glycation end products (AGEs) assessment

The evaluation of the anti-glycation activity of Madhugrit was done as per Starowicz et al. (34) with slight modifications. Briefly, glucose (90 mg/ml) and BSA (10 mg/ml) were separately dissolved in DPBS. Then, Madhugrit (0-100 µg/ml) or Metformin (2 mM) were mixed with a BSA-glucose solution. The use of 0.01% sodium azide was done to prevent microbe development. After 1 week of incubation at 37°C, the fluorescence of AGEs was measured at Ex.350/Em.420 nm and the inhibition of AGEs formation was evaluated. Data were presented as mean ± SEM (n=3).

## Assessment of THP-1 monocyte (suspension cells) to macrophage (adherent cells) differentiation

THP-1 monocytes ($5\times10^5$ cells) were pre-treated with Madhugrit (10, 30, and 100 µg/ml) or Metformin (2 mM) in T-25 flasks for 24 hr. Afterward, the cells were centrifuged, washed with DPBS, and plated at a density of $3\times10^4$ cells/well in a 96-well plate. The cells were again treated with Madhugrit or Metformin in presence of 20 ng/ml PMA for 24 hr. All treatments were performed with NG (5.5 mM) culture media. Post incubation the cells were washed and Alamar blue assay was performed. Data were presented as mean ± SEM (n=3).

## Assessment of LPS-induced TNF-α and IL-6 cytokine release in THP-1 macrophages

THP-1 monocytes were plated at a density of $1\times10^5$ cells per well. The cells were differentiated to macrophages and pre-treated with Madhugrit (10, 30, and 100 µg/ml) or Metformin (2 mM) for 24 hr. Following incubation, the cells were washed and stimulated with 100 ng/ml LPS in presence of Madhugrit (10, 30, and 100 µg/ml) or Metformin (2 mM) for 24 hr. Untreated control (UC) group was taken as normal control. All treatments were performed with NG (5.5 mM) culture media. The cell supernatant was then collected and assessed for TNF-α and IL-6 release by sandwich ELISA as per the manufacturer's instructions. Data were presented as mean ± SEM (n=4).

## Assessment of LPS-induced NF-κB, TNF-α, and IL-1β activity under high glucose conditions

THP-1 macrophages were pre-treated with Madhugrit (10, 30, and 100 µg/ml) or Metformin (2 mM) for 24 hr. Later on, the cells were stimulated for 24 hr by LPS (500 ng/ml) and divided into 5 groups: (1) UC NG (5.5 mM), (2) LPS NG (5.5 mM), (3) UC HG (25 mM), (4) LPS HG (25 mM) and (5) LPS HG (25 mM) with Madhugrit (10, 30, 100 µg/ml) or Metformin (2 mM). After 24 hr the cell supernatant was collected and incubated with the NF-κB, TNF-α, and IL-1β reporter cells. Subsequently, based on the secreted embryonic alkaline phosphatase (SEAP) levels released by the reporter cells the activity of NF-κB, TNF-α and IL-1β was evaluated by QUANTI-Blue reagent as per the manufacturer's instructions. The plates were read at an optical density of 630 nm by Envision multimode plate reader. Data were presented as mean ± SEM (n=3).

## Scratch wound healing assay

HaCaT cells ($2\times10^5$/well) were cultured in 12 well plates and pre-treated with Madhugrit (10, 30, 100 µg/ml) or Metformin (2 mM) for 24 hr. Later on, the cells were washed with DPBS and induced with mitomycin C (5 µg/ml) to inhibit proliferation. The cells were washed and wounded by a 10 µl plastic pipette tip and further rinsed with DPBS to remove cell debris. The cells were treated and divided into 5 groups: (1) UC NG (5.5 mM), (2) UC HG (25 mM), and (3) HG (25 mM) with Madhugrit (10, 30, 100 µg/ml) or Metformin (2 mM). Images were acquired at 0 hr and 24 hr. Analysis of % wound closure and rate of migration (µm/hr) were done by Fiji, ImageJ (NIH, USA) (13, 35). Data were presented as mean ± SEM (n=3).

## Maintenance and treatment of *Caenorhabditis elegans*

The N2 (wild type) *C. elegans* strain was procured from the Caenorhabditis Genetics Center (CGC) and maintained in NGM (nematode growth medium) seeded with *E. coli* OP50 at 20°C. A synchronization technique was used to separate the eggs from the worms by treatment with an alkaline hypochlorite solution (25, 36). The hatched eggs released the L1 larvae, used for exposure to various treatments. The L1 nematodes were exposed to different concentrations of Madhugrit (3, 10, and 30 µg/ml) or Metformin (2 mM) for 24 hr. After incubation, the nematodes were transferred to an NGM plate seeded with *E. coli* OP50 with or without high glucose (HG, 100 mM) supplementation along with Madhugrit (3, 10, and 30 µg/ml) or Metformin (2 mM). Treatment scheme and parameters analyzed on *C. elegans* experimental model are depicted in Figure 1.

## Brood size assessment

The nematodes were treated as described above and were maintained on NGM/*E. coli* OP50 plates until they reached larval stage L4. To evaluate progeny size, one nematode from each treated group was transferred to a new NGM plate seeded with *E. coli* OP50 with or without 100 mM glucose supplementation along with Madhugrit (3, 10, and 30 µg/ml) or Metformin (2 mM). The total number of progenies were counted by ZEISS Stemi 305 stereo microscope (Carl Zeiss, Germany). Data were presented as mean ± SEM (n=5).

## Analysis of aberrant behavior (curling) in C. elegans

After pre-treatment, 30 worms of the L4 stage were transferred to new NGM plates seeded with *E. coli* OP50 with or without 100 mM glucose supplementation along with Madhugrit (3, 10, and 30 µg/ml) or Metformin (2 mM). The worms that displayed a curling behavior (37) were counted by ZEISS Stemi 305 stereo microscope (Carl Zeiss, Germany). Data were presented as mean ± SEM (n=5).

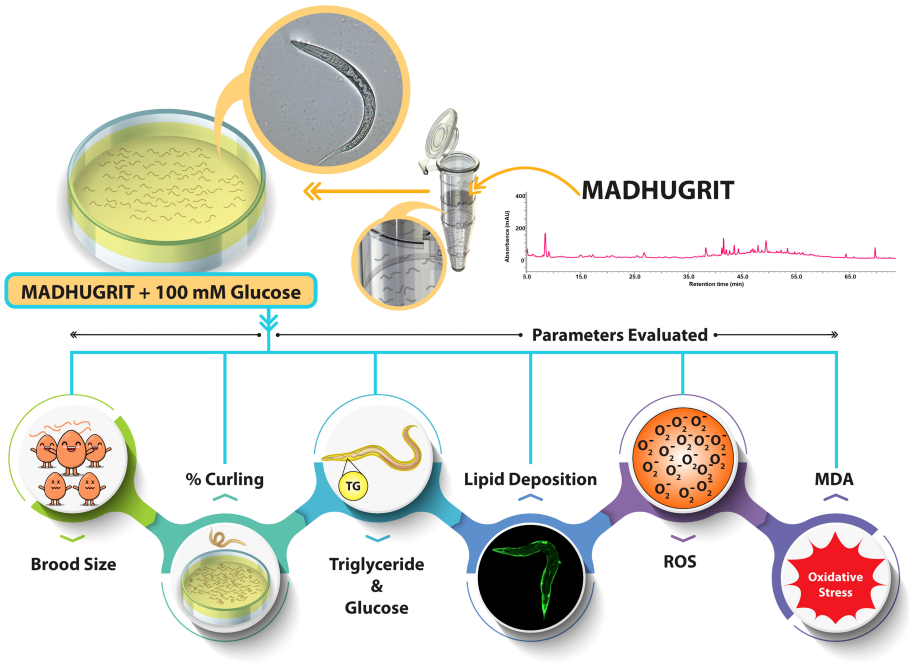


FIGURE 1
Schematic of *C. elegans* treatment and parameters evaluated.

## Assessment of glucose and triglyceride accumulation in *C. elegans*

The pre-treated L4 stage nematodes were transferred to a new NGM plate seeded with *E. coli* OP50 with or without 100 mM glucose supplementation along with Madhugrit (3, 10, and 30 µg/ml) or Metformin (2 mM). On Day 5, worms were washed off from the plates and centrifuged at 600×g for 1 min. Worms were washed rigorously and placed in lysis buffer (Tris 100 mM, NaCl 150 mM, EGTA 1 mM, EDTA 1 mM, Triton X-100 1%, and sodium deoxycholate 0.5%) supplemented with protease inhibitor cocktail (Thermo Fisher Scientific, USA) and passed through three cycles of freeze-thaw and centrifuged at 14000×g for 10 min. The supernatant was collected and analyzed for glucose and triglyceride levels by Erba 200 biochemical analyzer (Erba Mannheim, Germany). Protein concentration was determined using the Pierce BCA protein assay kit. The obtained values were further normalized with protein concentration. Data were presented as mean ± SEM (n=3).

## Microscopy of lipid deposition in *C. elegans* by Nile red stain

After treatment, worms were washed off from the plates and centrifuged at 600×g for 1 min. The worms were washed thrice and fixed with 40% isopropanol for 3 min, centrifuged at 600×g for 1 min, and stained with Nile red as per the protocol of Escorcia et al. (38). The images were acquired using a FITC filter on an Olympus BX43 microscope equipped with a Mantra imaging platform (PerkinElmer, USA) and further processed on Inform 2.2 software suite (PerkinElmer, USA).

## Evaluation of ROS levels in *C. elegans*

ROS levels in *C. elegans* were detected by the $H_2$DCFDA dye as mentioned by Zhou et al. (39) with slight modifications. Briefly, worms were lysed, centrifuged and the supernatant was incubated with $H_2$DCFDA (200 µM) at 37°C for 1 hr. The plates were read at Ex. 495/Em.523 nm by Envision multimode plate reader and the fluorescence values were normalized with protein concentration (40). Data were presented as mean ± SEM (n=3).

## Assessment of lipid peroxidation in *C. elegans*

The MDA content from the lysate of treated nematodes was measured by the TBA-TCA method (41). The optical density was read at 532 nm by Envision multimode plate reader and the amount of MDA present in the samples was determined from the standard curve. The data was further normalized with protein concentration. Data were presented as mean ± SEM (n=3).

## Data analysis

Statistical analysis was performed using one-way ANOVA with Dunnett's multiple comparisons *post-hoc* test. Data were analyzed using GraphPad Prism 7 (GraphPad Software, USA). Results were considered to be statistically significant at a probability level of $p < 0.05$.

# Results

## Phytometabolite analysis of Madhugrit

The quantitative analysis of phytometabolites using standard marker compounds (Figure 2) confirmed the presence of rutin, ellagic acid, gallic acid, protocatechuic acid, methyl gallate, magnoflorine, corilagin, palmatine, coumarin, cinnamic acid and piperine in Madhugrit. The quantitative analysis of phytochemicals using reference standards is mentioned in Table 1.

## Cell viability analysis of Madhugrit

The effect of Madhugrit on the viability of cells was assessed on rat pancreatic exocrine like AR42J cells (Figures 3A, F), rat L6 myotubes (Figures 3B, G), human monocytic THP1 cells (Figures 3C, H), human THP1 macrophages (Figures 3D, I) and human HaCaT epidermal keratinocytes (Figures 3E, J). The cell lines were subjected to various concentrations of Madhugrit (10, 30, and 100 µg/ml) and no significant decrease in cell viability was observed even at 100 µg/ml concentration in all the cell lines. These preliminary results indicated that Madhugrit is non-toxic at all physiologically relevant concentrations and has no effect on the metabolic functionality of cells.

## Madhugrit reduced α-amylase secretion from pancreatic acinar-like cells and increased glucose uptake in skeletal myotubes

The AR42J cells was differentiated into an exocrine acinar-like pancreatic cell line (31) as the undifferentiated cells secrete less α-amylase in response to starch (Figure 4A). The bioactivity of Madhugrit in presence of starch load which mimics the physiological postprandial condition was determined on the

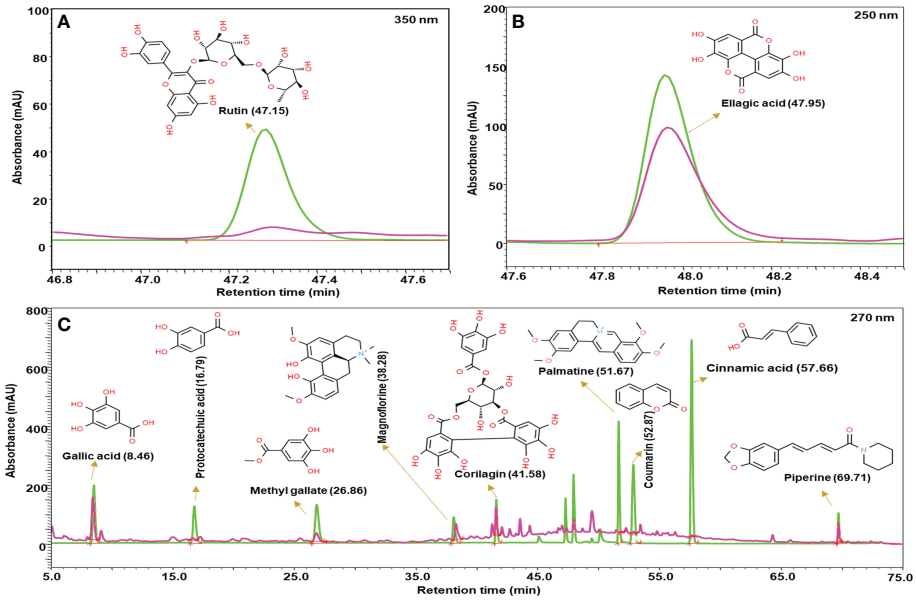


FIGURE 2
Phytometabolite analysis of Madhugrit by HPLC. Overlap chromatogram of standards (green line) and Madhugrit (pink line). Rutin was quantified at 350 nm **(A)**, Ellagic acid at 250 nm **(B)**, and Gallic acid, Protocatechuic acid, Methyl gallate, Magnoflorine, Corilagin, Palmatine, Coumarin, Cinnamic acid, and Piperine at 270 nm wavelength **(C)**.

differentiated cells. It was observed that Madhugrit (10, 30, and 100 µg/ml) treated cells released significantly ($p < 0.01$) less α-amylase compared to control (Figure 4A) in response to 1% (w/v) starch. Next, to confirm the hypoglycemic activity of Madhugrit we evaluated its effect on glucose uptake levels in L6 cells (42). When compared with the control group, Madhugrit treatment with 10, 30, and 100 µg/ml significantly ($p < 0.05$) promoted the uptake of glucose by 1.64, 2.48, and 2.84-fold respectively, in a concentration-dependent manner (Figure 4B). The results were at par with the positive control drug Metformin (2 mM) which also significantly ($p < 0.05$) enhanced the glucose uptake levels by 2.53-fold compared to normal control.

TABLE 1 Quantitative analysis of phytometabolites in Madhugrit.

| Sr. No. | Compound name | Retention time (min) | Amount (in µg/mg) |
|---|---|---|---|
| 1 | Gallic acid | 8.46 | 1.158 |
| 2 | Magnoflorine | 38.28 | 0.950 |
| 3 | Corilagin | 41.58 | 0.770 |
| 4 | Piperine | 69.71 | 0.449 |
| 5 | Methyl gallate | 26.86 | 0.305 |
| 6 | Rutin | 47.15 | 0.278 |
| 7 | Ellagic acid | 47.95 | 0.198 |
| 8 | Protocatechuic acid | 16.79 | 0.081 |
| 9 | Coumarin | 52.87 | 0.026 |
| 10 | Cinnamic acid | 57.66 | 0.021 |
| 11 | Palmatine | 51.67 | 0.014 |

HPLC quantified major metabolites present in as deciphered from the chromatogram shown in Figure 2.

## Madhugrit inhibited the *in vitro* AGEs formation

Advanced glycation end products (AGEs) are formed in high amounts during diabetes which get accumulated and develop oxidative stress (43). It was observed that Madhugrit (3-100 µg/ml) inhibited the *in vitro* formation of AGEs in a concentration-dependent manner (Figure 4C). An inhibition of more than 15% was observed in the Madhugrit (100 µg/ml) treated group. Hence, it was established that Madhugrit possesses a property to inhibit AGEs formation.

## Madhugrit decreased inflammation by inhibition of monocyte to macrophage differentiation and release of TNF-α and IL-6 cytokines

The differentiation of monocytes to macrophages is a critical event that activates various pro-inflammatory signaling networks. The anti-inflammatory properties of Madhugrit were confirmed by the use of the *in vitro* model of THP1

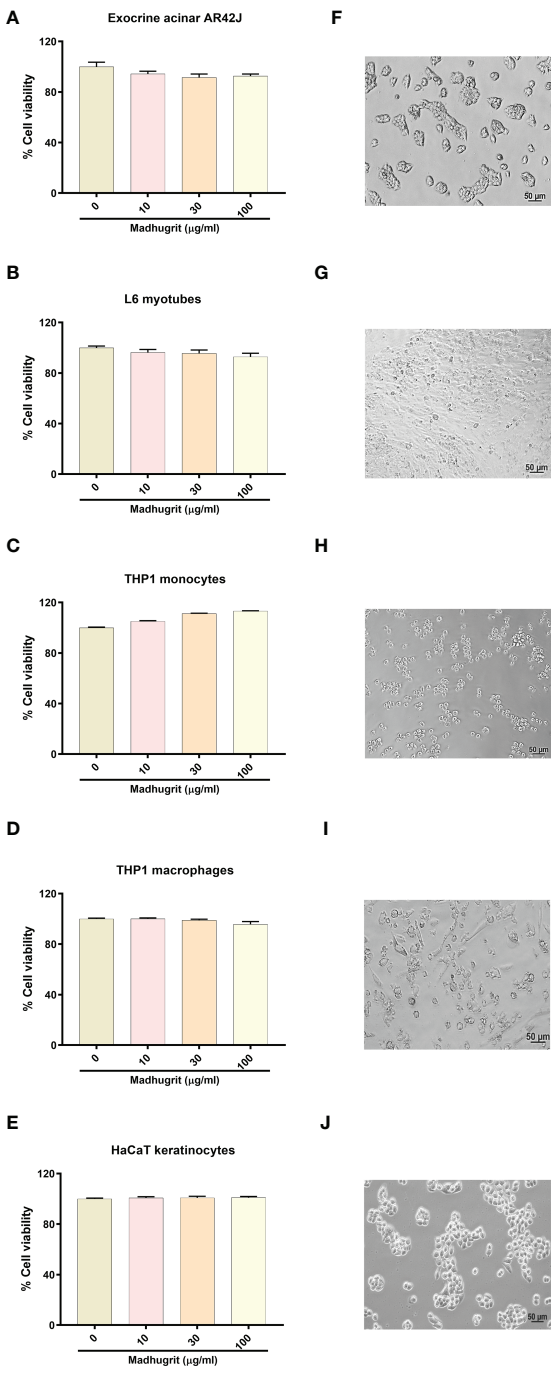


FIGURE 3
Cell viability analysis of Madhugrit. Cell viability of Madhugrit (10, 30, and 100 µg/ml) was performed on Exocrine acinar AR42J cells **(A)**, L6 myotubes **(B)**, THP1 monocytes **(C)**, THP1 macrophages **(D)** and HaCaT keratinocytes **(E)** by Alamar blue assay. Corresponding representative images of the cell lines used for the analysis **(F-J)**.

monocyte to macrophage differentiation by PMA. It was observed that compared to control, Madhugrit at the concentration of 100 µg/ml significantly ($p < 0.01$) decreased the conversion of monocytes to macrophages in presence of PMA (Figure 5A) as depicted by Alamar blue assay. Similarly, a significant ($p < 0.05$) decrease was also observed in Metformin (2 mM) treated cells which was also previously reported by Vasamsetti et al. (28). Furthermore, the levels of LPS induced pro-inflammatory cytokines namely TNF-α and IL-6 were also evaluated post-Madhugrit treatment. An increase in the levels of LPS is observed due to an imbalance of gut microbiota during diabetes. LPS upon binding to toll-like receptor 4, found on immune cells activates a series of pro-inflammatory cascades, generally accompanied by an increase in levels of TNF-α and IL-6 (14, 44, 45). Madhugrit (10, 30, and 100 µg/ml) treated THP1 macrophages inhibited the release of LPS (100 ng/ml) induced TNF-α and IL-6 release, in a concentration-dependent manner (Figures 5B, C). The inhibitory effect of Madhugrit at 100 µg/ml concentration was more pronounced than Metformin (2 mM) in the case of TNF-α (Figure 5B) and IL-6 release (Figure 5C). Taken together, Madhugrit has anti-inflammatory properties, evident by its potential to inhibit macrophage differentiation and release of pro-inflammatory cytokines which is helpful to control the low-grade inflammation during diabetes.

## Madhugrit inhibited the activity of NF-κB, TNF-α, and IL-1β in THP-1 macrophages under hyperglycemic conditions

Macrophages under hyperglycemic state constantly express a pro-inflammatory phenotype which is more prominent in presence of exogenous stimulants (endotoxins) (3). In high glucose (25 mM) conditions, it was observed that THP1 macrophages without any LPS (500 ng/ml) challenge, compared to normal glucose (5.5 mM) conditions, showed an increase in their pro-inflammatory phenotype which became more pronounced upon LPS stimulation (Figures 5D–F). It was observed that Madhugrit (10, 30, and 100 µg/ml) treated macrophages, in a concentration-dependent manner, were able to decrease their pro-inflammatory phenotype when exposed to high glucose and LPS, evident from the significantly decreased activity of NF-κB, TNF-α, and IL-1β (Figures 5D–F). Similar findings were observed in the Metformin (2 mM) treated group as well (Figures 5D–F). Taken together, these results suggest that Madhugrit has potentials to reduce persistent inflammatory phenotype of macrophages exposed to high glucose and bacterial endotoxins, in chronic diabetic conditions.

## Madhugrit normalized wound healing process under high glucose enviornment

One of the common complication of diabetes is delayed and impaired wound healing process (46). A controlled inflammation and re-epithelization of the wound are paramount for effective

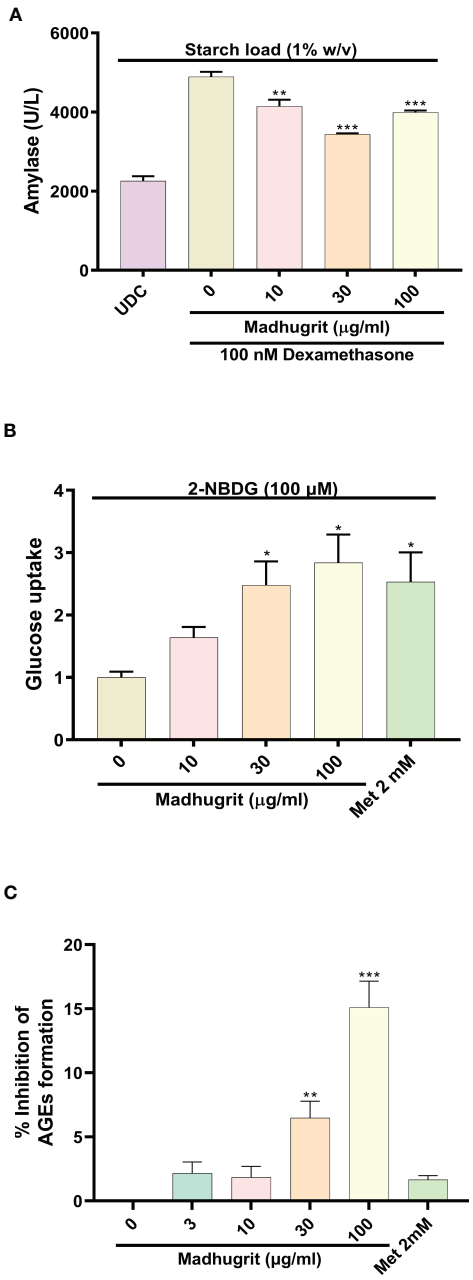


FIGURE 4
Analysis of amylase release, glucose uptake and inhibition of AGEs in presence of Madhugrit. **(A)** The release of amylase in dexamethasone differentiated AR42J cells was performed after induction with starch (1% w/v) in presence of Madhugrit. Undifferentiated cells (UDC) were taken as a normal control. **(B)** The uptake of glucose post Madhugrit treatment was evaluated in L6 myotubes by the fluorescent glucose analog 2-NBDG. **(C)** Evaluation of inhibitory potential of Madhugrit against AGEs formation. The statistical significance of the observed differences in the means compared to the Madhugrit (0 µg/ml) group was analyzed through one-way ANOVA followed by Dunnett's multiple comparison test and represented as *, ** or *** depending on whether the calculated p value was <0.05, <0.01 or <0.001.

wound healing. Keratinocyte migration, which is an integral part of re-epithelization is inhibited in high glucose conditions (13). Based on Madhugrit's ability to resolve inflammation, we sought to examine its activity on wound healing under hyperglycemic conditions. As the HaCaT cells were induced with mitomycin C, the cell proliferation process was inhibited to remove any confounding observations related to the rate of migration. The HaCaT cells under high glucose (25 mM) condition displayed a visible defect in the wound healing process. In comparison, the cells treated with Madhugrit (10, 30, and 100 µg/ml) showed a

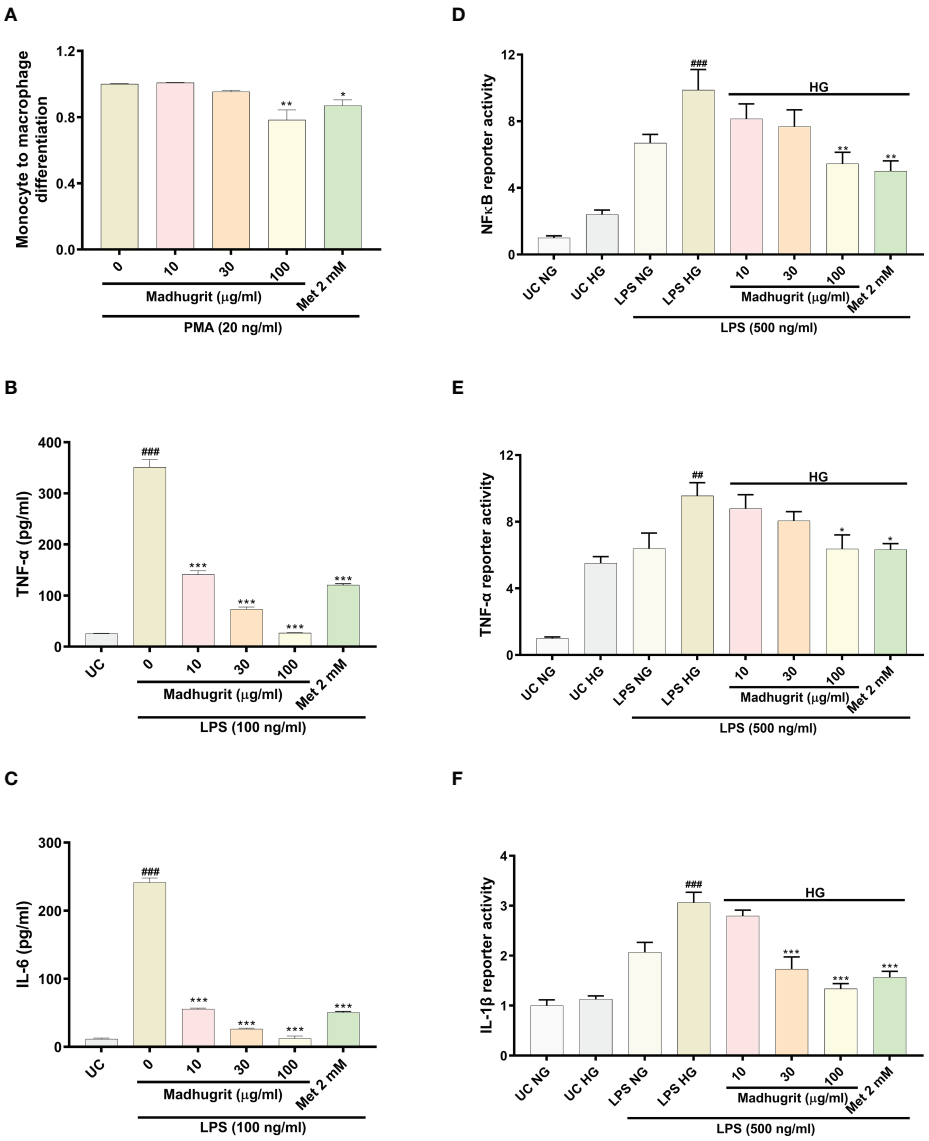


FIGURE 5
Madhugrit reduced monocyte to macrophage differentiation, release and activity of pro-inflammatory cytokines and NF-κB response. **(A)** Madhugrit inhibited the THP1monocyte to macrophage conversion in presence of PMA (20 ng/ml) represented as fold change. **(B, C)** The levels of released TNF-α and IL-6 (pg/ml) in presence of Madhugrit (0-100 µg/ml) or Metformin (2 mM) after LPS (100 ng/ml) induction. **(D-F)** Activity of NF-κB, TNF-α and IL-1β under normal glucose (NG) and high glucose (HG) conditions in presence of Madhugrit (0-100 µg/ml) or Metformin (2 mM) after LPS (500 ng/ml) induction. The statistical significance of the observed differences in the means compared to the **(A)** Madhugrit (0 µg/ml) was analyzed through one-way ANOVA followed by Dunnett's multiple comparison test and represented as * ($p<0.05$) or ** ($p<0.01$). Statistical significance between Untreated control (UC) and Madhugrit (0 µg/ml) group **(B, C)** is represented as ### ($p<0.001$) and between UC HG and LPS HG group **(D-F)** as ## ($p<0.01$) or ### ($p<0.001$). Comparison of the treatments with Madhugrit (0 µg/ml) or LPS HG group was represented as *, ** or *** depending on whether the calculated p value was <0.05, <0.01 or <0.001.

prominent ability for wound healing, but it was not apparent in the Metformin (2 mM) treated group (Figure 6A). Based on the image analysis a significant ($p<0.05$) decrease in the percentage of wound closure and rate of cell migration was observed when HaCaT cells were kept in high glucose conditions (Figures 6B, C). Upon Madhugrit treatment, the cells started to display effective wound healing in a concentration-dependent manner. Notably, at 100 µg/ml concentration of Madhugrit the rate of migration and percentage of wound closure was equivalent to that of HaCaT cells kept in normal glucose (5.5 mM) condition (Figures 6B, C). These results suggest that Madhugrit has a potential to normalize the wound healing process in a high glucose condition.

## Madhugrit decreased the toxic effects on progeny and aberrant behavior of *C. elegans* in high glucose condition

A constant level of high glucose leads to multi-organ dysfunction which underlies the complications of diabetes (47). To confirm the potency of Madhugrit *in vivo*, the non-mammalian model of *C. elegans* was utilized as the effects of glucose toxicity have been previously reported on the nematode (25). The effect of standalone Madhugrit (3-30 µg/ml) treatment on Brood size was evaluated which showed that it had no toxic effect (data not shown). Further experiments were performed using the same concentrations of Madhugrit. The worms exposed to high glucose (100 mM) showed a significant ($p < 0.001$) reduction in their brood size but the worms exposed to 30 µg/ml concentration of Madhugrit were able to significantly ($p < 0.001$) counteract the negative effects of glucose on their egg laying capacity. Similar effects were observed in the case of Metformin (Figure 7A). Under high glucose exposure, *C. elegans* displayed aberrant behavior like curling. Nearly, 80% of the worms were observed to have curling behavior due to glucose-induced stress. Madhugrit (3, 10, and 30 µg/ml) treated worms showed a decrease in the incidences of curling behavior in a concentration-dependent manner (Figure 7B). The positive control drug Metformin (2 mM) also reduced % curling in the high glucose exposed worms. The observed increase in brood size and a decrease in % curling suggests that Madhugrit has a strong potential to negate the effects of glucose toxicity on normal physiology.

## Madhugrit normalized the glucose and lipid levels in *C. elegans* under high glucose exposure

The qualitative assessment of the lipid content post glucose exposure and Madhugrit treatment was evaluated by Nile red staining. The worms exposed to 100 mM glucose clearly showed increased lipid accumulation compared to worms grown without added glucose. Madhugrit (3, 10, and 30 µg/ml) treated worms showed a visible reduction in lipid content in a dose-dependent manner. Worms with Metformin (2 mM) treatment also displayed less lipid deposition (Figure 7C). Furthermore, the worms exposed to high glucose (100 mM) showed a significant ($p < 0.05$) increase in their glucose (0.92 mM/mg protein) and triglyceride (137.8 mg/mg protein) levels compared to worms grown without added glucose (Figures 7D, E). Such biochemical alterations were significantly reduced in the Madhugrit (3, 10, and 30 µg/ml) treated nematodes. Metformin (2 mM) treated worms also efficiently resisted the biochemical changes in response to high glucose exposure. The worms treated with 30 µg/ml of Madhugrit had nearly normalized levels of glucose and triglyceride levels (Figures 7D, E).

## Madhugrit decreased ROS levels and lipid peroxidation in *C. elegans* exposed to high glucose

The evaluation of changes in ROS levels was done by the normalized fluorescence intensity of dichlorofluorescein (DCF) (48). High glucose exposure significantly ($p < 0.001$) increased the DCF fluorescence compared to worms grown without added glucose (Figure 7F). Madhugrit (3, 10, 30 µg/ml) treated nematodes were able to counteract the development of ROS in response to high glucose as observed by the dose-dependent decrease in fluorescence (Figure 7F). An increase in ROS causes the overproduction of MDA, an indicator of oxidative stress (49). The worms exposed to 100 mM glucose displayed a significant ($p < 0.001$) increase in MDA (404.9 nM/mg protein) levels (Figure 7G). Whereas, Madhugrit (3, 10, 30 µg/ml) treated worms were able to offset the generation of oxidative stress in a dose-dependent fashion (Figure 7G). The 30 µg/ml Madhugrit treated worms had MDA (121.4 nM/mg protein) levels equivalent to the worms grown without added glucose (121.3 nM/mg protein). Collectively, these results implied that Madhugrit possesses robust anti-oxidant properties.

# Discussion

Globally, the pandemic of obesity, inappropriate diet, and sedentary lifestyle has led to an increase in the prevalence of diabetes, decade after decade (50). In 2015 the global economic burden of diabetes was estimated to be more than $1.3 trillion (51). The current pharmacotherapy for diabetes involves insulin secretagogues, insulin sensitizers, alpha-glucosidase inhibitors, biguanides, incretin mimetics, sodium-glucose co-transport-2 inhibitors, amylin antagonists, and insulin. Monotherapy of conventional oral hypoglycemic agents often fail to achieve therapeutic goals and so the use of dual drug therapy is on the rise. Such combinatorial therapies lead to increased incidences of adverse effects like diarrhoea, lactic acidosis, and hepatotoxicity which leads to a decline in patient compliance (52, 53). Anti-diabetic agents from ethnopharmacological origins may be an attractive alternative due to their low cost, better safety profile, and other beneficial pleiotropic effects. Additionally, they might alleviate metabolic abnormalities and abrogate the development of comorbidities associated with diabetes (6).

The present study aimed to characterize the phytochemistry and bioactivity of the Ayurvedic anti-diabetic medicine Madhugrit, a herbo-mineral formulation composed of extracts from 29 herbs and a mineral pitch. The phytometabolite characterization of Madhugrit revealed the presence of several bioactive compounds namely gallic acid, magnoflorine, corilagin, piperine, methyl gallate, rutin, ellagic acid, protocatechuic acid, coumarin, cinnamic acid, and palmatine.

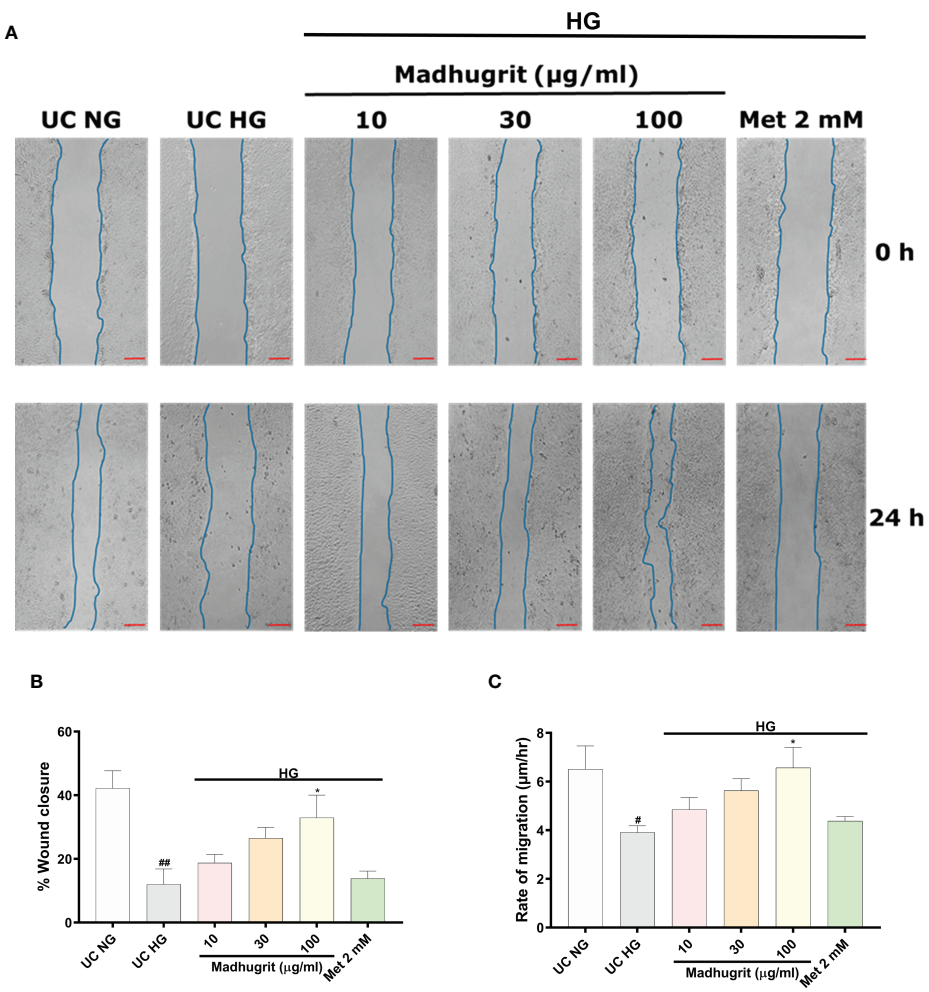


FIGURE 6
Madhugrit enhanced keratinocyte (HaCaT) migration capacity. **(A)** Representative pictures of scratched wound of HaCaT monolayers (0 and 24 hr) placed in normal glucose (NG) or high glucose (HG) conditions in presence of Madhugrit (10, 30, and 100 µg/ml) or Metformin (2 mM). Blue lines represent wounded area. Scale bar (red) = 100 µm. **(B, C)** Graph quantifying the average wound closure and rate of migration of the wounded HaCaT cells in presence of Madhugrit (10, 30, and 100 µg/ml) or Metformin (2 mM). The statistical significance of the observed differences in the means compared to the UC NG group was analyzed through one-way ANOVA followed by Dunnett's multiple comparison test and represented as # ($p<0.05$) or ## ($p<0.01$). Comparison of the treatments with UC HG group was represented as * ($p<0.05$).

These phytochemicals have been reported to possess anti-diabetic, anti-inflammatory, antioxidant, and wound healing properties (6, 7, 54). To assess the collective pharmacological effects of these phytometabolites, we determined the effects of Madhugrit on various *in vitro* models of diabetes and related complications. After establishing the therapeutic properties of Madhugrit we determined its effectiveness on a non-mammalian *in vivo* model of the nematode *C. elegans*. Thus, various *in vitro* and *in vivo* methods were employed to determine the therapeutic potentials of Madhugrit.

Before beginning pharmacological screening of Madhugrit its effect on cell viability was evaluated on rat pancreatic acinar cells (AR42J), rat skeletal myotubes (L6), human monocyte and macrophage (THP-1) cells, and human epidermal keratinocytes (HaCaT). Madhugrit was found to be viable at all physiologically relevant concentrations. The cell viability profile of Madhugrit allowed us to rule out any confounding bias in our obtained results. In order to assess the anti-diabetic properties of Madhugrit, we mainly studied its effect on α-amylase release. Post-prandial hyperglycemia is one of the major symptoms of diabetes. As amylase helps in the breakdown of complex carbohydrates obtained from diet to simple sugars, it promotes the rise of glucose levels in the blood. Therefore, amylase inhibition can help in the effective control of raised glucose levels after meals (10, 32, 33). Madhugrit was found to retard the release of α-amylase from rat pancreatic acinar cells post a starch load. Upon confirmation of the α-amylase inhibitory activity of Madhugrit, we further evaluated its effect on glucose uptake as

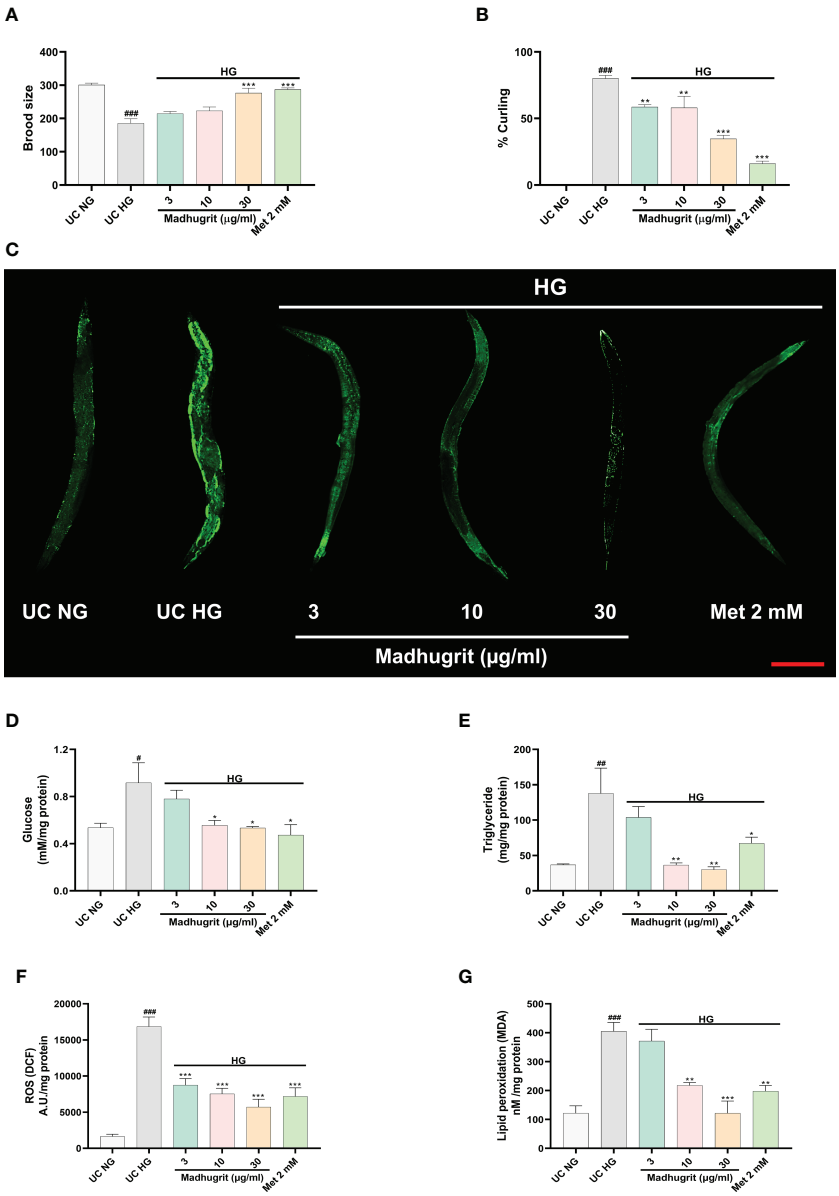


FIGURE 7
Madhugrit staved off the glucose toxicity markers in *C. elegans* exposed to high glucose (HG) conditions. **(A)** Brood size of the nematodes placed under HG was determined in presence or absence of Madhugrit (3, 10, and 30 µg/ml) or Metformin (2 mM). **(B)** Aberrant behavior of the worms in HG was observed in the form of curling and the number of worms in curled state were quantified in presence or absence of Madhugrit (3, 10, and 30 µg/ml) or Metformin (2 mM). **(C)** Lipid deposition (green) in the nematodes exposed to HG was qualitatively determined by Nile red staining in presence of different treatments. Scale bar (red)=200 µm. **(D-G)** Glucose, triglyceride accumulation, ROS generation and MDA levels in the nematodes were evaluated in presence in presence or absence of Madhugrit (3, 10, and 30 µg/ml) or Metformin (2 mM). The statistical significance of the observed differences in the means compared to the UC NG group was analyzed through one-way ANOVA followed by Dunnett's multiple comparison test and represented as # ($p<0.05$), ## ($p<0.01$), or ### ($p<0.001$). Comparison of the treatments with UC HG group was represented *, ** or *** depending on whether the calculated p value was <0.05, <0.01 or <0.001.

both work in synergy to maintain euglycemia. The potential of Madhugrit to enhance glucose uptake was performed on rat skeletal myotubes using Metformin as a positive control. It was found that Madhugrit substantially improved the glucose uptake activity of L6 cells as observed by the uptake of fluorescent glucose analog 2-NBDG. The hypoglycemic properties of Madhugrit can be attributed to the presence of gallic acid as one of its major phytoconstituents (55). Gallic acid *in vitro*is reported to directly inhibit α-amylase activity in an *in vitro* model system (56). A study described that when isolated rat

skeletal muscles were treated with gallic acid-rich Pu-erh tea extract, glucose transport was stimulated by the enhanced insulin signal transduction in the absence of insulin. This raises the possibility that gallic acid, a major content in Madhugrit, might be an insulin-mimetic agent (57).

Inflammation of the intestinal epithelium observed in obese diabetic patients is reportedly associated with changes in gut microflora. It has been reported that LPS derived from gut microbiota is involved in the onset and progression of the chronic low-grade inflammation observed in obesity (58). Furthermore, the activation of various inflammatory signaling networks initiates the monocyte to macrophage differentiation (28). The present data confirmed that Madhugrit might be able to decrease the LPS-mediated inflammation as observed by the reduced release of TNF-α and IL-6 from the LPS-stimulated THP1 macrophages. Moreover, the conversion of THP1 monocytes to macrophages in the presence of PMA is also reduced by Madhugrit. Such properties of Madhugrit might be able to stave off diabetes-related complications like metabolic endotoxemia and atherosclerosis (27, 28, 58). These pleiotropic effects of Madhugrit can be correlated with the presence of corilagin which is known to be effective in the prevention of LPS-induced inflammation by the inhibition of TLR4 involved in the inflammatory cascade (59, 60).

Inflammation related to diabetes seems to be involved in the development of renal, ophthalmological, cardiovascular, and several other co-morbidities (61). Macrophages under hyperglycemic conditions constantly express a pro-inflammatory phenotype even in the absence of any infection or tissue damage (3). A constant high glucose exposure to macrophages enhances NF-κB activity which further augments TNF-α and IL-1β activity (3, 62–64). In our study, we found that high glucose primed THP1 macrophages even after the LPS challenge, displayed a considerably decreased activity of NF-κB, TNF-α, and IL-1β in presence of Madhugrit. This validates that Madhugrit might possess a potent anti-inflammatory property in addition to being an effective anti-diabetic agent. The presence of magnoflorine and methyl gallate in Madhugrit might explain its potent anti-inflammatory effects. Magnoflorine has been reported to ameliorate inflammation in the *in vivo* diabetic nephropathy model in rats (65). Also, methyl gallate is known to modulate the NF-κB signaling pathway which is majorly responsible for pro-inflammatory cytokine release (66). Thus, in combination, both the phytochemicals might be more effective in lessening the burden of inflammation-related diabetic complications.

Delayed wound healing in diabetes is mainly described as persistent inflammation and an imbalance in extracellular matrix regulation. The production of various growth factors is compromised which results in malfunctioning of cell migration and wound re-epithelization (3, 67). Chronic wounds are highly prone to infection, which can eventually lead to septicemia and other morbidities (68). As Madhugrit considerably staved off inflammation we further investigated its effects on keratinocyte migration, a key process of wound-healing which is also hampered in hyperglycemic conditions (13, 46). When a scratch was applied on the monolayer of high glucose exposed human epidermal keratinocytes (HaCaT cells), a visible reduction of wound closure was observed which was in response to the impaired keratinocyte migration. Madhugrit was able to enhance the migration of keratinocytes exposed to high glucose and accelerate wound closure. This effect of Madhugrit might be due to the presence of a plethora of phytochemicals namely ellagic acid, coumarin, cinnamic acid, and palmatine which are known to enhance wound healing (69–72). Also, it has been reported that cinnamic acid-based formulations in addition to wound healing, have antimicrobial properties as well (73). This further augments the therapeutic potential of Madhugrit.

A prolonged hyperglycemic state leads to the formation of glycated proteins and AGEs which are responsible for various co-morbidities due to the loss of function in proteins in response to crosslink formation. Moreover, AGEs also cause tissue injury by enhancing oxidative stress and inflammation (74). Madhugrit inhibited the formation of AGEs which further bolsters its effectiveness as an anti-diabetic agent. Rutin, a major phytochemical in Madhugrit is known to ameliorate AGEs formation as observed in an *in vitro* model system of protein glycation (75).

After we established the pharmacological effects of Madhugrit using various *in vitro* models we sought to further evaluate its effectiveness in a whole-body organism. Further evaluations were then performed *in vivo* on *C. elegans*. In contrast to *in vivo* rodent models, the short lifespan of the nematode makes it an ideal model to study the detrimental effects of high glucose exposure (76). The insulin signaling pathway is conserved across diverse metazoan. In *C. elegans* the pathway regulates fat storage and reproduction. Disturbances in this pathway are a major contributor to the pathogenesis of obesity and diabetes, and the use of the nematode can be done to study the effects of anti-diabetic agents that may modulate this pathway. Moreover, various natural phytochemicals like quercetin have been reported to prevent high-glucose-induced toxicity in *C. elegans* (77). One of the preliminary physiological defects observed in high glucose exposed *C. elegans* was a decrease in the brood size and aberrant behavior like curling. But these effects were observed in a low frequency in Madhugrit treated groups. Similar attenuation of high glucose-induced reduction in brood size is reported after treatment of worms with leaves of *Aquilaria crassna* (agarwood) (78). Secondly, we observed that high levels of glucose accumulation in the nematode promoted lipogenesis and enhanced triglyceride formation which was visually inspected by Nile red staining. This was not observed in the case of Madhugrit treatment as the worms displayed a normalized

lipid deposition. Akin to our findings one study reported that *Apios americana* Medik flower extract treated *C. elegans* showed a drastic reduction in glucose and lipid levels under hyperglycemic conditions (79). A study on the flavonoid-rich extracts of *Citrus aurantium* L. var. *amara* Engl. also showed that the extract-fed *C. elegans* lowered lipid accumulation in the nematodes by affecting the fatty acid synthesis pathway (80). Here, the lipid and glucose-lowering bioactivity of Madhugrit can be correlated with the presence of piperine as one of its constituents (81). It has been documented that high-glucose conditions result in a substantial accumulation of modified mitochondrial proteins and a steady increase in ROS formation in *C. elegans* (82). Hence, we also evaluated the potency of Madhugrit against the formation of ROS and lipid peroxidation products like MDA in high glucose-exposed *C. elegans*. The observed decrease in the ROS and MDA levels can be attributed to the presence of protocatechuic acid as phenolic compounds have been reported to reduce the ROS generation in *C. elegans* (83, 84).

In summary, Madhugrit was found to have robust anti-diabetic, anti-inflammatory, and antioxidant properties which were assessed in various *in vitro* models and on a nematode model. Most of the pharmacological effects of Madhugrit were at par with that of Metformin, the classical anti-diabetic agent (29, 30) but Madhugrit displayed a superior wound healing and anti-oxidant ability than Metformin. Also, due to adverse effects of Metformin, like gastrointestinal disturbances, pancreatitis, hepatitis, vitamin B12 and coagulation abnormalities, and reactive hypoglycemia make its long-term use rather limited (85). Collectively, Madhugrit was able to display a myriad of pharmacological actions against diabetes and related complications. This study also advocates detailed clinical investigations of Madhugrit on human subjects of hyperglycemia and associated co-morbidities.

## Conclusion

This study explored the anti-diabetic, anti-inflammatory, anti-oxidant, wound healing, and lipid-lowering capacity of the ayurvedic prescription medicine Madhugrit. The α-amylase inhibitory and glucose uptake-enhancing properties of the phytomedicine support its purported use as a glucose-lowering agent. The ability of Madhugrit to abrogate pro-inflammatory cytokine production *via* modulation of the NF-κB pathway and hindering the monocyte to macrophage conversion hints towards its use as an effective anti-inflammatory agent as well. The enhanced rate of migration of epidermal keratinocytes under hyperglycemic conditions in presence of Madhugrit evidences its use in the mitigation of diabetic wounds and ulcers. The *in vivo* observations of reduced triglyceride and glucose accumulation, and a decrease of ROS and MDA levels in high glucose-induced *C. elegans* state that Madhugrit might also be able to mitigate the co-morbidities associated with diabetes. Furthermore, given the normalization of brood size and lack of aberrant behavior in the Madhugrit-fed nematodes, it can be acknowledged that the phytomedicine might help retain normal physiological functions under hyperglycemic conditions. Therefore, Madhugrit could be utilized as an effective medicinal product to manage diabetes and associated co-morbidities.

## Data availability statement

The raw data supporting the conclusions of this article will be made available by the authors, without undue reservation.

## Author contributions

AB: Conceptualization, planning, visualization, supervision, writing - review & editing. VG: Conceptualization, planning, visualization, methodology, investigation, data curation, formal analysis, writing original draft. NP: Methodology, investigation, formal analysis. MT: Methodology, investigation, formal analysis. MR: Methodology, investigation, formal analysis. RD: Data curation, writing - review & editing, visualization, project administration, supervision. AV: Writing - review & editing, project administration, conceptualization, visualization, supervision. All authors contributed to the article and approved the submitted version.

## Funding

This research work was funded internally by Patanjali Research Foundation Trust, Haridwar, India.

## Acknowledgments

We extend our gratitute to Dr. Tapan Dey, Ms Moumita Manik, Ms. Deepika Rajput, Mr. Sudeep Verma and Dr. Jyotish Srivastava for their support in the analysis. We are also grateful to Mr. Tarun Rajput, Mr. Gagan Kumar, and Mr. Lalit Mohan for their swift administrative support.

## Conflict of interest

The test article was provided by Divya Pharmacy, Haridwar, Uttarakhand, India. AB is an honorary trustee in Divya Yog Mandir Trust, which governs Divya Pharmacy, Haridwar. In addition, he holds an honorary managerial position in Patanjali Ayurved Ltd., Haridwar, India. Other than providing the test

formulation (Madhugrit), Divya Pharmacy was not involved in any aspect of the research reported in this study.

The remaining authors declare that the research was conducted in the absence of any commercial or financial relationships that could be construed as a potential conflict of interest.

## Publisher's note

All claims expressed in this article are solely those of the authors and do not necessarily represent those of their affiliated organizations, or those of the publisher, the editors and the reviewers. Any product that may be evaluated in this article, or claim that may be made by its manufacturer, is not guaranteed or endorsed by the publisher.

## Supplementary material

The Supplementary Material for this article can be found online at: https://www.frontiersin.org/articles/10.3389/fendo.2022.1064532/full#supplementary-material

## References


1. Pradeepa R, Mohan V. Epidemiology of type 2 diabetes in India. *Indian J Ophthalmol* (2021) 69(11):2932–8. doi: 10.4103/ijo.IJO_1627_21

2. Alam S, Hasan MK, Neaz S, Hussain N, Hossain MF, Rahman T. Diabetes mellitus: Insights from epidemiology, biochemistry, risk factors, diagnosis, complications and comprehensive management. *Diabetology* (2021) 2(2):36–50. doi: 10.3390/diabetology2020004

3. Grosick R, Alvarado-Vazquez PA, Messersmith AR, Romero-Sandoval EA. High glucose induces a priming effect in macrophages and exacerbates the production of pro-inflammatory cytokines after a challenge. *J Pain Res* (2018) 11:1769–78. doi: 10.2147/JPR.S164493

4. Dhanya R, Arun KB, Nisha VM, Syama HP, Nisha P, Santhosh Kumar TR, et al. Preconditioning L6 muscle cells with naringin ameliorates oxidative stress and increases glucose uptake. *PloS One* (2015) 10(7):e0132429-e. doi: 10.1371/journal.pone.0132429

5. Pontarolo R, Conegero Sanches AC, Wiens A, Perlin CM, Tonin FS, Borba HHL, et al. Pharmacological treatments for type 2 diabetes. *Treat Type 2 Diabetes* (2015) . p:147–84. doi: 10.5772/59204

6. Jugran AK, Rawat S, Devkota HP, Bhatt ID, Rawal RS. Diabetes and plant-derived natural products: From ethnopharmacological approaches to their potential for modern drug discovery and development. *Phytother Res* (2021) 35 (1):223–45. doi: 10.1002/ptr.6821

7. Blahova J, Martiniakova M, Babikova M, Kovacova V, Mondockova V, Omelka R. Pharmaceutical drugs and natural therapeutic products for the treatment of type 2 diabetes mellitus. *Pharm (Basel)* (2021) 14(8):806. doi: 10.3390/ph14080806

8. Scheen AJ. Pharmacotherapy of 'Treatment resistant' type 2 diabetes. *Expert Opin Pharmacother* (2017) 18(5):503–15. doi: 10.1080/14656566.2017.1297424

9. O'Brien MJ, Karam SL, Wallia A, Kang RH, Cooper AJ, Lancki N, et al. Association of second-line antidiabetic medications with cardiovascular events among insured adults with type 2 diabetes. *JAMA Netw Open* (2018) 1(8):e186125. doi: 10.1001/jamanetworkopen.2018.6125

10. Kaur N, Kumar V, Nayak SK, Wadhwa P, Kaur P, Sahu SK. Alpha-amylase as molecular target for treatment of diabetes mellitus: A comprehensive review. *Chem Biol Drug Des* (2021) 98(4):539–60. doi: 10.1111/cbdd.13909

11. Bashary R, Vyas M, Nayak SK, Suttee A, Verma S, Narang R, et al. An insight of alpha-amylase inhibitors as a valuable tool in the management of type 2 diabetes mellitus. *Curr Diabetes Rev* (2020) 16(2):117–36. doi: 10.2174/1573399815666190618093315

12. Rizwan H, Pal S, Sabnam S, Pal A. High glucose augments ros generation regulates mitochondrial dysfunction and apoptosis *Via* stress signalling cascades in keratinocytes. *Life Sci* (2020) 241:117148. doi: 10.1016/j.lfs.2019.117148

13. Li L, Zhang J, Zhang Q, Zhang D, Xiang F, Jia J, et al. High glucose suppresses keratinocyte migration through the inhibition of P38 Mapk/Autophagy pathway. *Front Physiol* (2019) 10:24. doi: 10.3389/fphys.2019.00024

14. Tsalamandris S, Antonopoulos AS, Oikonomou E, Papamikroulis GA, Vogiatzi G, Papaioannou S, et al. The role of inflammation in diabetes: Current concepts and future perspectives. *Eur Cardiol* (2019) 14(1):50–9. doi: 10.15420/ecr.2018.33.1

15. Wanjari MM, Mishra S, Dey YN, Sharma D, Gaidhani SN, Jadhav AD. Antidiabetic activity of chandraprabha vati - a classical ayurvedic formulation. *J Ayurveda Integr Med* (2016) 7(3):144–50. doi: 10.1016/j.jaim.2016.08.010

16. Alam S, Sarker MMR, Sultana TN, Chowdhury MNR, Rashid MA, Chaity NI, et al. Antidiabetic phytochemicals from medicinal plants: Prospective candidates for new drug discovery and development. *Front Endocrinol* (2022) 13:800714. doi: 10.3389/fendo.2022.800714

17. Kim SK, Jung J, Jung JH, Yoon N, Kang SS, Roh GS, et al. Hypoglycemic efficacy and safety of momordica charantia (Bitter melon) in patients with type 2 diabetes mellitus. *Complement Therapies Med* (2020) 52:102524. doi: 10.1016/j.ctim.2020.102524

18. Aleem A, Kabir H. Review on swertia chirata as traditional uses to its pyhtochemistry and pharmacological activity. *J Drug Deliv Ther* (2018) 8:73–8. doi: 10.22270/jddt.v8i5-s.1957

19. Kamat JP, Boloor KK, Devasagayam TP, Venkatachalam SR. Antioxidant properties of asparagus racemosus against damage induced by gamma-radiation in rat liver mitochondria. *J Ethnopharmacol* (2000) 71(3):425–35. doi: 10.1016/s0378-8741(00)00176-8

20. Al-Nablsi S, El-Keblawy A, Ali MA, Mosa KA, Hamoda AM, Shanableh A, et al. Phenolic contents and antioxidant activity of Citrullus Colocynthis fruits, growing in the hot arid desert of the UAE, influenced by the fruit parts, accessions, and seasons of fruit collection. *Antioxid (Basel)* (2022) 11(4):656. doi: 10.3390/antiox11040656

21. Pattonder RK, Chandola HM, Vyas SN. Clinical efficacy of shilajatu (Asphaltum) processed with agnimantha (Clerodendrum phlomidis linn.) in sthaulya (Obesity). *Ayu* (2011) 32(4):526–31. doi: 10.4103/0974-8520.96127

22. Philip S, Tom G, Balakrishnan Nair P, Sundaram S, Velikkakathu Vasumathy A. Tinospora cordifolia chloroform extract inhibits lps-induced inflammation *Via* nf-κb inactivation in thp-1cells and improves survival in sepsis. *BMC Complement Med Therapies* (2021) 21(1):97. doi: 10.1186/s12906-021-03244-y

23. Karthikeyan M, Balasubramanian T, Kumar P. *In-vivo* animal models and *in-vitro* techniques for screening antidiabetic activity. *J Develop Drugs* (2016) 5:153. doi: 10.4172/2329-6631.1000153

24. Shen P, Yue Y, Zheng J, Park Y. Caenorhabditis elegans: A convenient *in vivo* model for assessing the impact of food bioactive compounds on obesity, aging, and alzheimer's disease. *Annu Rev Food Sci Technol* (2018) 9:1–22. doi: 10.1146/annurev-food-030117-012709

25. Alcántar-Fernández J, Navarro RE, Salazar-Martínez AM, Pérez-Andrade ME, Miranda-Ríos J. Caenorhabditis elegans respond to high-glucose diets through a network of stress-responsive transcription factors. *PloS One* (2018) 13(7): e0199888. doi: 10.1371/journal.pone.0199888

26. Carretero M, Solis GM, Petrascheck MC. Elegans as model for drug discovery. *Curr Topics Medicinal Chem* (2017) 17(18):2067–76. doi: 10.2174/1568026617666170131114401

27. Hattori Y, Hattori K, Hayashi T. Pleiotropic benefits of metformin: Macrophage targeting its anti-inflammatory mechanisms. *Diabetes* (2015) 64 (6):1907–9. doi: 10.2337/db15-0090

28. Vasamsetti SB, Karnewar S, Kanugula AK, Thatipalli AR, Kumar JM, Kotamraju S. Metformin inhibits monocyte-to-Macrophage differentiation *Via* ampk-mediated inhibition of Stat3 activation: Potential role in atherosclerosis. *Diabetes* (2014) 64(6):2028–41. doi: 10.2337/db14-1225

29. Bailey CJ. Metformin: Historical overview. *Diabetologia* (2017) 60(9):1566–76. doi: 10.1007/s00125-017-4318-z

30. Zhou T, Xu X, Du M, Zhao T, Wang J. A preclinical overview of metformin for the treatment of type 2 diabetes. *Biomedi Pharmacother* (2018) 106:1227–35. doi: 10.1016/j.biopha.2018.07.085

31. Eum WS, Li MZ, Sin GS, Choi SY, Park JB, Lee JY, et al. Dexamethasone-induced differentiation of pancreatic Ar42j cell involves P21(Waf1/Cip1) and map kinase pathway. *Exp Mol Med* (2003) 35(5):379–84. doi: 10.1038/emm.2003.50

32. Ponnusamy S, Haldar S, Mulani F, Zinjarde S, Thulasiram H, RaviKumar A. Gedunin and azadiradione: Human pancreatic alpha-amylase inhibiting limonoids from neem (Azadirachta indica) as anti-diabetic agents. *PloS One* (2015) 10(10): e0140113. doi: 10.1371/journal.pone.0140113

33. Ngoh Y-Y, Tye GJ, Gan C-Y. The investigation of A-amylase inhibitory activity of selected Pinto bean peptides *Via* preclinical study using Ar42j cell. *J Funct Foods* (2017) 35:641–7. doi: 10.1016/j.jff.2017.06.037

34. Starowicz M, Zieliński H. Inhibition of advanced glycation end-product formation by high antioxidant-leveled spices commonly used in European cuisine. *Antioxidants* (2019) 8(4):100. doi: 10.3390/antiox8040100

35. Suarez-Arnedo A, Torres Figueroa F, Clavijo C, Arbelaez P, Cruz JC, Munoz-Camargo C. An image J plugin for the high throughput image analysis of *in vitro* scratch wound healing assays. *PloS One* (2020) 15(7):e0232565. doi: 10.1371/journal.pone.0232565

36. Byerly L, Cassada RC, Russell RL. The life cycle of the nematode caenorhabditis elegans. i. wild-type growth and reproduction. *Dev Biol* (1976) 51 (1):23–33. doi: 10.1016/0012-1606(76)90119-6

37. Shirdhankar R, Sorathia N, Rajyadhyaksha M. Short-term hyperglycaemia induces motor defects in C. elegans. *bioRxiv* (2017). doi: 10.1101/240473

38. Escorcia W, Ruter DL, Nhan J, Curran SP. Quantification of lipid abundance and evaluation of lipid distribution in caenorhabditis elegans by Nile red and oil red O staining. *J Visual Experiments JOVE* (2018) 133:e57352. doi: 10.3791/57352

39. Zou CG, Tu Q, Niu J, Ji XL, Zhang KQ. The daf-16/Foxo transcription factor functions as a regulator of epidermal innate immunity. *PloS Pathog* (2013) 9(10): e1003660. doi: 10.1371/journal.ppat.1003660

40. Reiniers MJ, de Haan LR, Reeskamp LF, Broekgaarden M, van Golen RF, Heger M. Analysis and optimization of conditions for the use of 2',7'-dichlorofluorescein diacetate in cultured hepatocytes. *Antioxid (Basel)* (2021) 10 (5):674. doi: 10.3390/antiox10050674

41. Heath RL, Packer L. Photoperoxidation in isolated chloroplasts. i. kinetics and stoichiometry of fatty acid peroxidation. *Arch Biochem Biophys* (1968) 125 (1):189–98. doi: 10.1016/0003-9861(68)90654-1

42. Zhao P, Ming Q, Qiu J, Tian D, Liu J, Shen J, et al. Ethanolic extract of folium sennae mediates the glucose uptake of L6 cells by GLUT4 and Ca(2). *Mol (Basel Switzerland)* (2018) 23(11):2934. doi: 10.3390/molecules23112934

43. Komura T, Yamanaka M, Nishimura K, Hara K, Nishikawa Y. Autofluorescence as a noninvasive biomarker of senescence and advanced glycation end products in caenorhabditis elegans. *NPJ Aging Mech Dis* (2021) 7 (1):12. doi: 10.1038/s41514-021-00061-y

44. Al Bander Z, Nitert MD, Mousa A, Naderpoor N. The gut microbiota and inflammation: An overview. *Int J Environ Res Public Health* (2020) 17(20):7618. doi: 10.3390/ijerph17207618

45. Scheithauer TPM, Rampanelli E, Nieuwdorp M, Vallance BA, Verchere CB, van Raalte DH, et al. Gut microbiota as a trigger for metabolic inflammation in obesity and type 2 diabetes. *Front Immunol* (2020) 11:571731. doi: 10.3389/fimmu.2020.571731

46. Yang DJ, Moh SH, Son DH, You S, Kinyua AW, Ko CM, et al. Gallic Acid promotes wound healing in normal and hyperglucidic conditions. *Mol (Basel Switzerland)* (2016) 21(7):899. doi: 10.3390/molecules21070899

47. Teshiba E, Miyahara K, Takeya H. Glucose-induced abnormal egg-laying rate in caenorhabditis elegans. *Biosci Biotechnol Biochem* (2016) 80(7):1436–9. doi: 10.1080/09168451.2016.1158634

48. Huang RT, Huang Q, Wu GL, Chen CG, Li ZJ. Evaluation of the antioxidant property and effects in caenorhabditis elegans of xiangxi flavor vinegar, a hunan local traditional vinegar. *J Zhejiang Univ Sci B* (2017) 18(4):324–33. doi: 10.1631/jzus.B1600088

49. Ji P, Li H, Jin Y, Peng Y, Zhao L, Wang XC. Elegans as an *in vivo* model system for the phenotypic drug discovery for treating paraquat poisoning. *PeerJ* (2022) 10:e12866. doi: 10.7717/peerj.12866

50. Lin X, Xu Y, Pan X, Xu J, Ding Y, Sun X, et al. Global, regional, and national burden and trend of diabetes in 195 countries and territories: An analysis from 1990 to 2025. *Sci Rep* (2020) 10(1):14790. doi: 10.1038/s41598-020-71908-9

51. Siopis G, Wang L, Colagiuri S, Allman-Farinelli M. Cost effectiveness of dietitian-led nutrition therapy for people with type 2 diabetes mellitus: A scoping review. *J Hum Nutr Diet* (2021) 34(1):81–93. doi: 10.1111/jhn.12821

52. Padhi S, Nayak AK, Behera A. Type ii diabetes mellitus: A review on recent drug based therapeutics. *Biomedi Pharmacother* (2020) 131:110708. doi: 10.1016/j.biopha.2020.110708

53. Abdel Raoof GF, Mohamed KY. Chapter 10 - natural products for the management of diabetes. In: Atta ur R, editor. *Studies in natural products chemistry*. Amsterdam: Elsevier (2018). 59:323–74.

54. Anwar S, Khan S, Almatroudi A, Khan AA, Alsahli MA, Almatroodi SA, et al. A review on mechanism of inhibition of advanced glycation end products formation by plant derived polyphenolic compounds. *Mol Biol Rep* (2021) 48 (1):787–805. doi: 10.1007/s11033-020-06084-0

55. Uddin SJ, Afroz M, Zihad SMNK, Rahman MS, Akter S, Khan IN, et al. A systematic review on anti-diabetic and cardioprotective potential of Gallic acid: A widespread dietary phytoconstituent. *Food Rev Int* (2022) 38(4):420–39. doi: 10.1080/87559129.2020.1734609

56. Adefegha SA, Oboh G, Ejakpovi II, Oyeleye SI. Antioxidant and antidiabetic effects of Gallic and protocatechuic acids: A structure–function perspective. *Comp Clin Pathol* (2015) 24(6):1579–85. doi: 10.1007/s00580-015-2119-7

57. Ma X, Tsuda S, Yang X, Gu N, Tanabe H, Oshima R, et al. Pu-Erh tea hot-water extract activates akt and induces insulin-independent glucose transport in rat skeletal muscle. *J Medicinal Food* (2013) 16(3):259–62. doi: 10.1089/jmf.2012.2520

58. Anhê FF, Desjardins Y, Pilon G, Dudonné S, Genovese MI, Lajolo FM, et al. Polyphenols and type 2 diabetes: A prospective review. *PharmaNutrition* (2013) 1 (4):105–14. doi: 10.1016/j.phanu.2013.07.004

59. Li Y, Wang Y, Chen Y, Wang Y, Zhang S, Liu P, et al. Corilagin ameliorates atherosclerosis in peripheral artery disease *Via* the toll-like receptor-4 signaling pathway *in vitro* and *in vivo*. *Front Immunol* (2020) 11:1611. doi: 10.3389/fimmu.2020.01611

60. Widowati W, Kusuma HSW, Arumwardana S, Afifah E, Wahyuni CD, Wijayanti CR, et al. Corilagin potential in inhibiting oxidative and inflammatory stress in lps-induced murine macrophage cell lines (Raw 264.7). *Iranian J Basic Med Sci* (2021) 24(12):1656–65. doi: 10.22038/ijbms.2021.59348.13174

61. Donath MY. Multiple benefits of targeting inflammation in the treatment of type 2 diabetes. *Diabetologia* (2016) 59(4):679–82. doi: 10.1007/s00125-016-3873-z

62. Dai J, Jiang C, Chen H, Chai Y. Rapamycin attenuates high glucose-induced inflammation through modulation of Mtor/Nf-kappab pathways in macrophages. *Front Pharmacol* (2019) 10:1292. doi: 10.3389/fphar.2019.01292

63. Dasu MR, Devaraj S, Jialal I. High glucose induces il-1beta expression in human monocytes: Mechanistic insights. *Am J Physiol Endocrinol Metab* (2007) 293(1):E337–46. doi: 10.1152/ajpendo.00718.2006

64. Lee JY, Kang Y, Kim HJ, Kim DJ, Lee KW, Han SJ. Acute glucose shift induces the activation of the Nlrp3 inflammasome in thp-1 cells. *Int J Mol Sci* (2021) 22(18):9952. doi: 10.3390/ijms22189952

65. Chang L, Wang Q, Ju J, Li Y, Cai Q, Hao L, et al. Magnoflorine ameliorates inflammation and fibrosis in rats with diabetic nephropathy by mediating the stability of lysine-specific demethylase 3a. *Front Physiol* (2020) 11:580406. doi: 10.3389/fphys.2020.580406

66. Correa LB, Seito LN, Manchope MF, Verri WAJr., Cunha TM, Henriques MG, et al. Methyl gallate attenuates inflammation induced by toll-like receptor ligands by inhibiting mapk and nf-κb signaling pathways. *Inflammation Res Off J Eur Histamine Res Soc [et al]* (2020) 69(12):1257–70. doi: 10.1007/s00011-020-01407-0

67. Spampinato SF, Caruso GI, De Pasquale R, Sortino MA, Merlo S. The treatment of impaired wound healing in diabetes: Looking among old drugs. *Pharmaceuticals* (2020) 13(4):60. doi: 10.3390/ph13040060

68. Guimarães I, Baptista-Silva S, Pintado M, Oliveira LA. Polyphenols: A promising avenue in therapeutic solutions for wound care. *Applied Sciences* (2021) 11(3):1230. doi: 10.3390/app11031230

69. Afshar M, Hassanzadeh- Taheri M, Zardast M, Honarmand M. Efficacy of topical application of coumarin on incisional wound healing in Balb/C mice. *Iranian J Dermatol* (2020) 23(2):56–63. doi: 10.22034/ijd.2020.110925

70. Naghavi M, Tamri P, Soleimani Asl S. Investigation of healing effects of cinnamic acid in a full-thickness wound model in rabbit. *Jundishapur J Natural Pharm Products* (2021) 16(1):e97669. doi: 10.5812/jjnpp.97669

71. Primarizky H, Misaco Yuniarti W, Lukiswanto B. Ellagic acid activity in healing process of incision wound on Male albino rats (Rattus norvegicus). *KnE Life Sci* (2017) 3:224. doi: 10.18502/kls.v3i6.1131

72. Schilrreff P, Alexiev U. Chronic inflammation in non-healing skin wounds and promising natural bioactive compounds treatment. *Int J Mol Sci* (2022) 23 (9):4928. doi: 10.3390/ijms23094928

73. Mingoia M, Conte C, Di Rienzo A, Dimmito MP, Marinucci L, Magi G, et al. Synthesis and biological evaluation of novel cinnamic acid-based antimicrobials. *Pharm (Basel)* (2022) 15(2):228. doi: 10.3390/ph15020228

74. Singh VP, Bali A, Singh N, Jaggi AS. Advanced glycation end products and diabetic complications. *Korean J Physiol Pharmacol* (2014) 18(1):1–14. doi: 10.4196/kjpp.2014.18.1.1

75. Dias D, Palermo K, Motta B, Kaga A, Lima T, Brunetti I, et al. Rutin inhibits the in vitroformation of advanced glycation products and protein oxidation more

efficiently than quercetin. *Rev Ciências Farmacêutica Básica e Aplicadas - RCFBA* (2021) 42:e718. doi: 10.4322/2179-443X.0718

76. Franco-Juárez B, Gómez-Manzo S, Hernández-Ochoa B, Cárdenas-Rodríguez N, Arreguin-Espinosa R, Pérez de la Cruz V, et al. Effects of high dietary carbohydrate and lipid intake on the lifespan of c. elegans. *Cells* (2021) 10 (9):2359. doi: 10.3390/cells10092359

77. Liao VH-C. Use of caenorhabditis elegans to study the potential bioactivity of natural compounds. *J Agric Food Chem* (2018) 66(8):1737–42. doi: 10.1021/acs.jafc.7b05700

78. Pattarachotanant N, Sornkaew N, Warayanon W, Rangsinth P, Sillapachaiyaporn C, Vongthip W, et al. Aquilaria crassna leaf extract ameliorates glucose-induced neurotoxicity *in vitro* and improves lifespan in caenorhabditis elegans. *Nutrients* (2022) 14(17):3668. doi: 10.3390/nu14173668

79. Zhou S, Chen J, Fan F, Pan Y, Feng X, Yu L, et al. Apios Americana medik flower extract protects high-Glucose-Treated hepatocytes and caenorhabditis elegans. *Food Biosci* (2022) 45:101473. doi: 10.1016/j.fbio.2021.101473

80. Shen CY, Wan L, Wang TX, Jiang JG. Citrus aurantium l. var. amara engl. inhibited lipid accumulation in 3t3-L1 cells and caenorhabditis elegans and prevented obesity in high-fat diet-fed mice. *Pharmacol Res* (2019) 147:104347. doi: 10.1016/j.phrs.2019.104347

81. Tripathi AK, Ray AK, Mishra SK. Molecular and pharmacological aspects of piperine as a potential molecule for disease prevention and management: Evidence from clinical trials. *Beni-Suef Univ J Basic Appl Sci* (2022) 11(1):16. doi: 10.1186/s43088-022-00196-1

82. Mendler M, Schlotterer A, Morcos M, Nawroth PP. Understanding diabetic polyneuropathy and longevity: What can we learn from the nematode caenorhabditis elegans? *Exp Clin Endocrinol Diabetes Off Journal German Soc Endocrinol [and] German Diabetes Assoc* (2012) 120(4):182–3. doi: 10.1055/s-0032-1304570

83. Bhattacharjee N, Dua TK, Khanra R, Joardar S, Nandy A, Saha A, et al. Protocatechuic acid, a phenolic from sansevieria roxburghiana leaves, suppresses diabetic cardiomyopathy *Via* stimulating glucose metabolism, ameliorating oxidative stress, and inhibiting inflammation. *Front Pharmacol* (2017) 8:251. doi: 10.3389/fphar.2017.00251

84. Aranaz P, Navarro-Herrera D, Zabala M, Romo-Hualde A, López-Yoldi M, Vizmanos JL, et al. Phenolic compounds reduce the fat content in caenorhabditis elegans by affecting lipogenesis, lipolysis, and different stress responses. *Pharmaceuticals* (2020) 13(11):355. doi: 10.3390/ph13110355

85. Shurrab NT, Arafa E-SA. Metformin: A review of its therapeutic efficacy and adverse effects. *Obes Med* (2020) 17:100186. doi: 10.1016/j.obmed.2020.100186

frontiers | Frontiers in Endocrinology

TYPE Original Research
PUBLISHED 26 January 2023
DOI 10.3389/fendo.2023.1099134



OPEN ACCESS

EDITED BY
Alexandre Gabarra Oliveira,
São Paulo State University, Brazil

REVIEWED BY
Fabiana S. Evangelista,
University of São Paulo, Brazil
Yan Jia,
First Hospital, Peking University, China

*CORRESPONDENCE
Qiming Liu
qimingliu@csu.edu.cn
Na Liu
naliu1025@csu.edu.cn

†These authors have contributed equally to this work and share first authorship

SPECIALTY SECTION
This article was submitted to Obesity, a section of the journal Frontiers in Endocrinology

RECEIVED 15 November 2022
ACCEPTED 13 January 2023
PUBLISHED 26 January 2023

CITATION
Wu K, Li B, Ma Y, Tu T, Lin Q, Zhu J, Zhou Y, Liu N and Liu Q (2023) Nicotinamide mononucleotide attenuates HIF-1α activation and fibrosis in hypoxic adipose tissue *via* NAD$^+$/SIRT1 axis. *Front. Endocrinol.* 14:1099134. doi: 10.3389/fendo.2023.1099134



# Nicotinamide mononucleotide attenuates HIF-1α activation and fibrosis in hypoxic adipose tissue *via* NAD$^+$/SIRT1 axis

Keke Wu[1†], Biao Li[1,2†], Yingxu Ma[1], Tao Tu[1], Qiuzhen Lin[1], Jiayi Zhu[1], Yong Zhou[1], Na Liu[1*] and Qiming Liu[1*]

[1]Department of Cardiovascular Medicine, Second Xiangya Hospital, Central South University, Changsha, Hunan, China, [2]Department of Cardiology, Shenzhen Traditional Chinese Medicine Hospital, Shenzhen, Guangdong, China

**Background:** Fibrosis is increasingly considered as a major contributor in adipose tissue dysfunction. Hypoxic activation of hypoxia-inducible factor 1α (HIF-1α) induces a profibrotic transcription, leading to adipose fibrosis. Nicotinamide mononucleotide (NMN), a member of the vitamin $B_3$ family, has been shown to relieve hepatic and cardiac fibrosis, but its effects on hypoxic adipose fibrosis and the underlying mechanism remain unclear. We aimed to elucidate the roles of NMN in regulating HIF-1α and fibrosis in hypoxic adipose tissue.

**Methods:** Mice were placed in a hypobaric chamber for four weeks to induce adipose fibrosis. NMN (500 mg/kg, every three days) was administered by intraperitoneal injection. *In vitro*, Stromal vascular fractions (SVF) cells were treated by hypoxia with or without NMN (200μM), sirtinol (25μM, a SIRT1 inhibitor) and $CoCl_2$ (100μM, a HIF1α enhancer). The effects of NMN on hypoxia-associated adipose fibrosis, inflammation, NAD$^+$/SIRT1 axis alteration, and HIF-1α activation were evaluated by real-time polymerase chain reaction (PCR), western blots, immunohistochemistry staining, immunoprecipitation, and assay kits.

**Results:** Mice placed in a hypoxic chamber for four weeks showed obvious adipose fibrosis and inflammation, which were attenuated by NMN. NMN also restore the compromised NAD$^+$/SIRT1 axis and inhibited the activation of HIF-1α induced by hypoxia. In hypoxia-induced SVFs, the SIRT1 inhibitor sirtinol blocked the anti-fibrotic and anti-inflammatory effects of NMN, upregulated the HIF-1α and its acetylation level. The HIF1α stabilizer $CoCl_2$ showed similar effects as sirtinol.

**Conclusion:** NMN effectively attenuated HIF-1α activation-induced adipose fibrosis and inflammation by restoring the compromised NAD$^+$/SIRT1 axis.

KEYWORDS

**nicotinamide mononucleotide, adipose tissue fibrosis, inflammation, HIF-1α activation, NAD +/SIRT1 axis**

# Introduction

Obesity is commonly considered as a persistent low-level inflammatory state closely related to insulin resistance, metabolic syndromes, and cardiovascular diseases (1, 2). This inflammatory state is closely related to adipose tissue hypoxia (3). A pivotal step to becoming obese is the rapid expansion of adipose tissue (AT) (4). The progression is accompanied by the shortage of oxygen due to the inability of the vascular system to keep up with the massive expansion. Hypoxia is therefore emerging as a causative factor for adipose dysfunction in obesity (4). The hypoxia state in AT induces the accumulation of hypoxia-inducible factor 1α (HIF-1α), which regulates many cellular anti-hypoxic responses (5, 6). Evidence from many laboratories suggests that the oxygen shortage of AT leads to several pathological processes, such as fibrosis, adipocytokine dysregulation, and inflammation, which are closely associated with adipose dysfunction and metabolic disorders (3, 6, 7).

HIF1α is considered as a significant initiating factor in adipocytes for fibrotic and inflammatory response, directly linked to metabolic dysfunction in AT under hypoxic conditions (3, 8). Unlike its action in the tumor, HIF1α cannot promote an adaptive proangiogenic reaction in AT (8). Instead, HIF1α induces an alternative transcriptional program, mainly entailing enhanced synthesis of extracellular matrix (ECM) components (9). The excessive collagen deposition in AT impairs ECM flexibility and tissue plasticity, thereby limiting AT's overexpansion, which triggers adipocyte necrosis (4, 8). The proinflammatory M1 macrophages are recruited to remove dead adipocytes, which eventually results in inflammation (10). HIF1α may also directly upregulate proinflammatory factors, such as IL-6 and MIF. These proinflammatory factors increase the infiltration of M1 macrophages, which in turn causes adipose fibrosis. These events raise the possibility that suppression of HIF-1α can prevent fibrotic and inflammatory changes induced by hypoxia or obesity (11, 12).

Nicotinamide mononucleotide (NMN), a member of the vitamin $B_3$ family, is a defined biosynthetic precursor of nicotinamide adenine dinucleotide ($NAD^+$). The effect of NMN on restoring $NAD^+$ homeostasis and activating sirtuins has been extensively investigated in the past decades (13, 14). Through restoring $NAD^+$ homeostasis, NMN can regulate mitochondrial metabolism and oxidative signaling pathway, which are closely related to adipose inflammation and fibrosis. NMN can also activate sirtuins, known to be the key regulators of aging and longevity, which have been linked to the regulating of adipose tissue function, including adipogenesis, WAT inflammation, and adipokine secretion (15–17). For example, SIRT1, the most well-known and prevalent sirtuin, has been reported to inhibit adipose inflammation. Genetic Sirt1 deficiency in rodents leads to elevated inflammation characterized by increased macrophage infiltration and mRNA expression of inflammatory cytokines in WAT under the High Fat Diet (HFD) condition (17–19). Moreover, SIRT1 has been involved in cardiac and renal fibrosis by regulating the TGF-β/Smads signaling pathway (20, 21). However, few studies have investigated whether SIRT1 inhibits hypoxia-induced inflammation and fibrosis by regulating HIF1α signaling pathway, especially in WAT. On the other hand, NMN has entered the stage of preclinical research due to its fewer unfavorable side effects and higher orally bioavailable (22). It has been well-documented that NMN delayed aging and ameliorated diseases caused by $NAD^+$ depletion, such as Alzheimer's disease, heart failure, diabetes, and complications associated with obesity (23–25). A recent study has shown that one adaptive metabolic pathway mediated by nicotinamide phosphor-ribosyl-transferase (NAMPT, the rate-limiting enzyme in $NAD^+$ biosynthesis) and SIRT1 is severely compromised in white adipose tissue (WAT) by HFD, thus leading to diabetes, whereas NMN ameliorates these changes (26). Although several preliminary studies have reported the effect of NMN on diet-and age-induced metabolic dysfunction, little is known about its role in hypoxia induced adipose fibrosis and inflammation.

In the present study, we aimed to find out: (a) whether NAMPT/$NAD^+$/SIRT1 axis is compromised by hypoxia, thus leading to adipose fibrosis and inflammation; (b) whether NMN inhibits hypoxia-related adipose fibrosis and inflammation with an emphasis on regulating HIF1α by restoring the compromised $NAD^+$/SIRT1 axis.

# Methods

## Chemical and reagents

Nicotinamide mononucleotide (B7878) was purchased from APExBIO Technology (Houston, United States) (98% purity, as detected by high-performance liquid chromatography analysis). Sirtinol was obtained from MedchemExpress (Sollentuna, Sweden). $CoCl_2$ was obtained from Sigma-Aldrich Co (St. Louis, MO, United States). The reverse-transcription assay kit was obtained from Thermo Fisher Scientific (USA). Antibodies against the following proteins were obtained from Abcam: TGF-β1 (ab92486), SIRT1 (ab110304), adiponectin (APN, ab5694), and NAMPT(ab236874). Antibodies against HIF1α (NB100-105) were purchased from Novus Biologicals. Antibodies against acetyl-lysine (9441S) were purchased from Cell Signaling Technology. Antibodies against MMP9(27306-1-AP), TIMP1(16644-1-AP), IL-6 (66146-1-lg), GAPDH, and β-actin were obtained from the Proteintech Group.

## Animal experiments

Male C57/B6 mice (8-10 weeks) weighing 20.2 ± 2g were purchased from the Institute of Laboratory Animal Science, Hunan SJA Laboratory Animal Co., Ltd (Changsha, China). All animal experiments were under the approval of the Animal Care and Use Committee of Second Xiangya Hospital of Central South University and were performed in strict accordance with the recommendations in the Guide for the Care and Use of Laboratory Animals of the National Institutes of Health. Mice were housed in a specific-pathogen-free (SPF) environment with a regular 12/12h day/night cycle, a humidity of 70%, and a temperature of 22°C for seven days before experiments. Mice were randomly divided into three groups (n = 8), namely, Control, hypoxia, and hypoxia + NMN. Hypoxia group mice were placed in a hypoxic chamber (54.02 kPa, 10.8% $O_2$) for four weeks. The chamber was opened daily for 30 min to clean and replenish food and water. NMN (500mg/kg, i.p, every three days) was delivered to mice 5-days before hypoxic treatment and one week after hypoxic treatment finished (25). The mice in the hypoxia and control groups were delivered equal volumes of saline. After anesthetic

induction, the mice are sacrificed by cervical dislocation. Lay the mouse in a supine position. Secure the upper and lower limbs to the dissection pan. Remove the skin, locate the testes and use forceps to lift up the epididymal white adipose tissue (eWAT). Use iris scissors to carefully excise the WAT from the epididymis. Fix one part of eWAT in 10% neutral buffered formalin for 24 h prior to histological processing and store the rest in a -80°C refrigerator.

## Histological study

After overnight fixation in 4% paraformaldehyde, the obtained eWAT was embedded in paraffin and sliced into 5-μm-thick sections. The change in eWAT structure and adipocyte size was examined by hematoxylin and eosin (H&E)-stained sections. The extent of interstitial fibrosis in WAT was evaluated from Masson-stained sections. It was calculated as the mean ratio of the blue-stained fibrotic area to the total tissue area. For each section, five optical fields were analyzed using digital analysis software (Image J) in a blinded manner.

We performed immunohistochemical staining to assess the level of SIRT1 expression and macrophage infiltration in the eWAT. After the sections were blocked using 8% goat serum in phosphate buffer saline (PBS), they were incubated with primary antibody against SIRT1 or the macrophage marker F4/80 at four °C overnight. Next, the sections were incubated with GT VisionTM+Detection System/Mo&Rb reagent for one hour at room temperature and developed using a peroxide-based substrate diaminobenzidine (DAB) kit (Gene Tech, Shanghai, China). Eventually, we dehydrated and cleared these sections in ethanol and xylene, respectively, and took the fields of view at the magnification of 200 ×. For each adipose depot, five optical fields per section were analyzed.

## Primary cell culture from the stromal vascular fraction of adipose tissue

Stromal vascular fraction (SVF) cells in epididymal fat depots from male C57BL/6 mice were isolated and cultured as described previously (27, 28). Briefly, fat tissues were minced into one $mm^3$ piece, then digested by type I collagenase (1 mg/ml) under agitation for 30-40 min at a 37 °C water bath. SVF cells were separated from the top layer of mature adipocytes by centrifugation (700 g, 10 min), then suspended in DMEM/F12 (Gibco) with 10% FBS and 100 U/ml penicillin-streptomycin and filtered by the cell strainer. Next, we centrifuged and re-suspended the SVF pellets in fresh media. Two hours after culturing cells under normal conditions (at 37°C in 95% $O_2$ and 5% $CO_2$), we washed the cells with PBS twice to remove red blood cells, immune cells, and other contaminants, and fresh media were added. All cells between 3-5 passages were used in this experiment. After serum starvation for 24 h, cells were randomly placed in cell culture chamber with 1% $O_2$ for 24h to conduct hypoxia. NMN was dissolved in sterile PBS and diluted to the desired final concentrations (200μM). NMN was added simultaneously with hypoxia treatment. Sirtinol (25μM) was used to block SIRT1 expression in SVFs. $CoCl_2$ (100μM) was used to enhance HIF1α expression in SVFs. Sirtinol or $CoCl_2$ was also added simultaneously with NMN.

## Western blot and real-time quantitative PCR

Immunoblotting analysis and qPCR were performed according to previous articles (29). In brief, Protein-extracts of snap-frozen eWAT and whole-cell lysates of SVF were prepared using standard procedures. Protein concentrations in the supernatants were measured using Bicinchoninic acid (BCA) assay (ASPEN, USA). Proteins were separated on SDS-polyacrylamide gels and transferred to PVDF membranes. After blocking with QuickBlock™ Western (P0252, Beyotime Biotechnology, China), the membranes were incubated with the primary antibodies overnight at 4°C, washed in PBST three times, and incubated with a secondary goat anti-rabbit polyclonal antibody (SA00001-2, Proteintech Group) at room temperature for 1h. Finally, the signals were tested by WesternBright™ Sirius ECL kit (K-12043-D20, Advansta, USA). Protein expression levels were normalized to β-actin.

Total mRNA was extracted from eWAT or SVF cells with GeneJET RNA Purification Kit (K0731, Thermo Fisher Scientific, USA). Reverse transcribed into cDNA using RevertAid First strand cDNA Synthesis kit (K1622, Thermo Fisher Scientific, USA). The StepOne Real-Time PCR (Life tech, Alameda, CA) was used for real-time qPCR analysis. The primers used are described in Table S1. β-actin was used as an internal control. The relative expression quantity $2^{-\Delta\Delta Ct}$ value was calculated to compare the differences among groups.

## Immunoprecipitation

For immunoprecipitation experiments, total homogenates from adipose tissue and cultured cells were treated with RIPA lysis buffer (P0013B, Beyotime Biotechnology, China), vortexed for the 30s, and centrifuged for 15 min at 12000 r/min. The tissue or cell extracts was subjected to immunoprecipitation with HIF1α primary antibody at 4° C overnight. The antibody-bound proteins were precipitated with 20 μL protein A/G PLUS-Agarose (Santa Cruz Biotechnology, sc-2003) and rotated for 1 h, then incubated overnight at 4°C. The beads were then gently centrifuged at 1000 r/min for 5 minutes at 4°C. After four RIPA buffer washes, the immunoprecipitates were diluted with 40 μL of 1 × SDS loading buffer (CW0027, Cowin Biotech, China) and boiled at 100°C for 2-3 min to separate complexes from the protein A/G PLUS-Agarose. The samples were then subjected to SDS-PAGE and transferred to polyvinylidene difluoride (PVDF) membranes (Bio-Rad, USA). After blocking with QuickBlock™ Western (P0252, Beyotime Biotechnology, China), the membranes were incubated with an anti-acetylated-lysine antibody (Cell Signaling Technology, #9441) overnight at 4°C, washed in PBST three times, and incubated with a secondary goat anti-rabbit polyclonal antibody (SA00001-2, Proteintech Group) at room temperature for 1h. Finally, the signals were tested by WesternBright™ Sirius ECL kit (K-12043-D20, Advansta, USA).

## $NAD^+$ measurements

In order to measure the $NAD^+$, EnzyChrom $NAD^+$/NADH Assay Kit (ECND100, Bioassay Systems, Hayward, California) was used

according to the manufacturer's instructions. In brief, mice eWAT weighing 20 mg for each sample or cells pelleted about $10^5$ for each sample were taken and homogenized in 100 μL $NAD^+$ or NADH extraction buffer, respectively. Extracts were heated for 5 min at 60°C, and 20 μL of assay buffer was added into extracts, followed by 100 μL of the opposite extraction buffer (to neutralize the extracts). Mixtures were vortexed and centrifuged at 12,000 g for 5 min. Supernatants (40 μL) were then mixed with a working reagent (80 μL) in each well. The optical density of supernatants at 565nm were measured at 0 and 15min intervals using a 96-well plate reader spectrophotometer. $NAD^+$/NADH concentration and their ratio were calculated using the manufacturers' equation.

### Statistical analysis

Statistical analyses were performed using GraphPad Prism version 7.0 software (San Diego, CA, USA). All values are expressed as mean ± standard deviation of the mean (SD). If the data fit normal distribution by taking Kolmogorov-Smirnov tests, the statistical comparisons between two groups were performed using Student's t-test, and comparisons among multiple groups were performed using one-way ANOVA followed by Tukey's *post hoc* test. $P < 0.05$ was considered statistically significant.

## Results

### NMN inhibits the aberrant deposition of ECM in the eWAT of hypoxia-induced mice

Adipose tissue structure remodeling is closely related to fibrosis. To learn whether NMN inhibits hypoxia induced adipose tissue structure change, we detected the adipocytes morphology and fibrotic area of the eWAT by HE Staining and Masson staining respectively (Figures 1A, B). Collagen fibers from the hypoxia-induced eWAT were increased and mainly distributed around adipocytes compared with the control group (7.556 ± 0.703 *vs.* 1.445 ± 0.1626, *P<0.05*). In contrast, the observed abnormal collagen deposition was reduced in NMN-treated eWAT (2.421 ± 0.1732 *vs.* 7.556 ± 0.703, *P<0.05*) (Figures 1B, C). Next, we measured the mRNA levels of collagen type I (Col1a1), type III (Col3a1), as well as matrix metalloproteinase 2 (MMP-2), MMP-9, tissue inhibitors of MMPs (TIMP-1), lysyl oxidase (LOX), and fibronectin (FN) by real-time quantitative PCR. As shown in Figure 1D, the above fibrotic genes were significantly upregulated in hypoxia-induced eWAT, whereas NMN reversed these changes. Moreover, the reduction of MMP9 and TIMP-1 protein expression levels due to NMN administration was further confirmed by Western blot (Figures 1E, F).

### Effect of NMN on dysregulated adipokines secretion and macrophage infiltration in the eWAT of hypoxia-induced mice

WAT is an active endocrine organ that produces many adipokines related to adipose dysfunction, especially the inflammatory and fibrotic factors. Therefore, we detected the protein level of APN, IL-6, and TGF-β in the eWAT of each group by Western blot. Hypoxia significantly increased pro-inflammatory and profibrotic factors levels, including IL-6 and TGF-βand decreased protective adipokine level, such as APN, whereas NMN attenuated these changes. (Figures 2A, B). The mRNA levels of the adipokines, including Leptin, Ang, Resistin, IL-6, and TGF-β, were significantly higher in the hypoxia group while APN expression was decreased (Figure 2C); NMN reversed these changes of the above adipokines.

We next examined the expression of macrophage marker F4/80 by immunohistochemistry (IHC) and qPCR. NMN significantly reduced the amounts of macrophages in the eWAT (Figures 2D, E). To further assess the effect of NMN on macrophage polarization in the eWAT, we evaluated the mRNA levels of TNFα and iNOS (M1 phenotype markers) and two other proteins, Arg1 and Ym1 (M2 phenotype markers). Compared with the hypoxia group, mice treated with NMN had lower levels of TNFα and iNOS but higher Arg1 and Ym1 levels (Figures 2F, G).

### NMN restores NAMPT/NAD+/SIRT1 axis and inhibits HIF-1α in white adipose tissue of hypoxia-induced mice

As a biosynthetic precursor of $NAD^+$, NMN was reported to boost the $NAD^+$ pool *in vivo* and regulate its related pathway. Thus, we evaluated NAMPT/NAD+/SIRT1 axis in the eWAT of three groups. The protein levels of NAMPT were significantly decreased in the eWAT of hypoxia-induced mice, and the impairment was restored by NMN(Figure 3A). $NAD^+$ levels and the $NAD^+$/NADH ratio in eWAT were reduced by hypoxia treatment but were replenished by NMN (Figures 3B, C). We next examined the protein expression of SIRT1 in the hypoxia group by IHC and Western blot (Figures 3D–F). It was significantly decreased in hypoxia-induced eWAT and was notably increased by NMN. HIF-1α is a key regulator in hypoxia-induced eWAT fibrosis. Thus, we examined the effects of NMN on HIF-1α in the eWAT of three groups (Figures 3D, G) and found it can diminish HIF-1α expression in hypoxia.

### NMN suppresses HIF-1α signaling-associated upregulation of fibrogenic and inflammatory genes in a SIRT1-dependent manner *in vitro*.

To further assess whether the inhibitory effect of NMN on eWAT structure remodeling is dependent on SIRT1 and its possible downstream target-HIF1α, SVF cells isolated from eWATof lean mice were exposed to hypoxia with or without NMN (200μM), Sirtinol (a SIRT1 inhibitor, 25μM) and $CoCl_2$ (a HIF1α enhancer, 100μM). The protein levels of NAMPT were significantly decreased in hypoxia-induced SVF cells, and NMN restored the impairment independently of Sirtinol or $CoCl_2$ treatment (Figure 4A). $NAD^+$ levels and the $NAD^+$/NADH ratio in SVF cells were reduced by hypoxia treatment but were replenished by NMN (Figures 4B, C). SVF cells showed a significantly hypoxia-induced downregulation of SIRT1 and upregulation of HIF1α and ac-HIF1α (Figures 4D–F). NMN treatment reversed the above changes. Interestingly, sirtinol

10.3389/fendo.2023.1099134

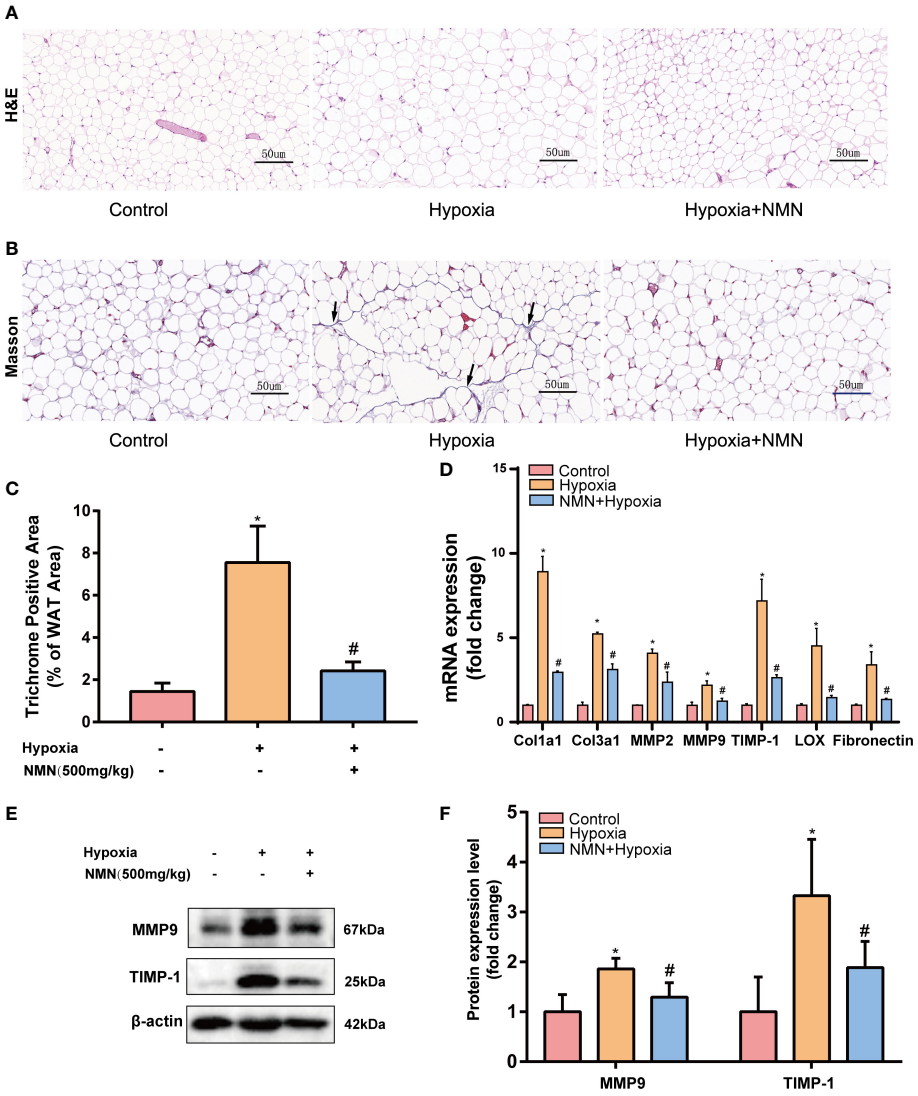


FIGURE 1
NMN alleviates the abnormal degradation and synthesis of ECM components in the eWAT of hypoxia-induced mice. **(A, B)** Representative images of eWAT adipocytes morphology and fibrosis as reflected by the H&E staining and Masson staining (400×magnification, scale bar=50 μm). **(C)** Statistical result for the interstitial fibrosis of eWAT (n = 6). **(D)** The relative mRNA levels of Col1a1, Col3a1, MMP-2, MMP-9, TIMP-1, LOX, and FN normalized to β-actin in eWAT (n = 3). **(E, F)** The relative protein levels of MMP9 and TIMP1 normalized to β-actin in eWAT (n = 5). $^{*}P < 0.05$ versus control group, $^{\#}P < 0.05$ versus hypoxia group.

partially blocked the activation of SIRT1 by NMN, accompanied by increased HIF1α and ac-HIF1α. $CoCl_2$ also augmented the level of HIF1α and ac-HIF1α after NMN treatment (Figures 4D, F).

We next examined the expression of fibrogenic and inflammatory genes associated with HIF1α signaling in SVF cells, including Col1a1, FN, TGF-β, IL-6, MIF, and TNF-α. The expression of the above genes was significantly increased in hypoxia-induced SVF cells, and this effect was reversed by NMN (Figures 5A–F). However, the suppressive effects of NMN on these genes were partly abolished by sirtinol (a SIRT1 inhibitor) or CoCl2 (a HIF1α enhancer).

## Discussion

Adipose tissue hypoxia and the activation of HIF-1α in obesity contribute to insulin resistance and type 2 diabetes. The mice raised in the hypoxia chamber presented similar pathophysiological processes, such as adipose fibrosis and inflammation, compared with HFD-fed mice (3, 12, 30). Recently, $NAD^+$ depletion is emerging as a major contributor to the pathogenesis of metabolic diseases, with the rise of studies on $NAD^+$ repletion strategies as countermeasure (14). In obesity, one of the main factors causing $NAD^+$ depletion in AT is that energy or fat excess, such as HFD-feeding, inhibits NAMPT expression (26, 31, 32). However, whether hypoxia is involved in the compromised NAMPT-mediated $NAD^+$ biosynthesis, thus leading to adipose fibrosis and inflammation is unknown. We previously demonstrated that NMN attenuates the development of cardiac fibrosis by inhibiting oxidative stress and the TGF-β/Smad signaling pathway, but whether NMN plays a role in adipose fibrosis and its mechanism is dependent on HIF1α are unclear. To fill this knowledge gap, we explored the effect of NMN on hypoxia-induced $NAD^+$ metabolism, fibrosis, and inflammation in the eWAT of mice.

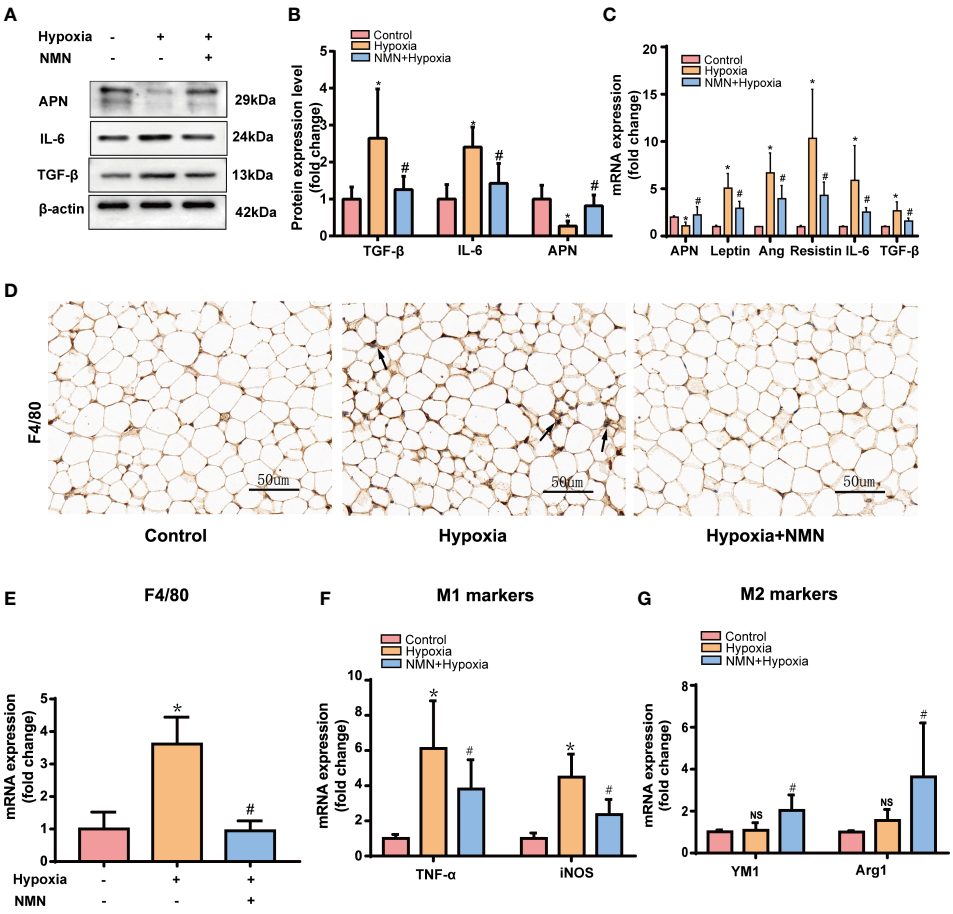


FIGURE 2
NMN alleviates dysregulated adipokines secretion and macrophage infiltration in the eWAT of hypoxia induced mice. **(A, B)** The relative protein levels of APN, TGFβ, and IL-6 normalized to β-actin in eWAT (n = 5). **(C)** The relative mRNA levels of APN, leptin, ang, resistin, IL-6, and TGF-β normalized to β-actin in eWAT (n = 6). **(D)** Representative images of macrophage marker F4/80 in eWAT as reflected by the IHC staining (400 × magnification, scale bar = 50μm). **(E)** The relative mRNA levels of F4/80 in eWAT (n = 6). **(F, G)** The relative mRNA levels of genes encoding TNFα, iNOS, Arg1 and Ym1 in eWAT (n = 6). $^{*}P < 0.05$ versus control group, $^{\#}P < 0.05$ versus hypoxia group.

In the present study, hypoxia- induced NAMPT down-regulation, $NAD^+$ depletion, fibrosis, and inflammation in eWAT, whereas the $NAD^+$ precursor NMN attenuated the changes, indicating the involvement of $NAD^+$ depletion in hypoxic insult. NMN attenuated HIF1α expression, suggesting that $NAD^+$ depletion may contribute to the HIF-1α accumulation in response to hypoxia. $NAD^+$ depletion and HIF-1α accumulation are the stress response to AT hypoxic state in the long term. In this context, the inhibitory role of NMN in $NAD^+$ depletion and hypoxia in AT was an attempt to restore cellular homeostasis.

The induction of HIF-1α in a hypoxia state fails to activate the angiogenic program in AT and turns to initiate a profibrotic response instead, causing fibrosis and inflammation in adipose tissue (4, 8). Inhibition of HIF -1α is the key point to attenuating adipose fibrosis and inflammation. In the present study, we found that NMN can inhibit HIF-1α activation and, as a result, effectively inhibit these profibrotic gene expressions. Consistent with the above results, the reduced Masson's staining further confirmed the anti-fibrotic effects of NMN. In addition, excessive collagen accumulation in AT is closely related to inflammation characterized by inflammatory cytokines dysregulation and macrophage infiltration (7), and HIF-1α can induce NF-κB-dependent inflammation (7, 33). In the AT of hypoxia-induced mice, NMN decreased the pro-inflammatory cytokines (TNF-α, TGF-β, and IL-6) and deleterious adipokines secretion (Leptin and Resistin) but increased the expression of adiponectin (APN). APN is a vital adipokine with insulin-sensitizing and anti-inflammation activities (34–36), but hypoxia could potentially inhibit APN and subsequently lead to inflammation and M1 macrophage infiltration in AT (37, 38). The anti-inflammatory activity of NMN may also be partly attributed to the regulation of APN. In the adipose tissue of hypoxia mice, NMN not only reduced the F4/80 (an indicator for the amounts of macrophage) but also inhibited M1 macrophage polarization, indicating the effect of NMN on blocking the inflammatory interplay between macrophages and adipocytes. The above evidence showed the protective role of NMN aganist adipose fibrosis and inflammation may be associated with the inhibition of HIF -1α.

NMN has been reported to be a multifunctional compound. In addition to replenishing $NAD^+$ and inhibiting oxidative stress, it can activate SIRT1, contributing to its effects on fibrosis and inflammation (21, 26, 39). In our *in vitro* study, the anti-fibrotic and anti-inflammatory effects of NMN on hypoxia-induced SVF were

10.3389/fendo.2023.1099134

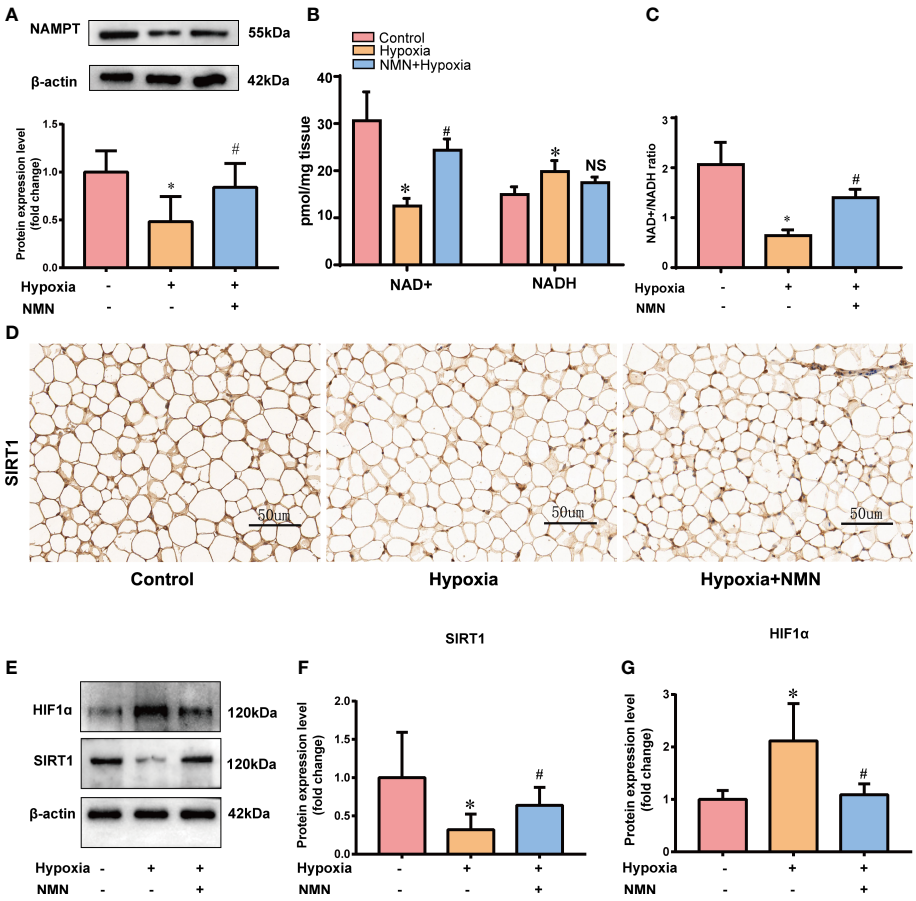


FIGURE 3
NMN restores NAMPT/NAD+/SIRT1 axis and inhibited HIF-1α acetylation in eWAT of hypoxia induced mice. **(A)** The relative protein levels of NAMPT normalized to β-actin in eWAT (n = 5). **(B, C)** Statistical results for $NAD^+$/NADH contents and $NAD^+$/NADH ratio in eWAT (n = 6). **(D)** Representative images of immunohistochemical staining for the SIRT1 protein in eWAT sections (400× magnification, scale bar=50μm). **(E–G)** The relative protein levels of SIRT1 and HIF1α in eWAT (n = 5). $^*P < 0.05$ versus control group, $^{\#}P < 0.05$ versus hypoxia group. NS indicates no significant difference compared with the matched group.

blocked by Sirtinol (a SIRT1 inhibitor), indicating the involvement of SIRT1 in NMN treatment. As an energy sensor, SIRT1 regulates cellular homeostasis, and therefore, we wanted to know whether NMN inhibited HIF-1α accumulation by activating SIRT1. Gomes et al. have found that SIRT1 is constantly required to ensure the efficient degradation of HIF1α under normal oxygen condition (40). During aging or hypoxia, $NAD^+$ depletion reduces the activity of SIRT1, leading to the activation of HIF1α (40, 41). Consistently, whether *in vivo* or *in vitro*, our results showed that the hypoxia-induced HIF1α upregulation was accompanied by reduced $NAD^+$ levels and SIRT1 activity. NMN treatment failed to reverse the above process with the disturbance of Sirtinol, indicating that NMN reduced HIF-1α accumulation by promoting proteasomal degradation in a SIRT1-dependent manner. Although the HIF-1α stabilizer $CoCl_2$ treatment can enhance the HIF1α expression with the existence of NMN, it failed to block the activation of SIRT1, further demonstrating that HIF-1α is the downstream target of SIRT1. In addition, several studies have shown that SIRT1 inactivated HIF1α by deacetylating it and consequently inhibited HIF-1 target genes (41, 42). In the present study, Sirtinol attenuated the enhanced effect of NMN on HIF1α deacetylation, indicating a possible role of SIRT1 in HIF1α activation. The above evidence is probably why SIRT1 has a role in the effect of NMN on HIF1α.

In summary, our study showed that NMN inhibited HIF-1α activation-induced adipose tissue fibrosis and inflammation, while the underlying mechanism may be associated with the $NAD^+$ repletion and the regulation of SIRT1 (Figure 6). These results provided further evidence for the beneficial effects of NMN on regulating adipose function in hypoxia. The benefit of NAD precursors in mouse model of metabolic diseases, in particularly NMN and NR, has been extensively investigated for a long time (23, 26, 39, 43). Currently, there are several ongoing human clinical trials or recently reported trials (NCT02191462, NCT02689882, NCT02921659, NCT02303483, NCT02678611, NCT03151239, UMIN000021309, UMIN000025739, UMIN000030609). All reported clinical trials of nicotinamide riboside (NR) or NMN demonstrated that it is safe, well tolerated, and can significantly increase plasma $NAD^+$ levels in healthy or obese volunteers (44–48). Besides, a recent study showed that 10 weeks of NMN administration in doses of 250mg/d improved skeletal muscle insulin sensitivity and insulin signaling in women with prediabetes (48). As $NAD^+$ metabolism can be a potential target for pathophysiological processes, including mitochondrial metabolism,

10.3389/fendo.2023.1099134

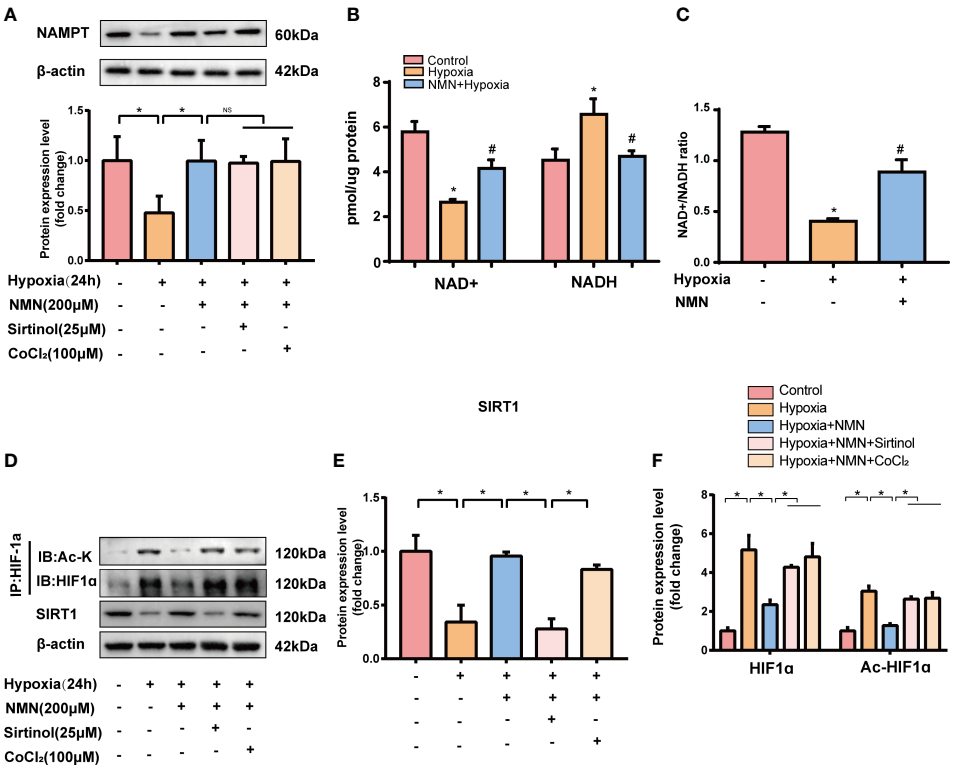


FIGURE 4
NMN restores NAMPT/NAD+/SIRT1 axis and inhibited HIF-1α acetylation in SVF cells. **(A)** The relative protein levels of NAMPT normalized to β-actin in SVF cells (n = 3). **(B, C)** Statistical results for $NAD^+$/NADH contents and $NAD^+$/NADH ratio in SVF cells (n = 3). **(D–F)** The relative protein levels of SIRT1 and HIF1α in SVF cells (n = 3). $^*P < 0.05$ versus control group, $^{\#}P < 0.05$ versus hypoxia group. NS indicates no significant difference compared with the matched group.

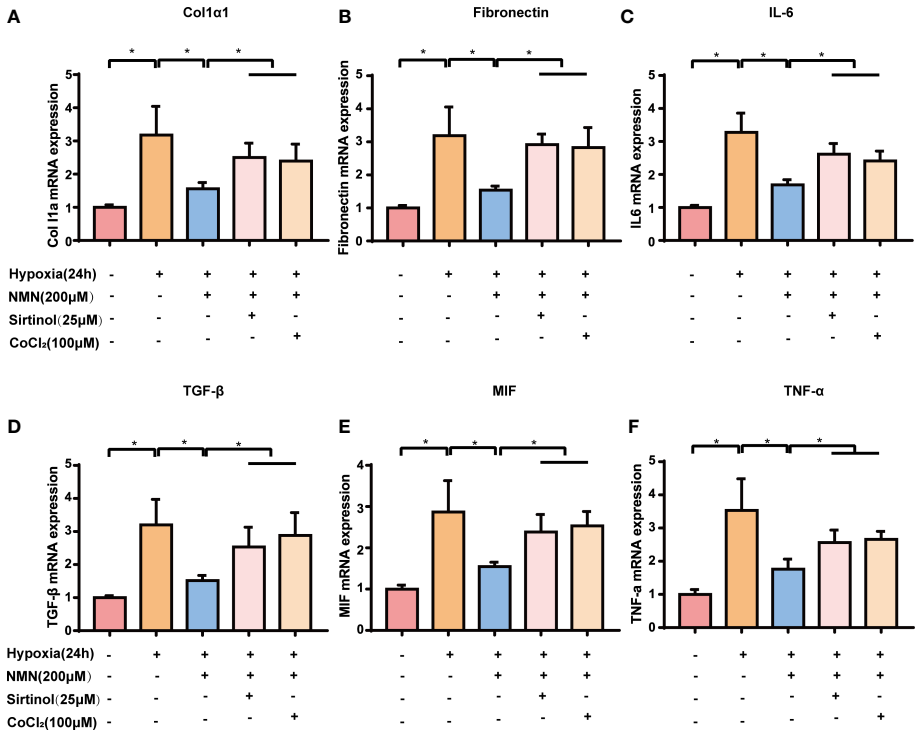


FIGURE 5
NMN suppresses HIF-1α signalling-associated upregulation of fibrogenic and inflammatory gene in a SIRT1-dependent manner. **(A–F)** The relative mRNA levels of Col1α, Fibronectin, IL-6, TGF-β, MIF and TNF-α normalized to β-actin in SVF cells (n = 3). $^*P < 0.05$ versus control group, $^{\#}P < 0.05$ versus hypoxia group.

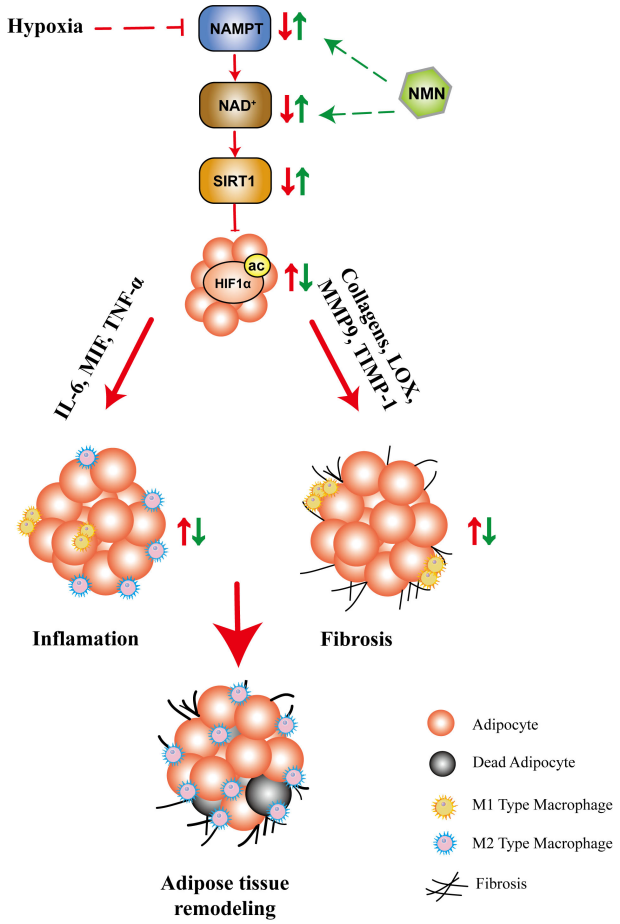


FIGURE 6
The proposed mechanisms for the protective role of NMN in hypoxia-induced adipose tissue remodeling. Hypoxia led to compromised NAMPT/$NAD^+$/SIRT1 axis, which further promoted HIF1α activation. As a result, the fibrotic and inflammatory response are significantly increased, accompanied by adipocytokine dysregulation, which ultimately lead to adipose tissue remodeling. NMN restored the NAMPT/$NAD^+$/SIRT1 axis and inhibited HIF1α activation, which further attenuated adipose tissue remodeling.

oxidative stress, inflammation, and fibrosis, NMN or NR may become a therapeutic option. The above evidence increases the possibility of $NAD^+$ precursors' clinical application, but its efficacy in patients with metabolic disorders remains unclear, and more studies are needed.

## Data availability statement

The original contributions presented in the study are included in the article/Supplementary Material. Further inquiries can be directed to the corresponding authors.

## Ethics statement

The animal study was reviewed and approved by the Animal Ethical and Welfare Committee of Second Xiangya Hospital of Central South University.

## Author contributions

KW, BL, NL, and QML designed the research. KW and BL performed the experiments. KW was a major contributor in writing the manuscript. YM and BL revised the manuscript. QML and NL supplied financial support and revised the manuscript. All authors read and approved the final manuscript.

## Funding

This research was supported by grants from the Hunan Province Innovative Project (no. 2020SK1013), the National Natural Science Foundation of China (no. 82070356), and the Natural Science Foundation of Hunan Province, China (nos. 2021JJ30033 and 2021JJ40870).

## Conflict of interest

The authors declare that the research was conducted in the absence of any commercial or financial relationships that could be construed as a potential conflict of interest.

## Publisher's note

All claims expressed in this article are solely those of the authors and do not necessarily represent those of their affiliated organizations, or those of the publisher, the editors and the reviewers. Any product that may be evaluated in this article, or claim that may be made by its manufacturer, is not guaranteed or endorsed by the publisher.

## Supplementary material

The Supplementary Material for this article can be found online at: https://www.frontiersin.org/articles/10.3389/fendo.2023.1099134/full#supplementary-material

## References

1. Van Gaal LF, Mertens IL, De Block CE. Mechanisms linking obesity with cardiovascular disease. *Nature* (2006) 444(7121):875–80. doi: 10.1038/nature05487

2. Fantuzzi G. Adipose tissue, adipokines, and inflammation. *J Allergy Clin Immunol* (2005) 115(5):911–9. doi: 10.1016/j.jaci.2005.02.023

3. Trayhurn P. Hypoxia and adipose tissue function and dysfunction in obesity. *Physiol Rev* (2013) 93(1):1–21. doi: 10.1152/physrev.00017.2012

4. Sun K, Tordjman J, Clement K, Scherer PE. Fibrosis and adipose tissue dysfunction. *Cell Metab* (2013) 18(4):470–7. doi: 10.1016/j.cmet.2013.06.016

5. Semenza GL. Hypoxia-inducible factors in physiology and medicine. *Cell* (2012) 148 (3):399–408. doi: 10.1016/j.cell.2012.01.021

6. Hosogai N, Fukuhara A, Oshima K, Miyata Y, Tanaka S, Segawa K, et al. Adipose tissue hypoxia in obesity and its impact on adipocytokine dysregulation. *Diabetes* (2007) 56(4):901–11. doi: 10.2337/db06-0911

7. Sun K, Kusminski CM, Scherer PE. Adipose tissue remodeling and obesity. *J Clin Invest* (2011) 121(6):2094–101. doi: 10.1172/jci45887

8. Halberg N, Khan T, Trujillo ME, Wernstedt-Asterholm I, Attie AD, Sherwani S, et al. Hypoxia-inducible factor 1 alpha induces fibrosis and insulin resistance in white adipose tissue. *Mol Cell Biol* (2009) 29(16):4467–83. doi: 10.1128/mcb.00192-09

9. Khan T, Muise ES, Iyengar P, Wang ZV, Chandalia M, Abate N, et al. Metabolic dysregulation and adipose tissue fibrosis: Role of collagen vi. *Mol Cell Biol* (2009) 29 (6):1575–91. doi: 10.1128/mcb.01300-08

10. Castoldi A, de Souza CN, Camara NOS, Moraes-Vieira PM. The macrophage switch in obesity development. *Front Immunol* (2016) 6:637. doi: 10.3389/fimmu.2015.00637

11. Sun K, Halberg N, Khan M, Magalang UJ, Scherer PE. Selective inhibition of hypoxia-inducible factor 1 alpha ameliorates adipose tissue dysfunction. *Mol Cell Biol* (2013) 33(5):904–17. doi: 10.1128/mcb.00951-12

12. Li XL, Li J, Wang LL, Li AY, Qiu ZX, Qi LW, et al. The role of metformin and resveratrol in the prevention of hypoxia-inducible factor 1 accumulation and fibrosis in hypoxic adipose tissue. *Br J Pharmacol* (2016) 173(12):2001–15. doi: 10.1111/bph.13493

13. Hershberger KA, Martin AS, Hirschey MD. Role of nad(+) and mitochondrial sirtuins in cardiac and renal diseases. *Nat Rev Nephrol* (2017) 13(4):213–25. doi: 10.1038/nrneph.2017.5

14. Jokinen R, Pirnes-Karhu S, Pietilainen KH, Pirinen E. Adipose tissue nad (+)-homeostasis, sirtuins and Poly(Adp-ribose) polymerases - important players in mitochondrial metabolism and metabolic health. *Redox Biol* (2017) 12:246–63. doi: 10.1016/j.redox.2017.02.011

15. Picard F, Kurtev M, Chung NJ, Topark-Ngarm A, Senawong T, de Oliveira RM, et al. Sirt1 promotes fat mobilization in white adipocytes by repressing ppar-gamma. *Nature* (2004) 429(6993):771–6. doi: 10.1038/nature02583

16. Gillum MP, Kotas ME, Erion DM, Kursawe R, Chatterjee P, Nead KT, et al. Sirt1 regulates adipose tissue inflammation. *Diabetes* (2011) 60(12):3235–45. doi: 10.2337/db11-0616

17. Chalkiadaki A, Guarente L. High-fat diet triggers inflammation-induced cleavage of Sirt1 in adipose tissue to promote metabolic dysfunction. *Cell Metab* (2012) 16(2):180–8. doi: 10.1016/j.cmet.2012.07.003

18. Mayoral R, Osborn O, McNelis J, Johnson AM, Oh DY, Izquierdo CL, et al. Adipocyte Sirt1 knockout promotes ppar gamma activity, adipogenesis and insulin sensitivity in chronic-hfd and obesity. *Mol Metab* (2015) 4(5):378–91. doi: 10.1016/j.molmet.2015.02.007

19. Zhou Y, Song T, Peng J, Zhou Z, Wei H, Zhou R, et al. Sirt1 suppresses adipogenesis by activating Wnt/Beta-catenin signaling in vivo and in vitro. *Oncotarget* (2016) 7(47):77707–20. doi: 10.18632/oncotarget.12774

20. Huang X-Z, Wen D, Zhang M, Xie Q, Ma L, Guan Y, et al. Sirt1 activation ameliorates renal fibrosis by inhibiting the tgf-Beta/Smad3 pathway. *J Cell Biochem* (2014) 115(5):996–1005. doi: 10.1002/jcb.24748

21. Wu K, Li B, Lin Q, Xu W, Zuo W, Li J, et al. Nicotinamide mononucleotide attenuates isoproterenol-induced cardiac fibrosis by regulating oxidative stress and Smad3 acetylation. *Life Sci* (2021) 274. doi: 10.1016/j.lfs.2021.119299

22. Poddar SK, Sifat AE, Haque S, Nahid NA, Chowdhury S, Mehedi I. Nicotinamide mononucleotide: Exploration of diverse therapeutic applications of a potential molecule. *Biomolecules* (2019) 9(1). doi: 10.3390/biom9010034

23. Mills KF, Yoshida S, Stein LR, Grozio A, Kubota S, Sasaki Y, et al. Long-term administration of nicotinamide mononucleotide mitigates age-associated physiological decline in mice. *Cell Metab* (2016) 24(6):795–806. doi: 10.1016/j.cmet.2016.09.013

24. Yoshino J, Baur JA, Imai S-i. Nad(+) intermediates: The biology and therapeutic potential of nmn and nr. *Cell Metab* (2018) 27(3):513–28. doi: 10.1016/j.cmet.2017.11.002

25. Lee CF, Chavez JD, Garcia-Menendez L, Choi Y, Roe ND, Chiao YA, et al. . doi: 10.1161/circulationaha.116.022495

26. Yoshino J, Mills KF, Yoon MJ, Imai S-i. Nicotinamide mononucleotide, a key nad (+) intermediate, treats the pathophysiology of diet- and age-induced diabetes in mice. *Cell Metab* (2011) 14(4):528–36. doi: 10.1016/j.cmet.2011.08.014

27. Aune UL, Ruiz L, Kajimura S. Isolation and differentiation of stromal vascular cells to Beige/Brite cells. *Jove-Journal Visualized Experiments* (2013) 73). doi: 10.3791/50191

28. Wang QA, Scherer PE, Gupta RK. Improved methodologies for the study of adipose biology: Insights gained and opportunities ahead. *J Lipid Res* (2014) 55(4):605–24. doi: 10.1194/jlr.R046441

29. Li B, Po SS, Zhang BJ, Bai F, Li JY, Qin F, et al. Metformin regulates adiponectin signalling in epicardial adipose tissue and reduces atrial fibrillation vulnerability. *J Cell Mol Med* (2020) 24(14):7751–66. doi: 10.1111/jcmm.15407

30. Lee YS, J-w K, Osborne O, Oh DY, Sasik R, Schenk S, et al. Increased adipocyte O-2 consumption triggers hif-1 alpha, causing inflammation and insulin resistance in obesity. *Cell* (2014) 157(6):1339–52. doi: 10.1016/j.cell.2014.05.012

31. Jukarainen S, Heinonen S, Ramo JT, Rinnankoski-Tuikka R, Rappou E, Tummers M, et al. Obesity is associated with low Nad(+)/Sirt pathway expression in adipose tissue of bmi-discordant monozygotic twins. *J Clin Endocrinol Metab* (2016) 101(1):274–82. doi: 10.1210/jc.2015-3095

32. Mercader J, Granados N, Caimari A, Oliver P, Bonet ML, Palou A. Retinol-binding protein 4 and nicotinamide Phosphoribosyltransferase/Visfatin in rat obesity models. *Hormone Metab Res* (2008) 40(7):467–72. doi: 10.1055/s-2008-1065324

33. Rius J, Guma M, Schachtrup C, Akassoglou K, Zinkernagel AS, Nizet V, et al. Nf-kappa b links innate immunity to the hypoxic response through transcriptional regulation of hif-1 alpha. *Nature* (2008) 453(7196):807–U9. doi: 10.1038/nature06905

34. Fruhbeck G, Catalan V, Rodriguez A, Ramirez B, Becerril S, Salvador J, et al. Involvement of the leptin-adiponectin axis in inflammation and oxidative stress in the metabolic syndrome. *Sci Rep* (2017) 7. doi: 10.1038/s41598-017-06997-0

35. Kantartzis K, Rittig K, Balletshofer B, Machann J, Schick F, Porubska K, et al. The relationships of plasma adiponectin with a favorable lipid profile, decreased inflammation, and less ectopic fat accumulation depend on adiposity. *Clin Chem* (2006) 52(10):1934–42. doi: 10.1373/clinchem.2006.067397

36. Luo N, Liu J, Chung BH, Yang Q, Klein RL, Garvey WT, et al. Macrophage adiponectin expression improves insulin sensitivity and protects against inflammation and atherosclerosis. *Diabetes* (2010) 59(4):791–9. doi: 10.2337/db09-1338

37. Ye J, Gao Z, Yin J, He Q. Hypoxia is a potential risk factor for chronic inflammation and adiponectin reduction in adipose tissue of Ob/Ob and dietary obese mice. *Am J Physiology-Endocrinol Metab* (2007) 293(4):E1118–E28. doi: 10.1152/ajpendo.00435.2007

38. Ohashi K, Parker JL, Ouchi N, Higuchi A, Vita JA, Gokce N, et al. Adiponectin promotes macrophage polarization toward an anti-inflammatory phenotype. *J Biol Chem* (2010) 285(9):6153–60. doi: 10.1074/jbc.M109.088708

39. Caton PW, Kieswich J, Yaqoob MM, Holness MJ, Sugden MC. Nicotinamide mononucleotide protects against pro-inflammatory cytokine-mediated impairment

of mouse islet function. *Diabetologia* (2011) 54(12):3083–92. doi: 10.1007/s00125-011-2288-0

40. Gomes AP, Price NL, Ling AJY, Moslehi JJ, Montgomery MK, Rajman L, et al. Declining nad(+) induces a pseudohypoxic state disrupting nuclear-mitochondrial communication during aging. *Cell* (2013) 155(7):1624–38. doi: 10.1016/j.cell.2013.11.037

41. Lim J-H, Lee Y-M, Chun Y-S, Chen J, Kim J-E, Park J-W. Sirtuin 1 modulates cellular responses to hypoxia by deacetylating hypoxia-inducible factor 1 alpha. *Mol Cell* (2010) 38(6):864–78. doi: 10.1016/j.molcel.2010.05.023

42. Geng H, Harvey CT, Pittsenbarger J, Liu Q, Beer TM, Xue C, et al. Hdac4 protein regulates Hif1 alpha protein lysine acetylation and cancer cell response to hypoxia. *J Biol Chem* (2011) 286(44):38095–102. doi: 10.1074/jbc.M111.257055

43. Canto C, Houtkooper RH, Pirinen E, Youn DY, Oosterveer MH, Cen Y, et al. The nad (+) precursor nicotinamide riboside enhances oxidative metabolism and protects against high-fat diet-induced obesity. *Cell Metab* (2012) 15(6):838–47. doi: 10.1016/j.cmet.2012.04.022

44. Airhart SE, Shireman LM, Risler LJ, Anderson GD, Gowda GAN, Raftery D, et al. An open-label, non-randomized study of the pharmacokinetics of the nutritional supplement nicotinamide riboside (Nr) and its effects on blood nad plus levels in healthy volunteers. *PLos One* (2017) 12(12). doi: 10.1371/journal.pone.0186459

45. Martens CR, Denman BA, Mazzo MR, Armstrong ML, Reisdorph N, McQueen MB, et al. Chronic nicotinamide riboside supplementation is well-tolerated and elevates nad(+) in healthy middle-aged and older adults. *Nat Commun* (2018) 9. doi: 10.1038/s41467-018-03421-7

46. Trammell SAJ, Schmidt MS, Weidemann BJ, Redpath P, Jaksch F, Dellinger RW, et al. Nicotinamide riboside is uniquely and orally bioavailable in mice and humans. *Nat Commun* (2016) 7. doi: 10.1038/ncomms12948

47. Dollerup OL, Christensen B, Svart M, Schmidt MS, Sulek K, Ringgaard S, et al. A randomized placebo-controlled clinical trial of nicotinamide riboside in obese men: Safety, insulin-sensitivity, and lipid-mobilizing effects. *Am J Clin Nutr* (2018) 108(2):343–53. doi: 10.1093/ajcn/nqy132

48. Yoshino M, Yoshino J, Kayser BD, Patti GJ, Franczyk MP, Mills KF, et al. Nicotinamide mononucleotide increases muscle insulin sensitivity in prediabetic women. *Science* (2021) 372(6547):1224–+. doi: 10.1126/science.abe9985

frontiers | Frontiers in Endocrinology

TYPE Systematic Review
PUBLISHED 27 January 2023
DOI 10.3389/fendo.2023.1115321



OPEN ACCESS

EDITED BY
Guilherme Zweig Rocha,
State University of Campinas, Brazil

REVIEWED BY
Lorenzo Nesti,
University of Pisa, Italy
Alfredo Caturano,
University of Campania Luigi Vanvitelli, Italy

*CORRESPONDENCE
Tao Liu
nclt456@sina.com

SPECIALTY SECTION
This article was submitted to Obesity, a section of the journal Frontiers in Endocrinology

RECEIVED 03 December 2022
ACCEPTED 11 January 2023
PUBLISHED 27 January 2023

CITATION
Liu X, Chen Y, Liu T, Cai L, Yang X and Mou C (2023) The effects of Sodium-glucose cotransporter 2 inhibitors on adipose tissue in patients with type 2 diabetes: A meta-analysis of randomized controlled trials.
*Front. Endocrinol.* 14:1115321.
doi: 10.3389/fendo.2023.1115321



# The effects of Sodium-glucose cotransporter 2 inhibitors on adipose tissue in patients with type 2 diabetes: A meta-analysis of randomized controlled trials

Xindong Liu, Ying Chen, Tao Liu*, Ling Cai, Xiaofeng Yang and Chuan Mou

Department of Cardiovascular Medicine, Nanchong Central Hospital, The Second Clinical Medical College of North Sichuan Medical College, Nanchong, China

**Purpose:** To systematically evaluate the effect of Sodium-glucose cotransporter 2 (SGLT2) inhibitors on adipose tissue in patients with type 2 diabetes.

**Methods:** We searched PubMed, Cochrane Library, EMBASE, and Web of science databases for literature pertaining to Randomized controlled trials (RCTs) of SGLT2 inhibitors in treating type 2 diabetes patients. The retrieval time was from the date of establishment of the databases to September 1, 2022. Meta-analysis was performed using RevMan5.4 software.

**Results:** Totally 551 patients were included in 10 articles. Meta-analysis results showed that compared with the control group, the visceral adipose tissue (WMD = -16.29 $cm^2$, 95% CI: -25.07 ~ -7.50, P<0.00001), subcutaneous adipose tissue (WMD = -19.34 $cm^2$, 95% CI: -36.27 ~ -2.41, P<0.00001), body weight (WMD = -2.36 kg, 95% CI: -2.89 ~ -1.83, P<0.00001) and triglyceride (WMD = -24.41 mg/dl, 95% CI: -45.79 ~ -3.03, P = 0.03) of the trial group significantly reduced.

**Conclusion:** SGLT2 inhibitors cause significant reductions in visceral adipose tissue, subcutaneous adipose tissue, body weight and triglycerides in type 2 diabetes patients, which may be attributed to the protective effect of the inhibitors on cardiovascular system.

KEYWORDS

**Sodium-glucose cotransporter 2 inhibitors, SGLT2, type 2 diabetes, adipose tissue, meta-analysis**

# 1 Introduction

Cardiovascular disease remains one of the leading causes of death worldwide, posing huge health risks and economic burdens. SGLT2 inhibitors are novel hypoglycemic agents that lower blood glucose by inhibiting the reabsorption of glucose in the kidneys and allowing excess glucose to be excreted from the urine. In recent years, a number of large randomized controlled clinical trials (the EMPAREG OUTCOME trial (1), CANVAS Program (2) and DECLARETIMI 58 trial (3), etc.) have confirmed that SGLT2 inhibitors can significantly reduce all-cause mortality, cardiovascular mortality and heart failure hospitalization rates in patients with type 2 diabetes, among others. However, their potential mechanism of cardiovascular protection is not completely clear.

There is considerable evidence that overweight, obesity and their comorbidities increase the morbidity and mortality of cardiovascular disease, independent of age and gender (4–6). A meta-analysis showed that SGLT2 inhibitors significantly reduced body weight in type 2 diabetes patients as compared to placebo (7). Studies using dual-energy X-ray absorptiometry (DEXA) and bioelectrical impedance analysis (BIA) confirmed that the SGLT2 inhibitor-associated weight loss was attributed to the reduction in (viscera and subcutaneous) adipose tissue mass, instead of the lean tissue mass which remained unchanged (8, 9). Type 2 diabetes patients are often accompanied by obesity, and obese type 2 diabetics have a greater propensity for ectopic and visceral fat deposition (10). It has been suggested that SGLT2 inhibitors significantly lowered weight and adiposity indices, with the potential to improve cardiometabolic risk among patients with type 2 diabetes mellitus (11). At present, the effects of SGLT2 inhibitors on visceral adipose tissue (VAT) and subcutaneous adipose tissue (SAT) are uncertain, and large-scale clinical trials are lacking. Therefore, we conducted a meta-analysis to assess the impact of SGLT2 inhibitors on VAT and SAT in patients with type 2 diabetes.

# 2 Methods

The meta-analysis was undertaken in accordance with the recommendations of the Preferred Reporting Items for Systematic Reviews and Meta-Analyses (PRISMA) guidelines (12). The literature search, literature screening, data extraction and risk of bias assessment were carried out independently by two researchers. Any disagreement was resolved by discussion or a third author. All studies included in this paper complied with the Declaration of Helsinki and were approved by the local ethics committee.

## 2.1 Data source and research search strategy

We searched the PubMed, Cochrane Library, EMBASE and Web of science databases from conception to September 1, 2022, for the data from RCTs of SGLT2 inhibitors in treating type 2 diabetes. The main search terms include “Diabetes Mellitus, Type 2”, “Sodium Glucose Transporter 2 Inhibitors”, and “Adipose Tissue”. The detailed information regarding the search strategy is shown in Supplementary Table 1. Additionally, we manually searched the references of relevant articles to obtain more literature.

## 2.2 Study selection

Inclusion criteria: 1) articles with type 2 diabetes patients aged ≥ 18 years; 2) trials that used SGLT2 inhibitors in the treatment group and placebo or conventional hypoglycemic drugs in the control group; 3) articles with randomized controlled trial (RCT); and 4) articles with outcome indicators including VAT or SAT that was reported in square centimeters. Exclusion criteria: 1) articles with missing, incomplete or unreasonable trial data; 2) articles with unavailable or converted primary outcome indicators; 3) duplicate literature data; and 4) articles examining animal studies.

## 2.3 Data extraction and assessment of risk of bias

A data extraction form was created to pre-extract information from the eligible literature, and then the data extraction form was further refined. The extracted data included 1) study characteristics (first author, publication date, study design, intervention, follow-up time); 2) study subject characteristics (number of patients, age, gender, weight, body mass index (BMI), duration of diabetes); 3) intervention characteristics (drug name, route of administration, dose, duration of treatment, etc.); 4) primary outcome indicators (visceral adipose tissue area, subcutaneous adipose tissue area and relative measurement methods); and 5) secondary outcome indicators (body weight, BMI, total cholesterol, triglycerides, low density lipoprotein cholesterol (LDL-C), high density lipoprotein cholesterol (HDL-C)). We assessed the treatment-related changes according to the change in the mean values and standard deviations (SD) of the outcome indicators before and after treatment. Detailed information on the changes pre- and post-treatment are shown in Supplementary Table 2.

The Cochrane risk-of-bias tool was used to assess the risk of bias based on the following seven criteria: random sequence generation, allocation concealment, blinding of participants and personnel, blinding of outcome assessment, incomplete outcome data, selective reporting, and other bias. Each study was judged to be at ‘low’, ‘high’ or ‘unclear’ risk of bias.

## 2.4 Data synthesis and analysis

All outcome indicators were continuous outcome data, expressed by weighted mean difference (WMD). Meta-analysis was performed using RevMan 5.4 software to calculate combined effect sizes and 95% confidence interval (CI) for each group. Heterogeneity was assessed using $I^2$ statistics, with $I^2$ of 25-50%, 50%-75% and >75% representing small, moderate and large heterogeneity, respectively. Considering that the heterogeneity among the included studies may be large, all the results are pooled using random effect models. Subgroup analyses were performed according to possible sources of heterogeneity. Statistical descriptions were made using forest plots, and

publication bias was assessed by funnel plots. $P<0.05$ was considered statistically significant.

# 3 Results

## 3.1 Study selection

Figure 1 illustrates the literature screening process. A total of 1051 articles were obtained after searching the databases based on the search strategy. The specific databases and corresponding literature quantity were as follows: PubMed (134), Cochrane Library (227), EMBASE (466), Web of science (224). 336 duplicates were removed by using Noteexpress software, 67 articles remained after the initial screening by reading the abstracts and full text. After excluding non-RCTs, trials failing to comply with study design protocols, trials lacking main outcome indicators, articles with missing data, and duplicate literature, 10 studies were included in the final meta-analysis (9, 13–21). 2 literature were sub-studies (13, 14), some research data of which were obtained from their original studies (22, 23).

## 3.2 Characteristics of the included studies

The baselines of all the included studies are comparable between groups. Table 1 shows the characteristics of the included studies. A total of 551 patients were enrolled, including 306 in the intervention group and 245 in the control group. Three SGLT2 inhibitors were evaluated in the studies, namely empagliflozin, dapagliflozin and ipragliflozin. The follow-up time was 3 or 6 months for most studies, and 26 months for only one study.

## 3.3 Quality assessment

All studies provided methods of random allocation. 3 studies were double-blinded and 7 studies were unblinded trials. One of the articles was a conference literature with incomplete information (13), so its "incomplete outcome data" and "other bias" were classified as unclear risk. Two trials funded by pharmaceutical companies were classified as high risk for 'other bias' according to guidance provided by Cochrane (24). Another trial also funded by a pharmaceutical company was classified as low risk for the 'other bias' item, because the authors declared that the funder had no role in study design, data collection and analysis, publication decisions or manuscript preparation. Supplementary Figure 1 provides the quality assessment details.

## 3.4 Meta-analysis of outcomes

### 3.4.1 VAT and SAT

All studies reported results for VAT and 7 studies reported results for SAT. Meta-analysis results showed that compared with the control group, VAT (WMD = -16.29 $cm^2$, 95% CI: -25.07 ~ -7.50, $P<0.00001$) and SAT (WMD = -19.34 $cm^2$, 95% CI: -36.27 ~ -2.41, $P<0.00001$) in the SGLT2 inhibitors treatment group were significantly reduced (Figures 2, 3). We observed a high degree of heterogeneity in both VAT ($P<0.00001$, $I^2 = 91\%$) and SAT ($P<0.00001$, $I^2 = 97\%$). Funnel plot results for both VAT and SAT showed that the scatter points corresponding to each study was largely distributed on the midline or largely symmetrically distributed, with no significant publication bias in either outcome, as shown in Figures 4, 5.

Considering the high heterogeneity of VAT and SAT, we further conducted sensitivity analysis and subgroup analysis (Table 2). In the

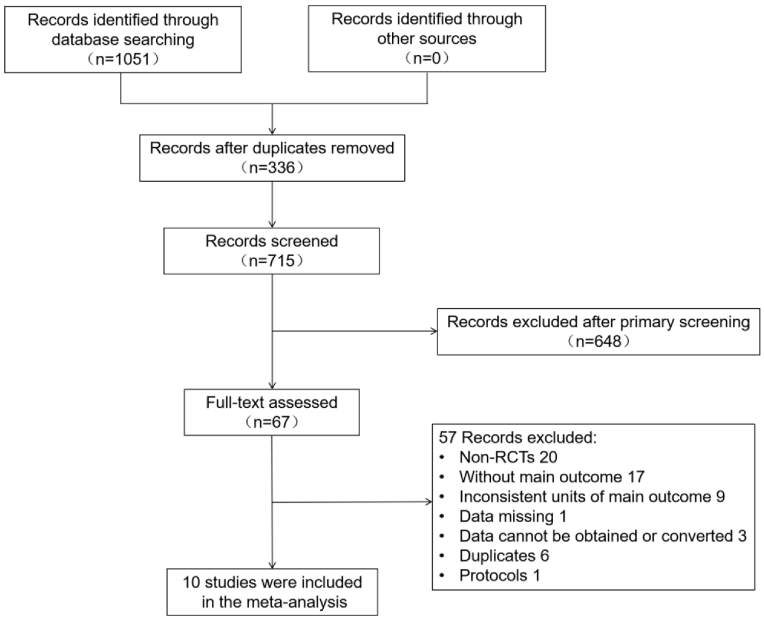


FIGURE 1
Flow chart of literature screening.

10.3389/fendo.2023.1115321

TABLE 1 Characteristics of the included studies.

| Study | Age (y) | BMI (kg/m$^2$) | Diabetes duration (y) | Follow-up (weeks) | Number of patients | Intervention | Instrument |
|---|---|---|---|---|---|---|---|
| Kim 2014 (13) | 55.7 ± 10.4 | 31.9 ± 4.9 | / | 104 | 29 | empagliflozin 25mg qd + metformin | MRI |
| | | | | | 22 | glimepiride 1-4mg qd + metformin | |
| Bando 2017 (14) | 55.0 ± 8.6 | 27.6 ± 3.6 | 9.7 ± 4.4 | 12 | 40 | ipragliflozin 50 mg qd | CT |
| | | | | | 22 | continued previous treatment | |
| Ito 2017 (15) | 58.2 ± 10.9 | 30.3 ± 5.6 | 9.1 ± 5.8 | 24 | 32 | ipragliflozin 50 mg qd | CT |
| | | | | | 34 | pioglitazone 15–30 mg qd | |
| Inoue 2019 (9) | 60.7 ± 10.9 | 27.8 ± 4.2 | 17. 5± 9.4 | 24 | 24 | ipragliflozin 50 mg qd | MRI |
| | | | | | 24 | continued previous treatment | |
| Shimizu 2019 (16) | 56.6 ± 12.4 | 27.9 ± 4.2 | / | 24 | 33 | dapagliflozin 5mg qd | BIA |
| | | | | | 24 | standard treatment | |
| Han 2020 (18) | 53.9 ± 10.9 | 30.3 ± 4.6 | 9.4 ± 5.8 | 24 | 30 | ipragliflozin 50mg qd + metformin + pioglitazone | CT |
| | | | | | 15 | metformin + pioglitazone | |
| Sakurai 2020 (17) | 58.6 ± 12.5 | 27.6 ± 6.0 | / | 12 | 31 | empagliflozin 10 mg qd | BIA |
| | | | | | 18 | standard treatment | |
| Chehrehgosha 2021 (20) | 51.2 ± 8.1 | 30.5 ± 3.9 | 6.3 ± 4.7 | 24 | 35 | empagliflozin 10 mg qd | DEXA |
| | | | | | 37 | placebo | |
| Gaborit 2021 (19) | 56.9 ± 9.6 | 34.9 ± 6.0 | 11.1 ± 6.7 | 12 | 26 | empagliflozin 10 mg qd | MRI |
| | | | | | 25 | placebo | |
| Horibe 2022 (21) | 60.9 ± 9.7 | 27.8 ± 3.9 | 12.5 ± 8.1 | 24 | 26 | dapagliflozin 5 mg qd | MRI |
| | | | | | 24 | standard treatment | |

CT, computed tomography; MRI, magnetic resonance imaging; DEXA, dual-energy x-ray absorptiometry; BIA, bioelectrical impedance analysis.

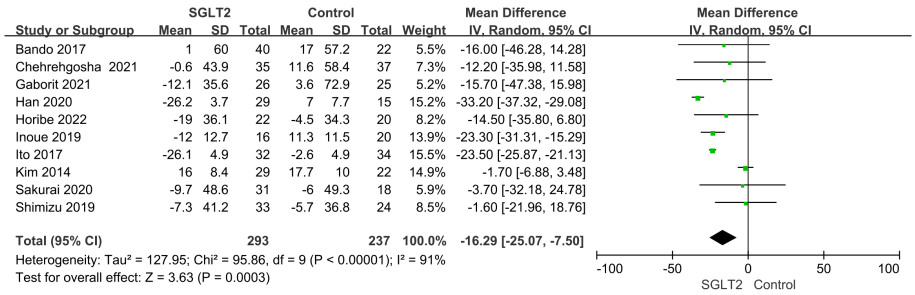


FIGURE 2
Forest plot of VAT.

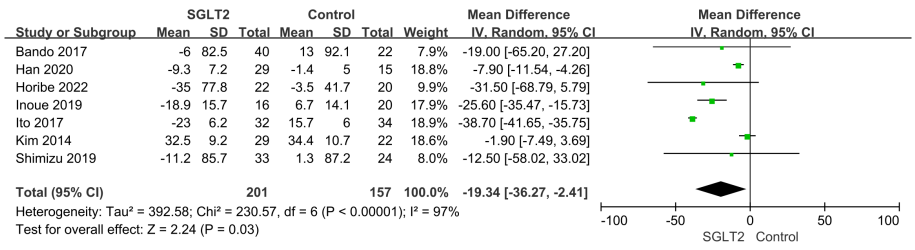


FIGURE 3
Forest plot of SAT.

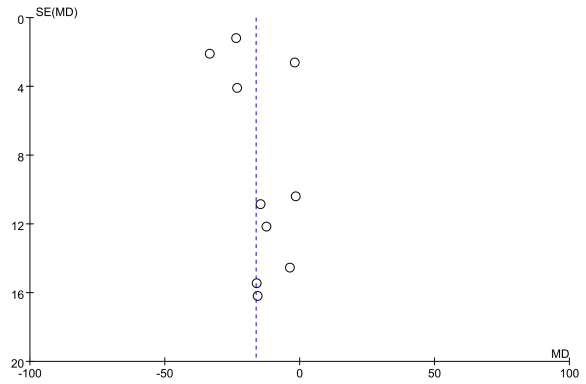


FIGURE 4
Funnel plot of VAT.

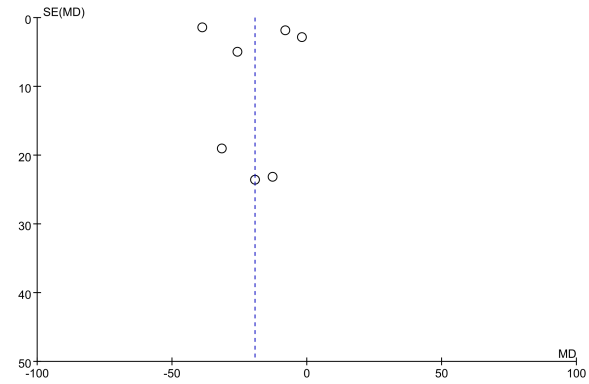


FIGURE 5
Funnel plot of SAT.

sensitivity analysis, removing any of the included studies caused no significant change in the results of VAT and SAT. Subsequently, subgroup analyses were performed based on the type of SGLT2, baseline BMI level, and duration of follow-up. The results showed that ipragliflozin significantly reduced VAT and SAT, while neither empagliflozin nor dapagliflozin reached statistical significance. As compared to the subgroup with BMI≥28 kg/m$^2$, treatment with SGLT2 resulted in a more significant reduction in SAT (WMD = -25.17 cm$^2$, 95% CI: -34.32 ~ -16.02, $P$<0.00001) in the subgroup with BMI<28 kg/m$^2$. In addition, neither VAT nor SAT reached statistical significance in the subgroup with < 24 weeks of follow-up ($P$>0.05).

### 3.4.2 Body weight and BMI

7 trials reported body weight, with high heterogeneity among the studies ($P$<0.00001, $I^2$ = 88%). Meta-analysis results showed that as compared to the control group, the body weight (WMD = -2.36 kg, 95% CI: -2.89 ~ -1.83, $P$<0.00001) of patients in the SGLT2 inhibitor treatment group was significantly reduced. Only 4 trials reported BMI, and no heterogeneity existed among the studies ($P$ = 0.84, $I^2$ = 0%). The results also indicated that relative to the control group, patients in the SGLT2 inhibitor treated group had a significantly lower BMI (WMD = -0.8 kg/m$^2$, 95% CI: -0.91 ~ -0.69, $P$<0.00001) (Table 3).

### 3.4.3 Blood lipids

According to the meta-analysis, triglycerides (WMD = -24.41 mg/dl, 95% CI: -45.79 ~ -3.03, $P$ = 0.03) were significantly lower and HDL cholesterol (WMD = 1.63 mg/dl, 95% CI: 0.62 ~ 2.64, $P$ = 0.002) was significantly higher in SGLT2 inhibitor-treated patients as compared to controls, while total cholesterol and LDL cholesterol failed to reach statistical significance (Table 3).

## 4 Discussion

In the meta-analysis involving 10 publications and 551 patients, we demonstrated that SGLT2 inhibitors, in addition to significantly reducing body weight and triglycerides, considerably lowered VAT and SAT in patients with type 2 diabetes.

Subgroup analysis of SGLT2 inhibitors drug categories by VAT and SAT revealed that ipragliflozin led to significant reductions in VAT and SAT, whereas empagliflozin and dapagliflozin seemingly caused no significant changes in VAT and SAT in patients with type 2 diabetes.

Differences in the drugs themselves may be one possible reason for the result. Neeland et al. analyzed the effects of empagliflozin on total body and visceral adiposity in over 6000 type 2 diabetes patients with high cardiovascular risk, finding that the drug significantly reduced indices of visceral adiposity and total body fat (11), which is inconsistent with our research results, even if the outcome indicators are different. In the case of our meta-analysis, only two studies used dapagliflozin treatment. Therefore, more or large clinical trials are needed for demonstrating the effects of the two drugs on VAT and SAT. Differences in the methods of measuring the main outcome indicators may be another reason for heterogeneity. Studies of ipragliflozin have mainly used computed tomography (CT) scan to determine VAT and SAT, whereas studies pertaining to empagliflozin and dapagliflozin have measured VAT and SAT by magnetic resonance imaging (MRI), DEXA, BIA.

We found that SGLT2 inhibitors treatment significantly reduced VAT and SAT when the follow-up time was longer than 6 months, whereas this positive result was not observed in trials with follow-up period of less than 6 months. A study indicated that the weight loss caused by SGLT2 inhibitors treatment was observed in the first week, and reached a stable level after 6 months (25). In our study, patients in all trials with follow-up time less than 6 months received a 3-month treatment, and such short treatment time may lead to the negative results.

Consistent with the results of several studies, we demonstrated that SGLT2 inhibitors considerably lower triglyceride levels in patients with type 2 diabetes (26, 27). At present, much controversy exists regarding the effect of SGLT2 inhibitor treatment on serum HDL-C and LDL-C levels. Calapkulu et al. found a decrease of 13.4 mg/dL in the LDL-C level in type 2 diabetes patients who had taken dapagliflozin (10mg/d) for 6 months (26). However, a study by Rau et al. showed that after 3 months of treatment for patients with type 2 diabetes, empagliflozin (10mg/d) led to an increase of 9 mg/dL in LDL-C (28). This growth is likely to be due to increased lipoprotein-lipase activity and delayed LDL turnover in the circulation (29).

TABLE 2 Subgroup analysis.

| Study characteristics | VAT ($cm^2$) | | | | SAT ($cm^2$) | | | |
|---|---|---|---|---|---|---|---|---|
| | Study number | Patient number | WMD [95% CI] | *P*-value | Study number | Patient number | WMD [95% CI] | *P*-value |
| Empagliflozin | 4 | 223 | -2.55 [-7.47, 2.37] | 0.31 | 1 | 51 | -1.90 [-7.49, 3.69] | 0.50 |
| Dapagliflozin | 2 | 99 | -10.01 [-27.05, 7.04] | 0.25 | 2 | 99 | -23.87 [-52.72, 4.98] | 0.10 |
| Ipragliflozin | 4 | 208 | -26.38 [-33.20, -19.57] | 0.0008 | 4 | 208 | -23.42 [-44.82, -2.03] | 0.03 |
| BMI ≥ 28($kg/m^2$) | 5 | 284 | -18.22 [-30.67, -5.76] | 0.004 | 3 | 161 | -16.24 [-40.27, 7.80] | 0.19 |
| BMI < 28($kg/m^2$) | 5 | 246 | -16.78 [-25.85, -7.71] | 0.0003 | 4 | 197 | -25.17 [-34.32, -16.02] | <0.00001 |
| Follow-up ≥ 24weeks | 7 | 368 | -17.65 [-27.40, -7.90] | 0.0004 | 6 | 296 | -19.37 [-37.08, -1.67] | 0.03 |
| Follow-up <24weeks | 3 | 162 | -11.34 [-28.70, 6.01] | 0.2 | 1 | 62 | -19.00 [-65.20, 27.20] | 0.42 |

Therefore, further research is needed to explore the effect of SGLT2 inhibitor on blood lipids.

In healthy populations, normal adipose tissue has such functions as protecting internal organs, storing energy, producing heat and reducing inflammation. Obesity, insulin resistance, diabetes and inflammation are all associated with the phenotype and biological changes of adipose tissue (30). In obesity and diabetes, adipose tissue is infiltrated by increasing numbers of inflammatory and immune cells, losing its own homeostatic function and developing chronic low-grade inflammation (31). Dysfunctional adipose tissue reduces the release of protective factors (e.g. lipocalin, nitric oxide or protective prostaglandins) and increased activation of stress-related pathways, leading to the release of pathological adipokines (e.g. resistin, visceral adiponectin and leptin) and the development of low-grade inflammation, and promoting metabolic and cardiovascular dysfunction (32). Dysfunctional adipose tissue may also increase the production of tissue factors and bioactive isoprostanes, damage the sensitivity of platelets to insulin signals, enhance coagulation and impair fibrinolysis, and promote thrombosis (33). Nesti L et al. showed that in type 2 diabetic patients with normal cardiac function, higher epicardial adipose tissue thickness was associated with lower peak oxygen uptake, reduced systolic reserve, higher natriuretic peptide levels, as well as chronotropic insufficiency and impaired heart rate recovery (34). Epicardial fat also causes a mechanical constriction of the diastolic filling leading to micro-circulatory dysfunction, which, together with the pro-inflammatory effect and fibrosis of the underlying myocardium, impairs the relaxability of the left ventricle and increases its filling pressure (35).

Contributing to reduced VAT and SAT, SGLT2 inhibitors also reduce ectopic adipose tissues, such as epicardial adipose tissue (36), hepatic adipose tissue (37) and perivascular adipose tissue (38), without affecting muscle mass and bone mineral content (9, 39). Sakurai et al. found that SGLT2 inhibitors reduced plasminogen activator inhibitor-1 (PAI-1) along with VAT, improved fibrinolysis, and increased serum high molecular weight adiponectin (17). In type 2 diabetes patients with non-alcoholic fatty liver disease, SGLT2 inhibitors can improve liver steatosis and fibrosis (18, 20), lowering serum aspartate aminotransferase (AST) and alanine aminotransferase (ALT) levels (37).

The mechanism by which SGLT2 inhibitors reduce adipose tissue is not completely clear. An animal study found that SGLT2 inhibitors triggered glycogen depletion signal and actuated liver-brain-adipose axis, promoting lipolysis (40). Lauritsen et al. showed that SGLT2 inhibition reduced GLUT4 gene and protein expression in adipose tissue, possibly by reducing glycerol formation and rebalancing substrate utilization away from glucose oxidation and lipid storage capacity (41). Moreover, SGLT2 inhibitors increase fat utilization by activating M2 macrophages (42). Undoubtedly, the role of SGLT2 inhibitors in ameliorating cardiovascular risk relates not only to the adipose tissue reduction, but, to their pleiotropic effect in reducing multiple risk factors (43).

TABLE 3 Meta-analysis results of body weight, BMI and blood lipids.

| Study characteristics | Study number | Patient number | WMD [95% CI] | *P*-value |
|---|---|---|---|---|
| Body weight (kg) | 7 | 381 | -2.36 [-2.89, -1.83] | <0.00001 |
| BMI ($kg/m^2$) | 4 | 222 | -0.80 [-0.91, -0.69] | <0.00001 |
| Total cholesterol (mg/dl) | 7 | 391 | -2.51 [-10.69, 5.67] | 0.55 |
| Triglyceride (mg/dl) | 7 | 397 | -24.41 [-45.79, -3.03] | 0.03 |
| LDL-C (mg/dl) | 9 | 497 | -1.31 [-9.97, 7.36] | 0.77 |
| HDL-C (mg/dl) | 8 | 446 | 1.63 [0.62, 2.64] | 0.002 |

There are some limitations to our study that should be noted. First, we included a limited number of trials and sample sizes, and thus more RCTs are needed to further validate the current results. Secondly, although all of these included studies were RCTs, seven of the ten included studies were not double-blinded, increasing the risk of performance bias. Third, the majority of RCTs included in the study were from Asia, so ethnic differences and Asian-specific lifestyles may have affected the results. Fourth, most trials included in the study had a short follow-up period, except one study that had a 26-month follow-up time. Fifth, significant heterogeneity was noted in the analysis of both the VAT and SAT, which may be due to different demographic characteristics and substantial differences in intervention type and design. Sixthly, another limitation is the difference of therapeutic drugs and doses used in each study, as well as various side effects caused by other drugs used in the trial population.

## 5 Conclusion

Our pooled results show that SGLT2 inhibitors significantly reduce VAT, SAT, body weight, and triglycerides in type 2 diabetes patients, which may correlate with the cardiovascular protective effects of the inhibitors and suggest a new therapeutic strategy for obese patients. Due to the limited sample size of the study and high heterogeneity of the included studies, the effects of SGLT2 inhibitors on adipose tissue need to be further investigated by resorting to a large sample of long-term RCTs.

## Data availability statement

The original contributions presented in the study are included in the article/Supplementary Material. Further inquiries can be directed to the corresponding author.

## Author contributions

XL and TL designed the study. XL and LC collected the data. YC performed the meta-analysis and drafted the manuscript. YC, XY, and CM partially planned the research. XL edited the manuscript. All authors contributed to the article and approved the submitted version.

## Conflict of interest

The authors declare that the research was conducted in the absence of any commercial or financial relationships that could be construed as a potential conflict of interest.

## Publisher's note



## Supplementary material

The Supplementary Material for this article can be found online at: https://www.frontiersin.org/articles/10.3389/fendo.2023.1115321/full#supplementary-material

## References

1. Zinman B, Wanner C, Lachin JM, Fitchett D, Bluhmki E, Hantel S, et al. Empagliflozin, cardiovascular outcomes, and mortality in type 2 diabetes. *N Engl J Med* (2015) 373:2117–28. doi: 10.1056/NEJMoa1504720

2. Neal B, Perkovic V, Mahaffey KW, de Zeeuw D, Fulcher G, Erondu N, et al. Canagliflozin and cardiovascular and renal events in type 2 diabetes. *N Engl J Med* (2017) 377:644–57. doi: 10.1056/NEJMoa1611925

3. Wiviott SD, Raz I, Bonaca MP, Mosenzon O, Kato ET, Cahn A, et al. Dapagliflozin and cardiovascular outcomes in type 2 diabetes. *N Engl J Med* (2019) 380:347–57. doi: 10.1056/NEJMoa1812389

4. Mongraw-Chaffin ML, Peters S, Huxley RR, Woodward M. The sex-specific association between BMI and coronary heart disease: A systematic review and meta-analysis of 95 cohorts with 1.2 million participants. *Lancet Diabetes Endocrinol* (2015) 3:437–49. doi: 10.1016/S2213-8587(15)00086-8

5. Choi S, Kim K, Kim SM, Lee G, Jeong SM, Park SY, et al. Association of obesity or weight change with coronary heart disease among young adults in south korea. *JAMA Intern Med* (2018) 178:1060–8. doi: 10.1001/jamainternmed.2018.2310

6. Khan SS, Ning H, Wilkins JT, Allen N, Carnethon M, Berry JD, et al. Association of body mass index with lifetime risk of cardiovascular disease and compression of morbidity. *JAMA Cardiol* (2018) 3:280–7. doi: 10.1001/jamacardio.2018.0022

7. Storgaard H, Gluud LL, Bennett C, Grondahl MF, Christensen MB, Knop FK, et al. Benefits and harms of sodium-glucose Co-transporter 2 inhibitors in patients with type 2 diabetes: A systematic review and meta-analysis. *PloS One* (2016) 11:e166125. doi: 10.1371/journal.pone.0166125

8. Bolinder J, Ljunggren O, Kullberg J, Johansson L, Wilding J, Langkilde AM, et al. Effects of dapagliflozin on body weight, total fat mass, and regional adipose tissue distribution in patients with type 2 diabetes mellitus with inadequate glycemic control on metformin. *J Clin Endocrinol Metab* (2012) 97:1020–31. doi: 10.1210/jc.2011-2260

9. Inoue H, Morino K, Ugi S, Tanaka-Mizuno S, Fuse K, Miyazawa I, et al. Ipragliflozin, a sodium-glucose cotransporter 2 inhibitor, reduces bodyweight and fat mass, but not muscle mass, in Japanese type 2 diabetes patients treated with insulin: A randomized clinical trial. *J Diabetes Investig* (2019) 10:1012–21. doi: 10.1111/jdi.12985

10. Levelt E, Pavlides M, Banerjee R, Mahmod M, Kelly C, Sellwood J, et al. Ectopic and visceral fat deposition in lean and obese patients with type 2 diabetes. *J Am Coll Cardiol* (2016) 68:53–63. doi: 10.1016/j.jacc.2016.03.597

11. Neeland IJ, McGuire DK, Chilton R, Crowe S, Lund SS, Woerle HJ, et al. Empagliflozin reduces body weight and indices of adipose distribution in patients with type 2 diabetes mellitus. *Diabetes Vasc Dis Res* (2016) 13:119–26. doi: 10.1177/1479164115616901

12. Liberati A, Altman DG, Tetzlaff J, Mulrow C, Gotzsche PC, Ioannidis JP, et al. The PRISMA statement for reporting systematic reviews and meta-analyses of studies that evaluate healthcare interventions: Explanation and elaboration. *BMJ* (2009) 339:b2700. doi: 10.1136/bmj.b2700

13. Kim G, Ridderstra Le M, Andersen KR, Zeller C, Woerle HJ, Broedl UC. Effect of empagliflozin compared with glimepiride as add-on to metformin for 2 years on the amount and distribution of body fat in patients with type 2 diabetes. *Diabetologia* (2014) 57:S330–1. doi: 10.1007/s00125-014-3355-0

14. Bando Y, Ogawa A, Ishikura K, Kanehara H, Hisada A, Notumata K, et al. The effects of ipragliflozin on the liver-to-spleen attenuation ratio as assessed by computed tomography and on alanine transaminase levels in Japanese patients with type 2 diabetes mellitus. *Diabetol Int* (2017) 8:218–27. doi: 10.1007/s13340-016-0302-y

15. Ito D, Shimizu S, Inoue K, Saito D, Yanagisawa M, Inukai K, et al. Comparison of ipragliflozin and pioglitazone effects on nonalcoholic fatty liver disease in patients with type 2 diabetes: A randomized, 24-week, open-label, active-controlled trial. *Diabetes Care* (2017) 40:1364–72. doi: 10.2337/dc17-0518

16. Shimizu M, Suzuki K, Kato K, Jojima T, Iijima T, Murohisa T, et al. Evaluation of the effects of dapagliflozin, a sodium-glucose co-transporter-2 inhibitor, on hepatic steatosis and fibrosis using transient elastography in patients with type 2 diabetes and non-alcoholic fatty liver disease. *Diabetes Obes Metab* (2019) 21:285–92. doi: 10.1111/dom.13520

17. Sakurai S, Jojima T, Iijima T, Tomaru T, Usui I, Aso Y. Empagliflozin decreases the plasma concentration of plasminogen activator inhibitor-1 (PAI-1) in patients with type 2 diabetes: Association with improvement of fibrinolysis. *J Diabetes Complications.* (2020) 34:107703. doi: 10.1016/j.jdiacomp.2020.107703

18. Han E, Lee YH, Lee BW, Kang ES, Cha BS. Ipragliflozin additively ameliorates non-alcoholic fatty liver disease in patients with type 2 diabetes controlled with metformin and pioglitazone: A 24-week randomized controlled trial. *J Clin Med* (2020) 9(1):259. doi: 10.3390/jcm9010259

19. Gaborit B, Ancel P, Abdullah AE, Maurice F, Abdesselam I, Calen A, et al. Effect of empagliflozin on ectopic fat stores and myocardial energetics in type 2 diabetes: The EMPACEF study. *Cardiovasc Diabetol* (2021) 20:57. doi: 10.1186/s12933-021-01237-2

20. Chehrehgosha H, Sohrabi MR, Ismail-Beigi F, Malek M, Reza BM, Zamani F, et al. Empagliflozin improves liver steatosis and fibrosis in patients with non-alcoholic fatty liver disease and type 2 diabetes: A randomized, double-blind, placebo-controlled clinical trial. *Diabetes Ther* (2021) 12:843–61. doi: 10.1007/s13300-021-01011-3

21. Horibe K, Morino K, Miyazawa I, Tanaka-Mizuno S, Kondo K, Sato D, et al. Metabolic changes induced by dapagliflozin, an SGLT2 inhibitor, in Japanese patients with type 2 diabetes treated by oral anti-diabetic agents: A randomized, clinical trial. *Diabetes Res Clin Pract* (2022) 186:109781. doi: 10.1016/j.diabres.2022.109781

22. Ridderstrale M, Andersen KR, Zeller C, Kim G, Woerle HJ, Broedl UC. Comparison of empagliflozin and glimepiride as add-on to metformin in patients with type 2 diabetes: A 104-week randomised, active-controlled, double-blind, phase 3 trial. *Lancet Diabetes Endocrinol* (2014) 2:691–700. doi: 10.1016/S2213-8587(14)70120-2

23. Bando Y, Tohyama H, Aoki K, Kanehara H, Hisada A, Okafuji K, et al. Ipragliflozin lowers small, dense low-density lipoprotein cholesterol levels in Japanese patients with type 2 diabetes mellitus. *J Clin Transl Endocrinol* (2016) 6:1–7. doi: 10.1016/j.jcte.2016.06.001

24. Lundh A, Lexchin J, Mintzes B, Schroll JB, Bero L. Industry sponsorship and research outcome. *Cochrane Database Syst Rev* (2017) 2:R33. doi: 10.1002/14651858.MR000033.pub3

25. Rajeev SP, Cuthbertson DJ, Wilding JP. Energy balance and metabolic changes with sodium-glucose co-transporter 2 inhibition. *Diabetes Obes Metab* (2016) 18:125–34. doi: 10.1111/dom.12578

26. Calapkulu M, Cander S, Gul OO, Ersoy C. Lipid profile in type 2 diabetic patients with new dapagliflozin treatment; actual clinical experience data of six months retrospective lipid profile from single center. *Diabetes Metab Syndr* (2019) 13:1031–4. doi: 10.1016/j.dsx.2019.01.016

27. Hayashi T, Fukui T, Nakanishi N, Yamamoto S, Tomoyasu M, Osamura A, et al. Dapagliflozin decreases small dense low-density lipoprotein-cholesterol and increases high-density lipoprotein 2-cholesterol in patients with type 2 diabetes: Comparison with sitagliptin. *Cardiovasc Diabetol* (2017) 16:8. doi: 10.1186/s12933-016-0491-5

28. Rau M, Thiele K, Korbinian Hartmann NU, Möllmann J, Wied S, Böhm M, et al. Effects of empagliflozin on lipoprotein subfractions in patients with type 2 diabetes: data from a randomized, placebo-controlled study. *Atherosclerosis* (2021) 330:8–13. doi: 10.1016/j.atherosclerosis.2021.06.915

29. Basu D, Huggins LA, Scerbo D, Obunike J, Mullick AE, Rothenberg PL, et al. Mechanism of increased LDL (Low-density lipoprotein) and decreased triglycerides with SGLT2 (Sodium-glucose cotransporter 2) inhibition. *Arterioscler Thromb Vasc Biol* (2018) 38:2207–16. doi: 10.1161/ATVBAHA.118.311339

30. Fuster JJ, Ouchi N, Gokce N, Walsh K. Obesity-induced changes in adipose tissue microenvironment and their impact on cardiovascular disease. *Circ Res* (2016) 118:1786–807. doi: 10.1161/CIRCRESAHA.115.306885

31. Oikonomou EK, Antoniades C. The role of adipose tissue in cardiovascular health and disease. *Nat Rev Cardiol* (2019) 16:83–99. doi: 10.1038/s41569-018-0097-6

32. Guzik TJ, Skiba DS, Touyz RM, Harrison DG. The role of infiltrating immune cells in dysfunctional adipose tissue. *Cardiovasc Res* (2017) 113:1009–23. doi: 10.1093/cvr/cvx108

33. Vilahur G, Ben-Aicha S, Badimon L. New insights into the role of adipose tissue in thrombosis. *Cardiovasc Res* (2017) 113:1046–54. doi: 10.1093/cvr/cvx086

34. Nesti L, Pugliese NR, Chiriaco M, Trico D, Baldi S, Natali A. Epicardial adipose tissue thickness is associated with reduced peak oxygen consumption and systolic reserve in patients with type 2 diabetes and normal heart function. *Diabetes Obes Metab* (2023) 25:177–88. doi: 10.1111/dom.14861

35. Salvatore T, Galiero R, Caturano A, Vetrano E, Rinaldi L, Coviello F, et al. Dysregulated epicardial adipose tissue as a risk factor and potential therapeutic target of heart failure with preserved ejection fraction in diabetes. *Biomolecules* (2022) 12(2):176. doi: 10.3390/biom12020176

36. Masson W, Lavalle-Cobo A, Nogueira JP. Effect of SGLT2-inhibitors on epicardial adipose tissue: A meta-analysis. *Cells-Basel* (2021) 10(8):2150. doi: 10.3390/cells10082150

37. Wei Q, Xu X, Guo L, Li J, Li L. Effect of SGLT2 inhibitors on type 2 diabetes mellitus with non-alcoholic fatty liver disease: A meta-analysis of randomized controlled trials. *Front Endocrinol (Lausanne).* (2021) 12:635556. doi: 10.3389/fendo.2021.635556

38. Cowie MR, Fisher M. SGLT2 inhibitors: Mechanisms of cardiovascular benefit beyond glycemic control. *Nat Rev Cardiol* (2020) 17:761–72. doi: 10.1038/s41569-020-0406-8

39. Sugiyama S, Jinnouchi H, Kurinami N, Hieshima K, Yoshida A, Jinnouchi K, et al. Dapagliflozin reduces fat mass without affecting muscle mass in type 2 diabetes. *J Atheroscler Thromb* (2018) 25:467–76. doi: 10.5551/jat.40873

40. Sawada Y, Izumida Y, Takeuchi Y, Aita Y, Wada N, Li E, et al. Effect of sodium-glucose cotransporter 2 (SGLT2) inhibition on weight loss is partly mediated by liver-brain-adipose neurocircuitry. *Biochem Biophys Res Commun* (2017) 493:40–5. doi: 10.1016/j.bbrc.2017.09.081

41. Lauritsen KM, Voigt JH, Pedersen SB, Hansen TK, Moller N, Jessen N, et al. Effects of SGLT2 inhibition on lipid transport in adipose tissue in type 2 diabetes. *Endocr Connect.* (2022) 11(4):e210558. doi: 10.1530/EC-21-0558

42. Xu L, Ota T. Emerging roles of SGLT2 inhibitors in obesity and insulin resistance: Focus on fat browning and macrophage polarization. *Adipocyte* (2018) 7:121–8. doi: 10.1080/21623945.2017.1413516

43. Sasso FC, Simeon V, Galiero R, Caturano A, De Nicola L, Chiodini P, et al. The number of risk factors not at target is associated with cardiovascular risk in a type 2 diabetic population with albuminuria in primary cardiovascular prevention. *Post-hoc Anal NID-2 trial. Cardiovasc Diabetol* (2022) 21:235. doi: 10.1186/s12933-022-01674-7

frontiers | Frontiers in Endocrinology

TYPE Original Research
PUBLISHED 27 January 2023
DOI 10.3389/fendo.2022.1089938



OPEN ACCESS

EDITED BY
Alexandre Gabarra Oliveira,
São Paulo State University, Brazil

REVIEWED BY
Aisha Musaazi Sebunya Nakitto,
Victoria University, Uganda
Zahra Abedi Kichi,
LMU Munich University Hospital, Germany
Giovanni Tarantino,
University of Naples Federico II, Italy

*CORRESPONDENCE
Ana Flávia Marçal Pessoa
ana.pessoa@fm.usp.br

†These authors have contributed equally to this work

SPECIALTY SECTION
This article was submitted to Obesity, a section of the journal Frontiers in Endocrinology

RECEIVED 04 November 2022
ACCEPTED 26 December 2022
PUBLISHED 27 January 2023

CITATION
Nehmi-Filho V, Santamarina AB, de Freitas JA, Trarbach EB, de Oliveira DR, Palace-Berl F, de Souza E, de Miranda DA, Escamilla-Garcia A, Otoch JP and Pessoa AFM (2023) Novel nutraceutical supplements with yeast β-glucan, prebiotics, minerals, and *Silybum marianum* (silymarin) ameliorate obesity-related metabolic and clinical parameters: A double-blind randomized trial. *Front. Endocrinol.* 13:1089938. doi: 10.3389/fendo.2022.1089938



# Novel nutraceutical supplements with yeast β-glucan, prebiotics, minerals, and *Silybum marianum* (silymarin) ameliorate obesity-related metabolic and clinical parameters: A double-blind randomized trial

Victor Nehmi-Filho[1,2†], Aline Boveto Santamarina[3†], Jéssica Alves de Freitas[1,2], Ericka Barbosa Trarbach[4], Daniela Rodrigues de Oliveira[1,5], Fanny Palace-Berl[1], Erica de Souza[6], Danielle Araujo de Miranda[7], Antonio Escamilla-Garcia[8], José Pinhata Otoch[1,2,8] and Ana Flávia Marçal Pessoa[1,2,9*]

[1]Natural Products and Derivatives Laboratory (LIM-26), Department of Surgery, University of São Paulo Medical School, São Paulo, SP, Brazil, [2]Research and Development Efeom Nutrition S/A, São Paulo, SP, Brazil, [3]Department of Biosciences, Federal University of São Paulo (UNIFESP), Santos, SP, Brazil, [4]Laboratory of Cellular and Molecular Endocrinology (LIM25), Division of Endocrinology and Metabology, Clinics Hospital, University of São Paulo Medical School, São Paulo, SP, Brazil, [5]Department of Pharmacology & Toxicology, Medical College of Wisconsin, Milwaukee, WI, United States, [6]Monte Azul Ambulatory, São Paulo, SP, Brazil, [7]Departament of Physiology, Escola Paulista de Medicina/ Universidade Federal de São Paulo, São Paulo, SP, Brazil, [8]University Hospital of the University of São Paulo, University of São Paulo Medical School, São Paulo, SP, Brazil, [9]Natural Products Committee, Brazilian Academic Consortium for Integrative Health (CABSIN), São Paulo, Brazil

**Purpose:** It is known that obesity has a multifactorial etiology that involves genetic and environmental factors. The WHO estimates the worldwide prevalence of 1.9 billion overweight adults and more than 650 million people with obesity. These alarming data highlight the high and growing prevalence of obesity and represent a risk factor for the development and aggravation of other chronic diseases, such as nonalcoholic fatty liver disease (NAFLD) that is frequently considered the hepatic outcome of type 2 diabetes. The use of non-pharmacological therapies such as food supplements, nutraceuticals, and natural integrative therapies has grown as an alternative tool for obesity-related diseases compared to conventional medications. However, it is a still little explored research field and lacks scientific evidence of therapeutic effectiveness. Considering this, the aim is to evaluate whether a new nutraceutical supplement composition can improve and supply essential mineral nutrients, providing an improvement of obesity-related metabolic and endocrine parameters.

**Methods:** Sedentary volunteers (women and men) with body mass index (BMI) ≤34.9 kg/m$^2$ were divided into two groups: Novel Nutraceutical Supplement_(S) (n = 30) and Novel Nutraceutical Supplement (n = 29), differing in the absence (S) or

presence of silymarin, respectively. Volunteers were instructed to take two capsules in the morning and two capsules in the evening. No nutritional intervention was performed during the study period. The data (anthropometrics and anamneses) and harvest blood (biochemistry and hormonal exams) were collected at three different time points: baseline time [day 0 (T0)], day 90 (T90), and day 180 (T180) post-supplementation.

**Results:** In the anthropometric analysis, the waist circumference in middle abdomen (WC-mid) and waist circumference in iliac crest (WC-IC) were reduced. Also, the waist-to-height ratio (WHt R) and waist-to-hip ratio (WHR) seem to slightly decrease alongside the supplementation period with both nutraceutical supplements tested as well as transaminase enzyme ratio [aspartate aminotransferase (AST)/alanine aminotransferase (ALT) ratio (AAR)], a known as a biomarker of NAFLD, and endocrine hormones cortisol and thyroid-stimulating hormone (TSH) at 90 and 180 days post-supplementation.

**Conclusions:** In a condition associated with sedentary and no nutritional intervention, the new nutraceutical supplement composition demonstrated the ability to be a strong and newfangled tool to improve important biomarkers associated with obesity and its comorbidities.

KEYWORDS

**nutraceutics, supplement, *Silybum marianum*, prebiotic, obesity, endocrine parameters, transaminases**

## 1 Introduction

The etiology of chronic non-communicable diseases such as obesity is multifactorial, including genetics and the environment (1). These diseases are the world's leading cause of mortality (2, 3). Data from the World Health Organization (WHO) estimate the worldwide prevalence of 1.9 billion overweight adults [body mass index (BMI) ≥25 kg/m$^2$] and more than 650 million people with obesity (BMI ≥30 kg/m$^2$) (3). Recently, during the critical phase of the pandemic, the prevalence of chronic non-communicable diseases was closely related to higher mortality in hospitalization due to coronavirus disease 2019 (COVID-19) (4). These alarming data highlight the high and growing prevalence of obesity that represents a risk factor for the development and aggravation of other metabolic diseases.

Considering this, the incessant search for nutritional intervention strategies is essential to pursue the mitigation of obesity and its comorbidities. In this sense, the use of natural products and derivatives as non-pharmacological strategies can be an alternative in the prevention and treatment of acute or chronic diseases. These tools could contribute to preventing or reducing obesity-related negative outcomes, promoting longer life spans and better-quality lives (5). Thus, the use of food supplements, nutraceuticals, and natural integrative therapies has grown compared to conventional medications, which are still necessary and indispensable for the adequate treatment of some conditions (6, 7). Indeed, non-pharmacological therapies seem to be promising strategies for the prevention and treatment of metabolic–inflammatory diseases, such as obesity, metabolic syndrome, dyslipidemia, and type 2 diabetes (8–10).

Nevertheless, in this study, we also intend to contribute to the construction of knowledge for clinical practice using anthropometric assessment and serum tests reachable to practitioners' daily routines. Previous studies have shown that increased neck circumference in obese adults is related to increased cardiovascular and inflammatory risk, acting as an anthropometric predictor of cardiovascular and inflammatory risk (11). Also, the waist-to-height ratio (WHtR), a measure with significant statistical representation, works as a good predictor of metabolic syndrome and appears to be directly proportional to inflammatory levels and correlated with poor eating habits (12–14).

Several cellular mechanisms are involved in obesity pathologies such as the metabolic pathways activated by directly influencing the insulin signaling in insulin-target tissues such as the liver, eventually leading to insulin resistance (15). Thus, nonalcoholic fatty liver disease (NAFLD) is frequently considered the hepatic outcome of type 2 diabetes. Indeed, insulin resistance also plays a central role in the development of the fatty liver (16), since hepatic fatty acid oxidation is reduced by mitochondrial dysfunctions triggered by obesity, resulting in hepatic accumulation of triacylglycerols (17, 18). Another common metabolic alteration in obesity is persistent and systemic low-grade inflammation (19, 20), which has been termed metainflammation. Metainflammation is closely linked to insulin resistance mechanisms that feedback each other, perpetuating long-term metabolic dysfunction (21). The combination of low-grade inflammation processes and insulin

resistance establishment is an important link between obesity and its comorbidities.

The increased incidence and prevalence of obesity-related comorbidities is a concern still unsolved by worldwide public health regulators. Despite efforts to mitigate obesity, little effect has been noticed on the increase of all diseases associated with it (22). Considering this, the benefits of several natural compounds have been investigated in the obesity research field nowadays. In this sense, the effect of isolated prebiotic compounds, such as fructooligosaccharides (FOSs) (23), galactooligosaccharides (GOSs) (24), and yeast β-glucans (25, 26), has been related to improved metabolic markers recovering the health status. Also, supplementation with minerals such as magnesium (27), zinc (28), and selenium (29) and plant-derived compounds such as *Silybum marianum* (silymarin) (30) has displayed positive effects in obesity models. Compounds such as FOS and GOS display a potential effect of modulating the gut microbiome, which is closely linked to inflammatory modulation (31). The same aspect might be related to yeast β-glucans (32), magnesium (27), zinc (28), and selenium (33), which are known for the immune system-strengthening action. Likewise, silymarin, the bioactive compound obtained from milk thistle (*S. marianum*), has been used over the centuries to primarily treat liver diseases and protect the liver against obesity injury, contributing to the restoration of hepatic function (34). The main bioactive compound of silymarin is the component called silybin. Silybin is a flavonolignan that has different activities such as antioxidant and anti-inflammatory properties (35). In this sense, preclinical protocols testing a combination of these compounds have shown their benefits in the improvement of mitochondrial activity and key inflammatory molecules involved in the pathogenesis of several non-communicable chronic diseases such as type 2 diabetes, obesity, and cardiovascular diseases (9, 10). The preclinical model compared the effect of the supplement components separately and in combination, and findings suggest that the nutraceutical compounds might have a stronger synergic effect, representing an innovative tool for obesity and insulin resistance management.

Therefore, in this study, we aim to apply our previously developed supplement composition containing yeast β-glucan, prebiotics, minerals, and *S. marianum* (milk thistle or silymarin) (9, 10) as a tool to modulate inflammatory and metabolic responses in a population with obesity. The main hypothesis is that the supplements can improve and supply essential micronutrients such as zinc, magnesium, and selenium, which are usually deficient in populations with obesity (36), providing an improvement of fatty liver diseases through metabolic and endocrine pathways.

# 2 Materials and methods

## 2.1 Ethics committee approval

This work was approved by the HC-FMUSP Research Ethics Committee under the CAAE number 39984320.5.0000.0068. This research project was carried out following the relevant guidelines and regulations and was approved by the Ethics Committee for the Analysis of Research Projects (CAPPesq). This study received approval from the Brazilian National System of Genetic Registration (SisGen), under the number AC29D69, and registered as a clinical trial under identification number NCT04810572 (ClinicalTrials.gov).

## 2.2 Recruitment of volunteers and experimental design

The "Novel Nutraceutical Supplement Trial" is a randomized controlled trial addressing sedentary people with three assessment points (baseline and 90 and 180 days post-supplementation) from Monte Azul Ambulatory, São Paulo, SP, Brazil, and online invitation between March and June 2021 (n = 133). Stratified randomization was applied to ensure a balance of baseline key factors between groups. In this study, age, BMI, and gender were considered baseline characteristics for sample stratification before randomization. The pharmaceutical team responsible for preparing the supplement capsules was the blind spot between participants and researchers until the end of the study. The sample size enrolled was based on a calculation determined using the G*Power software (37). Assuming an F test with a type I error of 5% at 95% power and a success rate (effect size) of 0.2, the required total sample size was 66. Due to the long-term period of supplementation protocol and the progress of the COVID-19 pandemic during the protocol, to account for a potential dropout of 20%, we inflate this to at least 80 participants.

The inclusion criteria were as follows: healthy volunteers of both genders aged between 44 and 64 years; BMI ≤34.9 kg/m$^2$; no diet intervention; and sedentary lifestyle. To guarantee that the volunteers had a sedentary lifestyle, we applied International Physical Activity Questionnaire (IPAQ)-Short Version (38) and presented it in Table 1. The exclusion criteria were as follows: volunteers who are allergic to some of the components of the nutraceutical formulation; the use of insulin, corticoids, and non-steroidal anti-inflammatory drugs for more than 15 days; AIDS; hepatitis; pregnancy; and patients under treatment with chemotherapy.

TABLE 1 Population physical activity level is classified by the International Physical Activity Questionnaire (IPAQ).

| Physical activity level | Novel Nutraceutical Supplement_(S) | | | Novel Nutraceutical Supplement | | |
|---|---|---|---|---|---|---|
| | T0 | T90 | T180 | T0 | T90 | T180 |
| **Inactive** | 63.33% (n=19) | 63.33% (n=19) | 66.66% (n=20) | 62.06% (n=18) | 62.06% (n=18) | 62.06% (n=18) |
| **Minimally active** | 36.66% (n=11) | 36.66% (n=11) | 33.33% (n=10) | 37.93% (n=11) | 37.93% (n=11) | 37.93% (n=11) |
| **HEPA active** | - | - | - | - | - | - |

HEPA active, health-enhancing physical activity.

10.3389/fendo.2022.1089938

All volunteers signed a term of free and informed consent before starting the study and could withdraw the consent at any time. Therefore, volunteers were divided into two groups: Novel Nutraceutical Supplement_(S) (n = 30) and Novel Nutraceutical Supplement (n = 29) Volunteers were instructed to take two capsules of the supplements in the morning and two capsules in the evening. The participants were instructed to maintain their eating habits, and no nutritional intervention was performed during the study period.

We used a Consolidated Standards of Reporting Trials (CONSORT) (39) flow diagram to display the trial. Initially, during the enrollment process, a total of 133 volunteers were assessed. At that stage, 42 people were excluded because they did not meet the inclusion criteria (n = 9) or declined to participate (n = 33). Thus, 91 participants were randomized into the two experimental groups, the Novel Nutraceutical Supplement_(S) group (n = 47) and the Novel Nutraceutical Supplement group (n = 44), and initiated the supplementation period. During the study follow-up at the T90 in the Novel Nutraceutical Supplement_(S) group, 13 participants declined the protocol because of time constraints (n = 7) or for no alleged reason (n = 6) and 34 participants kept on with the study. In the Novel Nutraceutical Supplement group at T90, a total of nine participants declined the study because of time constraints (n = 4) or for no alleged reason (n = 5) and 35 participants were followed in the study. At T180 on Novel Nutraceutical Supplement_(S), four people were excluded from the protocol for COVID-19 diagnosis (n = 2) or no alleged reasons (n = 2); a total of 30 participants then completed the study. In the Novel Nutraceutical Supplement group, six participants were excluded because of COVID-19 diagnosis (n = 1) or no alleged reasons (n = 5); 29 participants completed the supplementation protocol as demonstrated in the CONSORT flowchart (Figure 1). The data and harvested blood were obtained from the volunteers at three different time points: baseline time [day 0 (T0)] and day 90 (T90) and day 180 (T180) post-supplementation as shown in Table 2.

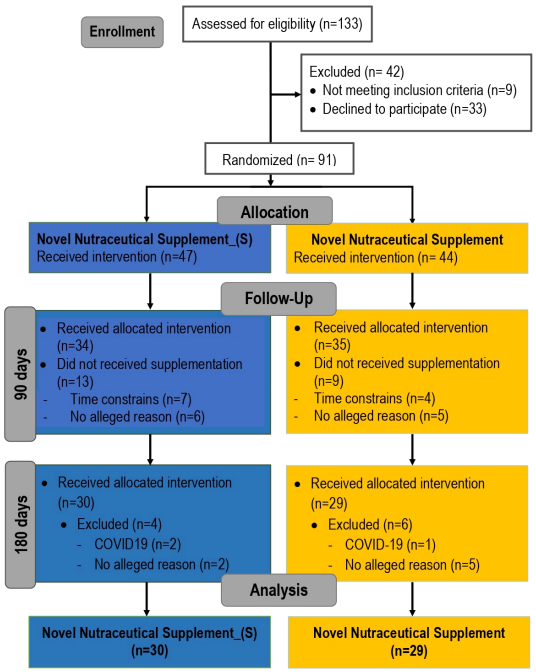


FIGURE 1
Consolidated Standards of Reporting Trials (CONSORT) flowchart describing the recruitment of volunteers and the experimental design carried out on this clinical trial.

TABLE 2 Anthropometric and demographic characterization of the study population.

| | Novel Nutraceutical Supplement_(S) | | | Novel Nutraceutical Supplement | | | *p* |
|---|---|---|---|---|---|---|---|
| **Variables** | **T0** | **T90** | **T180** | **T0** | **T90** | **T180** | |
| **Sample Size** | 30 | | | 29 | | | |
| **Age (years)** | 54.10 ± 5.52 | | | 54.83 ± 4.59 | | | – |
| **Height (cm)** | 162.0 (153.0-171.0) | | | 161.5 (155.8-186.0) | | | – |
| **Body Mass (kg)** | 72.10 ± 12.50 | 72.17 ± 11.69 | 72.44 ± 12.34 | 73.47 ± 12.34 | 73.85 ± 12.47 | 74.03 ± 12.64 | – |
| **BMI (kg/m$^2$)** | 27.23 ± 3.28 | 27.29 ± 3.10 | 27.38 ± 3.31 | 27.65 ± 3.45 | 27.80 ± 3.58 | 27.88 ± 3.64 | – |
| **Neck (cm)** | 35.55 ± 3.16 | 35.70 ± 4.06 | 35.03 ± 3.08 | 36.12 ± 3.02 | 35.94 ± 3.51 | 35.78 ± 3.34 | – |
| **WC-mid (cm)** | 90.68 ± 9.64 | 89.77 ± 9.76 | 88.89 ± 9.82 | 92.12 ± 10.66 | 91.64 ± 11.00 | 90.53 ± 10.48 | 0.010[a]; 0.030[b] |
| **Hip (cm)** | 105.29 ± 6.88 | 103.74 ± 8.52 | 104.79 ± 7.00 | 104.54 ± 7.01 | 104.15 ± 8.06 | 105.00 ± 7.21 | – |
| **WC-IC (cm)** | 99.46 ± 8.25 | 100.18 ± 8.14 | 99.74 ± 9.25 | 100.06 ± 8.44 | 102.76 ± 8.20 | 99.81 ± 9.01 | 0.010[c]; <0.010[d] |
| **WHtR** | 0.57 ± 0.59 | 0.56 ± 0.06 | 0.55 ± 0.05 | 0.59 ± 0.06 | 0.57 ± 0.06 | 0.56 ± 0.06 | – |
| **WHR** | 0.86 ± 0.07 | 0.87 ± 0.08 | 0.87 ± 0.07 | 0.91 ± 0.07 | 0.88 ± 0.07 | 0.88 ± 0.09 | – |

BMI, body mass index; WC-mid, waist circumference in middle abdomen; WC-IC, waist circumference in iliac crest; WHtR, waist-to-height ratio; WHR, waist-to-hip ratio.
Data values are expressed as mean ± SEM.
[a] Significant difference Supplement_(S) T0 vs. T180.
[b] Significant difference Supplement_(S) T90 vs. T180.
[c] Significant difference Novel Supplement T0 vs. T90.
[d] Significant difference Novel Supplement T90 vs. T180.
T0, day 0; T90, 90 days post-supplementation; T180, 180 days post-supplementation.

## 2.3 Novel nutraceutical supplement formulations

We prepared two formulations (Patent number: BR 10 2020 016156 3): Formulation 1 (n = 30): Novel Nutraceutical Supplement_(S) (without silymarin), developed and tested in the present study, contained the following components: zinc (Zn) 1%, magnesium (Mg) 1% (Purifarma Distribuidora Quımica e Farmacêutica, São Paulo, Brazil), FOSs 45% (NutraFlora®, Westchester, Illinois, USA), selenomethionine (Se) 0.01%, GOSs 10%, tixosil 5%, and 1.3/1.6-(b-glycosidic bonds) yeast b-glucans (Saccharomyces cerevisiae) 6% (Biorigin, São Paulo, Brazil); and Formulation 2 (n = 29): zinc (Zn) 1%, magnesium (Mg) 1% (Purifarma Distribuidora Química e Farmacêutica, São Paulo, Brazil), FOSs 45% (NutraFlora®, Westchester, Illinois, USA), selenomethionine (Se) 0.01%, GOSs 10%, tixosil 5%, 1.3/1.6-(b-glycosidic bonds) yeast b-glucans (Saccharomyces cerevisiae) 6% (Biorigin, São Paulo, Brazil), and S. marianum (silymarin extract 9%) (SM Empreendimento Farmacê utica LTDA, São Paulo, Brazil). The percentages of the Novel Nutraceutical Supplement were determined following recommendations and parameters published by the European Food Safety Authority (EFSA) (40). The formulations of the novel nutraceutical supplements were manipulated by the compounding pharmacy "Solis Magistral Farmácia Homeopática Sensitiva (São Paulo, Brazil)," which kept the double blinding point of this clinical study.

## 2.4 Anthropometric parameters

Anthropometric parameters were collected and analyzed at baseline time (T0) and T90 and T180 post-supplementation. The volunteers were weighed using the Body Composition Scale 2 (Xiaomi Mi, Beijing, China). The hip (cm), iliac crest (cm), waist (cm), and neck (cm) circumferences and height (cm) were measured using a plastic tape measurer. BMI was calculated by dividing weight (kg) by the square of height (m).

## 2.5 Aspartate aminotransferase (AST) and alanine aminotransferase (ALT) ratio (AAR), biochemistry, and endocrine parameters

The volunteers' blood sample was collected on T0 and T90 and T180 post-supplementation. All samples were collected between 7:00 a.m. and 9:00 a.m. in the morning. The samples were processed on the same day of collection to immediately perform biochemical analysis and endocrine parameters. Total cholesterol, triglycerides (TGs), non-high-density lipoprotein (HDL)-cholesterol, low-density lipoprotein (LDL)-cholesterol, very-low-density lipoprotein (VLDL)-cholesterol, HDL-cholesterol, aspartate aminotransferase (AST), alanine aminotransferase (ALT), alkaline phosphatase, gamma-glutamyl transferase (gamma-GT), creatinine, insulin, cortisol, thyroxine (T4), thyroid-stimulating hormone (TSH), and C-reactive protein (CRP) were analyzed in the serum, and plasma glucose levels obtained. Biochemical analyses and endocrine parameters were measured at the partner laboratory "Fleury Medicina e Saúde." AST/ALT ratio (AAR) was calculated according to Rief et al. (41). Atherogenic index (AI) was determined following the formula AI = [log10(TAG÷HDL-c)].

## 2.6 Statistical analysis

All statistical analyses were conducted following the CONSORT recommendations (39). Data were classified as parametric or nonparametric based on the Shapiro–Wilks test. Parametric data are represented as mean ± standard deviation, and nonparametric data are represented as median and interquartile range. Comparisons between groups involving parametric data were performed with repeated-measures analysis of variance (ANOVA). Comparisons between groups involving nonparametric data were performed using the Friedman test. Analyses were performed using STATA® 14.0 (Stata Corp. LCC, College Station, TX, USA) and GraphPad Prism 9.0 (GraphPad Software, La Jolla, CA, USA) software.

# 3 Results

## 3.1 Novel nutraceutical supplements reduce anthropometric parameters

Accessing the data of the participant's physical activity level evaluated by the IPAQ-Short Version, we can notice that the sample is composed mostly of inactive people, with a small percentage of minimally active people and without individuals practicing health-enhancing physical activity (HEPA active). This characteristic was maintained for both groups throughout the study period, as shown in Table 1. Analyzing the population characterization is noteworthy for the homogeneity between groups through age, height, body mass, and BMI, displaying similar data. Regarding the waist circumference, in the middle abdomen (WC-mid), we have found a significant reduction in the Supplement_(S) group at T0 and T90 compared to T180. We also have found an increase in waist circumference in the iliac crest (WC-IC) at T0 vs. T90 followed by a significant reduction at T90 compared to T180 in the novel supplement group. The BMI, neck, and hip circumference did not differ among the evaluations. Despite the absence of a statistical difference, the WHtR and waist-to-hip ratio (WHR) seem to slightly decrease alongside the supplementation period in both groups. These data are presented in Table 2.

## 3.2 Lipid profile under the nutraceutical supplement effect

We evaluated the serum total cholesterol, TGs, and lipoproteins in all volunteers who received the Novel Nutraceutical Supplement_(S) (n = 30) and the Novel Nutraceutical Supplement (n = 29) (Figure 1). Neither of the supplements changed the total cholesterol (Figure 2A), TGs (Figure 2B), non-HDL-cholesterol (Figure 2C), HDL-cholesterol (Figure 2D), LDL-cholesterol (Figure 2E), VLDL-cholesterol (Figure 2F), and AI (Figure 2G) at 90 and 180 days post-supplementation.

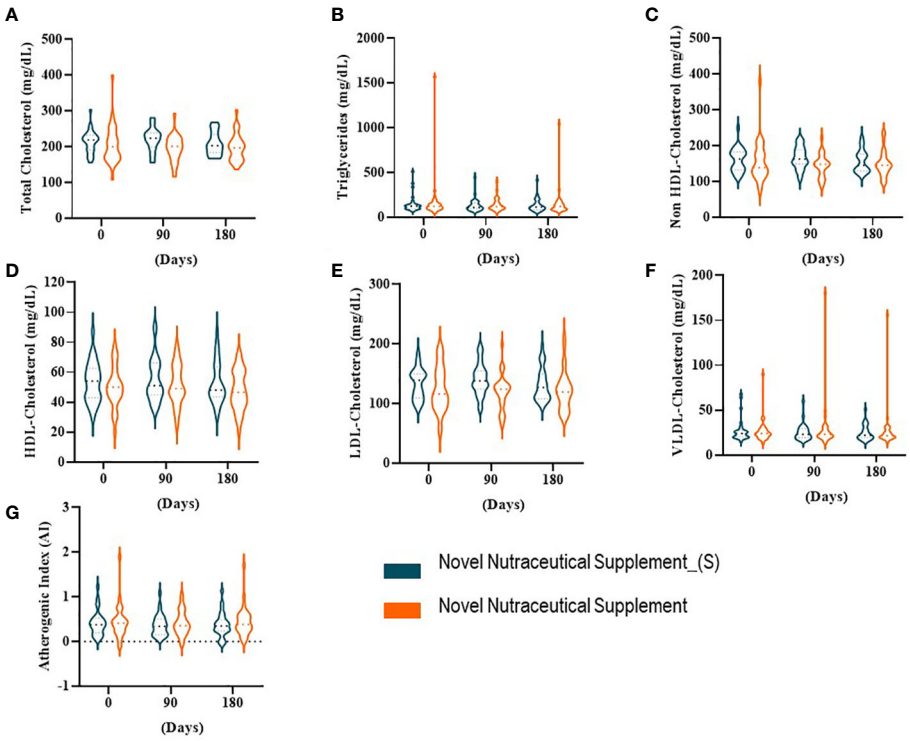


FIGURE 2
Lipid profile at baseline time (Day 0) and 90 and 180 days post-supplementation. **(A)** Total cholesterol. **(B)** Triglycerides. **(C)** Non-HDL-cholesterol. **(D)** HDL-cholesterol. **(E)** LDL-cholesterol. **(F)** VLDL-cholesterol. **(G)** Atherogenic index (AI). Novel Nutraceutical Supplement_(S) (n = 30) and Novel Nutraceutical Supplement (n = 29). Values are expressed as mean ± SEM or median (min to max, box plot) by plot violin graphic. HDL, high-density lipoprotein; LDL, low-density lipoprotein; VLDL, very-low-density lipoprotein.

## 3.3 Novel nutraceutical supplements modulate biomarkers associated with non-alcoholic fatty liver disease (NAFLD)

In our cohort, liver and renal functions were estimated by liver enzymes and creatinine, respectively. The liver enzymes AST (Figure 3A), alkaline phosphatase (Figure 3C), and gamma-GT (Figure 3E), even creatinine (Figure 3F), did not show differences between baseline time and 90 and 180 days post-supplementation in both groups. However, the ALT enzyme (Figure 3B) in Nutraceutical Supplement_(S) increased only 180 days post-supplementation as compared with 90 days post-supplementation. While in the Novel Nutraceutical Supplement group, we observed that the ALT enzyme (Figure 3B) increased at 90 and 180 days post-supplementation as compared with baseline time. An elevated AAR (Figure 3D) (above 1.0) has been associated with fibrosis/cirrhosis prevalence in NAFLD (41). All groups in baseline time demonstrate elevated AAR (>2.20) (Figure 3D), and Novel Nutraceutical Supplement and Supplement_(S) were able to decrease AAR at 90 and 180 days post-supplementation.

## 3.4 Carbohydrate metabolism and novel nutraceutical supplements

The influence of the supplements on carbohydrate metabolism was measured by glycemia, insulin, and Homeostatic Model Assessment of Insulin Resistance (HOMA-IR). When we analyzed the effects of the supplements on glycemia (Figure 4A) and insulin (Figure 4B) after 90 and 180 days compared to baseline time (day 0), we did not observe changes. While the Nutraceutical Supplement increased glycemia as compared with Novel Nutraceutical Supplement_(S) at 90 days post-supplementation. HOMA-IR (Figure 4C) follows the same pattern compared to the baseline time with the supplementations. Although HOMA-IR increased at the 180-day compared to the 90-day post-supplementation in the Novel Nutraceutical Supplement_(S) group there was no statiscal differences.

## 3.5 Novel nutraceutical supplements influence endocrine hormones

Endocrine hormones cortisol, thyroxine (T4), thyroid-stimulating hormone (TSH), and inflammatory marker C-reactive protein were evaluated at 90 and 180 days post-supplementation. Serum cortisol (Figure 5A) decreased at 90 and 180 days post the Nutraceutical Supplement_(S) vs. the baseline time (day 0), while the Nutraceutical Supplement was not able to modulate this steroid hormone produced by adrenal glands. The thyroid hormone gland T4 and C-reactive protein (Figures 5B, D) were not influenced by either of the supplements during the 180 days of supplementation. While TSH (Figure 5C) decreased in the Novel Nutraceutical Supplement_(S) group when compared to baseline time at all points evaluated, but not in the Novel Nutraceutical Supplement group.

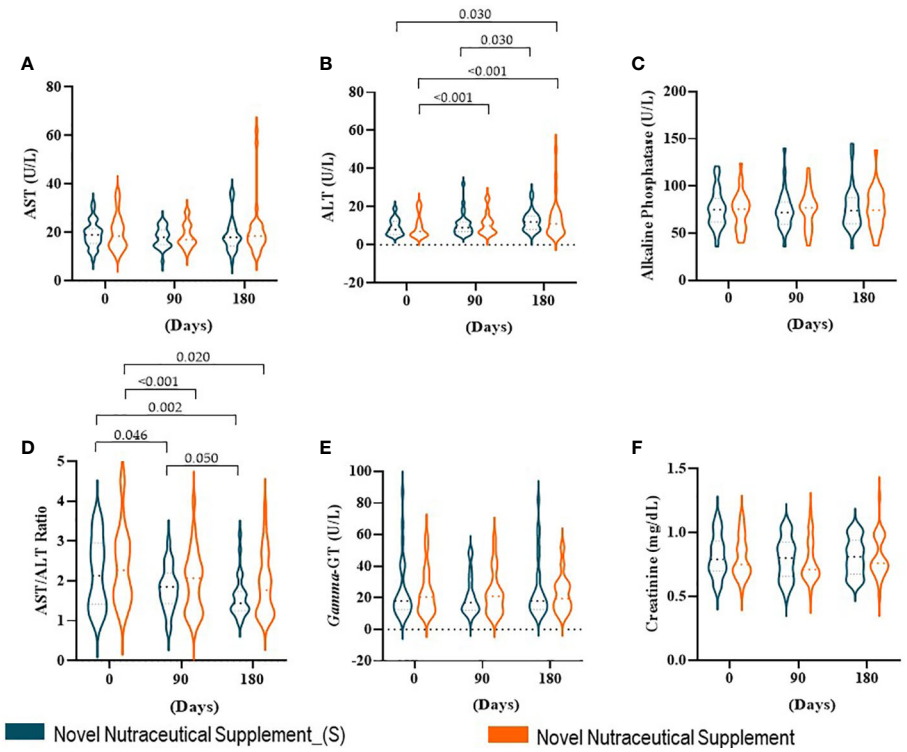


FIGURE 3
Liver enzymes, AST/ALT ratio (AAR), and creatinine at baseline time (Day 0) and 90 and 180 days post-supplementation. **(A)** AST. **(B)** ALT. **(C)** Alkaline phosphatase. **(D)** AAR. **(E)** Gamma-GT. **(F)** Creatinine. Novel Nutraceutical Supplement_(S) (n = 30) and Novel Nutraceutical Supplement (n = 29). Values are expressed as mean ± SEM or median (min to max, box plot) by plot violin graphic. AST, aspartate aminotransferase; ALT, alanine aminotransferase; gamma-GT, gamma-glutamyl transferase.

## 4 Discussion

The application of natural products or their derivatives for the prevention or treatment of several pathologies represents a reasonable and accessible way for clinical practitioners and the general population to use natural resources as viable alternative therapies for health promotion and disease intervention. The development of new products containing different molecules and natural derivatives that interact synergistically has shown beneficial potential, acting holistically and producing few adverse effects on the human body (5). Our recently published findings show the synergistic effects between yeast β-glucan, prebiotic, minerals (selenium, zinc, magnesium), and *S. marianum* of an innovative supplement with nutraceutical properties in a preclinical model of diet-induced obesity (9, 10). These preclinical investigations have shown that after 4 weeks of supplementation, the new nutraceutical reduced fasting glycemia, insulin, HOMA-IR, HOMA-β, dyslipidemia, ectopic fat deposition, and hepatic fibrosis levels. It was probably mediated by molecules

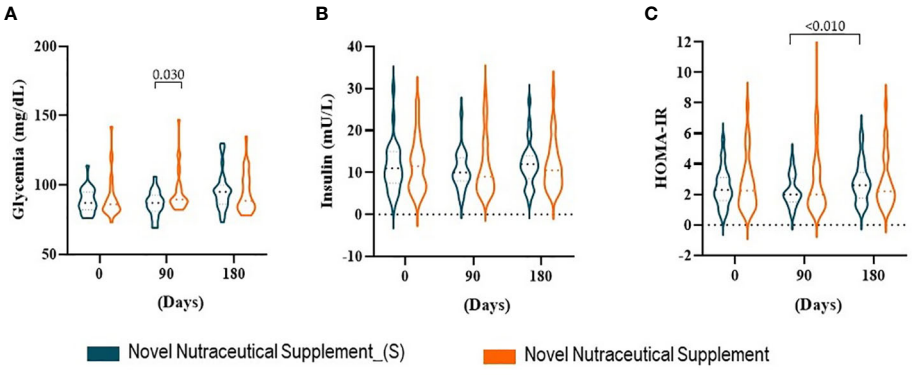


FIGURE 4
Carbohydrate profile at baseline time (Day 0) and 90 and 180 days post-supplementation. **(A)** Glycemia. **(B)** Insulin. **(C)** HOMA-IR. Novel Nutraceutical Supplement_(S) (n = 30) and Novel Nutraceutical Supplement (n = 29). Values are expressed as mean ± SEM or median (min to max, box plot) by plot violin graphic. HOMA-IR, Homeostatic Model Assessment of Insulin Resistance.

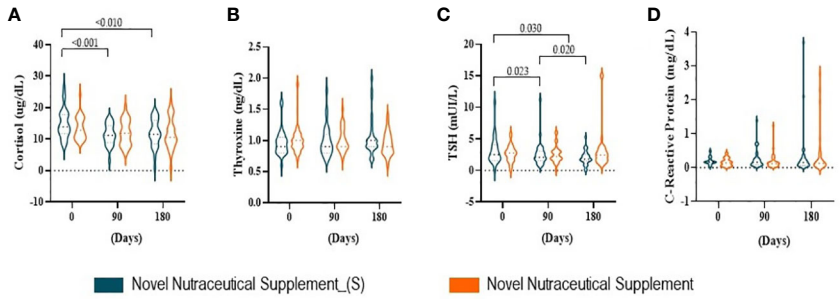


FIGURE 5
Hormones produced by the adrenal and thyroid gland at baseline time (Day 0) and 90 and 180 days post-supplementation. Novel Nutraceutical Supplement_(S) (n = 30) and Novel Nutraceutical Supplement (n = 29). **(A)** Cortisol. **(B)** Thyroxine (T4). **(C)** TSH. **(D)** C-reactive protein. Values are expressed as mean ± SEM or median (min to max, box plot) by plot violin graphic. TSH, thyroid-stimulating hormone.

such as Peroxisome proliferator- activated receptor gamma (PPARg) coactivator 1 α (PGC-1α), interleukin-6 (IL-6), and IL-10, since our previous preclinical study has shown the modulation of this pathway by gene and protein expression changes (9, 10). The glutathione-S-transferase activity status was also modulated by the supplement displaying antioxidant effects. The preclinical studies also display enhanced metabolism promoted by molecules such as PPARα, adenosine monophosphate-activated protein kinase (AMPK)-PGC-1α, and Mitochondrial transcription factor A (TFAM) signaling pathways. Notably, the cortisol/C-reactive protein ratio, a well-characterized marker of the hypothalamic–pituitary–adrenal axis immune interface status, was found to be modulated by the supplement (9, 10).

Based on these preclinical studies and aiming to build up the evidence pyramid in this rapidly growing area of research, we have initiated a double-blind randomized clinical trial applying this supplement formula to participants who were overweight or obese. In this clinical trial, we began by focusing on evaluating clinical, biochemical, and anthropometric parameters. This is relevant because it brings scientific criteria for the investigation and analysis of parameters affordable to clinical practitioners who work in the area of obesity prevention and treatment. In this way, we hope to generate knowledge and scientific support for the advancement and updating of clinical practice in this research area.

Regarding the results of our randomized double-blind clinical trial, it is important to note that there was no indication of dietary interventions, encouragement of physical activity, or sort of a change in the participants' lifestyle. Therefore, our results reflect the effects that can be directly and exclusively attributed to the consumption of the nutraceutical formula applied in the study.

The characterization of the anthropometric and demographic data shows that there are no significant differences between the groups at the beginning of the study. This is relevant to state the similarity of both groups in our sample to guarantee the reliability of data. Analyzing the anthropometrics among the supplementation groups at different time points, it is noteworthy that the WC reduction in both groups was promoted by the supplementation throughout the time. Despite the lack of weight loss, the reduction of WC represents a marker of decreased cardiovascular risk for the participants. It is well established that high WC reflects abdominal fat deposition, and it is strongly associated with the development of non-communicable chronic diseases (42). The indicators of abdominal obesity are better to discriminate inflammatory status and metabolic risk than the indicator and generalized obesity as BMI. In this sense, considering the cutoff points of WHtR and WHR preconized by health guidelines, it is possible to note that both markers decreased from the T0 time point to T180 time point, returning to low-risk values. The WHtR and WHR are easily collected anthropometric measures and reliable indicators for the diagnosis of obesity mainly related to increased visceral adiposity. Thus, they also represent a relevant clinical parameter to assess cardiovascular risk that is strongly related to visceral fat deposition. When increased, WHtR is a good predictor of metabolic syndrome and appears to be directly proportional to the inflammatory indicators and directly correlated with poor eating habits (12–14). Also, the neck circumference was slightly reduced by both supplements at the end of the treatment compared to the beginning; this finding is related to the natural course of obesity, since the volunteers were instructed not to change their lifestyle throughout the supplementation period, in addition to not having nutritional intervention and lifestyle changes in this study. Results from previous studies show that increased neck circumference in obese adults is related to increased cardiovascular and inflammatory risks, acting as an anthropometric predictor of cardiovascular and inflammatory risks for this population (11).

In our data, the supplements with a combination of minerals, fibers, and bioactive compounds were able to restore low cardiovascular risk levels without the need for medicines or dietary interventions. It might be related to high metabolic rates and an increase in energy expenditure promoted by the supplement compounds that are described to enhance molecules related to fatty acid metabolism activation (9). In a review, (43) described the effect of reducing adiposity by intake of bioactive natural compounds in obese populations. In particular, compounds such as FOSs (44) and GOSs (45) have shown an adiposity-reducing effect through activation of β-oxidation markers, such as acetyl CoA-carboxylase (ACC) inactivation, AMPK activation, and mitochondrial oxidation *via* allosteric regulation of carnitine palmitoyl transferase 1 (CPT-1) (43). In this sense, studies that used acute bioactive compound supplementation found similar results without changes in body weight, but in other specific biomarkers (46, 47). These changes may not yet be evident in anthropometric data; however, these results allow us to believe that long-term consumption could exert more

pronounced effects on weight loss or parameters such as WHtR and BMI. Thus, in clinical practice, these anthropometric changes might be a good sign of improvement in cardiometabolic status.

Considering the biochemical parameters analyzed in serum samples collected at the end of the experimental protocol, there were no significant changes in serum concentrations of total cholesterol and its fractions or TGs. The improvement of the serum lipoprotein profile through the consumption of nutraceutical compounds such as fibers and antioxidants is recognized in the literature as a strategy to control dyslipidemia and prevent the onset of cardiovascular diseases, among other metabolic changes (48). Preclinical models of obesity that chronically consumed different bioactive compounds showed improvement in serum lipids (TG, HDL-cholesterol, and LDL-cholesterol) and insulin sensitivity associated with weight (49–52). Specifically, the supplement formula with silymarin can improve insulin sensitivity and reduce pro-inflammatory cytokines such as tumor necrosis factor-alpha (TNF-α) and IL-6 in mice (9, 10). It might be attributed to silymarin compounds such as silibinin, which has been proven to be an immune modulator *in vivo*, inhibiting hepatic activation of Nuclear Factor-kappaB and consequently modulating the production of pro-inflammatory cytokines such as TNF-α, interferon-gamma, IL-4, IL-2, and Inducible nitric oxide synthase (iNOS) and upregulating anti-inflammatory cytokines such as IL-10 (35). However, these effects may also be related to the increased intake of daily fiber from FOSs and GOSs and antioxidant compounds by the supplement tested. Furthermore, these findings were not confirmed in the clinical study, showing the limitation of preclinical studies that are not able to mimic factors ranging from preexisting diseases and lifestyle, genetic predispositions and variability, and even factors such as the composition of the intestinal microbiota that can influence the response to supplement consumption.

To investigate other markers related to NAFLD, serum concentrations of AST and ALT as well as the AAR were evaluated. AST, ALT, and gamma-GT are accessible clinical markers to check for liver damage. It is known that ALT is found mainly in the hepatocyte cytoplasm, while AST is present in the mitochondria. Therefore, in cases of mild liver damage, ALT is altered in the serum, while in severe liver damage, there is an increase in AST in the bloodstream (53). Despite the absence of statistical differences in gamma-GT, it might represent an indicator of risk for advanced fibrosis in NAFLD and must be carefully watched by clinical practitioners (40). Based on this, our results allow us to suggest that there was no severe liver damage despite the mild liver damage displayed by both groups at all time points. It is important to consider that obesity and overweight are a strong risk factor for NAFLD *per se*, as the participants started the study with a high level of ALT, which was maintained until the end of the study. It is also noteworthy that the new supplement had its consumption safety reinforced, since, over time, there were no worsening or severe liver damage signs in this study. In fact, the AAR was reduced by the supplementation over time. These data are interesting, since, in alcoholic liver disease, the AAR is usually higher than 2, while in NAFLD, this index tends to be between 1 and 2. Recently, some studies have proposed the use of the AAR as the main laboratory parameter for the diagnosis of NAFLD. NAFLD is a chronic inflammatory liver disease with the evolutionary potential to cirrhosis. Currently, cases of cirrhosis in obese patients, previously diagnosed as cryptogenic, have been attributed to the evolution of NAFLD (41). Thus, AAR is an extremely relevant clinical parameter that reflects and helps in the diagnosis of hepatic complications. The supplement recovers the AAR, promoting hepatoprotective effects. This effect might be promoted by the supplement and can be explained by its rich composition. In this sense, the application of silymarin extract stands out by its hepatoprotective effects, enhancement of insulin receptor (IR) sensitivity, and immune modulation, besides its beneficial effects against cardiovascular and neurological diseases and some types of cancer among other positive effects (34). Also, the yeast β-glucan is an immunomodulatory molecule and might also contribute to the hepatoprotective effect (54). Notably, there are many drug therapies available in the pipeline that have been shown to be effective in the treatment of NAFLD/Nonalcoholic steatohepatitis (NASH) (55). However, nutraceutical supplements and integrative therapies should be considered as options for clinical frontline professionals as complementary tools and not substitutes for well-established drug treatments.

In obesity, the classic chronic low-grade inflammatory state, also known as metainflammation, is associated with increased inflammatory processes; the reactive oxygen species (ROS) is also increased. We did not find alterations in the C-reactive protein; however, this can be considered a nonspecific inflammatory marker and therefore not very sensitive to the discreet changes promoted by the metainflammation of obesity. Hyperglycemia and hyperinsulinemia are also known to trigger an inflammatory process and oxidative stress environment (56). In parallel, insulin resistance is also established by visceral fat deposition that increases the activation of the lipolysis process (57, 58). In turn, an increased flow of portal vein free fatty acids (FFAs) occurs, exposing the liver to a greater influx of FFAs modifying hepatic metabolic patterns, contributing to the maintenance of systemic hyperinsulinemia and insulin resistance (59). As observed in our results, insulin resistance comes alongside overweight/obesity and represents a persistent metabolic issue with a major concern for practitioners due to its complex management.

Accessing the endocrine profile, we found a significant reduction in cortisol levels promoted by the new supplement tested. Cortisol is a hormone well known for its key role in responding to stressful stimuli. Despite its physiological role, in obesity, it is known that high levels of cortisol promote body weight gain and increase appetite with a preference for energy-dense food, contributing to a high cardiometabolic risk. Also, chronic exposure to glucocorticoids such as cortisol is known to promote the specifically abdominal obesity metabolic syndrome and eventually cardiovascular diseases. In addition, the reduction in cortisol is related to the improvement in sleep quality, which is also directly linked to the prevalence of obesity (60). Our results demonstrate an improvement in cortisol levels, contributing to a reduction in abdominal obesity and a better metabolic prognosis without any lifestyle change intervention. In this way, the new supplement proves to be a tool capable of modulating endocrine pathways of cortisol production.

In this way, our primary clinical data allow us to conclude that the new supplement has an innovative combination of nutrients and

bioactive compounds capable of promoting the improvement of biochemical and endocrine parameters in overweight/obesity. Its effect was pronounced, since it was able to promote metabolic improvement without the association of lifestyle change therapies such as diet intervention and physical activity. Although the nutrients of this supplement are accessible through a healthy diet, epidemiological data show that the consumption of these nutrients is usually deficient in a large part of the population. Thus, supplementation proves to be an important alternative to maintain adequate intake levels when the diet does not meet this demand. Therefore, the supplementation of beneficial compounds can be a valuable tool for preventing the onset of chronic diseases in the long term, avoiding the need for medication treatments. Nevertheless, these data represent an initial study of this new supplement. For more robust conclusions to be obtained, further studies are necessary with a larger sample size of both genders equally distributed. Further research also needs to address refined and in-depth biomolecular analyses that would provide a basis for a discussion on the reported clinical findings of robust cellular pathways, which might be considered another limitation of the present study. Nonetheless, the present results allow us to suggest that the parameters analyzed in this study can also be evaluated in clinical practice as an indication of endocrine and metabolic changes, bringing the research for the development of new nutraceuticals closer to the clinical practice of medical professionals, which has proven to be a major barrier between scientific research and practice application.

## Data availability statement

The raw data supporting the conclusions of this article will be made available by the authors, without undue reservation.

## Ethics statement

The studies involving human participants were reviewed and approved by the HC-FMUSP Research Ethics Committee under the CAAE number 39984320.5.0000.0068 and registered as a Clinical Trial under identification number NCT04810572 (ClinicalTrials.gov). The patients/participants provided their written informed consent to participate in this study.

## Author contributions

Conceptualization, AS and AP; Methodology, JF, DM and AP; Investigation, VN and AP; Resources, VN; Data curation, ET, FP-B, and AP; Writing—original draft preparation, AS, JF and AP; writing—review, editing and visualization, AE-G, ES, and DO; Supervision, AP and JO; Project administration, AP; funding acquisition, VN. All authors contributed to the article and approved the submitted version.

## Funding

This study received funding from Efeom Nutrição S.A. The funder was not involved in the study design, collection, analysis, interpretation of data, the writing of this article, or the decision to submit it for publication. All authors declare no other competing interests.

## Acknowledgments

The authors would like to thank Márcia Alves at Efeom Nutrition S.A., the data collection team Beatriz Itikawa, Thais Marques, Sumaia Sobral, Fabiana Sampaio, Sabrina Lira, and the employees of the LIM26 for technical support. Aline Boveto Santamarina thanks Fundação de Amparo à Pesquisa do Estado de São Paulo scholarship (FAPESP 2020/04448-0).

## Conflict of interest

The authors declare that the research was conducted in the absence of any commercial or financial relationships that could be construed as a potential conflict of interest.

## Publisher's note

All claims expressed in this article are solely those of the authors and do not necessarily represent those of their affiliated organizations, or those of the publisher, the editors and the reviewers. Any product that may be evaluated in this article, or claim that may be made by its manufacturer, is not guaranteed or endorsed by the publisher.

## References

1. Darnton-Hill I, Nishida C, James W. A life course approach to diet, nutrition and the prevention of chronic diseases. *Public Health Nutr* (2007) 7:101–21. doi: 10.1079/PHN2003584

2. WHO. The power of cities: tackling noncommunicable diseases and road safety. Geneva: World Health Organization; 2019 (WHO/NMH/PND/2019.9). Licence: CC BY-NC-SA 3.0 IGO.

3. Calder PC, Ahluwalia N, Brouns F, Buetler T, Clement K, Cunningham K, et al. Dietary factors and low-grade inflammation in relation to overweight and obesity. *Br J Nutr* (2011) 106:S5–S78. doi: 10.1017/S0007114511005460

4. Jean-Louis G, Turner AD, Jin P, Liu M, Boutin-Foster C, McFarlane SI, et al. Increased metabolic burden among blacks: A putative mechanism for disparate covid-19 outcomes. *Diabetes Metab Syndr Obes Targets Ther* (2020) 13:3471–9. doi: 10.2147/DMSO.S267952

5. Tarantino G, Balsano C, Santini SJ, Brienza G, Clemente I, Cosimini B, et al. It is high time physicians thought of natural products for alleviating nafld. *Is there sufficient evidence to Use them? Int J Mol Sci* (2021) 22. doi: 10.3390/ijms222413424

6. Rosenzweig T, Sampson SR. Activation of insulin signaling by botanical products. *Int J Mol Sci* (2021) 22:1–20. doi: 10.3390/ijms22084193

7. Konstantinidi M, Koutelidakis AE. Functional foods and bioactive compounds: A review of its possible role on weight management and obesity's metabolic consequences. *Medicines* (2019) 6:94. doi: 10.3390/medicines6030094

8. Chen L, Yu J. Modulation of toll-like receptor signaling in innate immunity by natural products. *Int Immunopharmacol* (2016) 37:65–70. doi: 10.1016/j.intimp.2016.02.005

9. Nehmi VA, Murata GM, de Moraes RCM, Lima GCA, De Miranda DA, Radloff K, et al. A novel supplement with yeast β-glucan, prebiotic, minerals and silybum marianum

synergistically modulates metabolic and inflammatory pathways and improves steatosis in obese mice. *J Integr Med* (2021) 19:439–50. doi: 10.1016/j.joim.2021.05.002

10. Santamarina AB, Moraes RCM, Nehmi Filho V, Murata GM, de Freitas JA, de Miranda DA, et al. The symbiotic effect of a new nutraceutical with yeast β-glucan, prebiotics, minerals, and silybum marianum (Silymarin) for recovering metabolic homeostasis *via* pgc-1α, il-6, and il-10 gene expression in a type-2 diabetes obesity model. *Antioxidants* (2022) 11:1–26. doi: 10.3390/antiox11030447

11. Jamar G, Pisani LP, Oyama LM, Belote C, Masquio DCL, Furuya VA, et al. Is the neck circumference an emergent predictor for inflammatory status in obese adults? *Int J Clin Pract* (2013) 67:217–24. doi: 10.1111/ijcp.12041

12. Haun DR, Pitanga FJG, Lessa I. Razão cintura/estatura comparado a outros indicadores antropométricos de obesidade como preditor de risco coronariano elevado. *Rev Assoc Med Bras* (2009) 55:705–11. doi: 10.1590/S0104-42302009000600015

13. Rodrigues SL, Baldo MP, Mill JG. Associação entre a razão cintura-estatura e hipertensão e. *Arq Bras Cardiol* (2010) 95:186–91. doi: 10.1590/S0066-782X2010005000073

14. Thompson AL, Adair L, Gordon-Larsen P, Zhang B, Popkin B. Environmental, dietary, and behavioral factors distinguish Chinese adults with high waist-to-Height ratio with and without inflammation. *J Nutr* (2015) 145:1335–44. doi: 10.3945/jn.114.20610202

15. Akbari M, Hassan-Zadeh V. IL-6 signalling pathways and the development of type 2 diabetes. *Inflammopharmacology* (2018) 26:685–98. doi: 10.1007/s10787-018-0458-0

16. Medina J, Fernández-Salazar LI, García-Buey L, Moreno-Otero R. Approach to the pathogenesis and treatment of nonalcoholic steatohepatitis. *Diabetes Care* (2004) 27:2057–66. doi: 10.2337/diacare.27.8.2057

17. Gregor MF, Hotamisligil GS. Inflammatory mechanisms in obesity. *Annu Rev Immunol* (2011) 29:415–45. doi: 10.1146/annurev-immunol-031210-101322

18. Iossa S, Lionetti L, Mollica MP, Crescenzo R, Botta M, Barletta A, et al. Effect of high-fat feeding on metabolic efficiency and mitochondrial oxidative capacity in adult rats. *Br J Nutr* (2003) 90:953–60. doi: 10.1079/BJN2003000968

19. Rogero M, Calder P. Obesity, inflammation, toll-like receptor 4 and fatty acids. *Nutrients* (2018) 10:432. doi: 10.3390/nu10040432

20. Tilg H, Moschen AR. Adipocytokines: Mediators linking adipose tissue, inflammation and immunity. *Nat Rev Immunol* (2006) 6:772–83. doi: 10.1038/nri1937

21. Fernández-Sánchez A, Madrigal-Santillán E, Bautista M, Esquivel-Soto J, Morales-González Á, Esquivel-Chirino C, et al. Inflammation, oxidative stress, and obesity. *Int J Mol Sci* (2011) 12:3117–32. doi: 10.3390/ijms12053117

22. Cena H, Calder PC. Defining a healthy diet: Evidence for the role of contemporary dietary patterns in health and disease. *Nutrients* (2020) 12:1–15. doi: 10.3390/nu12020334

23. Sabater-Molina M, Larqué E, Torrella F, Zamora S. Dietary fructooligosaccharides and potential benefits on health. *J Physiol Biochem* (2009) 65:315–28. doi: 10.1007/BF03180584

24. Torres DPM, Gonçalves M do PF, Teixeira JA, Rodrigues LR. Galacto-oligosaccharides: Production, properties, applications, and significance as prebiotics. *Compr Rev Food Sci Food Saf* (2010) 9:438–54. doi: 10.1111/j.1541-4337.2010.00119.x

25. Andrade EF, Lima ARV, Nunes IE, Orlando DR, Gondim PN, Zangeronimo MG, et al. Exercise and beta-glucan consumption (Saccharomyces cerevisiae) improve the metabolic profile and reduce the atherogenic index in type 2 diabetic rats (HFD/STZ). *Nutrients* (2016) 8. doi: 10.3390/nu8120792

26. Lobato RV, Silva V de O, Andrade EF, Orlando DR, Zangerônimo MG, de Souza RV, et al. Metabolic effects of β-glucans (Saccharomyces cerevisae) per os administration in rats with streptozotocin-induced diabetes. *Nutr Hosp* (2015) 32:256–64. doi: 10.3305/nh.2015.32.1.9013

27. Nielsen FH. Magnesium, inflammation, and obesity in chronic disease. *Nutr Rev* (2010) 68:333–40. doi: 10.1111/j.1753-4887.2010.00293.x

28. Kim J, Ahn J. Effect of zinc supplementation on inflammatory markers and adipokines in young obese women. *Biol Trace Elem Res* (2014) 157:101–6. doi: 10.1007/s12011-013-9885-3

29. Rayman MP. Selenium and human health. *Lancet* (2012) 379:1256–68. doi: 10.1016/S0140-6736(11)61452-9

30. Izzo AA, Abenavoli L, Santini A, Capasso R, Cicala C. Milk thistle (silybum marianum): A concise overview on its chemistry, pharmacological, and nutraceutical uses in liver diseases. *Journal title: Phytotherapy Research* (2018) 32:1–12. doi: 10.1002/ptr.6171

31. Liu F, Li P, Chen M, Luo Y, Prabhakar M, Zheng H, et al. Fructooligosaccharide (FOS) and galactooligosaccharide (GOS) increase bifidobacterium but reduce butyrate producing bacteria with adverse glycemic metabolism in healthy young population. *Sci Rep* (2017) 7:1–12. doi: 10.1038/s41598-017-10722-2

32. Stothers CL, Burelbach KR, Owen AM, Patil NK, McBride MA, Bohannon JK, et al. β-glucan induces distinct and protective innate immune memory in differentiated macrophages. *J Immunol* (2021) 207:2785–98. doi: 10.4049/jimmunol.2100107

33. Avery JC, Hoffmann PR. Selenium, selenoproteins, and immunity. *Nutrients* (2018) 10. doi: 10.3390/nu10091203

34. MacDonald-Ramos K, Michán L, Martínez-Ibarra A, Cerbón M. Silymarin is an ally against insulin resistance: A review. *Ann Hepatol* (2021) 23. doi: 10.1016/j.aohep.2020.08.072

35. Schümann J, Prockl J, Kiemer AK, Vollmar AM, Bang R, Tiegs G. Silibinin protects mice from T cell-dependent liver injury. *J Hepatol* (2003) 39:333–40. doi: 10.1016/S0168-8278(03)00239-3

36. Banach W, Nitschke K, Krajewska N, Mongiałło W, Matuszak O, Muszyński J, et al. The association between excess body mass and disturbances in somatic mineral levels. *Int J Mol Sci* (2020) 21:1–14. doi: 10.3390/ijms21197306

37. Faul F, Erdfelder E, Lang A-G, Buchner A. G*Power 3: A flexible statistical power analysis program for the social, behavioral, and biomedical sciences. *Behav Res Methods* (2007) 39:175–91. doi: 10.3758/BF03193146

38. Matsudo S, Araújo T, Matsudo V, Andrade D, Andrade E, Oliveira LC, et al. Questionário internacional de atividade física (Ipaq): Estupo de validade e reprodutibilidade no brasil. *Rev Bras Atividade Física Saúde* (2012) 6:5–18. doi: 10.12820/rbafs.v.6n2p5-18

39. Schulz KF, Altman DG, Moher D. CONSORT 2010 statement: Updated guidelines for reporting parallel group randomized trials. *Open Med* (2010) 4. doi: 10.1016/j.ijsu.2010.09.006

40. Tahan V, Canbakan B, Balci H, Dane F, Akin H, Can G, et al. Serum gamma-glutamyltranspeptidase distinguishes non-alcoholic fatty liver disease at high risk. *Hepatogastroenterology* (2008) 55:1433–8.

41. Rief P, Pichler M, Raggam R, Hafner F, Gerger A, Eller P, et al. The AST/ALT (De-ritis) ratio. *Med (Baltimore)* (2016) 95:e3843. doi: 10.1097/md.0000000000003843

42. Han TS, Lean ME. A clinical perspective of obesity, metabolic syndrome and cardiovascular disease. *JRSM Cardiovasc Dis* (2016) 5:1–13. doi: 10.1177/2048004016633371

43. Rupasinghe HPV, Sekhon-Loodu S, Mantso T, Panayiotidis MI. Phytochemicals in regulating fatty acid β-oxidation: Potential underlying mechanisms and their involvement in obesity and weight loss. *Pharmacol Ther* (2016) 165:153–63. doi: 10.1016/j.pharmthera.2016.06.005

44. Costa GT, Guimarães SB, Sampaio HAC. Fructo-oligosaccharide effects on blood glucose. an overview [Efeitos dos fruto-oligossacar{í}deos no controle glic{ê}mico. revis{ã}o]. *Acta Cir Bras* (2012) 27:279–82. doi: 10.1590/S0102-86502012000300013

45. Hashmi A, Naeem N, Farooq Z, Masood S, Iqbal S, Naseer R. Effect of prebiotic galacto-oligosaccharides on serum lipid profile of hypercholesterolemics. *Probiotics Antimicrob Proteins* (2016) 8:19–30. doi: 10.1007/s12602-016-9206-1

46. Mullan A, Delles C, Ferrell W, Mullen W, Edwards CA, McColl JH, et al. Effects of a beverage rich in (poly)phenols on established and novel risk markers for vascular disease in medically uncomplicated overweight or obese subjects: A four week randomized trial. *Atherosclerosis* (2016) 246:169–76. doi: 10.1016/j.atherosclerosis.2016.01.004

47. Nogueira L de P, Nogueira Neto JF, Klein MRST, Sanjuliani AF. Short-term effects of green tea on blood pressure, endothelial function, and metabolic profile in obese prehypertensive women: A crossover randomized clinical trial. *J Am Coll Nutr* (2016) 5724:1–8. doi: 10.1080/07315724.2016.1194236

48. Oliveira V, Marinho R, Vitorino D, Santos GA, Moraes JC, Dragano N, et al. Diets containing alfa-linolenic (omega-3) or oleic (omega-9) fatty acids rescues obese mice from insulin resistance. *Endocrinology* (2015) 156:4033–46. doi: 10.1210/en.2014-1880

49. Qin B, Anderson RA. An extract of chokeberry attenuates weight gain and modulates insulin, adipogenic and inflammatory signalling pathways in epididymal adipose tissue of rats fed a fructose-rich diet. *Br J Nutr* (2012) 108:581–7. doi: 10.1017/S000711451100599X

50. Heyman L, Axling U, Blanco N, Sterner O, Holm C, Berger K. Evaluation of beneficial metabolic effects of berries in high-fat fed C57BL/6J mice. *J Nutr Metab* (2014) 2014:1–12. doi: 10.1155/2014/403041

51. Dragano NRV, Marques A y C, Cintra DEC, Solon C, Morari J, Leite-Legatti AV, et al. Freeze-dried jaboticaba peel powder improves insulin sensitivity in high-fat-fed mice. *Br J Nutr* (2013) 110:447–55. doi: 10.1017/S0007114512005090

52. Burton-Freeman BM, Sandhu AK, Edirisinghe I. Red raspberries and their bioactive polyphenols: Cardiometabolic and neuronal health links. *Adv Nutr Int Rev J* (2016) 7:44–65. doi: 10.3945/an.115.009639

53. Lala V, Goyal A, Minter DA. *Liver function tests*. Treasure Island (FL (2022). Available at: http://www.ncbi.nlm.nih.gov/pubmed/29494096.

54. Cao Y, Zou S, Xu H, Li M, Tong Z, Xu M, et al. Hypoglycemic activity of the baker's yeast β-glucan in obese/type 2 diabetic mice and the underlying mechanism. *Mol Nutr Food Res* (2016) 60:2678–90. doi: 10.1002/mnfr.201600032

55. Negi CK, Babica P, Bajard L, Bienertova-Vasku J, Tarantino G. Insights into the molecular targets and emerging pharmacotherapeutic interventions for nonalcoholic fatty liver disease. *Metabolism* (2022) 126:154925. doi: 10.1016/j.metabol.2021.154925

56. Rani V, Deep G, Singh RK, Palle K, Yadav UCS. Oxidative stress and metabolic disorders: Pathogenesis and therapeutic strategies. *Life Sci* (2016) 148:183–93. doi: 10.1016/j.lfs.2016.02.002

57. Shoelson SE. Inflammation and insulin resistance. *J Clin Invest* (2006) 116:1793–801. doi: 10.1172/JCI29069

58. Ye J. Mechanisms of insulin resistance in obesity. *Front Med* (2013) 7:14–24. doi: 10.1007/s11684-013-0262-6

59. Byrne CD. Ectopic fat, insulin resistance and non-alcoholic fatty liver disease. *Proc Nutr Soc* (2013) 72:1–8. doi: 10.1017/S0029665113001249

60. Makhoul E, Aklinski JL, Miller J, Leonard C, Backer S, Kahar P, et al. A review of COVID-19 in relation to metabolic syndrome: Obesity, hypertension, diabetes, and dyslipidemia. *Cureus* (2022) 14. doi: 10.7759/cureus.27438

frontiers | Frontiers in Endocrinology

TYPE Mini Review
PUBLISHED 21 February 2023
DOI 10.3389/fendo.2023.1090039



OPEN ACCESS

EDITED BY
Bruno Melo Carvalho,
Universidade de Pernambuco, Brazil

REVIEWED BY
Elisa Villalobos,
Newcastle University, United Kingdom
Xavier Prieur,
U1087 Institut du Thorax (INSERM), France

*CORRESPONDENCE
Ana Paula Davel
anadavel@unicamp.br

SPECIALTY SECTION
This article was submitted to Obesity, a section of the journal Frontiers in Endocrinology

RECEIVED 04 November 2022
ACCEPTED 10 February 2023
PUBLISHED 21 February 2023

CITATION
Freitas IN, da Silva JA Jr, Oliveira KM, Lourençoni Alves B, Dos Reis Araujo T, Camporez JP, Carneiro EM and Davel AP (2023) Insights by which TUDCA is a potential therapy against adiposity. *Front. Endocrinol.* 14:1090039. doi: 10.3389/fendo.2023.1090039



# Insights by which TUDCA is a potential therapy against adiposity

Israelle Netto Freitas[1,2], Joel Alves da Silva Jr[2], Kênia Moreno de Oliveira[2], Bruna Lourençoni Alves[2], Thiago Dos Reis Araújo[2], João Paulo Camporez[3], Everardo Magalhães Carneiro[1,2] and Ana Paula Davel[1,2]*

[1]Department of Structural and Functional Biology, Institute of Biology, University of Campinas, Campinas, SP, Brazil, [2]Obesity and Comorbidities Research Center, University of Campinas, Campinas, SP, Brazil, [3]Department of Physiology, Ribeirao Preto Medical School, University of Sao Paulo, Ribeirao Preto, SP, Brazil

Adipose tissue is an organ with metabolic and endocrine activity. White, brown and ectopic adipose tissues have different structure, location, and function. Adipose tissue regulates energy homeostasis, providing energy in nutrient-deficient conditions and storing it in high-supply conditions. To attend to the high demand for energy storage during obesity, the adipose tissue undergoes morphological, functional and molecular changes. Endoplasmic reticulum (ER) stress has been evidenced as a molecular hallmark of metabolic disorders. In this sense, the ER stress inhibitor tauroursodeoxycholic acid (TUDCA), a bile acid conjugated to taurine with chemical chaperone activity, has emerged as a therapeutic strategy to minimize adipose tissue dysfunction and metabolic alterations associated with obesity. In this review, we highlight the effects of TUDCA and receptors TGR5 and FXR on adipose tissue in the setting of obesity. TUDCA has been demonstrated to limit metabolic disturbs associated to obesity by inhibiting ER stress, inflammation, and apoptosis in adipocytes. The beneficial effect of TUDCA on perivascular adipose tissue (PVAT) function and adiponectin release may be related to cardiovascular protection in obesity, although more studies are needed to clarify the mechanisms. Therefore, TUDCA has emerged as a potential therapeutic strategy for obesity and comorbidities.

KEYWORDS

**TUDCA, tauroursodeoxycholic acid, obesity, endoplasmic reticulum (ER) stress, adipose tissue, perivascular adipose tissue, adipocyte**

## 1 Introduction

Obesity is a global public health problem. Data from 2016 showed that about 1.9 billion adults worldwide were overweight, while 650 million were considered obese (1). Yet, studies indicate that, in 2025, almost 2.3 billion adults will be overweight; and more than 700 million will be obese (2). About public expenses with health, it is postulated that the costs of caring for

obese patients will double by 2050 (US$10.1 billion) compared to 2010 (US$5.8 billion) (3). According to the Global Burden of Disease study, 4.7 million people died prematurely in 2017 as a result of obesity (4). Obesity is a risk factor for developing many disorders such as diabetes mellitus, hypertension, cardiovascular events, obstructive sleep apnea syndrome, cancer, and musculoskeletal diseases (5). Obesity also has a negative impact on quality of life and increases the costs of healthcare (6).

Adipose tissue is an endocrine organ with high metabolic activity. It corresponds to 20-28% of the body mass of healthy individuals and may represent up to 80% of the body mass in obese individuals (7). It is a specialized connective tissue composed predominantly by adipocytes and separated by a thin layer of extracellular matrix (8). It was believed that adipose tissue operated only as an energy store in the form of triglycerides, however, this tissue also works as an endocrine organ capable of secreting numerous hormones and adipokines that contribute to energy homeostasis (9). Besides these metabolism-related functions, adipose tissue regulates other physiological processes related to reproduction, immunity, angiogenesis, extracellular matrix restructuring, steroid metabolism, and body temperature (7).

White adipose tissue (WAT) is composed primarily of white and a few beige adipocytes, depending on its location. White adipocytes have a vacuole with a single lipid droplet and few cellular organelles and can vary in size according to the amount of stored triglycerides. Its main function is energy storage, but WAT also secretes a wide variety of adipokines, such as leptin and adiponectin, which are the first two proteins discovered (10). In addition, beige or brite adipocytes are generally found scattered amongst the white adipocytes and have the potential to generate heat when facing cold exposure or adrenergic receptors stimulation (11, 12). On the other hand, brown adipose tissue (BAT) adipocytes present several lipid droplets vacuolized and a large number of mitochondria, which gives the tissue a brown color. Its main function is the production of energy in the form of heat, a process accomplished by the uncoupling protein-1 (UCP-1), which is considered its phenotypic characteristic protein (10, 13).

**Abbreviations:** ATF6, transcription factor 6; BAs, bile acid; BAT, brown adipose tissue; BiP, binding immunoglobulin protein; CA, cholic acid; CDCA, chenodeoxycholic acid; CIDEA; cell death-inducing DNA fragmentation factor alpha-like effector A; Cox8b, Cytochrome c oxidase subunit 8b; CYP7A1, cholesterol 7α-hydroxylase; DCA, deoxycholic acid; ER, endoplasmic reticulum; eIF2α, eukaryotic initiation factor 2 alpha; GPDH, glycerol-3-phosphate dehydrogenase; GRP78, glucose-regulated protein-78; hASCs, human adipose derived stem cells; iNOS, inducible nitric oxide synthase; IRE1α, inositol-requiring enzyme 1α; LCA, lithocholic acid; NASH, non-alcoholic steatohepatitis; NLRP3, NOD- LRR- and pyrin domain-containing protein 3; Pgc1a, Peroxisome proliferator-activated receptor-gamma coactivator; PPARγ, peroxisome proliferator-activated receptor γ; PVAT, perivascular adipose tissue; PERK, protein kinase R (PKR)-like endoplasmic reticulum kinase; ROS, reactive oxygen species; TUDCA, tauroursodeoxycholic acid; TNF-α, tumor necrosis factor-α; UCP-1, uncoupling protein-1; UDCA, ursodeoxycholic acid; UPR, unfolded protein response; WAT, white adipose tissue; XBP-1, X Box Protein 1; Cytochrome c oxidase subunit 8b (Cox8b); Peroxisome proliferator-activated receptor-gamma coactivator (Pgc1a); cell death-inducing DNA fragmentation factor alpha-like effector A (CIDEA).

Adipose tissues regulate energy homeostasis, providing energy in nutrient-deficient conditions and storing it in high-supply conditions (14). However, when the excess of stored energy exceeds the expenditure, obesity can be established (15). Therefore, studies involving the comprehension, prevention, and treatment of obesity are extremely important. Here, we review endoplasmic reticulum (ER) stress as a mechanism involved in adipose tissue morphological, functional and molecular changes on the setting of obesity highlighting recent advances in therapeutic actions of the tauroursodeoxycholic bile acid (TUDCA).

## 2 Changes in adipose tissue depots in obesity: A role for ER stress

### 2.1 ER stress

The ER is an important organelle of eukaryotic cells responsible for maintaining calcium homeostasis, for the biosynthesis of phospholipids and for the synthesis and folding of proteins that will be directed to the plasma membrane or to secretory vesicles (16). However, inflammation, nutrient deprivation, hypoxia, acidosis, and oxidative stress can disturb the homeostasis of ER leading to ER stress (17–19). ER stress is established when an imbalance occurs between the demand and the capacity of the ER for protein folding, resulting in the accumulation of misfolded/unfolded proteins. To normalize ER homeostasis and reestablish protein folding, cells rely on a defense mechanism called unfolded protein response (UPR) (20, 21).

UPR monitors protein folding in the ER and adjusts folding capacity to match the amount of synthesis. For this, three sensors that are present in the ER membrane are required: protein kinase R-like ER kinase (PERK), transcription factor 6 (ATF6), and inositol requiring enzyme 1α (IRE1α) (20, 21). Under physiological conditions, these sensors are bonded to a chaperone protein named as glucose-regulated protein 78 (GRP78) an ER chaperone also referred to as the immunoglobulin heavy chain binding protein (BiP), which keeps them inactivated. However, when levels of misfolded proteins increase, BiP dissociates from PERK, ATF6 and IRE1α activating three distinct signaling pathways (22). When BiP dissociates from IRE1α, IRE1α is autophosphorylated and activates the transcription factor X Box Protein 1 (XBP-1) that regulates the expression of chaperones and enzymes involved in the degradation of misfolded proteins arising from the ER (23, 24). PERK phosphorylates eukaryotic initiation factor 2 (eIF2α) and induces ATF4 translation, one of the UPR-dependent signaling proteins. In general, these pathways regulate protein synthesis rate, biosynthesis of new chaperones, protein trafficking within the ER, protein degradation, and finally, apoptosis, if ER homeostasis is not reestablished (20–22).

ER stress is linked to oxidative stress (23) as protein misfolding produces reactive oxygen species (ROS) (24, 25) that further impairs protein folding and depletes ER $Ca^{2+}$ levels, aggravating ER stress (26, 27). In addition, IRE1α/XBP-1 and PERK/eIF2α induce the expression of C/EBP homologous protein (CHOP) that contribute to ROS generation and apoptosis (28).

## 2.2 ER stress in WAT and BAT during obesity

ER stress has been associated with dysfunctional WAT and BAT during obesity. In WAT, high-fat diet (HFD)-induced obesity enhances expression of UPR markers such as PERK, ATF-6, IRE1-α, ATF-4, and CHOP (29–31). Furthermore, ER stress affects adipokine secretion and action by impairing adiponectin synthesis and secretion (30, 31) and by inducing leptin resistance (32). Lipogenesis and adipogenesis are also modulated by ER stress (33). In line with this, activation of ER stress increases triglycerides, SREBP-1c, and FAS in human mature adipocytes (34). CHOP upregulation limits beige adipocyte differentiation by inhibiting UCP-1, Cox8b, Cidea, Prdm16, and PGC-1α (35), while CHOP deficiency upregulates PPARγ and adiponectin (29). IRE1α impedes beige fat activation in white and beige adipocytes, degrades PGC1-α mRNA, and limits thermogenesis (36).

During obesity, ER stress can be a mechanism potentiating proinflammatory state in WAT and UPR pathways converge with inflammatory signaling pathways (37, 38). CHOP deficiency enhances M2 macrophages abrogating WAT inflammation (29). In addition, IRE1α favors M1/M2 adipose tissue macrophages polarization and impairs WAT browning (30). Therefore, ER stress can modulate WAT adipocytes morphology and WAT inflammation in the setting of obesity.

In humans and in animal models of obesity, density and thermogenic activity of brown adipocytes is lower, as they go through a process called whitening, due but not limited to the excess of lipids (39, 40). Enlarged white-like brown adipocytes may present accumulation of large lipid droplets, mitochondrial dysfunction, and oxidative stress (41–44). The inflammatory profile triggered in BAT during obesity reduces the expression of UCP-1 and BAT thermogenic activity. Furthermore, inflammatory mediators have been shown to prevent the expansion of BAT in obesity, by promoting cell apoptosis *via* tumor necrosis factor-α (TNF-α) or reducing tissue proliferation, inhibiting catecholamine signaling (45).

In BAT of obese mice, genes related to ER stress and UPR such as GRP78, CHOP, ATF4 and ATF6 are enhanced while thermogenic genes UCP-1 and PGC1-α are reduced; induction of ER stress resulted in brown adipocytes apoptosis *in vitro* and *in vivo* (46). UCP-1 deficiency increases CHOP and XBP1 transcript levels and eIF2α phosphorylation, linking deficient thermogenesis to ER stress in BAT (47). However, the role of UPR response elements in BAT are still under investigation. The IRE1α/XBP1 pathway seem to be highly activated compared with other UPR branches during the induction of UCP-1 transcription in BAT, and its induction mechanism is independent of ER stress (48). Also, in brown adipocytes, PERK has a function independent of UPR, and seems to be essential for mitochondrial thermogenesis (49). Therefore, the role of ER stress in BAT in response to metabolic challenges as obesity still needs to be clarified.

## 2.3 Ectopic fat

In addition to classic fat depots, adipose tissue can accumulate ectopically during the development of obesity, which can contribute to impaired function in the deposited tissues (50), such as blood vessels and liver (51). In this sense, it is known that a progressive increase in the deposition of lipids in the liver leads to inflammation, hepatocellular degeneration, and collagen deposition, resulting in non-alcoholic steatohepatitis (NASH) (52), which, if not reversed, leads to irreversible liver cirrhosis and also increases the risk for the occurrence of hepatocellular carcinoma (53, 54). ER stress and UPR pathways are molecular mechanisms associated with NASH. CHOP, Bip, IRE1α and XBP1 are involved in hepatic lipid metabolism (55). In the livers of obese mice, ER stress associated with IRE1α and PERK activation, and CHOP upregulation activate the NLRP3 inflammasome and induce hepatocyte inflammation and apoptosis (56). Therefore, long-term ER stress leads can result in liver injury in obesity. The importance of ER stress to hepatic lipid metabolism in obesity and NASH was the topic of a recent review (57).

The obesity has also been demonstrated to alter the perivascular adipose tissue (PVAT) (58, 59). PVAT presents morphological characteristics that vary according to the vascular bed, resembling WAT in mesenteric arteries and abdominal aorta or BAT/beige in thoracic aorta (60–62). PVAT synthesizes and releases a variety of vasoactive substances that paracrinally influence peripheral vascular resistance and, therefore, blood pressure. PVAT may lose its vasoregulatory capacity due to a decrease in the release of vasodilating adipokines (63, 64). The expansion of PVAT in obesity is associated with immune cells infiltration, reduced adiponectin and increased leptin secretion, greater ROS production, and inducible nitric oxide synthase (iNOS) expression (63–67). In PVAT depots, ER stress is associated with the expression of pro-inflammatory factors including NF-kB, impaired vascular function (vasodilation and contraction) and atherosclerotic plaque destabilization (68, 69).

Given the metabolic and cardiovascular importance of PVAT and other ectopic fat depots, further studies need to be conducted in order to better elucidate the impact and pathophysiological of obesogenic diets and ER stress in ectopic fat. It is also relevant to identify pharmacological tools targeting ER stress in PVAT that could be a coadjuvant approach to the treatment and prevention of vascular complications associated with cardiometabolic diseases.

# 3 Actions of TUDCA in adiposity

## 3.1 Molecular mechanisms of TUDCA

Bile acids (BAs) are synthesized in hepatocytes by the enzyme cholesterol 7α-hydroxylase (CYP7A1) from cholesterol, generating primary BAs such as cholic acid (CA) and chenodeoxycholic acid (CDCA). In the intestine, through deconjugation, oxidation and epimerization reactions carried out by the intestinal microbiota, primary BAs give rise to secondary BAs such as deoxycholic acid (DCA), lithocholic acid (LCA) and ursodeoxycholic acid (UDCA). After the formation of secondary BAs, some BAs are conjugated in hepatocytes with the amino acids glycine as glycocholic acid (GCA), or taurine, as TUDCA, which makes these compounds obtain greater solubility and ionization in the intestinal lumen (70, 71).

At first, it was believed that BAs served only to assist in the process of digestion of lipids and fat-soluble vitamins (71, 72). However, recent data show that these molecules can regulate lipid and glycemic metabolism, BA synthesis, and the immune system, presenting metabolic and endocrine functions (71–73). These effects result from signaling through receptors such as the Farnesoid X receptor (FXR), the G protein-coupled BA receptor (TGR5) and Sphingosine-1-phosphate receptor 2 (S1PR2) (72–74). FXR is a nuclear receptor while TGR5 and S1PR2 are membrane receptors. These three receptors are classically expressed in the liver and digestive tract, but also have been identified in other tissues such as the heart, blood vessels, and adipocytes (75, 76). Additionally, preadipocytes and mature adipocytes express other factors involved in BA metabolism, such as BSEP (bile salt exporting pump), a hepatic protein that functions as a bile salt export pump in liver cells mediating BA transport into the bile canaliculi (77, 78). BAs conjugation with taurine increases affinity to the membrane and nuclear receptors (75).

Inhibition of ER stress could be a therapeutic intervention against morphofunctional alterations of overall adipose tissue depots in obesity. In this sense, the ER stress inhibitor TUDCA, a BA conjugated to taurine with chemical chaperone activity, has emerged as a therapeutic strategy to minimize adipose tissue dysfunction and metabolic alterations associated with obesity (79, 80).

## 3.2 Effects of TUDCA and its receptors in obesity

TUDCA was recently demonstrated to be an important mediator of beneficial metabolic effects on diet-induced obesity models, as by activating FXR and TGR5, taurine-conjugated BAs can improve glucose homeostasis, lipid metabolism and BAT thermogenesis (81, 82).

The activation of TGR5 increases energy expenditure in HFD-induced obese mice, limiting obesity and insulin resistance (83). TGR5 signals through cyclic adenosine monophosphate/protein kinase A (cAMP/PKA) and deiodinase-2 activation in mouse and human brown adipocytes and increased thermogenic activity (84–86). This pathway can also mediate beiging of WAT by increasing mitochondrial content and fission in white adipocytes from HFD mice (85). In BAT, TGR-5 induces thermogenesis (83). FXR activation can reduce both weight gain and inflammatory markers in WAT of HFD-induced obese mice, as well as limit the expansion of WAT under obesogenic conditions (87–89). Therefore, BA receptors activation seems to limit lipid accumulation, inflammation and metabolic changes in WAT during obesity. However, it was demonstrated that FXR-deficiency can attenuate WAT expansion, body weight and insulin resistance in mouse models of genetic and diet-induced obesity (90). Controversial data is also observed in ectopic fat as reduced or increased fat liver accumulation was observed following FXR activation (88, 89). Therefore, further studies are needed to clear the molecular mechanism of BA receptors in adipocytes during obesity.

Our group has demonstrated that TUDCA has a beneficial effect on glucose-induced insulin secretion through TGR5/PKA signaling in beta cells (91). Interestingly, increased insulin secretion is induced by TUDCA in isolated pancreatic islets under thapsigargin-induced ER stress (72). Therefore, it is likely that ER stress inhibition in beta cells is involved in TUDCA effects. In agreement, by modulating ER stress, administration of TUDCA in obese and type 2 diabetic mice normalized glycemia, restored insulin sensitivity in liver, muscle and adipose tissues, as well as reduced fatty liver disease (92). Of note, TUDCA may act as an insulin receptor (IR) agonist, which, in addition, can contribute to its beneficial effects on insulin sensitivity (93).

TUDCA treatment of human adipose derived stem cells (hASCs) significantly decreases ER stress marker GRP78, adipogenic markers such as PPARγ and glycerol-3-phosphate dehydrogenase 1 (GPDH), and lipid accumulation (94) suggesting that ER inhibition by TUDCA is associated with decreased adipogenesis. Such actions of TUDCA were similar to the ER stress inhibitor 4-phenyl butyric acid (PBA). Further, TUDCA or PBA treatment decreased ER stress markers, free cholesterol, inflammatory cytokines level, and NF-kB activity in WAT of HFD-induced obese mice (37). Finally, ER stress inhibition induced by TUDCA is associated with the inhibition of ROS production and attenuated cleaved-caspase-3 expression, resulting in an antiapoptotic effect in white adipocytes exposed to high glucose (95). In BAT, ER stress inhibition is associated with increased UCP-1 and thermogenesis (96, 97). The major effects of TUDCA on WAT and BAT are summarized in Figure 1.

TUDCA treatment also has been suggested as beneficial for ectopic fat during obesity (Figure 1). Reduced ER stress markers PERK and IRE-1α phosphorylation is demonstrated in the liver of diabetic ob/ob mice associated with resolution of fat liver disease (92). TUDCA can limit hepatocyte lipoapoptosis by suppressing phosphorylation of eIF2α, XBP1 splicing, BiP and ATF4 expression (98). TUDCA may also have beneficial effects on PVAT. In line with this, TUDCA reduced ER stress markers GRP78 and ATF4 on PVAT from type 2 diabetic mice which was associated with improved endothelial function and reduced vascular stiffness (99). The ex vivo exposure to palmitate or thapsigargin both impaired insulin-induced vasorelaxation in the aorta which was prevented by TUDCA, associated with reduced expression of ER markers IRE1α and eIF-2α phosphorylation in PVAT (100). However, the mechanisms associated with TUDCA-induced PVAT mediated protective vascular effects still need to be addressed. As TUDCA increases adiponectin production in obese mice and in adipocytes (76, 101) this can be an additional beneficial mechanism associated with cardiovascular protection. Future studies need to be addressed to elucidate mechanisms of metabolic and vascular effects of TUDCA, focused on the involvement of ER stress inhibition and/or direct effects of this BA.

# 4 Conclusion

Here, we summarize the main findings on the effects of TUDCA and receptors TGR5 and FXR on adipose tissue in the setting of obesity. TUDCA has been demonstrated to limit metabolic disturbs

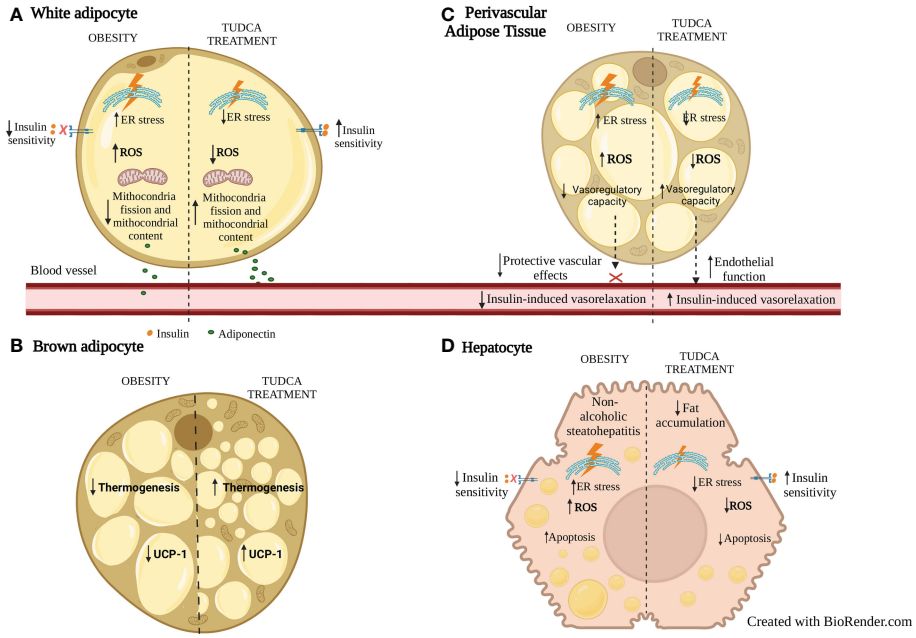


FIGURE 1
Effects of TUDCA treatment on WAT, BAT, PVAT and liver fat during obesity. **(A)** In WAT adipocytes, ER stress inhibition with TUDCA is associated with increased mitochondrial fission and content, decreased ROS, and increased insulin sensitivity and adiponectin secretion. **(B)** In BAT, TUDCA increases thermogenesis and expression of UCP-1. **(C)** In PVAT, ER stress inhibition with TUDCA is associated with decreased ROS, increased anticontractile and endothelial function. **(D)** In hepatocytes, in addition to inhibiting ER and oxidative stress, TUDCA treatment increases insulin sensitivity, decreases fat accumulation and adipocyte apoptosis. ER: endoplasmic reticulum; ROS: reactive oxygen species. UCP-1: uncoupling protein-1.

associated with obesity by inhibiting lipid accumulation, ER stress, inflammation, and apoptosis in adipocytes. TUDCA also improves insulin sensitivity in obese mice and may act as an IR agonist. The beneficial effect of TUDCA on PVAT function and adiponectin release may be related to cardiovascular protection in obesity, although more studies are needed to clarify the mechanisms. A limitation of the studies is to identify possible direct effects of TUDCA independent of ER stress inhibition, which are interesting for elucidating possible therapeutic targets in obesity and other diseases.

As summarized in this review, TUDCA can be considered a multi-targeted therapy, as this BA modulates glucose and lipid metabolism, inflammatory response, adipogenesis, macrophage differentiation and other general metabolic responses. TUDCA has been approved by the US administration for clinical use in diseases such as cholelithiasis and cholestatic liver disease (102, 103). Therefore, it may be suggested that TUDCA treatment could be also an important therapeutic agent for obesity and comorbidities.

## Author contributions

IF and AD contributed to the study conception, design and writing. JS, BA, TR, JC, and EC contributed to the writing and reviewing. KO made the figures. All authors contributed to the article and approved the submitted version.

## Funding

This work was supported by Fundação de Amparo à Pesquisa do Estado de São Paulo- FAPESP (grant numbers 2018/26080-4, 2019/15164-5, 2020/05146-7 and 2021/02734-8) and Conselho Nacional de Desenvolvimento Científico e Tecnológico- CNPq (308682/2019-0).

## Conflict of interest

The authors declare that the research was conducted in the absence of any commercial or financial relationships that could be construed as a potential conflict of interest.

## Publisher's note

# References


1. WHO. Word Health Organization. (2020) (Accessed September, 2022).

2. World Health Organization. The State of Food Security and Nutrition in the World 2019: Safeguarding Against Economic Slowdowns and Downturns. Rome: Food and Agriculture Organization of the United Nations (FAO); (2019).

3. Rtveladze K, Marsh T, Webber L, Kilpi F, Levy D, Conde W, et al. Health and economic burden of obesity in Brazil. *PloS One* (2013) 8. doi: 10.1371/journal.pone.0068785

4. Dai H, Alsalhe TA, Chalghaf N, Riccò M, Bragazzi NL, Wu J. The global burden of disease attributable to high body mass index in 195 countries and territories, 1990-2017: An analysis of the global burden of disease study. *PloS Med* (2020) 17(7): e1003198. doi: 10.1371/journal.pmed.1003198

5. Singh GM, Danaei G, Farzadfar F, Stevens GA, Woodward M, Wormser D, et al. The age-specific quantitative effects of metabolic risk factors on cardiovascular diseases and diabetes: a pooled analysis. *PloS One* (2013) 8(7):e65174. doi: 10.1371/journal.pone.0065174

6. Kolotkin RL, Andersen JR. A systematic review of reviews: exploring the relationship between obesity, weight loss and health-related quality of life. *Clin Obes* (2017) 7(5):273–89. doi: 10.1111/cob.12203

7. Frigolet ME, Gutiérrez-Aguilar R. The colors of adipose tissue. *Gac Med Mex* (2020) 156:142–9. doi: 10.24875/GMM.M20000356

8. Bastard JP, Fève B. Physiology and physiopathology of adipose tissue. *Springer-Verlag* (2013) 2:1–437. doi: 10.1007/978-2-8178-0343-2

9. Wozniak SE, Gee LL, Wachtel MS, Frezza EE. Adipose tissue: The new endocrine organ? a review article. *Dig Dis Sci* (2009) 54:1847–56. doi: 10.1007/s10620-008-0585-3

10. Saely CH, Geiger K, Drexel H. Brown versus white adipose tissue: A mini-review. *Gerontology* (2011) 58:15–23. doi: 10.1159/000321319

11. Cinti S. Between brown and white: Novel aspects of adipocyte differentiation. *Ann Med* (2011) 43. doi: 10.3109/07853890.2010.535557

12. Unamuno X, Gómez-Ambrosi J, Rodríguez A, Becerril S, Frühbeck G, Catalán V. Adipokine dysregulation and adipose tissue inflammation in human obesity. *Eur J Clin Invest* (2018) 48(9):e12997. doi: 10.1111/eci.12997

13. Villarroya F, Cereijo R, Gavaldà-Navarro A, Villarroya J, Giralt M. Inflammation of brown/beige adipose tissues in obesity and metabolic disease. *J Intern Med* (2018) 284:492–504. doi: 10.1111/joim.12803

14. Choe SS, Huh JY, Hwang IJ, Kim JI, Kim JB. Adipose tissue remodeling: Its role in energy metabolism and metabolic disorders. *Front Endocrinol* (2016) 7:30. doi: 10.3389/fendo.2016.00030

15. Kahn CR, Wang G, Lee KY. Altered adipose tissue and adipocyte function in the pathogenesis of metabolic syndrome. *J Clin Invest* (2019) 129:3990–4000. doi: 10.1172/JCI129187

16. Lin JH, Walter P, Yen TS. Endoplasmic reticulum stress in disease pathogenesis. *Annu Rev Pathol* (2008) 3:399–425. doi: 10.1146/annurev.pathmechdis.3.121806.151434

17. Tarayre JP, Aliaga M, Barbara M, Tisné-Versailles J. Hypotheses on a possible role of some mediators in various inflammatory reactions on mouse ear. *Methods Find Exp Clin Pharmacol* (1988) 10(10):623–7.

18. Dong L, Krewson EA, Yang LV. Acidosis activates endoplasmic reticulum stress pathways through GPR4 in human vascular endothelial cells. *Int J Mol Sci* (2017) 18 (2):278. doi: 10.3390/ijms18020278

19. Balsa E, Soustek MS, Thomas A, Cogliati S, García-Poyatos C, Martín-García E, et al. ER and nutrient stress promote assembly of respiratory chain supercomplexes through the PERK-eIF2α axis. *Mol Cell* (2019) 74(5):877–90.e6. doi: 10.1016/j.molcel.2019.03.031

20. Chadwick SR, Lajoie P. Endoplasmic reticulum stress coping mechanisms and lifespan regulation in health and diseases. *Front Cell Dev Biol* (2019) 7:84. doi: 10.3389/fcell.2019.00084

21. Chipurupalli S, Samavedam U, Robinson N. Crosstalk between ER stress, autophagy and inflammation. *Front Med* (2021) 8:758311. doi: 10.3389/fmed.2021.758311

22. Adams CJ, Kopp MC, Larburu N, Nowak PR, Ali MMU. Structure and molecular mechanism of ER stress signaling by the unfolded protein response signal activator IRE1. *Front Mol Biosci* (2019) 6:11. doi: 10.3389/fmolb.2019.00011

23. Chaudhari N, Talwar P, Parimisetty A, Lefebvre d'Hellencourt C, Ravanan P. A molecular web: endoplasmic reticulum stress, inflammation, and oxidative stress. *Front Cell Neurosci* (2014) 8:213. doi: 10.3389/fncel.2014.00213

24. Zeeshan HM, Lee GH, Kim HR, Chae HJ. Endoplasmic reticulum stress and associated ROS. *Int J Mol Sci* (2016) 17:327. doi: 10.3390/ijms17030327

25. Benjamin P, Jonathan S. Weissman; oxidative protein folding in eukaryotes: mechanisms and consequences. *J Cell Biol* (2004) 164(3):341–6. doi: 10.1083/jcb.200311055

26. Malhi H, Kaufman RJ. Endoplasmic reticulum stress in liver disease. *J Hepatol* (2011) 54(4):795–809. doi: 10.1016/j.jhep.2010.11.005

27. Bhandary B, Marahatta A, Kim HR, Chae HJ. An involvement of oxidative stress in endoplasmic reticulum stress and its associated diseases. *Int J Mol Sci* (2013) 14:434–56. doi: 10.3390/ijms14010434

28. Oyadomari S, Mori M. Roles of CHOP/GADD153 in endoplasmic reticulum stress. *Cell Death Differ* (2004) 11(4):381–9. doi: 10.1038/sj.cdd.4401373

29. Suzuki T, Gao J, Ishigaki Y, Kondo K, Sawada S, Izumi T, et al. ER stress protein CHOP mediates insulin resistance by modulating adipose tissue macrophage polarity. *Cell Rep* (2017) 18(8):2045–57. doi: 10.1016/j.celrep.2017.01.076

30. Shan B, Wang X, Wu Y, Xu C, Xia Z, Dai J, et al. The metabolic ER stress sensor IRE1α suppresses alternative activation of macrophages and impairs energy expenditure in obesity. *Nat Immunol* (2017) 18(5):519–29. doi: 10.1038/ni.3709

31. Torre-Villalvazo I, Bunt AE, Alemán G, Marquez-Mota CC, Diaz-Villaseñor A, Noriega LG, et al. Adiponectin synthesis and secretion by subcutaneous adipose tissue is impaired during obesity by endoplasmic reticulum stress. *J Cell Biochem* (2018) 119 (7):5970–84. doi: 10.1002/jcb.26794

32. Hosoi T, Sasaki M, Miyahara T, Hashimoto C, Matsuo S, Yoshii M, et al. Endoplasmic reticulum stress induces leptin resistance. *Mol Pharmacol* (2008) 74 (6):1610–9. doi: 10.1124/mol.108.050070

33. Menikdiwela KR, Guimarães JP, Ramalingam L, Kalupahana N, Dufour JM, Washburn L, et al. Mechanisms linking endoplasmic reticulum (ER) stress and microRNAs to adipose tissue dysfunction in obesity. *Crit Rev Biochem Mol Biol* (2021) 56:5. doi: 10.1080/10409238.2021.1925219

34. Zhu W, Niu X, Wang M, Li Z, Jiang HK, Li C, et al. Endoplasmic reticulum stress may be involved in insulin resistance and lipid metabolism disorders of the white adipose tissues induced by high-fat diet containing industrial trans-fatty acids. *Diabetes Metab Syndr Obes* (2019) 29:12. doi: 10.2147/DMSO.S218336

35. Lee JM, Park S, Lee D, Ginting RP, Lee MR, Lee MW, et al. Reduction in endoplasmic reticulum stress activates beige adipocytes differentiation and alleviates high fat diet-induced metabolic phenotypes. *Biochim Biophys Acta Mol Basis Dis* (2021) 1867(5):166099. doi: 10.1016/j.bbadis.2021.166099

36. Chen Y, Wu Z, Huang S, Wang X, He S, Liu L, et al. Adipocyte IRE1α promotes PGC1α mRNA decay and restrains adaptive thermogenesis. *Nat Metab* (2022) 4:1166–84. doi: 10.1038/s42255-022-00631-8

37. Chen Y, Wu Z, Zhao S, Xiang R. Chemical chaperones reduce ER stress and adipose tissue inflammation in high fat diet-induced mouse model of obesity. *Sci Rep* (2016) 6:1–8. doi: 10.1038/srep27486

38. Kawasaki N, Asada R, Saito A, Kanemoto S, Imaizumi K. Obesity-induced endoplasmic reticulum stress causes chronic inflammation in adipose tissue. *Sci Rep* (2012) 2:1–7. doi: 10.1038/srep00799

39. McGregor RA, Kwon EY, Shin SK, Jung UJ, Kim E, Park JHY, et al. Time-course microarrays reveal modulation of developmental, lipid metabolism and immune gene networks in intrascapular brown adipose tissue during the development of diet-induced obesity. *Int J Obes* (2013) 37:1524–31. doi: 10.1038/ijo.2013.52

40. Vitali A, Murano I, Zingaretti MC, Frontini A, Ricquier D, Cinti S. The adipose organ of obesity-prone C57BL/6J mice is composed of mixed white and brown adipocytes. *J Lipid Res* (2012) 53(4):619–29. doi: 10.1194/jlr.M018846

41. Stephens M, Ludgate M, Rees DA. Brown fat and obesity: the next big thing? *Clin Endocrinol* (2011) 74(6):661–70. doi: 10.1111/j.1365-2265.2011

42. Bournat JC, Brown CW. Mitochondrial dysfunction in obesity. *Curr Opin Endocrinol Diabetes Obes* (2010) 17(5):446–52. doi: 10.1097/MED.0b013e32833c3026

43. Shimizu I, Walsh K. The whitening of brown fat and its implications for weight management in obesity. *Curr Obes Rep* (2015) 4:224–9. doi: 10.1007/s13679-015-0157-8

44. Gao P, Jiang Y, Wu H, Sun F, Li Y, He H, et al. Inhibition of mitochondrial calcium overload by SIRT3 prevents obesity- or age-related whitening of brown adipose tissue. *Diabetes* (2020) 2:165–80. doi: 10.2337/db19-0526

45. Alcalá M, Calderon-Dominguez M, Serra D, Herrero L, Viana M. Mechanisms of impaired brown adipose tissue recruitment in obesity. *Front Physiol* (2019) 10:94. doi: 10.3389/fphys.2019.00094

46. Liu Z, Gu H, Gan L, Xu Y, Feng F, Saeed M, et al. Reducing Smad3/ATF4 was essential for Sirt1 inhibiting ER stress-induced apoptosis in mice brown adipose tissue. *Oncotarget* (2017) 8:9267–79. doi: 10.18632/oncotarget.14035

47. Bond LM, Burhans MS, Ntambi JM. Uncoupling protein-1 deficiency promotes brown adipose tissue inflammation and ER stress. *PloS One* (2018) 13(11):e0205726. doi: 10.1371/journal.pone.0205726

48. Asada R, Kanemoto S, Matsuhisa K, Hino K, Cui M, Cui X, et al. IRE1α-XBP1 is a novel branch in the transcriptional regulation of Ucp1 in brown adipocytes. *Sci Rep* (2015) 5:16580. doi: 10.1038/srep16580

49. Kato H, Okabe K, Miyake M, Hattori K, Fukaya T, Tanimoto K, et al. ER-resident sensor PERK is essential for mitochondrial thermogenesis in brown adipose tissue. *Life Sci Alliance* (2020) 3(3):e201900576. doi: 10.26508/lsa.201900576

50. Ferrara D, Montecucco F, Dallegri F, Carbone F. Impact of different ectopic fat depots on cardiovascular and metabolic diseases. *J Cell Physiol* (2019) 234:21630–41. doi: 10.1002/jcp.28821

51. Camporez JP, Wang Y, Faarkrog K, Chukijrungroat N, Petersen KF, Shulman GI. Mechanism by which arylamine n-acetyltransferase 1 ablation causes insulin

resistance in mice. *Proc Natl Acad Sci U.S.A.* (2017) 114(52):E11285–92. doi: 10.1073/pnas.1716990115

52. Camargo FN, Matos SL, Araujo LCC, Carvalho CRO, Amaral AG, Camporez JP. Western Diet-fed ApoE knockout Male mice as an experimental model of non-alcoholic steatohepatitis. *Curr Issues Mol Biol* (2022) 44(10):4692–703. doi: 10.3390/cimb44100320

53. Arab JP, Arrese M, Trauner M. Recent insights into the pathogenesis of nonalcoholic fatty liver disease. *Annu Rev Pathol Mech Dis* (2018) 13:321–50. doi: 10.1146/annurev-pathol-020117-043617

54. Buzzetti E, Pinzani M, Tsochatzis EA. The multiple-hit pathogenesis of non-alcoholic fatty liver disease (NAFLD). *Metabolism* (2016) 65:1038–48. doi: 10.1016/j.metabol.2015.12.012

55. Lee AH, Scapa EF, Cohen DE, Glimcher LH. Regulation of hepatic lipogenesis by the transcription factor XBP1. *Science* (2008) 320(5882):1492–6. doi: 10.1126/science.1158042

56. Lebeaupin C, Proics E, de Bieville CH, Rousseau D, Bonnafous S, Patouraux S, et al. ER stress induces NLRP3 inflammasome activation and hepatocyte death. *Cell Death Dis* (2015) 6(9):e1879. doi: 10.1038/cddis.2015.248

57. Zheng W, Sun Q, Li L, Cheng Y, Chen Y, Lv M, et al. Role of endoplasmic reticulum stress in hepatic glucose and lipid metabolism and therapeutic strategies for metabolic liver disease. *Int Immunopharmacol* (2022) 113(Pt B):109458. doi: 10.1016/j.intimp.2022.109458

58. Chang L, Milton H, Eitzman DT, Eugene Chen Y. Paradoxical roles of perivascular adipose tissue in atherosclerosis and hypertension. *Circ J* (2013) 77:11–8. doi: 10.1253/circj.CJ-12-1393

59. Victorio JA, Guizoni DM, Freitas IN, Araujo TR, Davel AP. Effects of high-fat and high-Fat/High-Sucrose diet-induced obesity on PVAT modulation of vascular function in Male and female mice. *Front Pharmacol* (2021) 10:720224. doi: 10.3389/fphar.2021.720224

60. Fitzgibbons TP, Kogan S, Aouadi M, Hendricks GM, Straubhaar J, Czech MP. Similarity of mouse perivascular and brown adipose tissues and their resistance to diet-induced inflammation. *Am J Physiol - Hear Circ Physiol* (2011) 301(4):H1425–37. doi: 10.1152/ajpheart.00376.2011

61. Police SB, Thatcher SE, Charnigo R, Daugherty A, Cassis LA. Obesity promotes inflammation in periaortic adipose tissue and angiotensin ii-induced abdominal aortic aneurysm formation. *Arterioscler Thromb Vasc Biol* (2009) 29. doi: 10.1161/ATVBAHA.109.192658

62. Padilla J, Jenkins NT, Vieira-Potter VJ, Harold Laughlin M. Divergent phenotype of rat thoracic and abdominal perivascular adipose tissues. *Am J Physiol - Regul Integr Comp Physiol* (2013) 304(7):R543–52. doi: 10.1152/ajpregu.00567.2012

63. Aghamohammadzadeh R, Unwin RD, Greenstein AS, Heagerty AM. Effects of obesity on perivascular adipose tissue vasorelaxant function: Nitric oxide, inflammation and elevated systemic blood pressure. *J Vasc Res* (2016) 52:299–305. doi: 10.1159/000443885

64. Greenstein AS, Khavandi K, Withers SB, Sonoyama K, Clancy O, Jeziorska M, et al. Local inflammation and hypoxia abolish the protective anticontractile properties of perivascular fat in obese patients. *Circulation* (2009) 119:1661–70. doi: 10.1161/CIRCULATIONAHA.108.821181

65. Gómez-Hernández A, Beneit N, Díaz-Castroverde S, Escribano Ó. Differential role of adipose tissues in obesity and related metabolic and vascular complications. *Int J Endocrinol* (2016). doi: 10.1155/2016/1216783

66. Araujo HN, Victorio JA, Valgas da Silva CP, Sponton ACS, Vettorazzi JF, de Moraes C, et al. Anti-contractile effects of perivascular adipose tissue in thoracic aorta from rats fed a high-fat diet: role of aerobic exercise training. *Clin Exp Pharmacol Physiol* (2018) 45(3):293–302. doi: 10.1111/1440-1681.12882

67. Victorio JA, Davel AP. Perivascular adipose tissue oxidative stress on the pathophysiology of cardiometabolic diseases. *Curr Hypertens Rev* (2020) 16(3):192–200. doi: 10.2174/1573402115666190410153634

68. Wang M, Xing J, Liu M, Gao M, Liu Y, Li X, et al. Deletion of seipin attenuates vascular function and the anticontractile effect of perivascular adipose tissue. *Front Cardiovasc Med* (2021) 8:706924. doi: 10.3389/fcvm.2021.706924

69. Ying R, Li SW, Chen JY, Zhang HF, Yang Y, Gu ZJ, et al. Endoplasmic reticulum stress in perivascular adipose tissue promotes destabilization of atherosclerotic plaque by regulating GM-CSF paracrine. *J Transl Med* (2018) 16(1):105. doi: 10.1186/s12967-018-1481-z

70. Ackerman HD, Gerhard GS. Bile acids in neurodegenerative disorders. *Front Aging Neurosci* (2016) 8:263. doi: 10.3389/fnagi.2016.00263

71. Hylemon PB, Zhou H, Pandak WM, Ren S, Gil G, Dent P. Bile acids as regulatory molecules. *J Lipid Res* (2009) 50:1509–20. doi: 10.1194/jlr.R900007-JLR200

72. Lee YY, Hong SH, Lee YJ, Chung SS, Jung HS, Park SG, et al. Tauroursodeoxycholate (TUDCA), chemical chaperone, enhances function of islets by reducing ER stress. *Biochem Biophys Res Commun* (2010) 397(4):735–9. doi: 10.1016/j.bbrc.2010.06.022

73. Kawamata Y, Fujii R, Hosoya M, Harada M, Yoshida H, Miwa M, et al. A G protein-coupled receptor responsive to bile acids. *J Biol Chem* (2003) 278:9435–40. doi: 10.1074/jbc.M209706200

74. Hanafi NI, Mohamed AS, Kadir SHSA, Othman MHD. Overview of bile acids signaling and perspective on the signal of ursodeoxycholic acid, the most hydrophilic bile acid, in the heart. *Biomolecules* (2018) 8(4):159. doi: 10.3390/biom8040159

75. Wan YJY, Sheng L. Regulation of bile acid receptor activity. *Liver Res* (2018) 2(4):180-5. doi: 10.1016/j.livres.2018.09.008

76. Schmid A, Schlegel J, Thomalla M, Karrasch T, Schäffler A. Evidence of functional bile acid signaling pathways in adipocytes. *Mol Cell Endocrinol* (2019) 483:1–10. doi: 10.1016/j.mce.2018.12.006

77. Hayashi H, Sugiyama Y. 4-phenylbutyrate enhances the cell surface expression and the transport capacity of wild-type and mutated bile salt export pumps. *Hepatology* (2007) 45:1506–16. doi: 10.1002/hep.21630

78. Telbisz Á, Homolya L. Recent advances in the exploration of the bile salt export pump (BSEP/ABCB11) function. *Expert Opin Ther Targets* (2016) 20:501–14. doi: 10.1517/14728222.2016.1102889

79. Yang JS, Kim JT, Jeon J, Park HS, Kang GH, Park KS, et al. Changes in hepatic gene expression upon oral administration of taurine-conjugated ursodeoxycholic acid in ob/ob mice. *PloS One* (2010) 5:1–10. doi: 10.1371/journal.pone.0013858

80. Kusaczuk M. Tauroursodeoxycholate-bile acid with chaperoning activity: Molecular and cellular effects and therapeutic perspectives. *Cells* (2019) 8(12):1471. doi: 10.3390/cells8121471

81. Dos Reis AT, Roberta Rodrigues MM, Lourençoni AB, Monali Barreto Dos SL, Fernandes BM, Alves da SJJ, et al. Tauroursodeoxycholic acid improves glucose tolerance and reduces adiposity in normal protein and malnourished mice fed a high-fat diet. *Food Res Int* (2022) 156:111331. doi: 10.1016/j.foodres.2022.111331

82. Münzker J, Haase N, Till A, Sucher R, Haange SB, Nemetschke L, et al. Functional changes of the gastric bypass microbiota reactivate thermogenic adipose tissue and systemic glucose control via intestinal FXR-TGR5 crosstalk in diet-induced obesity. *Microbiome* (2022) 10(1):96. doi: 10.1186/s40168-022-01264-5

83. Watanabe M, Houten SM, Mataki C, Christoffolete MA, Kim BW, Sato H, et al. Bile acids induce energy expenditure by promoting intracellular thyroid hormone activation. *Nature* (2006) 439(7075):484–9. doi: 10.1038/nature04330

84. Broeders EPM, Nascimento EBM, Havekes B, Brans B, Roumans KHM, Tailleux A, et al. The bile acid chenodeoxycholic acid increases human brown adipose tissue activity. *Cell Metab* (2015) 22(3):418-26. doi: 10.1016/j.cmet.2015.07.002

85. Velazquez-Villegas LA, Perino A, Lemos V, Zietak M, Nomura M, Pols TWH, et al. TGR5 signalling promotes mitochondrial fission and beige remodelling of white adipose tissue. *Nat Commun* (2018) 9(1):245. doi: 10.1038/s41467-017-02068-0

86. Saito M, Matsushita M, Yoneshiro T, Okamatsu-Ogura Y. Brown adipose tissue, diet-induced thermogenesis, and thermogenic food ingredients: From mice to men. *Front Endocrinol (Lausanne)* (2020) 11:222. doi: 10.3389/fendo.2020.00222

87. McIlvride S, Nikolova V, Fan HM, McDonald JAK, Wahlström A, Bellafante E, et al. Obeticholic acid ameliorates dyslipidemia but not glucose tolerance in mouse model of gestational diabetes. *Am J Physiol Endocrinol Metab* (2019) 317(2):E399–410. doi: 10.1152/ajpendo.00407.2018

88. van Zutphen T, Stroeve JHM, Yang J, Bloks VW, Jurdzinski A, Roelofsen H, et al. FXR overexpression alters adipose tissue architecture in mice and limits its storage capacity leading to metabolic derangements. *J Lipid Res* (2019) 60(9):1547–61. doi: 10.1194/jlr.M094508

89. Haczeyni F, Poekes L, Wang H, Mridha AR, Barn V, Geoffrey Haigh W, et al. Obeticholic acid improves adipose morphometry and inflammation and reduces steatosis in dietary but not metabolic obesity in mice. *Obesity* (2017) 25(1):155–65. doi: 10.1002/oby.21701

90. Prawitt J, Abdelkarim M, Stroeve JH, Popescu I, Duez H, Velagapudi VR, et al. Farnesoid X receptor deficiency improves glucose homeostasis in mouse models of obesity. *Diabetes* (2011) 60(7):1861–71. doi: 10.2337/db11-0030

91. Vettorazzi JF, Ribeiro RA, Borck PC, Branco RC, Soriano S, Merino B, et al. The bile acid TUDCA increases glucose-induced insulin secretion *via* the cAMP/PKA pathway in pancreatic beta cells. *Metabolism* (2016) 65(3):54–63. doi: 10.1016/j.metabol.2015.10.021

92. Ozcan U, Yilmaz E, Ozcan L, Furuhashi M, Vaillancourt E, Smith RO, et al. Chemical chaperones reduce ER stress and restore glucose homeostasis in a mouse model of type 2 diabetes. *Science* (2006) 313:1137–40. doi: 10.1126/science.1128294

93. da Silva JAJr, Figueiredo LS, Chaves JO, Oliveira KM, Carneiro EM, Abreu PA, et al. Effects of tauroursodeoxycholic acid on glucose homeostasis: Potential binding of this bile acid with the insulin receptor. *Life Sci* (2021) 285:120020. doi: 10.1016/j.lfs.2021.120020

94. Cha BH, Kim JS, Chan Ahn J, Kim HC, Kim BS, Han DK, et al. The role of tauroursodeoxycholic acid on adipogenesis of human adipose-derived stem cells by modulation of ER stress. *Biomaterials* (2014) 35:2851–8. doi: 10.1016/j.biomaterials.2013.12.067

95. Li A, Zhang S, Li J, Liu K, Huang F, Liu B. Metformin and resveratrol inhibit Drp1-mediated mitochondrial fission and prevent ER stress-associated NLRP3 inflammasome activation in the adipose tissue of diabetic mice. *Mol Cell Endocrinol* (2016) 434:36–47. doi: 10.1016/j.mce.2016.06.008

96. Contreras C, Fondevila MF, López M. Hypothalamic GRP78, a new target against obesity? *Adipocyte* (2018) 7(1):63–6. doi: 10.1080/21623945.2017.1405878

97. Jeong HW, Choi RH, Koh HJ. Obesity-induced TRB3 negatively regulates brown adipose tissue function in mice. *Biochem Biophys Res Commun* (2021) 547:29–35. doi: 10.1016/j.bbrc.2021.01.103

98. Cho EJ, Yoon JH, Kwak MS, Jang ES, Lee JH, Yu SJ, et al. Tauroursodeoxycholic acid attenuates progression of steatohepatitis in mice fed a methionine-choline-deficient diet. *Dig Dis Sci* (2014) 59(7):1461–74. doi: 10.1007/s10620-014-3217-0

99. Battson ML, Lee DM, Jarrell DK, Hou S, Ecton KE, Phan AB, et al. Tauroursodeoxycholic acid reduces arterial stiffness and improves endothelial dysfunction in type 2 diabetic mice. *J Vasc Res* (2017) 54(5):280–7. doi: 10.1159/000479967

100. Xu X, Chen Y, Song J, Hou F, Ma X, Liu B, et al. Mangiferin suppresses endoplasmic reticulum stress in perivascular adipose tissue and prevents insulin resistance in the endothelium. *Eur J Nutr* (2018) 57(4):1563–75. doi: 10.1007/s00394-017-1441-z

101. Vettorazzi JF, Kurauti MA, Soares GM, Borck PC, Ferreira SM, Branco RCS, et al. Bile acid TUDCA improves insulin clearance by increasing the expression of insulin-degrading enzyme in the liver of obese mice. *Sci Rep* (2017) 7(1):14876. doi: 10.1038/s41598-017-13974-0

102. Hetz C, Zhang K, Kaufman RJ. Mechanisms, regulation and functions of the unfolded protein response. *Nat Rev Mol Cell Biol* (2020) 21:421–38. doi: 10.1038/s41580-020-0250-z

103. Larghi A, Crosignani A, Battezzati PM, De Valle G, Allocca M, Invernizzi P, et al. Ursodeoxycholic and tauro-ursodeoxycholic acids for the treatment of primary biliary cirrhosis: a pilot crossover study. *Aliment Pharmacol Ther* (1997) 11:409–14. doi: 10.1046/j.1365-2036.1997.124295000

frontiers | Frontiers in Endocrinology

TYPE Original Research
PUBLISHED 12 May 2023
DOI 10.3389/fendo.2023.1120531



OPEN ACCESS

EDITED BY
Bruno Melo Carvalho,
Universidade de Pernambuco, Brazil

REVIEWED BY
Cecilia Castillo,
Nutriologa Infantil, Chile
Thinus Smit,
Sefako Makgatho Health Sciences University, South Africa
William Toet,
University of Cape Town, South Africa
Danie Van Zyl,
University of Pretoria, South Africa

*CORRESPONDENCE
Prabash Sadhai
prabashsadhai@gmail.com
Ankia Coetzee
ankiac@sun.ac.za

†These authors have contributed equally to this work and share first authorship

RECEIVED 10 December 2022
ACCEPTED 20 March 2023
PUBLISHED 12 May 2023

CITATION
Sadhai P, Coetzee A, Conradie-Smit M, Greyling CJ, van Gruting R, du Toit I, Lubbe J, van de Vyver M and Conradie M (2023) Nutritional deficiency in South African adults scheduled for bariatric surgery.
*Front. Endocrinol.* 14:1120531.
doi: 10.3389/fendo.2023.1120531



# Nutritional deficiency in South African adults scheduled for bariatric surgery

Prabash Sadhai [1*†], Ankia Coetzee [1,2*†], Marli Conradie-Smit [1,2], C. J. Greyling [3], Rutger van Gruting [1], Inge du Toit [4], Jeanne Lubbe [4], Mari van de Vyver [5] and Magda Conradie [1,2]

[1]Tygerberg Hospital, Faculty of Medicine and Health Sciences, Stellenbosch University, Cape Town, South Africa, [2]Division of Endocrinology, Department of Medicine, Faculty of Medicine and Health Sciences, Stellenbosch University, Cape Town, South Africa, [3]Specialist Physician & Endocrinologist, Durbanville Mediclinic and Kuilsriver Netcare Hospital, Cape Town, South Africa, [4]Department of Surgical Sciences, Division of Surgery, Faculty of Medicine and Health Sciences, Stellenbosch University, Cape Town, South Africa, [5]Division of Clinical Pharmacology, Department of Medicine, Faculty of Medicine and Health Sciences, Stellenbosch University, Cape Town, South Africa

**Background:** Globally, there is a rising trend in obesity, known to increase morbidity and mortality. Metabolic surgery and adequate weight loss decrease mortality but may worsen pre-existing nutrient deficiencies. Most data on pre-existing nutritional deficiencies in the population undergoing metabolic surgery is from the developed world, where an extensive micronutrient assessment is achievable. In resource-constrained environments, the cost of a comprehensive micronutrient assessment must be weighed against the prevalence of nutritional deficiencies and the potential harm if one or more nutritional deficiencies are missed.

**Methods:** This cross-sectional study investigated the prevalence of micronutrient and vitamin deficiencies in participants scheduled to undergo metabolic surgery in Cape Town, South Africa, a low-middle income country. 157 participants were selected and 154 reported on; who underwent a baseline evaluation from 12 July 2017 to 19 July 2020. Laboratory measurements were conducted, including vitamin B12 (Vit B12), 25-hydroxy vitamin D (25(OH)D), folate, parathyroid hormone (PTH), thyroid-stimulating hormone (TSH), thyroxine (T4), ferritin, glycated haemoglobin (HbA1c), magnesium, phosphate, albumin, iron, and calcium.

**Results:** Participants were predominantly female, aged 45 years (37-51), with a preoperative BMI of 50.4 kg/m$^2$ (44.6-56.5). A total of 64 individuals had Type 2 diabetes mellitus (T2D), with 28 undiagnosed cases at study entry (18% of study population). 25(OH)D deficiency was most prevalent (57%), followed by iron deficiency (44%), and folate deficiency (18%). Other deficiencies (vitamin B12, calcium, magnesium, phosphate) were rarely encountered and affected ≤1% of participants. Folate and 25(OH)D deficiency were related to obesity classification, with a higher prevalence in participants with a BMI ≥40 kg/m$^2$ ($p < 0.01$).

**Conclusion:** A higher prevalence of some micronutrient deficiencies was noted compared with data from similar populations in the developed world. The minimum baseline/preoperative nutrient evaluation in such populations should

include 25(OH)D, iron studies, and folate. Additionally, screening for T2D is recommended. Future efforts should seek to collate broader patient data on a national scale and include longitudinal surveillance after surgery. This may provide a more holistic picture of the relationship between obesity, metabolic surgery and micronutrient status inform more appropriate evidence-based care.

KEYWORDS

bariatric (weight loss) surgery, obesity, micronutrient deficiency, pre-bariatric aspects, diabetes, diabetes mellitus, vitamin D

# 1 Introduction

The unfavorable metabolic milieu associated with obesity is a worldwide concern and was recently highlighted by the Coronavirus Infectious Disease 2019 (COVID-19) pandemic (1–4). Epidemiological studies from around the globe have conclusively demonstrated a linear association between obesity and all-cause mortality, with mortality pre-dominantly attributable to cardiovascular disease (1, 5, 6). A recent meta-analysis suggests a rise in death rate as body mass index (BMI) increases above 25 kg/$m^2$ (7).

Obesity is often mistakenly assumed to be synonymous with a state of nutritional excess. The excess, however, only applies to the energy balance. As such obesity can paradoxically represent a state of nutritional deficiency. Obesity is often compounded by a change in diet to low-cost, readily available, high sugar, high carbohydrate, and nutrient-deficient meals. Therefore, excess weight can co-occur with malnutrition, known as the 'overfed but undernourished' phenomenon (8, 9).

Metabolic surgery effectively addresses the harmful effects of excess weight and has decreased morbidity and mortality associated with excess adiposity (10–13). The benefits of metabolic surgery performed in high volume centers outweigh the associated potential harm, provided that precautionary measures are taken to prevent long-term adversities (14–17).

In recent years reports of pre-existing micronutrient deficiency in patients scheduled for metabolic surgery have increased (18, 19). Krzizek et al. (19) demonstrated a high prevalence of micronutrient deficiencies preoperatively in Austria, with 25-hydroxy vitamin D (25(OH)D) deficiency significantly associated with higher BMI (19). Flancbaum reported preoperative deficiencies of 43.9% for iron, 8.4% for ferritin, and 68.1% for 25(OH)D in a cohort from New York (18). Geographical, socio-economical, and ethnic variables limit extrapolation of these findings to the South-African population undergoing surgery for obesity.

Since metabolic surgical procedures may further impact micronutrient status, correcting pre-existing deficiencies is standard care. It is thus recommended to evaluate and optimize the micronutrient status of all patients scheduled to undergo metabolic surgery preoperatively (20–22). In resource-limited environments, the cost of a comprehensive preoperative micronutrient assessment needs to be weighed against both the prevalence of deficiencies and the potential harm if these deficiencies remain undetected. Recommendations on preoperative testing should ideally be contextualized. The primary objective of this study was to determine the prevalence of micronutrient and vitamin deficiencies in obese patients scheduled to undergo metabolic surgery at a tertiary referral centre from a low-middle income country.

# 2 Materials and methods

This study, nested within a larger prospective OMIT (Obesity and Metabolic surgery Initiative Tygerberg) cohort study, followed a descriptive, cross-sectional design. The OMIT study was designed to evaluate the safety and efficacy of high-volume metabolic surgery in the public health sector at Tygerberg Hospital. Tygerberg Hospital is a tertiary level hospital that serves as a referral center for more than 3.4 million people residing in the Cape Town Metropole of South Africa.

The study protocol was approved by Stellenbosch University's Health Research Ethics Committee (S18/01/003) and conducted according to the 1964 Helsinki Declaration principles. All participants provided written informed consent.

## 2.1 Inclusion and exclusion criteria

All patients scheduled to undergo a Roux and Y-gastric bypass procedure or sleeve gastrectomy from 12 July 2017 to 19 July 2020, who underwent a thorough preoperative assessment, were considered for inclusion in this analysis.

### 2.1.1 Inclusion criteria

Obesity was defined based on the World Health Organization (WHO) classification (23). Obese individuals, aged 20-60-years, were eligible for surgical intervention and inclusion in the OMIT study, if they met the following criteria:

Individuals with

- BMI ≥40 kg/$m^2$ (WHO class III and above)

- o BMI 30.0-39.9 kg/m$^2$ (WHO class I and II) with a related co-morbid disease (diabetes, obstructive sleep apnea, osteoarthritis etc.), prior gestational diabetes (GDM) or current pre-diabetes (i.e., high risk for future diabetes)

### 2.1.2 Exclusion criteria

Potential participants were discussed by a multidisciplinary team (MDT) and were excluded from study entry if any of the following conditions were noted:

- o uncontrolled medical comorbidity(ies)
- o concurrent comorbidity(ies) deemed to be too high an operative risk following evaluation by a specialist anesthetist
- o contraindications to laparoscopic metabolic surgery including multiple prior open abdominal surgeries and the lack of commitment, support, resources, or other significant barriers to short, medium, and long-term adherence to the program.
- o active underlying malignancy or bowel disease such as peptic ulcer disease or inflammatory bowel disease
- o uncontrolled psychiatric illness or unwillingness to undergo psychiatric evaluation towards assessing psychological "fitness" for metabolic surgery
- o excessive, current, or previous alcohol or drug dependence/abuse
- o current pregnancy, breastfeeding, planning pregnancy in the next two years or unreliable contraception
- o immobile patients

## 2.2 Sociodemographic and anthropometric measurements

Data was collected prospectively. Gender and ethnic determination were made by self-declaration. Socio-economic status was categorized using the South African Department of Health's Uniform Patient Fee Schedule's (UPFS) classification code. The classification code, usually expressed in South African Rands, is reflected here as US Dollars for ease of reference. It is based on annual income brackets as follows: H0: Low – receiving grant or pension; H1: <$3800/person or <$5450/family; H2: $3800-$5450/person or $5450-$19070/family; H3: >$13620/person or > $19070/family; P: Private patients are those not subsidized by the state and, for this research, denotes participants with medical aid or the highest income category.

Basic anthropometric measurements (weight, height, waist circumference) were obtained by dedicated and permanent nursing staff. Weight was measured with minimal clothing using a Charder® digital scale placed on a flat surface and recorded to the nearest kilogram (kg) and height to the nearest one centimeter (cm) with a calibrated stadiometer. Body mass index (kg/m$^2$) was calculated as weight (kg) divided by square height (m) and participants were categorized according to the WHO classification (23): overweight (25-29.9 kg/m$^2$); Class I obesity (30-34.9 kg/m$^2$); Class II obesity (35-39.9 kg/m$^2$); Class III obesity (>40 kg/m$^2$) (23). Waist circumference (WC) was measured to the nearest 0.5 cm with a non-stretchable tape measure.

The clinical assessment also included blood pressure, urine dipstick, and a thorough surgical risk evaluation. Brachial blood pressure (BP) was measured, once, on the left arm while sitting down using a calibrated automated sphygmomanometer (Dinamap Carescape V100) with an appropriate cuff size. RightSign® multistix were used for urine analysis.

## 2.3 Biochemical analysis

All laboratory measurements were done by the National Health Laboratory Service (NHLS), a SANAS (South African National Accreditation System) accredited laboratory at Tygerberg Hospital (accreditation code M0390) using the Roche Cobas®6000 analyzer. The NHLS adheres to the Clinical and Laboratory Standards Institute (CLSI, previously National Committee for Clinical Laboratory Standards [NCCLS]) EP28-A3c (formerly C28-A3) guideline for Defining, Establishing and Verifying Reference Intervals in the Clinical Laboratory (24). Reference intervals used in our study are not population specific, but provided by the instrument manufacturer (24).

### 2.3.1 Micronutrient and hormonal assessment

Micronutrient status and associated hormonal regulators were determined *via* various laboratory techniques that included the following: electrochemiluminescence binding assay (immunoassay) for Vitamin B12 (Vit B12), 25(OH)D, folate, parathyroid hormone (PTH), thyroid-stimulating hormone (TSH), thyroxine (T4), and ferritin measurements; turbidimetric inhibition immunoassay for glycated hemoglobin (HbA1c); immunoturbidimetric assay to measure transferrin; colorimetric assay for magnesium, phosphate, albumin, and iron and spectrophotometric detection for calcium. Serum copper, zinc, selenium, vitamins B1, B3, B6, A, E, K, and C were not assessed. The HbA1c percentage was calculated with a programmed equation adhering to the international federation of clinical chemistry and laboratory standard recommendations (25).

Deficiencies were defined as follows: albumin <35 g/L, vitamin B12 <145 pmol/L, calcium <2.15 mmol/L, 25(OH)D deficient if ≤50 nmol/L; insufficient if 50.1-72.5 nmol/L and sufficient if ≥72.5 nmol/L (26); iron ≤13 ug/L, serum folate <8.8 nmol/L, magnesium <0.63 mmol/L, phosphate <0.78 mmol/L. Iron deficiency was defined as a ferritin <30 mcg/l or ferritin <100 mcg/l plus transferrin saturation <20 percent. Iron deficiency anemia was defined as a Hb <13 g/dl in male participants and <12 g/dl in female participants with biochemical features of iron deficiency (25).

Hormonal assessments were further defined or categorized. If the TSH was outside of the laboratory reference range (0.27–4.2 mIU/L), a free T4 and T3 were measured. Patients with a raised (PTH >6.9 pmol/L) or inappropriately normal PTH level (3.6-6.9

pmol/L) were diagnosed as having primary hyperparathyroidism if calcium was elevated (> 2.51 mmol/L). If calcium was not elevated, secondary hyperparathyroidism applied if 25(OH)D levels was noted to be deficient. Normocalcemic hyperparathyroidism was diagnosed if calcium and 25(OH)D were normal with a concomitant PTH >6.9 pmol/L.

### 2.3.2 Assessment of glycemic status

Glycemic status was not formally assessed with a 75-gram glucose 2-hour oral glucose tolerance test (OGTT). A diagnosis of pre-diabetes was based on a fasting plasma glucose (FPG) ≥5.6 mmol/L and <7 mmol/L and/or a HbA1c ≥5.7% and <6.5% (≥39 mmol/mol and <48 mmol/mol) (27). Diabetes mellitus was defined as a participant known with diabetes mellitus on anti-diabetic medication, or patients not known with diabetes mellitus with a FPG ≥7 mmol/L and/or HbA1c ≥6.5% (≥48 mmol/mol) (27).

## 2.4 Data management and statistical analysis

Structured standardized data sheets were used to capture demographic characteristics and relevant clinical data and subsequently gathered in the Bariatric Outcomes Longitudinal Database (BOLD), managed by the Surgical Review Corporation (SRC). The SRC, founded in 2003, is a United States of America-based independent and non-profit organization offering accreditation and assistance with data management. BOLD is web-based, and data was entered at each encounter or during bulk transfer from clinical notes. Statistical analysis was performed using GraphPad Prism (version 9) software. The Kolmogorov-Smirnov (K-S) normality test with Lilliefors correction was used ($p<0.05$) and normal distribution of data confirmed with the Shapiro-Wilk test. Non-parametric data is presented as median (IQR). Chi-square analysis and Fisher's exact tests were used to determine differences between stratified categories. Kruskal-Wallis ANOVA with Dunn's multiple comparison or Mann-Whitney test was done to determine differences between groups. Spearman's simple linear regression analysis was used to determine associations between variables. A probability value (p-value) of <0.05 was regarded as significant.

# 3 Results

## 3.1 Sociodemographic and anthropometric assessments

Of the 157 participants referred for metabolic surgery in the 3-year study-period, 154 (98%) were eligible for inclusion (Figure 1). Eleven participants (7%) were diagnosed with Class I or II obesity (<40 kg/m$^2$), while all others presented with Class III obesity or higher (>40 kg/m$^2$) (Supplementary Table S1). The median BMI of the total cohort was above the WHO Class III threshold [50.4 kg/m$^2$ (44.6-56.5)]. Most participants (136/154) were female with a median

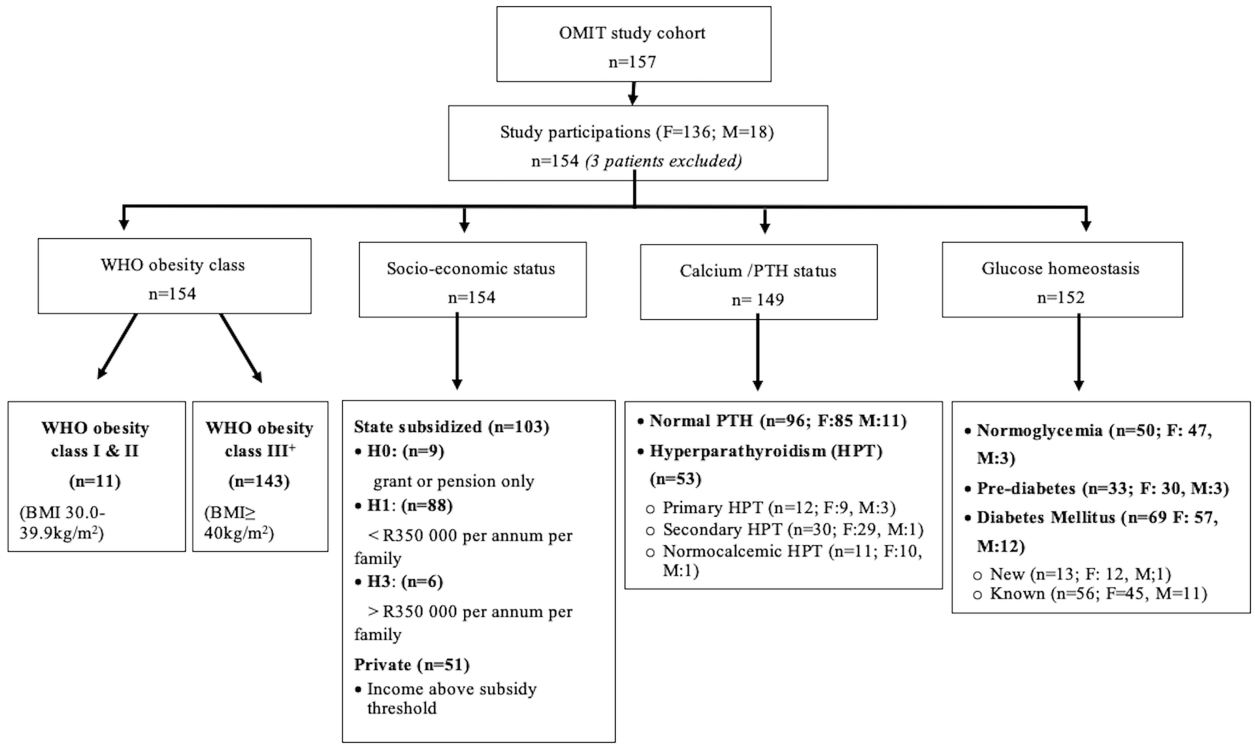


FIGURE 1
Overview of the study population and sstratification categories based on glycemic status and calcium homeostasis.

10.3389/fendo.2023.1120531

age of 45 years (37–51) and the majority either of mixed or Asian (65/154; 42%) or European (83/154; 54%) descent. Three patients were excluded due to concurrent comorbidity (significant chronic renal failure) deemed too high perioperative risk. Amongst the public-sector participants (n=103; 66% of study cohort), annual income in most participants was between $3800 and $5450 as individual and/or between $5450 and $19070 per family (categories H1-2) in 88/103 (85%). A small minority of public sector participants relied on state pension or medical disability (n=9; 9%; H0) or had a personal or family income more than $13620 or $19070 respectively (n=6; 6%; H3). Non-subsidized private participants on medical insurance comprised 33% of the study cohort.

## 3.2 Baseline micronutrient deficiencies and hormonal assessment

An overview of the micro-nutrient deficiencies in the study population at baseline is presented in Figure 2. The most common deficiency amongst the study population was a 25(OH)D deficiency, noted in 57% (88/154) of the cohort. Iron deficiency was present in 44% of participants, and folate deficiency in 18%. Deficiency of vitamin B12 (3%), calcium (1%), magnesium (1%) and phosphate (1%) were limited. None of the participants with vitamin B12 deficiency was on chronic metformin treatment and only one of the five was on a proton pump inhibitor (PPI). A total of 124 (80%) participants had 1-2 micronutrient deficiencies, 12 had >2 deficiencies and 18 did not have any deficiencies.

Baseline micronutrient deficiencies (Table 1) and diabetes status (Supplementary Table S1) were tabulated within population subcategories based on ethnicity, annual income and obesity class. Statistical evaluation was limited to ethnicity and obesity class on 25 (OH)D deficiency due to too small numbers for the other micronutrient deficiencies within the mentioned subpopulations.

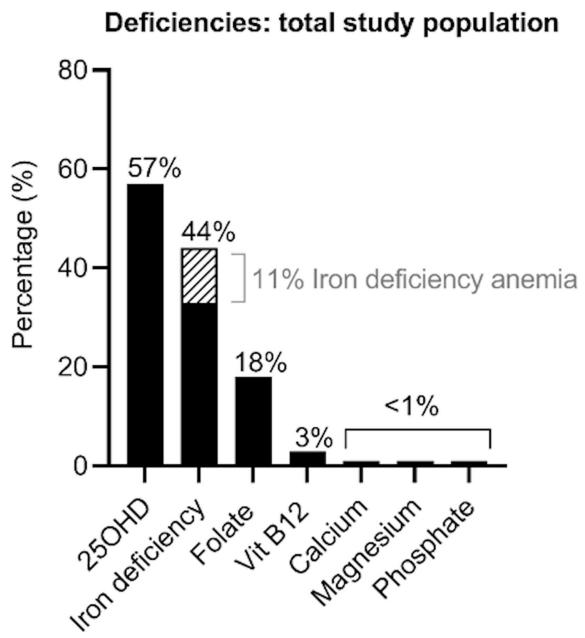


FIGURE 2
Overview of the deficiencies evident in the total study population.

A significant association between 25(OH)D deficiency (≤50 nmol/L) and ethnicity was noted in the study cohort (Table 1). 25 (OH)D deficiency was prevalent in 78% (51/65) (n/N) of participants with Mixed/Asian ancestry, in 67% (4/6) (n/N) of participants with Black African ancestry, and only in 40% (33/83) (n/N) of participants with European ancestry. There was furthermore a significant difference in the median 25(OH)D levels amongst WHO obesity categories. Class I and II obese participants (BMI<40kg.m$^2$) had higher 25(OH)D levels [62 (45–67) nmol/L] compared to class III obese participants (BMI>40 kg.m$^2$) [44 (36–60) nmol/L]. The majority (85/143; 59%) of individuals with BMI ≥40 kg/m$^2$ had 25(OH)D deficiency, compared to 27% (3/11) with a BMI <40 kg/m$^2$ (Figure 3A and Table 1).

Circulating plasma calcium levels were available in 154 participants and PTH status documented in 149. Calcium levels were low, normal, and elevated in 1% (2/154), 82% (127/154) and 16% (25/154) of patients at baseline respectively (Figure 3B). The two participants with low calcium levels had mild and asymptomatic hypocalcemia (i.e., uncorrected calcium levels of 2.02 mmol/L (albumin 42 g/dL) and 2.14 mmol/L (albumin 44 g/dL). A complete calcium and PTH dataset were available in 149 participants that included 17 of the 25 participants with hypercalcemia (Figure 3C). The diagnosis of primary hyperparathyroidism was based on the presence of hypercalcemia with either concomitant elevated PTH levels (4/12) or inappropriately normal, unsuppressed PTH values i.e., a PTH >3.5-6.9mmol/L (8/17). Primary hyperparathyroidism was present in 8% (12/149) [12/17 with hypercalcemia], secondary hyperparathyroidism in 20% (30/149), and normocalcemic hyperparathyroidism in 7% (11/149).

An expected inverse relationship between PTH and both calcium and 25(OH)D was observed (Figures 3D, E). The inverse relationship between PTH and 25(OH)D remained significant in the presence of normal circulating calcium levels (Figure 3F). Thirty four of the 88 participants with deficient 25 (OH)D levels had physiologically appropriate secondary hyperparathyroidism. WHO obesity class and glucose status had no statistically significant impact on circulating calcium levels.

Iron deficiency was the second most prevalent deficiency. Sixty-six participants (66/150; 44%) met the criteria for iron deficiency and 17/150 (11%) had iron-deficiency anaemia (Table 1). Folate deficiency was not present in any of participants in the BMI <40 kg/m$^2$ (0/11) (n/N) whereas 18% of participants with BMI ≥40 kg/m$^2$ (27/143) (n/N) presented with serum folate ≤8.8 nmol/L.

The median TSH of the total cohort was 1.97 (1.42-2.99) mIU/L. Of the 18 participants who had an elevated TSH level at baseline, the majority were known with primary hypothyroidism (10/18) on levothyroxine replacement therapy and of them 14 had subclinical hypothyroidism only (normal T4, TSH 4.2-9.9 mIU/L).

## 3.3 Glycemic status

A complete data set to evaluate glycemic status was available for 152 of the study participants (Figure 1). A concerning percentage of

TABLE 1 Baseline micronutrient deficiencies in the total cohort and within certain population categories.

| | 25(OH)D *(<50 nmol/L)* | Calcium *(<2,15 mmol/L)* | Iron *(<13 ug/L)* | Ferritin *(<30mcg/dL)* | Transferrin Sats (<20%) | Haemoglobin (<12 g/dL) | Albumin *(<35g/L)* | Iron deficiency[1] | Iron deficiency Anemia[2] | Folate *(<8,8 nmol/L)* |
|---|---|---|---|---|---|---|---|---|---|---|
| **Total study population: N=154** | | | | | | | | | | |
| *median (IQR)* | 46 (37-62) | 2.38 (2.3-2.47) | 10.95 (8.2-13.6) | 76 (38-170) | 16 (12-20) | 13.5 (12.5-14.3) | 44 (42-46) | | | 17.0 (10.3-28.4) |
| Total number of deficiencies | 88/154 (57%) | 2/154 (1%) | | | | | | 66/150 (44%) | 17/150 (11%) | 27/143 (18%) |
| **Number of deficiencies per category:** | | | | | | | | | | |
| **Gender** | | | | | | | | | | |
| Male | 9/18 (50%) | 0 | 8/18 (44%) | 0 | 11/18 (61%) | 0 | 0 | 3/18 (17%) | 1/18 (5%) | 3/18 (17%) |
| Female | 79/136 (58%) | 2/136 (1%) | 105/136 (77%) | 21/136 (15%) | 107/136 (78%) | 17/136 (12%) | 0 | 63/136 (46%) | 16/136 (12%) | 24/136 (18%) |
| **Ethnicity** | | | | | | | | | | |
| Mixed or Asian | 51/65 (78%) | 1/65 (2%) | 52/65 (80%) | 13/65 (20%) | 53/62 (85%) | 10/63 (16%) | 0 | 34/65 (52%) | 8/65 (12%) | 10/62 (16%) |
| European | 33/83 (40%) | 1/83 (1%) | 51/83 (61%) | 7/82 (9%) | 51/80 (64%) | 6/83 (7%) | 0 | 32/83 (39%) | 8/83 (10%) | 17/79 (22%) |
| Black African | 4/6 (67%) | 0 | 3/6 (50%) | 1/6 (17%) | 3/6 (50%) | 1/6 (17%) | 0 | 0 | 1/6 (17%) | 0 |
| *Chi-square* | **p<0.01* | | | | | | | | | |
| **Annual Income** | | | | | | | | | | |
| H0 | 4/9 (44%) | 0 | 7/9 (78%) | 1/9 (%) | 7/9 (78%) | 1/9 (11%) | 0 | 5/9 (56%) | 1/9 (11%) | 0 |
| H1-2 | 53/88 (60%) | 1/88 (1%) | 62/88 (70%) | 12/88 (14%) | 61/88 (69%) | 7/88 (8%) | 0 | 36/88 (41%) | 6/88 (7%) | 19/88 (22%) |
| H3 | 1/6 (17%) | 0/6 (0%) | 3/6 (50%) | 0 | 3/6 (50%) | 0 | 0 | 4/6 (67%) | 0 | 1/6 (17%) |
| P | 30/51 (59%) | 1/51 (2%) | 34/49 (69%) | 7/50 (%) | 36/45 (80%) | 9/48 (19%) | 0 | 21/49 (43%) | 2/49 (4%) | 6/46 (13%) |
| *Chi-square* | – | | | | | | | | | |
| **Obesity Class** | | | | | | | | | | |
| Class I-II BMI<40kg/$m^2$ | 3/11 (27%) | 0 | | | | | | 2/11 (18%) | 1/11 (9%) | 0 |
| Class III or above BMI>40kg/$m^2$ | 85/143 (59%) | 2/143 (1%) | | | | | | 64/143 (45%) | 16/143 (11%) | 27/143 (19%) |
| *Fishers Exact* | **p<0.01* | | | | | | | | | |

Statistical analysis, Fishers Exact & Chi-square analysis. *p<0.05 indicate significance.

the cohort had abnormal glucose homeostasis at baseline (n=102; 67%). T2D was present in 45% and included 69 participants, 56 with previously known and 13 with newly diagnosed T2D. The mean HbA1c in those with known T2D on treatment was 7.4 ± 1.8% and 7.3 ± 1.9% in those with newly diagnosed T2D prior to any intervention. Optimal glycemic control (treatment target HbA1c ≤ 7%) was only evident in 24 of the 56 participants with known T2D (42.8%). Pharmacological therapy in most was limited to monotherapy with metformin (n=40/56; 71%). Fourteen participants used combination oral therapy (metformin ± another oral agent) with or without insulin. Two participants were on insulin only.

# 4 Discussion

This study is the first to define preoperative micronutrient status in an African patient cohort scheduled for metabolic surgery. In South Africa, literature is available on the baseline patient profiles and outcomes after metabolic surgery, but little is known about the preoperative micronutrient status of bariatric cohorts (28). This study, in predominantly morbidly obese females, revealed significant deficiencies of some micronutrients at baseline indicative of obesity as a state of excess energy and is not synonymous with optimal nutrition. Like data from the developed world, vitamin D deficiency (57%) was the most prevalent, followed by iron deficiency (44%) and then folate deficiency (18%); with 88% (136/154) of the participants having at least one nutrient deficiency prior to surgery. Identification of the most prevalent micronutrient deficiencies preoperatively, enables clinicians to limit laboratory measurements in a resource constrained setting. The results suggest that the preoperative assessment of individuals scheduled for metabolic surgery should include, at minimum, the measurement of 25(OH)D, iron studies and folate.

While initial thinking framed obesity as a disease of the developed world, evidence indicates that the developing world is

10.3389/fendo.2023.1120531

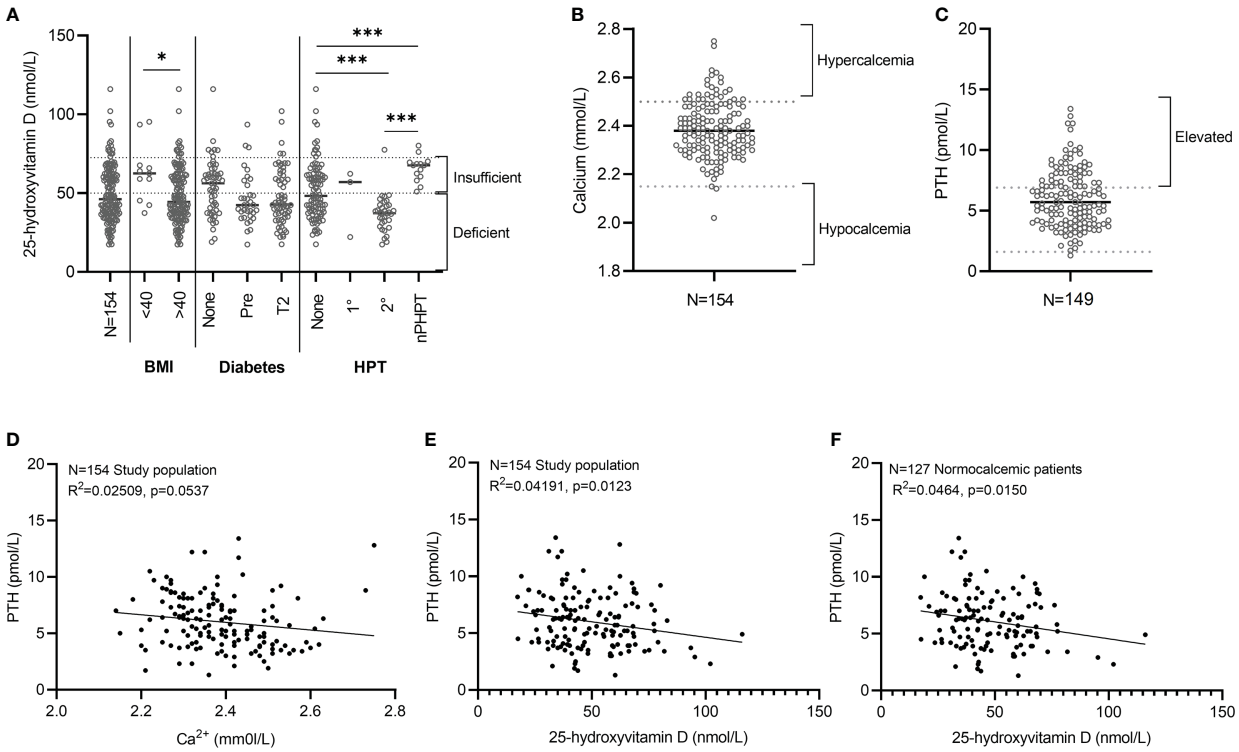


FIGURE 3
Relationship between PTH and 25(OH)D. **(A)** 25-hydroxyvitamin D (nmol/L). Individual data points are presented with the median for each group indicated using a grey line. The number of patients per category is as follow: BMI<40 kg/m$^2$ (N=11), BMI>40kg/m$^2$ (N=143), No diabetes (N=54), Pre-diabetes (N=34), Type 2 diabetes (N=64), Normal PTH levels (N=98), Primary hyperparathyroidism (HPT) (N=3), Secondary HPT (N=34), Normocalcemic HPT (N=14). *Statistical analysis.* BMI category: Mann-Whitney test. Hyperparathyroidism category: Kruskal-Wallis multiple comparisons test. *p<0.05, ***p<0.001 indicate significant difference between groups **(A)**. **(B)** Calcium levels (mmol/L) (N=154). **(C)** PTH levels (pmol/L) (N=154). Individual values are presented for the total study population (N=154) with the median indicated using a black line **(B, C)**. **(D–F)** Simple linear regression analysis between PTH and Calcium **(D)** and 25-hydroxyvitamin D **(E, F)**.

equally, if not more, prone to escalating rates of obesity (29, 30). An extensive systematic review and meta-analysis conducted in 199 countries from 1980–2008 showed that the average rate of BMI increase per decade is 0.4 kg/m$^2$ in men and 0.5 kg/m$^2$ in women (29). The meta-analysis revealed concerning statistics specifically for South Africa, noting an increase in BMI at a rate of 2.9 kg/m$^2$ per decade for males and 1.6 kg/m$^2$ per decade for females during 2000–2008. Longitudinal data derived from other South African studies support these findings and corroborate an upward trend in obesity (31). In developing countries, the obesity problem is compounded by urbanization, a change in diet to low-cost, easily accessible, high sugar, carbohydrate-dense, and nutrient-deficient diets, allowing for little variety (8). Obese individuals from lower-income settings or areas where food insecurity prevails, are expected to have more profound micronutrient deficiencies. Although this study is the largest to date to investigate baseline micronutrient deficiencies before metabolic surgery in an African population, the limited number of deficiencies per income category did not allow us to perform reliable statistical analysis to assess the interplay between socio-economic and nutritional status.

Sun exposure and the presence of melanin play a significant role in the metabolism of 25(OH)D. Higher melanin concentrations have advantages for those who live in areas of intense sunlight exposure by reducing the harmful effects of ultraviolet light on the skin; however, it does reduce the efficacy of 25(OH)D metabolism. South Africa has a heterogeneous population with marked variation in skin concentration of melanin. Skin pigmentation and concentration of melanin is known to influence activation of vitamin D in the skin and varies amongst the different ethnic groups in South Africa. Globally, people of African descent with higher skin melanin content are known to be predisposed to vitamin D deficiency and lower circulating 25(OH)D levels. 25 (OH)D levels were thus assessed at baseline as noted and compared amongst the different ethnic groups included in the study cohort.

A recent systematic review and meta-analysis describing 25 (OH)D deficiency in Africa, with high levels of sunlight, noted a pooled prevalence of low 25(OH)D status of 18.46% (32). Further, mean serum 25(OH)D levels were lower in South Africa compared to the rest of sub-Saharan Africa (30). This was attributed to lifestyle factors and increasing urbanization (32). The optimal serum 25 (OH)D for skeletal health is controversial, and concentrations for extra skeletal health have not been established. The Institute of Medicine (IOM) favors maintaining the serum 25(OH)D between 50 and 100 nmol/L for bone health (33). The US National Osteoporosis Foundation, the International Osteoporosis Foundation [IOF] and the American Geriatric Society suggest that a minimum level of 75 nmol/L is necessary to minimize fracture risk (34). Musculoskeletal health and fracture risk is a

concern in people who undergo metabolic surgery, and obesity is a predisposing factor for 25(OH)D deficiency, hence the rationale for adopting the higher threshold of 72.5 nmol/L in this study to denote sufficiency and to regard a circulating level of 25(OH)D ≤ 50nmol/L as deficient.

The prevalence of 25(OH)D deficiency was high (57%) in the relatively young cohort of these study participants (mean age 45 years; [37-51 years]). The highest percentage of 25(OH)D deficiency was documented in those of mixed ancestry/Asian decent (51/65; 78%) and in black Africans (4/6; 67%), a finding that supports the notion that melanin concentration does play a role in the skin activation of 25(OH)D. It is, however, noteworthy that the prevalence of 25(OH)D deficiency in the study participants was significantly higher than the figures reported for the general population in the region thereby implicating excess body weight, irrespective of skin melanin content, as a contributor to 25(OH)D deficiency (32).

The association between 25(OH)D and obesity has not been fully established, and various theories have been postulated (35). 25(OH)D metabolism hinges on sun exposure which may be reduced in obese individuals, who tend to partake in less outdoor physical activities (18, 36). Furthermore, 25(OH)D may be sequestered in the adipose tissue of obese persons and, as such, has a reduced bioavailability (36). While the pathophysiology of 25(OH)D deficiency in obesity remains uncertain, the important role of 25(OH)D sufficiency to ensure optimal skeletal health are widely accepted. This study documented an inverse correlation between PTH and 25(OH)D. PTH secretion is expected to increase with a decrease in bioavailable 25(OH)D and a negative calcium balance. Chronic exposure of the skeleton to elevated circulating PTH is known to contribute to bone loss and decreased skeletal integrity. The findings argue for the critical interpretation of PTH to inform the routine monitoring and appropriate supplementation of 25(OH)D in obese patients, particularly those scheduled for metabolic surgery.

Most of the study participants (136/154) were women with a median age of 45 years (37–51) and the majority were either of mixed/Asian (65/154; 42%) or European (83/154; 54%) descent. Iron deficiency was noted in near half (46%) of the women in this study, with iron deficiency anemia present in 12%. A study by Phatlhane et al. in otherwise healthy non-pregnant South African adults (median age 30 years) documented iron deficiency in a concerning 56,6% of their female participants and iron deficiency anemia in 9.8% (37); findings in keeping with those described here. Diagnostic criteria employed to define iron deficiency and iron deficiency anemia were similar in this study and Phatlhane et al. (37). They attributed the presence of iron deficiency in their cohort to menstrual blood loss and limited intake of iron rich foods. In another local study, the association between obesity and iron deficiency in women aged 25-49 years in rural areas in the Free State Province of South Africa was explored. Iron-deficiency was noted in a far lower percentage of their participants (4.1%) (38). Studies from elsewhere in the world looking at micronutrient status in the morbidly obese and prior to bariatric surgery document iron deficiency in a comparatively lower percentage of their cohorts (<10%) (18, 19, 39). Detailed dietary assessment and interrogation of menstrual patterns was not performed in this study making it impossible to define causality of these findings or explain the discrepancy compared to other published data. The high prevalence of iron deficiency in the South African setting prior to metabolic surgery is important and noteworthy and should prompt assessment of iron status prior to performing metabolic surgery.

25(OH)D, folate, and iron deficiencies were more prevalent in participants with a BMI ≥45 kg/m$^{2,}$ compared to those with a BMI <40kg/m$^2$, a finding also noted in other published studies (16). In fact, folate deficiency was exclusively seen in participants in the obesity class III or above. Interpretation of this data must, however, be done cautiously as only 11 study participants, representative of a minority of the cohort (7%) had a BMI <40 kg/m$^2$. Folate deficiency was observed in 18% of research participants, comparatively lower than other African studies, where folate deficiency was noted in 54% obese and non-obese women in Ghana (39). The Ghanaian study (40) notes that folate deficiency may be particularly high in West Africa where folate-deficient diets are consumed. In the same way, Modjadji et al. (41) demonstrated low folate levels in 28% of non-pregnant women of childbearing age in Limpopo, South Africa. This study was performed 4 years after the introduction of mandatory food fortification with folic acid in South Africa. Additionally, low folate levels have been linked to poor socio-economic circumstances (SES), but limited numbers precluded an evaluation of the association between folate and SES in this study (41).

We did not quantify nutrient (including folate) intake in our study, but the South African National Food Consumption Survey-Fortification Baseline (NFCS-FB) in women of reproductive age, reassuringly indicated low rates of folate deficiency nationally (42). Interestingly at the time, 60% did not look for the food fortification logo on maize, bread, or flour products (42). Provincially, women and children in the Western Cape, Northern Cape, the Free State and Eastern Cape had significantly lower mean serum and red blood cell folate compared to other provinces (42). Still, the mean folate levels in the Western Cape where 58% of women were obese or overweight was sufficient (42). It is well established that overweight and obese individuals have lower serum folate concentrations than normal-weight individuals (43). Female folate deficiency is still noted during pregnancy and lactation despite food fortification due to increased metabolic needs (40, 44). Globally the proposed contributing factors to folate deficiency in obese and overweight individuals include inflammation, insulin resistance and dysbiosis in the microbiome (43). Additional considerations are increased urinary excretion, dilution of blood volume, and impaired folate absorption by the intestinal epithelium (45). We could not identify comparable South African cohorts to juxtapose our findings scientifically and did not evaluate the influence of these factors in our study.

Clinicians should maintain a high index of suspicion and a low threshold to test for micronutrient deficiencies in obese patients, especially those with a BMI ≥40 kg/m$^2$, irrespective of whether they are scheduled for metabolic surgery or not.

Evaluation of glycemic status was limited to determination of a fasting blood glucose and HbA1c and was available in 152 of study participants. Abnormal glucose homeostasis was present in a concerning number of participants (102/152; 67%). Of those 33/

102 (32%) had newly diagnosed prediabetes and 13/102 (13%) unknown T2D thus representing 30% of this study cohort. Within obesity category III, 22% and 40% of women had prediabetes and T2D respectively, metabolic abnormalities not considered or required as inclusion criteria in this subgroup of the cohort. Optimal glycemic control was achieved in less than half of participants known with diabetes mellitus prior to study entry (42.8%). The high prevalence of undiagnosed prediabetes and T2D and the suboptimal control of known diabetes at baseline in subjects scheduled for bariatric surgery is noteworthy and must be addressed in clinical practice. It illustrates the significant number of unmet needs for T2D in sub-Saharan Africa (46). Evidence from the South African National Health and Nutrition Examination Survey (SANHANES-1 (2011–2012) indicated in people with T2D, 45.4% are unscreened and overall, that 80.6% of the T2D population had an unmet need for care (47). Obesity is one of the strongest risk factors for T2D and to limit the impact of this epidemic, urgent multilevel prevention and management actions are required.

This study has limitations. All participants were recruited from an existing pool of patients referred for metabolic surgery at a single tertiary hospital and extrapolation of the findings may thus not be applicable to the broader population. Findings in this study remain valuable as an initial step to uncover the baseline prevalence of micronutrient deficiencies in obese South Africans scheduled for metabolic surgery. With the projected increased prevalence of obesity on the African continent, the results caution for the judicial monitoring of patients considered for metabolic surgery as treatment method. Based on the data, it is recommended that a routine assessment of micronutrient status is performed; that as a minimum include the measurement of 25(OH)D, iron status and folate. Screening for T2D with an oral glucose tolerance test ± HbA1c determination and optimization of glycemic control in those known with T2D should be standard of care in obese individuals, including those scheduled for metabolic surgery.

## 5 Conclusion

In conclusion, the study documented micronutrient deficiencies and a concerning prevalence of abnormal glucose status in obese individuals scheduled for metabolic surgery. The appropriate detection and management of these nutritional deficiencies need to be moderated by the judicial use of resources and should include, at a minimum, the measurement of 25(OH)D and folate level and evaluation of iron status. Future efforts should seek to collate patient data on a national scale, to provide a more holistic, longitudinal picture of the relationship between obesity, metabolic surgery, and micronutrient status in the developing world, which may optimize evidence-based care.

## Data availability statement

The original contributions presented in the study are included in the article/Supplementary Material. Further inquiries can be directed to the corresponding authors.

## Ethics statement

The study protocol was approved by Stellenbosch University's Health Research Ethics Committee (S18/01/003) and conducted according to the 1964 Helsinki Declaration principles. All participants provided written informed consent. The patients/participants provided their written informed consent to participate in this study.

## Author contributions

All authors have met the requirements for authorship. All authors contributed to the article and approved the submitted version.

## Acknowledgments

The authors thank the participants of this study, who have helped to shed light on this important topic. We thank Polly Joubert, who assisted with data collection. We acknowledge Dr. Marizna Korf (nee Barkhuizen), Dr. Razia Bandeker and Dr. Keshanya Moodley, who assisted with details pertaining to laboratory analysis.

## Conflict of interest

The authors declare that the research was conducted in the absence of any commercial or financial relationships that could be construed as a potential conflict of interest.

## Publisher's note



## Supplementary material

The Supplementary Material for this article can be found online at: https://www.frontiersin.org/articles/10.3389/fendo.2023.1120531/full#supplementary-material

SUPPLEMENTARY TABLE 1
Baseline characteristics and stratification categories. The WHO classification of obesity was done according to BMI (kg/m$^2$): I – obese (30-34.9 kg/m$^2$); II – severely obese (35-39.9 kg/m$^2$); III – morbidly obese (>40 kg/m$^2$). Annual Income bracket is based on the Uniform Patient Fee Schedule's (UPFS) classification code. H0: Low – receiving grant or pension; H1: <R70 000/person or <R100 000/family; H2: R70 000- R100 000/person or R100 000-R350 000/family; H3: >R250 000/person or >R350 000/family; P: Private patients – not subsidized.

# References


1. Flegal KM, Kit BK, Orpana H, Graubard BI. Association of all-cause mortality with overweight and obesity using standard body mass index categories: a systematic review and meta-analysis. *Jama* (2013) 309(1):71–82. doi: 10.1001/jama.2012.113905

2. Gao F, Zheng KI, Wang X-B, Sun Q-F, Pan K-H, Wang T-Y, et al. Obesity is a risk factor for greater COVID-19 severity. *Diabetes Care* (2020) 43(7):e72–4. doi: 10.2337/dc20-0682

3. Popkin BM, Du S, Green WD, Beck MA, Algaith T, Herbst CH, et al. Individuals with obesity and COVID-19: A global perspective on the epidemiology and biological relationships. *Obes Rev* (2020) 21(11):e13128. doi: 10.1111/obr.13128

4. Tamara A, Tahapary DL. Obesity as a predictor for a poor prognosis of COVID-19: A systematic review. *Diabetes Metab Syn* (2020) 14(4):655–9. doi: 10.1016/j.dsx.2020.05.020

5. Sowers JR. Obesity as a cardiovascular risk factor. *Am J Med* (2003) 115(8):37–41. doi: 10.1016/j.amjmed.2003.08.012

6. Wilson PW, D'Agostino RB, Sullivan L, Parise H, Kannel WB. Overweight and obesity as determinants of cardiovascular risk: the framingham experience. *Arch Int Med* (2002) 162(16):1867–72. doi: 10.1001/archinte.162.16.1867

7. James PT, Leach R, Kalamara E, Shayeghi M. The worldwide obesity epidemic. *Obes Res* (2001) 9(S11):228S–33S. doi: 10.1038/oby.2001.123

8. Caballero B. A nutrition paradox–underweight and obesity in developing countries. *N Engl J Med* (2005) 352(15):1514–6. doi: 10.1056/NEJMp048310

9. Astrup A, Bügel S. Overfed but undernourished: recognizing nutritional inadequacies/deficiencies in patients with overweight or obesity. *Int J Obes* (2019) 43(2):219–32. doi: 10.1038/s41366-018-0143-9

10. Courcoulas AP, Yanovski SZ, Bonds D, Eggerman TL, Horlick M, Staten MA, et al. Long-term outcomes of bariatric surgery: a national institutes of health symposium. *JAMA Surg* (2014) 149(12):1323–9. doi: 10.1001/jamasurg.2014.2440

11. Schauer PR, Bhatt DL, Kirwan JP, Wolski K, Aminian A, Brethauer SA, et al. Bariatric surgery versus intensive medical therapy for diabetes–5-year outcomes. *N Engl J Med* (2017) 376:641–51. doi: 10.1056/NEJMoa1600869

12. Sjöström L, Peltonen M, Jacobson P, Sjöström CD, Karason K, Wedel H, et al. Bariatric surgery and long-term cardiovascular events. *Jama* (2012) 307(1):56–65. doi: 10.1001/jama.2011.1914

13. Vest AR, Heneghan HM, Agarwal S, Schauer PR, Young JB. Bariatric surgery and cardiovascular outcomes: a systematic review. *Heart* (2012) 98(24):1763–77. doi: 10.1136/heartjnl-2012-301778

14. Nguyen NT, Paya M, Stevens CM, Mavandadi S, Zainabadi K, Wilson SE. The relationship between hospital volume and outcome in bariatric surgery at academic medical centers. *Ann Surg* (2004) 240(4):586. doi: 10.1097/01.sla.0000140752.74893.24

15. Birkmeyer NJ, Dimick JB, Share D, Hawasli A, English WJ, Genaw J, et al. Hospital complication rates with bariatric surgery in Michigan. *Jama* (2010) 304(4):435–42. doi: 10.1001/jama.2010.1034

16. Pories WJ. Bariatric surgery: risks and rewards. *J Clin Endocrinol Metabol* (2008) 93(11):s89–96. doi: 10.1210/jc.2008-1641

17. MacDonald KG, Long SD, Swanson MS, Brown BM, Morris P, Dohm GL, et al. The gastric bypass operation reduces the progression and mortality of non-insulin-dependent diabetes mellitus. *J Gastrointest Surg* (1997) 1(3):213–20. doi: 10.1016/S1091-255X(97)80112-6

18. Krzizek EC, Brix JM, Herz CT, Kopp HP, Schernthaner GH, Schernthaner G, et al. Prevalence of micronutrient deficiency in patients with morbid obesity before bariatric surgery. *Obes Surg* (2018) 28(3):643–8. doi: 10.1007/s11695-017-2902-4

19. Flancbaum L, Belsley S, Drake V, Colarusso T, Tayler E. Preoperative nutritional status of patients undergoing roux-en-Y gastric bypass for morbid obesity. *J Gastrointest Surg* (2006) 10(7):1033–7. doi: 10.1016/j.gassur.2006.03.004

20. O'Kane M, Parretti HM, Pinkney J, Welbourn R, Hughes CA, Mok J, et al. British Obesity and metabolic surgery society guidelines on perioperative and postoperative biochemical monitoring and micronutrient replacement for patients undergoing bariatric surgery–2020 update. *Obes Rev* (2020) 21(11):e13087. doi: 10.1111/obr.13087

21. Parrott J, Frank L, Rabena R, Craggs-Dino L, Isom KA, Greiman L. American Society for metabolic and bariatric surgery integrated health nutritional guidelines for the surgical weight loss patient 2016 update: micronutrients. *Surg Obes Relat Dis* (2017) 13(5):727–41. doi: 10.1016/j.soard.2016.12.018

22. Mechanick JI, Youdim A, Jones DB, Garvey WT, Hurley DL, McMahon MM, et al. Clinical practice guidelines for the perioperative nutritional, metabolic, and nonsurgical support of the bariatric surgery patient–2013 update: cosponsored by American association of clinical endocrinologists, the obesity society, and American society for metabolic & bariatric surgery. *Surg Obes Relat Dis* (2013) 9(2):159–91. doi: 10.1016/j.soard.2012.12.010

23. World Health Organization. Obesity: preventing and managing the global epidemic, in: *Proceedings of the WHO Consultation on Obesity*, Geneva, 1997 June 3-5.

24. CLSI. *Defining, establishing, and verifying reference intervals in the clinical laboratory; approved guideline. 3rd ed*. Wayne, PA: Clinical and Laboratory Standards Institute (2008).

25. Jeppsson J, Kobold U, Barr J, Finke A, Hoelzel W, Hoshino T, et al. Approved IFCC reference method for the measurement of HbA1c in human blood. *Clin Chem Lab Med* (2002) 40(1):78–89. doi: 10.1515/CCLM.2002.016

26. Vieth R. Why the minimum desirable serum 25-hydroxyvitamin d level should be 75 nmol/L (30 ng/ml). *Best Pract Res Clin Endocrinol Metab* (2011) 25(4):681–91. doi: 10.1016/j.beem.2011.06.009

27. SEMDSA Guideline Committee. SEMDSA guideline for the management of type 2 diabetes mellitus. *J Endocrinol Metab Diabetes South Afr* (2012) 17(1):1–94.

28. Van der Merwe MT, Fetter G, Naidoo S, Wilson R, Drabble N, Gonçalves D, et al. Baseline patient profiling and three-year outcome data after metabolic surgery at a south African centre of excellence. *J Endocrin Metabol Diabetes S Afr* (2015) 20(3):16–27. doi: 10.1080/16089677.2015.1085700

29. Finucane MM, Stevens GA, Cowan MJ, Danaei G, Lin JK, Paciorek CJ, et al. National, regional, and global trends in body-mass index since 1980: systematic analysis of health examination surveys and epidemiological studies with 960 country-years and 9.1 million participants. *Lancet* (2011) 377(9765):557–67. doi: 10.1016/S0140-6736(10)62037-5

30. NCD Risk Factor Collaboration. Rising rural body-mass index is the main driver of the global obesity epidemic in adults. *Nature* (2019) 569(7755):260. doi: 10.1038/s41586-019-1171-x

31. Cois A, Day C. Obesity trends and risk factors in the south African adult population. *BMC Obes* (2015) 2(1):42. doi: 10.1186/s40608-015-0072-2

32. Mogire RM, Mutua A, Kimita W, Kamau A, Bejon P, Pettifor JM, et al. Prevalence of vitamin d deficiency in Africa: a systematic review and meta-analysis. *Lancet Global Health* (2020) 8(1):e134–142. doi: 10.1016/S2214-109X(19)30457-7

33. Sanders KM, Stuart AL, Williamson EJ, Simpson JA, Kotowicz MA, Young D, et al. Annual high-dose oral vitamin d and falls and fractures in older women: a randomized controlled trial. *JAMA* (2010) 303(18):1815–22. doi: 10.1001/jama.2010.594

34. AU Dawson-Hughes B, Mithal A, Bonjour JP, Boonen S, Burckhardt P, Fuleihan GE, et al. IOF position statement: vitamin d recommendations for older adults. *Osteoporos Int* (2010) 21(7):1151–4. doi: 10.1007/s00198-010-1285-3

35. Holick MF. Vitamin d deficiency. *New Engl J Med* (2007) 357(3):266–81. doi: 10.1056/NEJMra070553

36. Wortsman J, Matsuoka LY, Chen TC, Lu Z, Holick MF. Decreased bioavailability of vitamin d in obesity. *Am J Clin Nutr* (2000) 72(3):690–3. doi: 10.1093/ajcn/72.3.690

37. Phatlhane DV, Zemlin AE, Matsha TE, Hoffmann M, Naidoo N, Ichihara K, et al. The iron status of a healthy south African adult population. *Clinica Chimica Acta* (2016) 460(1):240–5. doi: 10.1016/j.cca.2016.06.019

38. Jordaan EM, van den Berg VL, van Rooyen FC, Walsh CM. Obesity is associated with anaemia and iron deficiency indicators among women in the rural free state, south Africa. *S Afr J Clin Nutr* (2020) 33(3):72–8. doi: 10.1080/16070658.2018.1553361

39. Ernst B, Thurnheer M, Schmid SM, Schultes B. Evidence for the necessity to systematically assess micronutrient status prior to bariatric surgery. *Obes Surg* (2009) 19(1):66–73. doi: 10.1007/s11695-008-9545-4

40. Christian AK, Steiner-Asiedu M, Bentil HJ, Rohner F, Wegmüller R, Petry N, et al. Co-Occurrence of Overweight/Obesity, anemia and micronutrient deficiencies among non-pregnant women of reproductive age in Ghana: Results from a nationally representative survey. *Nutrients* (2022) 14(7):1427. doi: 10.3390/nu14071427

41. Modjadji SE, Alberts M, Mamabolo RL. Folate and iron status of south African non-pregnant rural women of childbearing age, before and after fortification of foods. *South Afr J Clin Nutr* (2007) 20(3):89–93. doi: 10.1080/16070658.2007.11734132

42. Labadarios D ed. *National food consumption survey-fortification baseline (NFCS-FB)*. South Africa: Directorate: Nutrition, Department of Health (2008).

43. Köse S, Sözlü S, Bölükbaşi H, Ünsal N, Gezmen-Karadağ M. Obesity is associated with folate metabolism. *Int J Vitamin Nutr Res* (2019) 90:353–64. doi: 10.1024/0300-9831/a000602

44. Mamabolo RL, Alberts M, Steyn NP, de Waal HDV, Nthangeni NG, Levitt NS. Evaluation of the effectiveness of iron and folate supplementation during pregnancy in a rural area of Limpopo province. *South Afr J Clin Nutr* (2004) 17(1):15–21.

45. van der Windt M, Schoenmakers S, van Rijn B, Galjaard S, Steegers-Theunissen R, van Rossem L. Epidemiology and (patho) physiology of folic acid supplement use in obese women before and during pregnancy. *Nutrients* (2021) 13(2):331. doi: 10.3390/nu13020331

46. Manne-Goehler J, Atun R, Stokes A, Goehler A, Houinato D, Houehanou C, et al. Diabetes diagnosis and care in sub-Saharan Africa: pooled analysis of individual data from 12 countries. *Lancet Diabetes Endocrinol* (2016) 4(11):903–12. doi: 10.1016/S2213-8587(16)30181-4

47. Stokes A, Berry KM, Mchiza Z, Parker WA, Labadarios D, Chola L, et al. Prevalence and unmet need for diabetes care across the care continuum in a national sample of south African adults: Evidence from the SANHANES-1, 2011-2012. *PloS One* (2017) 12(10):e0184264. doi: 10.1371/journal.pone.0184264

# Frontiers in Endocrinology

**Explores the endocrine system to find new therapies for key health issues**

The second most-cited endocrinology and metabolism journal, which advances our understanding of the endocrine system. It uncovers new therapies for prevalent health issues such as obesity, diabetes, reproduction, and aging.

---

## Discover the latest Research Topics

See more →

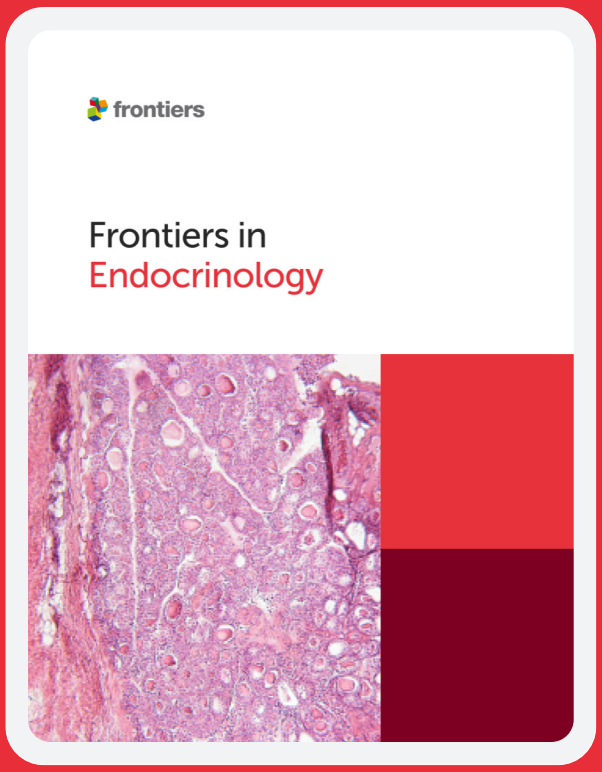


**Frontiers**

Avenue du Tribunal-Fédéral 34
1005 Lausanne, Switzerland
frontiersin.org

**Contact us**

+41 (0)21 510 17 00
frontiersin.org/about/contact